Impacts of Climate Change on European Electricity and Heating Systems

Smail Kozarcanin
PhD Thesis

Department of Engineering
Aarhus University
Denmark

Nov. 2019

Smail Kozarcanin
1st Edition, November 2019
Department of Engineering
Aarhus University
Inge Lehmanns Gade 10
DK-8000 Aarhus C

This document was typeset in LaTeX

Front cover illustration: From dreamstime.com

ISBN: 978-87-7507-477-8
DOI: 10.7146/aul.378

Contents

Résumé (English, Danish, Bosnian) . . . III
Preface . . . IX
Acknowledgement . . . XI

1 Introduction **1**
1.1 Motivation . . . 1
1.2 Project design . . . 10
1.3 Conversion and validation of energy system related data, in brief 11
1.4 Climate data . . . 13
1.5 Introduction to relevant pre-projects . . . 17
1.6 Structure . . . 22

Part I **24**

2 21st century climate change impacts on key properties of a large-scale renewable-based electricity system **25**
2.1 Introduction . . . 28
2.2 Experimental procedures . . . 33
2.3 Results and discussions . . . 37
2.4 Conclusion . . . 46

Part II **52**

3 Estimating country-specific space heating threshold temperatures from national consumption data **53**
3.1 Introduction . . . 55
3.2 Experimental procedures . . . 59
3.3 Results and discussions . . . 70
3.4 Conclusion . . . 83

4 Impact of climate change on the cost-optimal mix of decentralised heat pump and gas boiler technologies in Europe **87**
4.1 Introduction . . . 89
4.2 Experimental procedures . . . 92
4.3 Results . . . 100
4.4 Discussions . . . 114
4.5 Conclusions and policy implications . . . 124

5 Techno-economic benefits of a fully coupled European electricity and heating system in a 21st century climate **129**
5.1 Introduction . . . 131
5.2 Experimental procedures . . . 136
5.3 Results and discussions . . . 148
5.4 Conclusion . . . 159

6 General Conclusion **161**

Appendix **165**

7 21st century climate change impacts on key properties of a large-scale renewable-based electricity system **167**
7.1 Extended introduction . . . 168
7.2 Extended experimental procedures . . . 174
7.3 Statistical tests . . . 220
7.4 Additional results . . . 221

8 Estimating country-specific space heating threshold temperatures from national consumption data **235**
8.1 National electricity and gas consumption data . . . 236
8.2 Additional results . . . 236

9 Impact of climate change on the cost-optimal mix of decentralised heat pump and gas boiler technologies in Europe **245**
9.1 Extended experimental procedures . . . 246
9.2 Additional results . . . 251

10 Project contributions **263**

References **266**

About the author **303**

Résumé

The European Commission have developed a long-term energy strategy that, if successful, will result in net-zero greenhouse gas emissions in Europe. This may be achieved in part by designing future energy systems with a close link between the electricity and other end-use sectors. Such well-integrated systems take decades to engineer, which allows for additional climate change. Time is therefore a significant constraint and timely mitigation strategies are important. In this collection of research articles, I focus on the impact of climate change on future European electricity and heating systems and present a selection of my first-authored articles on this topic. Initially, I treat these sectors separately, but by the end, I focus on the potential benefits of designing a closely linked European electricity and heating system.

To represent a broad range of climate outcomes for the 21st century, I adopt three representative climate projections from the Intergovernmental Panel on Climate Change. Based on the underlying assumptions of these projections, the World Climate Research Programme developed state-of-the-art weather data for the 21st century that is made available for further research. I use weather data from nine independent climate models to generate climate change affected energy system data for this project. The large ensemble of data defines the foundation of this project and is used in all analyses.

The electricity sector is fundamental in the energy systems and with its rising share of renewable power production it becomes important to investigate into its resilience to climate change. In the chapter "*21st century climate change impacts on key properties of a large-scale renewable-based electricity system*", I have shown that highly renewable electricity systems might perform equally well at the end of this century as of now. This is in particular an interesting result for coupling other end-use sectors with the power sector.

Measured data on space heating are not available on country scale, nor are

highly granular estimates. To this end, I have developed a coherent method that can be used for this purpose. The method is presented in chapter "*Estimating country-specific space heating threshold temperatures from national consumption data*", and shows that current results can improve significantly by including weather and primary energy use.

In the chapter "*Impact of climate change on the cost-optimal mix of decentralised heat pump and gas boiler technologies in Europe*", I uncover that the need for space heating may reduce significantly depending on the degree of climate change. With a careful modelling of the coefficient of performance, I show that heat pumps become more economically feasible with rising ambient temperatures.

I conclude this collection with an ongoing research, which shows that a closely linked power and heating system reduces the system cost by up to 10%. The impact of climate change and the CO_2-constraints have a considerably higher impact, with system costs ranging from below 30% of the historical reference point to 100% above, depending on the projection.

This collection of research papers is backed up with an extended appendix, which contains detailed information on the procedures used in the research papers.

Resume

Europa-Kommissionen har udviklet en langsigtet energistrategi, som, hvis succesfuld, vil resultere i netto-nuludledning af drivhusgasser i Europa. Dette kan opnås til dels ved at udvikle fremtidige energisystemer med tæt kobling mellem elsektoren og andre slutbrugersektorer. Sådanne velintegrerede systemer vil tage årtier at udvikle og tillader derved yderligere klimaforandringer. Tid er således en væsentlig begrænsende faktor, og rettidige strategier for udbedring er essentielle. I denne samling af forskningsartikler fokuserer jeg på effekten af klimaforandringer på Europas fremtidige elektricitets- og varmesystemer og præsenterer et udvalg af artikler på området, på hvilke jeg er førsteforfatter. Til at starte med behandles disse sektorer hver for sig, men til slut fokuserer jeg på de potentielle fordele ved at udvikle et tæt koblet europæisk el- og varmesystem.

For at repræsentere et bredt spektrum af mulige klimaudfald i det 21. århundrede bruger jeg tre repræsentative klimaprognoser fra FN's klimapanel. Baseret på de underliggende antagelser i disse prognoser har World Climate Research Programme udviklet avanceret vejrdata for det 21. århundrede, som er tilgængeliggjort til brug for videre forskning. Jeg bruger i dette projekt vejrdata fra ni uafhængige klimamodeller for at generere energisystemdata, der er påvirket af klimaforandringer. Denne store samling af data udgør grundlaget for projektet og bruges i alle analyser.

Elsektoren er en grundlæggende del af energisystemerne, og med dens stigende andel af vedvarende energiproduktion er det vigtigt at undersøge dens robusthed over for klimaforandringer. I kapitlet "*21st century climate change impacts on key properties of a large-scale renewable-based electricity system*" viser jeg, at elektricitetssystemer med stor andel af vedvarende energi muligvis vil kunne yde lige så godt i slutningen af dette århundrede, som de gør i dag. Dette resultat er særligt interessant i forhold til koblingen af andre slutbrugersektorer til elsektoren.

Datamålinger på rumvarme er ikke tilgængelige på landsskala, ej heller er grove estimater. Jeg har derfor udviklet en konsekvent metode, der kan bruges til dette formål. Metoden præsenteres i kapitlet "*Estimating country-specific space heating threshold temperatures from national consumption data*" og viser, at nuværende resultater kan forbedres betydeligt ved at inkludere vejr og primær energiforbrug.

I kapitlet "*Impact of climate change on the cost-optimal mix of decentralised heat pump and gas boiler technologies in Europe*" viser jeg, at behovet for rumvarme muligvis vil reduceres betydeligt, afhængig af graden af klimaforandringer. Gennem omhyggelig modellering af ydelseskoefficienten viser jeg, at varmepumper er mere økonomisk realiserbare med stigende omgivelsestemperaturer.

Jeg konkluderer denne samling med igangværende forskning, der viser, at et tæt forbundet el- og varmesystem kan reducere systemomkostninger med op til 10%. Effekten af klimaforandringer og CO2-begrænsninger har en betydeligt højere påvirkning, med systemomkostninger, der kan variere fra 30% under det historiske udgangspunkt til 100% over, alt efter hvilken fremskrivning, der bruges.

Denne samling a forskningsartikler indeholder et udvidet supplerende tillæg, som indeholder detaljeret information om metoder, der blev brugt i forskningsartiklerne.

Rezime

Europska komisija razvila je dugoročnu energetsku strategiju koja će, ako bude uspješna, rezultirati neto-nultom emisijom stakleničkih plinova u Europi. To se dijelom može postići dizajniranjem budućih energetskih sustava koji su usko povezani između električne energije i ostalih krajnjih sektora. Za takve dobro integrirane sustave su potrebna desetlječa inženjerstva, što omogućava dodatne klimatske promjene. Vrijeme je stoga važno ograničenje a važne a zato su i važne pravovremene strategije ublažavanja. U ovoj zbirci članaka o istraživanju se fokusiram na utjecaj klimatskih promjena na buduće evropske sustave za električnu energiju i grijanje i predstavljam izbor svojih prvih autorskih članaka na ovu temu. U početku tretiram te sektore odvojeno, ali na kraju se usredotočujem na potencijalne prednosti dizajniranja usko povezanog europskog sustava električne energije i grijanja.

Kako bih predstavio širok raspon klimatskih rezultata za 21. stoljeće, usvajam tri reprezentativne projekcije klime iz Međuvladinog Panela o Klimatskim Promjenama. Na temelju temeljnih pretpostavki ovih projekcija, Svjetski Program Istraživanja Klime razvio je izuzetne vremenske podatke za 21. stoljeće koji su dostupni za daljnja istraživanja. Za ovaj projekt koristim vremenske podatke iz devet nezavisnih klimatskih modela za generiranje podataka energetskog sustava koji su utjecali na klimatske promjene. Velika skupina podataka definira temelje ovog projekta i koristi se u svim analizama.

Sektor električne energije je fundamentalan u energetskim sustavima, a s povećanim udjelom proizvodnje obnovljive energije postaje važno istražiti otpornost na klimatske promjene. U članku "*21st century climate change impacts on key properties of a large-scale renewable-based electricity system*" pokazao sam da bi visoko obnovljivi elektroenergetski sustavi mogli funkcionirati podjednako dobro krajem ovog stoljeća kao i sada. To je posebno zanimljiv rezultat za povezivanje ostalih krajnjih sektora s električnim sektorom.

Izmjereni podaci o grijanju prostora nisu dostupni na razini države, niti postoje vrlo detaljne procjene. Radi toga sam razvio metodu koja se može koristiti u tu svrhu. Metoda je opisana u radu "*Estimating country-specific space heating threshold temperatures from national consumption data*" i pokazuje da se trenutni rezultati mogu značajno poboljšati uključivanjem vremenskih prilika i korištenjem primarne energije.

U radu "*Impact of climate change on the cost-optimal mix of decentralised heat pump and gas boiler technologies in Europe*" otkrivam da se grijanje prostora može značajno smanjiti ovisno o stupnju klimatskih promjena. Pažljivim modeliranjem koeficijenta performansi pokazujem da toplinske crpke postaju ekonomski lakše izvedive s povećanjem temperature okoline.

Ovu zbirku zaključujem istraživanjem koje je u tijeku, a koje pokazuje da usko povezani sustav električne energije i grijanja smanjuje troškove sustava za do 10%. Utjecaj klimatskih promjena i proračun CO_2 ima znatno veći utjecaj, pri čemu se troškovi sustava kreću u rasponu od 30% ispod povijesne referentne točke do 100%, ovisno o projekciji.

Ova zbirka znanstvenih radova potpomognuta je proširenim dodatkom koji sadrži detaljne informacije o postupcima koji se koriste u istraživačkim radovima.

Preface

Roughly two years after finishing my Master's thesis, about May 2016, I was approached by Professor Martin Greiner and Associate Professor Gorm Bruun Andresen from the Department of Engineering, Aarhus University, about a vacant position for a Ph.D. project on the topic: *Impacts of Climate Change on European Electricity and Heating Systems*. After some consideration and encouragement from family, friends and former colleagues, I agreed to take up the challenge. This work is a collection of some of mine research articles, which serves as a final outcome of my research during this project.

The ultimate goal of this project is to investigate into the advantage of designing a fully coupled European electricity and heating system and characterise the value of establishing such a system in the context of climate change. Such a system comes with benefits in both sectors. Research on climate change mitigation has become a mature line of study during the past decades. The electricity sector is currently under a strong transition towards CO_2-neutrality. The heating sector is lacking severely behind and requires significantly more attention in order to reach similar goals. Therefore, I am mostly concerned with the latter in this project. As of now, it is crucial to develop timely mitigation strategies for climate change – either we invest heavily in green technologies or we proceed our *Business As Usual* tradition. Further research into sector coupling and cross-vector integration might lead to the right decision!

This collection is built up of three general parts. In *Part I*, which consists of one research chapter, I only focus on the electricity system and investigate into the impact of climate change on five key metrics that represent a highly weather dependent European electricity system. *Part II*, which consists of three research chapters, is initiated with a similar research question, but with a focus on the buildings heating sector. In the final and concluding chapter of *Part II*, I focus on the governing research question, which was introduced in the previous paragraph. Each chapter is built around a research article that is either published,

under revision or in preparation at the time of writing. I am the first author of all articles, but detailed information on the contributions is presented at the onset of each chapter. *Part III* is an appendix, which holds an extensive supplemental information that covers the research Chapters 2 - 4. The research in Chapters 3 and 4 were partially conducted during an extended research stay for six months at the Centre for Environmental Policy, Imperial College London.

Acknowledgement

This project would not have been possible if not for the assistance, patience, and support of many individuals. As a matter of priority, I would first like to express my gratitude to my supervisor Associate Professor Gorm Bruun Andresen for mentoring me during this project. I truly apologise to his family, friends and others for making him about 10 years older throughout the project period. He has helped me through lots of difficult times in all possible activities related to academia. I sincerely thank him for his confidence in me.

Next, I would like to thank Dr. Iain Staffell for his enthusiasm and time spent on the extensive collaboration of two common publications. Furthermore, I thank him for his courtesy and responsibility for providing me with a warm welcome during the extended research stay at the Centre for Environmental Policy, Imperial College London. I sincerely hope that you take good care of your llama and that you occasionally take it for a spin at the Yorkshire dales.

I cannot express enough appreciation to my external collaborators from various meteorological institutes around Europe for spending their valuable time in handing out state-of-the-art climate change data for this research. Without this data the project would not have been possible. I sincerely thank: Ole Bøssing Christensen and Frederik Boberg from the Danish Meteorological Institute for discussions and for supplying out data from the regional climate model HIRHAM5, Grigury Nikulin from the Swedish Meteorological and Hydrological Institute for supplying out data from the regional climate model RCA4, Erik van Meijgaard from Royal Netherlands Meteorological Institute for supplying out data from the regional climate model RACMO22E, Peter Lenzen from German Climate Computing Center for supplying out data from the regional climate model CCLM4.

I would like to thank my colleagues: Hailiang Liu, Kun Zhu, Magnus Dahl, Bo Tranberg, Leon Schwenk Nebbe and Marta Victoria, for their assistance and

fruitful discussions throughout the project period.

I would like to thank Professor Dirk Witthaut for assessing the mid-term progress of this project, Professor Martin Greiner and Dr. Tom Brown for their help and assistance. Thanks to Heidi Søndergaard and Mejrema Zvonic for their graphical inputs and Mette Stig Hansen for her writing inputs.

Thanks to you my beloved wife for lending me out to my supervisor for three years and thank you for understanding me and the time I had to put into this doctoral degree. Finally, I would like to thank my family without whose love, support and understanding I could never have finished this project.

This research was supported by Aarhus University Research Foundation, AUFF, with funding number AUFF-E-2015-FLS-7-26.

CHAPTER 1

Introduction

1.1 Motivation

A world perspective

Natural catastrophes are common consequences of rapid weather changes and have ravaged the Earth throughout its lifetime. Hurricanes, droughts, flooding etc. are catastrophes known to all humans. Despite the invariable long term history of natural disasters, our generation is witnessing increasing rates of destruction and generations to come will witness scales of destruction and catastrophes never seen before, if no undertakings are made. Figure 1.1b illustrates this trend by the type of catastrophe on a global scale. It is evident that catastrophes due to flooding, erratic weather and temperature related incidents have increased from a few events in 1930 to about 350 during this decade. This trend is a clear signal of a changing climate and it is the primary way that most people experience it. During the recent decades, researchers have aimed to explain the changing climate with multiple controversial arguments, but a recent study has shown, with a "golden standard", that anthropogenic CO_2-emission is the main driver [1]. Figure 1.1a illustrates the anthropogenic CO_2-emission for different world regions. It is clear that, although Europe was accounted for the largest share of emission in 1990, it has undergone a decreasing trend towards 2016. The current largest share is accounted for by Asia from which approximately half of this amount is accounted for by China. Adding up the emissions from Europe, America and Asia amounts to 32 Gt, which is a close approximation to the global level in 2016. Production of electricity and heat from main activ-

ity and auto producers and from fossil fuel combustion in the residential sector account for about half of this amount (or 16 Gt). Decarbonising these sectors is therefore a vital starting point towards a more CO_2-neutral energy economy, which can be achieved through energy system transition [2].

Sector coupling will become a major strategy in the process of decarbonisation [3, 4]. Electrification of end-use sectors is currently the most promising strategy towards a low-carbon economy, but is currently only applicable for less energy intensive applications as, e.g., in low temperature processes and in lightweight transportation. A complementary solution for the energy intensive sectors is cross-vector integration, which is a form of indirect electrification, where electricity is used to produce gaseous and liquid energy carriers that can be used in, e.g., industrial high temperature processes and heavyweight transportation. Nevertheless, the current techno-economic barriers are still relatively high and many technologies need further improvement in order to become competitive in many applications and regions. The market for many power-to-x technologies also need further development in order for these to compete with cheap fossil-fuel driven technologies. Many places in the world lack an integrated planning and operational schedule within the individual sectors, which certainly prevents strong synergies and flexible interconnections between different sectors. Immature energy and climate policies in several world regions are not directly addressing the issue of climate change, which further decelerates the process of energy system decarbonisation [5]. To summarise, even though a significant progress has been made, there is still work to be done in all segments of energy systems worldwide.

For the remaining of this collection, the focus is on the European energy system and narrow into the electricity and buildings heating sectors.

Climate policies in Europe, in brief

At the COP21 meeting in Paris on December 2015, the UNFCCC member parties reached an agreement to limit the global average temperature increase below 2 °C above pre-industrial levels and to pursue efforts to limit the increase by 1.5 °C [8]. Before the Paris agreement, the European Commission have already proposed a long-term energy strategy that, if successful, will result in a low-carbon economy by 2050 in Europe [9]. The goal was to reduce the CO_2-emission by 80% - 95% compared to 1990 values and thereby pursue efforts to limit the global temperature increase to 2 °C. For Europe to take the more stringent Paris agree-

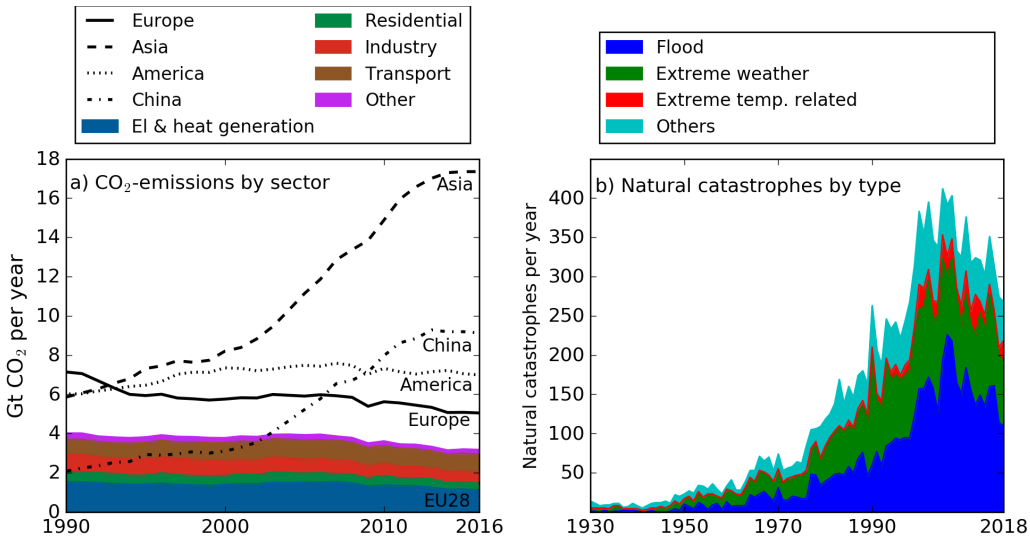

Figure 1.1: **Panel a: Sector aggregated CO_2-emission for a number of world regions. Emission by the EU28 is split into sectors and shown as areal plots.** The *electricity & heating* category refers to emission from main activity and auto producers of electricity and heat. The *residential* category refers to emission from fossil fuel combustion in households. The *industry* category refers to emission from fossil fuel combustion in manufacturing and construction activities, oil refineries for the purpose of coal mining, oil and gas extraction and others that are not mentioned. *Transport* accounts for emission from all transportation activities, except for international marine and aviation bunkers. Finally, the *others* category contains emission from the commercial sector, agriculture, foresting, fishing and others that are not mentioned. Figure redone from [6]. **Panel b: Natural catastrophes.** The *extreme temperature related* category defines catastrophes related to extreme temperatures and droughts. The *others* category covers natural catastrophes related to earthquakes, landslides, wildfire and volcanic activity. Figure redone with data from [7].

ment as a serious consideration and contribute to the process of reaching the 1.5 °C limit, the current roadmap had to be restructured. Therefore on November 2018, the European Commission adopted a new strategic long-term vision for reducing the net emission by 100% by 2050 [10].

Despite these efforts, there is still a 30-year gap with contentious greenhouse gas emission, though with lower rates in Europe. For this reason, Europeans might develop a moral courage, rectitude and a feeling of incorruptibility, but the global greenhouse gas emission will contentiously increase and the climate will continue to change. A study from 2019 by the Climate Action Tracker, reveals that there has only been a minor progress according to the Paris Agreement in 2019. They estimate that under current policies, the increase of the global average temperature will exceed 1.5 °C by the year of 2035, 2 °C by year 2053 and

3.2 °C by 2100 [11]. Another study expects a global average temperature increase of 2.0 - 4.9°C with a 3.2 °C median at the end of this century. The same study showed that the probability for staying below 2 °C is 5% while the probability for staying below 1.5 °C is as low as 1% [12]. Unfortunately, at the end of the day, it seems that the 2015 Paris Agreement [8] is just becoming "another order of business". It is now clear that the climate will continue to change, at least to some degree, but due to insecurities in energy and climate policies, technological innovations, markets etc., and due to missing global cooperation [13, 14] the degree of change remains unknown. Given this, it becomes important to incorporate projections of various degrees of climate change into studies on the design of future energy systems. In this report, three reconstructed concentration pathways, RCP [15] are applied, that represent very distinct, but plausible outcomes of the climate during the 21st century. These are a subset of the latest generation of climate projections adopted by the Intergovernmental Panel on Climate Change [16] in their fifth assessment report AR5 [17]. These are formally introduced in Section 1.5.

Advances in the European electricity sector

Production of electricity and heat in the EU28 accounts for the largest share of the CO_2-emission followed by transportation and industrial processes, as shown in Figure 1.1a. The EU28 power sector is a special case compared to other world regions. It has experienced a rapid transformation in all of its segments over the past decades. For example, the transmission and distribution grids have expanded significantly, the share of renewables is constantly increasing, electricity storage is becoming popular, renewable capacities has become cost-competitive to conventional production units, increasing consumer awareness, increasing social acceptance of renewable capacities and research has flourished within this area. Taking as an example the renewable penetration, a value of 32% (or a production of 1051 TWh) in 2018 made the European power sector the holder of the largest share of CO_2-neutral power production compared to other main regions [18]. In contrast, the US and Chinese power sectors held a corresponding share of 17% (or a production of 720 TWh) in 2018 and 24% (or a production of 1546 TWh) in 2017, respectively [19, 20]. It would be inaccurate to assign climate change mitigation as the only driver of the European advances, but certainly, it has a significant impact.

In the new long-term vision for Europe [10], the power sector appears to be the fastest to decarbonise and is expected to be emission-free by 2040. By means of

several studies [21, 22, 23, 24], this implies a strong transition towards a highly renewable electricity system. Nevertheless, with a renewable penetration of 20% in 2010, 32% in 2018 and a projected increase of 94 TWh/yr to reach 57% in 2030 [18], decarbonisation of the European electricity sector is already on a sure-fire way. Several studies also focus on the potential of large-scale storage options as, e.g., batteries, pumped hydro and hydrogen storages in future highly decarbonised energy systems and show that different types of storages qualify differently in different applications [25, 26, 27].

Advances in the European heating sector

In the same long-term strategy [10], the residential and commercial heating sectors are found to be fully decarbonised by 2050. Increasing energy efficiencies and renovating rates are already causing these sectors to decarbonise efficiently [10]. From a technological standpoint, the slow rate of innovation and the prohibitive costs of clean options for heating [28, 29] are at the moment not contributing significantly to the process of decarbonisation [30]. Decentralised heat generation is currently dominated by fossil-fuel driven boilers, which hold 61% of the total installed capacity. Biomass technologies hold the second largest share with 19% of the installed capacity. Direct electricity technologies as, e.g., electricity driven boilers and resistive heaters (which may be clean depending on the primary energy source for power generation) already hold a share of 13% of the installed capacity. Heat pumps are getting more attractive with 99% of the units installed after 2002 resulting in a share of 7% of the installed capacity [31]. The increasing interest in heat pumps is motivated by several factors as, e.g., investment subsidies supplied by governmental initiatives, increasing carbon taxes on heat generation by combustion of fossil fuels, increasing energy efficiency standards of buildings and increasing awareness towards information dissemination through campaigns and other events [32, 33]. The European Heat Pump Market Association projects that with the current sales of heat pumps, their market would double every 10 years which should result in a cost reduction of approximately 20% by 2024 [34].

A strong coupling of the electricity and heating systems can only take place through a large deployment of electricity driven technologies for heat generation. If heat generation is to be decarbonised, this requires an increased renewable penetration in the power system. This information leads naturally to the key questions of this project, which are briefly introduced in the following paragraphs with a detailed introduction in their respective research chapters.

Filling the gap of knowledge

Increasing the renewable penetration in energy systems will force them to rely more often on intermittent power generation for which it is expected, that challenges in constantly meeting the electricity demand will become increasingly complex. In addition to the short-term weather variations, climate change is expected to add another degree of long-term weather variability. It is therefore important to investigate into what extent long-term climate change might affect future highly renewable electricity systems. Such a study does not only quantify some of the key challenges that might occur in meeting the electricity demand, but the coupling to other sectors might be affected as well. This question is addressed in the first research chapter, Chapter 2. Here, research on the impact of climate change on power production from variable renewable electricity sources and power consumption via the electrified heating and cooling is presented. Next, five key metrics of a highly renewable European electricity system are defined and their resilience to climate change was analysed. The addition to the existing literature emanated by using a simplified top-down modelling approach of the electricity system that is, in particular, suitable for capturing the effect of weather on energy systems. Furthermore, the climate is allowed to affect both the demand and supply sides simultaneously. The study is strengthen by using carefully generated and validated energy system data. The use of climate change data from nine independent climate models contribute to the robustness of the results.

In Chapter 5, the benefits of introducing additional cooperation between the European electricity and heating systems is analysed and the value of such a system design is characterised in various degrees of climate change. This analysis requires an in-depth modelling of the buildings heat demand and supply sides. Contrary to the systematic control of electricity consumption, the decentralised ways of heating requires no smart monitoring systems to sustain system stability and metering equipment for heat consumption are therefore rare. Data on heat consumption are therefore either non-existing or not openly available and has to be estimated. Similarly, there are no open available estimates of the space heating requirements that fit the needs of this project. A model that can be used to estimate the space heating requirements and the non-heating summer seasons was therefore developed. The model must be given a temperature time series and a time series on the primary energy source(s) of the region in question. It is furthermore independent on the areal extent and can be applied to city as well as country or continental scales. It is also straight forward extended to estimate the need for cool. This modelling approach provides value to the exist-

ing literature through its prowess, simplicity and easy replication. This study is presented in research Chapter 3.

In Chapter 4, the investigation is on the impact of climate change on the buildings heat demand and on the impact of climate change on the cost-optimal options for future decentralised heating. Changes in the spatial temperature fluctuations and in the short and long-term temporal fluctuations will naturally affect the synergy between the demand and supply sides in future heating systems. As a consequence, the design of future cost-optimal heating infrastructures might look very different from the design of today's systems. By assuming no upper constraints on the supply of different energy carriers for heat generation as, e.g., electricity, gas and biomass, an analysis that assess the full potential of the different options for heating under the impact of climate change is allowed. This study is conducted by using climate change data with a high spatial resolution. This is an important approach that allows for capturing extreme temperature fluctuations across local regions. As in the aforementioned studies, the results are strengthen by using weather data from nine independent climate models.

In the final and concluding chapter, Chapter 5, investigation into the advantage of designing a fully coupled European electricity and heating system and characterise its value in the context of climate change is presented. Results of the previous two chapters are used for the modelling of the heating system. Since climate change is expected to strongly affect the heating sector through the temperature dependent demand and supply sides, the strong system coupling might perform differently in the different outcomes of climate change. A total of eight scenarios with different combinations of the system strengths and climate outcomes are evaluated and compared. For each scenario, the system costs, the technology composition and the system efficiency are quantified.

1.2 Project design

The biggest efforts of this interdisciplinary project were devoted to energy system analysis. Climate science enters the study through the application of vast amounts of climate change affected weather data and CO_2-constraints. The design of this project is illustrated with a schematic overview in Figure 1.2. The individual steps of this diagram are detailed in Section 1.5. The red coloured section illustrates the contributions to this project from other well-established projects. The green area illustrates how I build my research on top.

The very first part of this project was purely data technical and dealt with the acquisition of climate change affected weather data followed by the processes of cleaning and organisation. In a second step, this data were converted into necessary energy system related time series and if possible, these were bias-adjusted. This process was rather protracted, but important to conduct carefully, as the results of this process define the foundation of this project. This process is explained in greater detail in the Section 1.3.

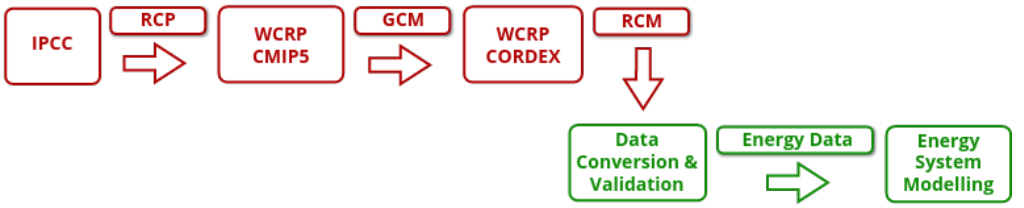

Figure 1.2: **A schematic overview of the project design.** Shown with red are the contributions from the Intergovernmental Panel on Climate Change IPCC, the World Climate Research Project WCRP and the Coordinated Regional Climate Downscaling Experiment CORDEX projects. Shown with green are my contributions to this project.

1.3 Conversion and validation of energy system related data, in brief

Throughout this project, data with a spatial and temporal resolution of 12 km x 12 km and 3 hours, respectively, were used. These are the results of the latest long-term projections of gridded weather data that are open-available for further research. They are currently seen as state-of-the-art within climatology and to the best of my knowledge, the best in the literature. The resolution of this data contributes significantly to an increased value and recognition of this project. Few climate variables with the highest demand as, e.g., the gridded temperature profiles can be found on various Earth System Grid Federation nodes, ESGF, but due to the high resolution in space and time most variables are not deployment on the ESGF nodes. Low resolution climate change affected weather data are most commonly found on the ESGF nodes. Great effort have therefore been put into contacting various meteorological institutes around Europe by person and requesting data. Data with 100 TB of climate change affected weather data were acquired from nine independent climate models. In Section 1.4, a selection of the climate variables that are used in this project are presented. For the remainder of this section, a brief introduction to the methods behind the conversion and validation processes is presented. An immense effort has been put into developing state-of-the-art methods for both. These processes are further detailed in the supplementary information of the article described in Chapter 2.

Starting with the electricity sector, 3-hourly country-wise wind and solar power potential time series have been created on the basis of data on the wind speed, surface roughness length, temperature and solar irradiation.

Wind power potential

The wind power potential has been evaluated on grid cell level and thereafter aggregated to country size. Based on the Wind Power database [35], turbines have been placed in grid cells that are closest to their actual positions. Turbine specific wind power curves have been used in the conversion from wind speeds to power production. Each power curve has been smoothed according to an optimised Gaussian convolution. This has previously shown to account very well for the limited temporal and spatial resolutions of the climate data [36]. The Gaussian convolution has been optimised by minimising the Kullback-Leibler divergence between the modelled wind power time series and an already bias-corrected time series provided by the Renewables.Ninja [37].

Solar power potential

A consistent database for PV-panels, their properties and information on their actual sites is currently non-existing. Therefore, one PV-panel has been placed in each grid cell. The conversion procedure from global radiation budgets to solar power potential time series follows a multi-step process that accounts for the geometry, direct, diffuse, and reflected irradiance on a tilted surface, temperature dependent efficiencies and inverter losses [36]. An optimised Weibull distribution has been used in the validation process. The optimised parameters of the Weibull distribution have been determined by validating against already bias-adjusted time series [38, 39], and seeks to minimise the Kullback-Leibler divergence metric.

Electricity consumption

The national electricity consumption was provided by the European Network of Transmission System Operators for Electricity [40]. To remove long-term trends in the consumption profiles, these were detrended for each country, and then concatenated in order to meet time span of the modelling period. The consumption was then corrected for impacts of electrified heating and cooling by means of the degree-day method and temperature data from the climate models.

Space heat consumption

National energy demand for space heating was estimated by using the theory of heating degree-days and the model-specific temperature data. The conversion from heating degree-days to actual energy consumption took place through values on the national energy demand provided by Heat Roadmap Europe [41].

1.4 Climate data

In Figures 1.3 – 1.5, a selection of the climate variables that are used in this project is presented. These are presented in terms of their spatial distribution with a 20-year average value in each grid cell for a historical period and for an end-of-century period in each climate pathway, RCP2.6, RCP4.5 and RCP8.5. The pathways are formally introduced in Section 1.5. These figures are excellent examples of the high spatial granularity of the climate variables that are used in this project. Clearly, the three projections span a broad outcome of possible climatic conditions throughout the 21st Century. Although, each individual pathway is based on internally socioeconomic assumptions, the RCPs cannot be treated as a consistent set of socioeconomic logic. As an example, RCP2.6 cannot be treated as a stringent socioeconomic reference scenario for the remaining RCPs, since the assumptions on socioeconomics, technology development etc. differ from the rest. The RCPs should therefore be treated as independent pathways representing a certain outcome of the future climate [42]. Examples are given in the following paragraphs.

Temperature

Figure 1.3 shows spatial distributions of the temperature. The historical period clearly illustrates increasing temperatures as a function of increasing latitudes with values ranging from an average value of 20 °C to below -10 °C. The RCP2.6 pathway leads to a temperature increase of up to 2 °C on the mainland, RCP4.5 of up to 4 °C and RCP8.5 of more than 6 °C.

Wind speed

Figure 1.4 shows similarly spatial distributions of the 10 meter wind speeds over Europe. In the historical frame, North-West Europe is dominated by the strongest winds, which reduce towards the mainland. The west chain of the Norwegian mountains and the Alps block, to a large extent, the wind from reaching East Scandinavia and the Balkans, respectively. As indicated earlier, the wind speeds are very different in the different climate projections. The least extreme climate pathway, RCP2.6, leads to increasing wind speeds by more than 2% around the British Isles, while the mainland is dominated by a decreasing trend. The intermediate pathway, RCP4.5, leads to increasing trends for most of Europe, while the most extreme climate projection, RCP8.5, leads to decreasing

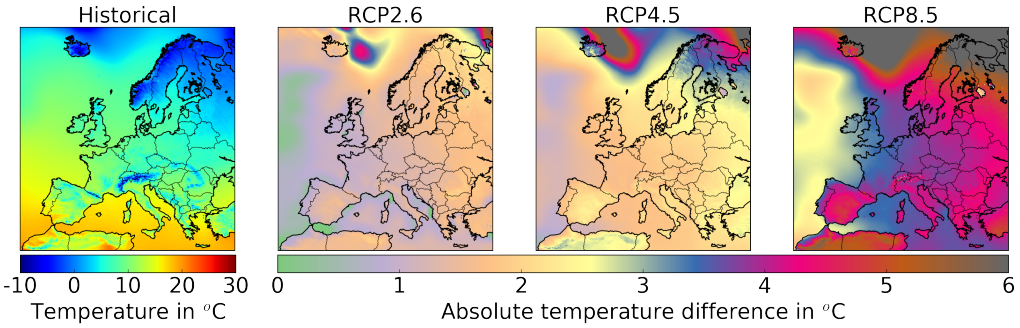

Figure 1.3: **Spatial distributions of the temperature profiles**. These are presented as 20-year average values. The historical frame spans the years from 1986 to 2006 while the cluster of climate pathways (RCP2.6, RCP4.5 and RCP8.5) spans an end-century period from 2080 to 2100. The figures are based on the HIRHAM5 regional climate model [43] downscaling the ICHEC-EC-EARTH global climate model [44].

trends. From these figures it becomes clear that the individual pathways are not continuations of each other and should be treated separately.

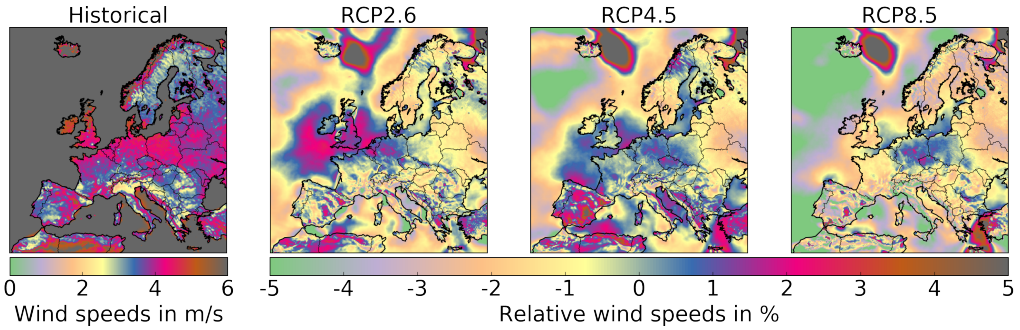

Figure 1.4: **Spatial distributions of the wind speed profiles**. These are presented as 20-year average values. The historical frame spans the years from 1986 to 2006 while the cluster of climate pathways (RCP2.6, RCP4.5 and RCP8.5) spans an end-century period from 2080 to 2100. The figures are based on the HIRHAM5 regional climate model [43] downscaling the ICHEC-EC-EARTH global climate model [44].

Shortwave irradiation

Figure 1.5 shows spatial distributions of the incoming shortwave radiation. The incoming radiation reduces naturally with increasing latitudes. The climate pathways show a clear pattern of changing incoming radiation as a function of the degree of climate change. From RCP2.6, RCP4.5 and RCP8.5 it is clear that

the radiation increases in South Europe while it is decreasing in the north. This is reasoned by an increasing cloud covering in the north with a decreasing trend in the south.

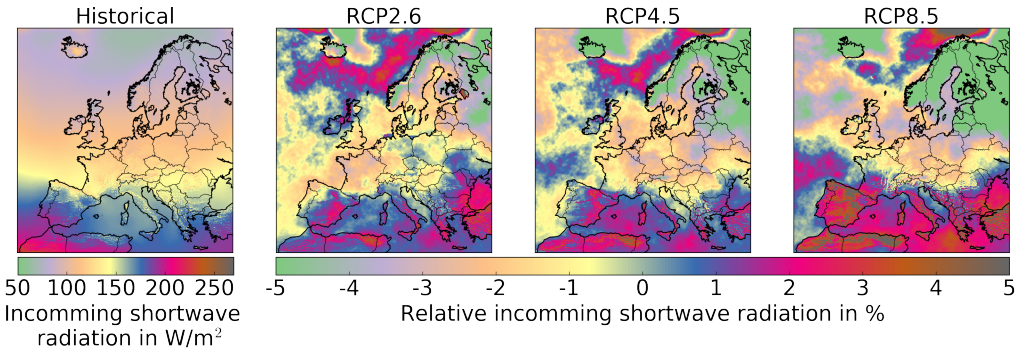

Figure 1.5: **Spatial distributions of the incomming shorwave radiation profiles**. These are presented as 20-year average values. The historical frame spans the years from 1986 to 2006 while the cluster of climate pathways (RCP2.6, RCP4.5 and RCP8.5) spans an end-century period from 2080 to 2100. The figures are based on the HIRHAM5 regional climate model [43] downscaling the ICHEC-EC-EARTH global climate model [44].

1.5 Introduction to relevant pre-projects

The bedrock of this project is built upon results from three well-established projects. These are described in the following.

Reconstructed Concentration Pathways, RCP

The first project showing its importance for this work is the development of the latest generation of climate projections by the Intergovernmental Panel on Climate Change [16], IPCC. IPCC is an organisation under the United Nations that is responsible for assessing the science related to climate change. In their Fifth Assessment Report, IPCC adopted four representative greenhouse gas concentration pathways, RCP, that describe possible outcomes of the climate for the 21st Century [15]. Integrated Assessment Models [45] have been used to develop the RCPs and include a diverse range of assumptions on socioeconomics, technology developments, biophysics etc. to project their consequences for the future climate system. The set of RCPs are defined by their total radiative forcing by 2100. RCP2.6 is a stringent mitigation pathway [46, 47, 48], which is a peak and decline scenario that reaches a radiative forcing level of 2.6 W/m^2 at 2100, as shown with green in Figure 1.6a. RCP2.6 is representative of keeping the global average temperature increase well below 2 °C above pre-industrial levels at 2100, as seen in panel d. This requires a peak in the CO_2-emission by the year of 2020 and eventually negative emission by the year 2080, as shown in panel b. The atmospheric concentration of CO_2 follows the curve topology of the radiative forcing, as shown in panel c. Next, IPCC adopts two intermediate scenarios, RCP4.5 [49, 50, 51, 52] and RCP6.0 [53, 54, 55], for which only RCP4.5 is considered in this project. Finally, IPCC adopt a scenario with increasing CO_2-emission throughout this century, RCP8.5 [56, 57], which is best known to the literature as the business as usual scenario. Figure 1.6 also shows the corresponding metrics of these pathways. Since the underlying logic of the pathways is broad and complex, a full description is avoided, but additional references have been assigned to each RCP for further reading.

Global Climate Modelling, GCM

The second project with an important role is the Coupled Model Intercomparison Project, CMIP, which is a framework of the World Climate Research Programme, WCRP, [58]. WCRPs Working Group on Coupled Modelling, WGCM,

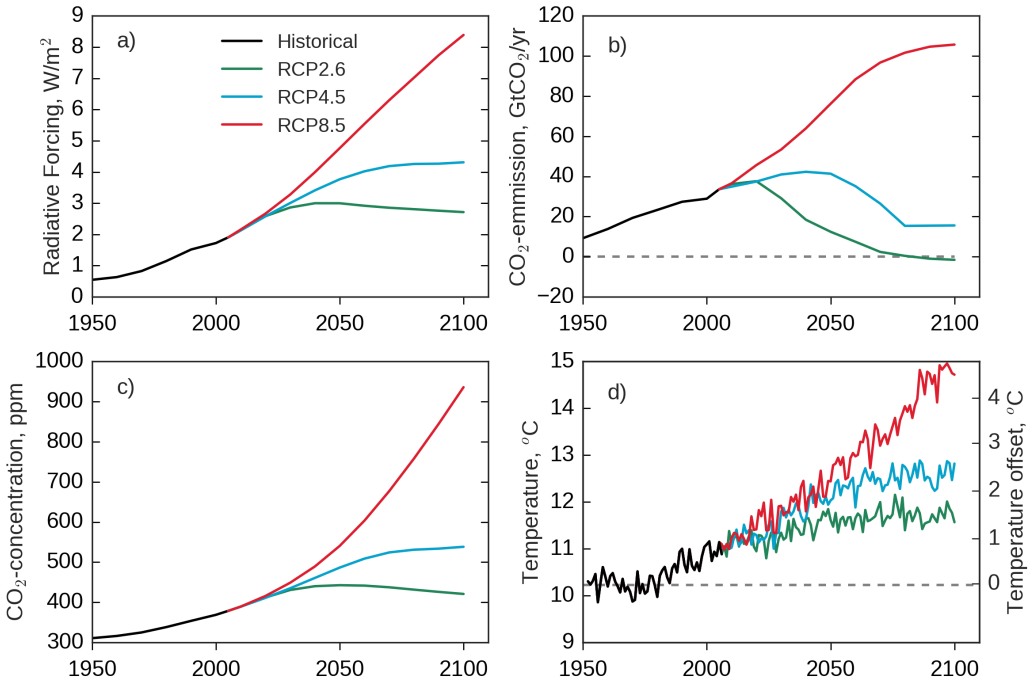

Figure 1.6: **Key metrics of the Reconstructed Concentration Pathways, RCP**. Panel a: Radiative forcing of the IPCC RCPs in W/m^2. Panel b: CO_2-emission of the IPCC RCPs in Gt CO_2 per year. Panel c: Atmospheric CO_2-concentrations of the IPCC RCPs in parts per million. Panel d: Temperature increase and offsets over Europe in the different IPCC RCPs in °C. The temperature profiles are computed from the HIRHAM5 regional climate model [43] downscaling the ICHEC-EC-EARTH global climate model [44].

along with the International Geosphere/Biosphere Programmes [59], IGBP, and the Integration and Modelling of the Earth System project [60], AIMES, designed a new set of climate model experiments. The outcome was a fifth phase of the Coupled Model Intercomparison Project, which is the most recent completed phase of global climate modelling [61]. The development of the CMIP5 project was influenced by climate modellers, climate scientists and the biogeochemistry community and resolves into a complex project organisation, see Figure 1 in [61].

For the GCMs to model climate change projections, they use information about emission of air pollutants and land use patterns from the RCPs. This process is shown as the first phase in Figure 1.2. Based on this information, the GCMs simulate the earth system and provide data on climate variables such as wind speeds, temperatures etc. GCMs are currently the most reliable tools, which include anthropogenic fingerprints and simulate their impact on the climate.

Global climate modelling results in weather data with, usually, monthly time scales and horizontal resolutions of hundreds of kilometres. The main reason for the coarse-grained resolution is the lack of computational power. With this resolution, the GCMs cannot capture local effects, which precludes them from accurately describing local weather variabilities. This provides a sincere limitation for research on regional scales. To allow for this, a downscaling of the GCMs have to take place. This leads to the next framework that is important for this project, which is described in the following section. For the rest of this section, the GCMs that were made available for this project are listed.

Five global climate models were made available from different climate institutes around Europe. These are listed here, but a more comprehensive description can be found in the supplementary information of the article described in Chapter 2 or in the attached citations. The following global climate models are considered: ICHEC-EC-Earth [44, 62], HadGEM2-ES [63, 64], MPI-ESM-LR [65], IPSL-CM5A-MR [66, 67] and CERFACS-CNRM-CM5 [68].

Coordinated Regional Climate Downscaling Experiment, CORDEX

The third project is the Coordinated Regional Climate Downscaling Experiment [69, 70], CORDEX, which is a framework of the WCRP. CORDEX holds the newest and the largest set of regional climate models, RCM, which supply the global climate modelling with, e.g., a higher resolution in space and time, which enables them to better represent local atmospheric processes and more complex landscapes and topographies [71]. In the most common downscaling technique, RCMs use large-scale atmospheric information supplied by the GCMs and feed these into the horizontal and vertical boundaries. This process is shown in the second step in Figure 1.2.

The CORDEX initiative results in highly granular climate affected weather data, which enables further research in various climate dependent fields. This is shown as the final red step in Figure 1.2. In this project, the focus is on the EURO-CORDEX domain [72], which is the European branch of the CORDEX initiative that covers the continent of Europe. Four regional climate models have been used in this research. These include HIRHAM5 [43], RCA4 [73, 74], RACMO22E [75] and CCLM4. A more comprehensive description can be found in the supplementary information of the article described in Chapter 2 or in the attached citations. The ensemble of regional and global climate models add up to nine climate models for this project. These are presented in Table 1.1.

The ability of the Global Climate Models (GCM) to accurately model the near surface air temperatures is receiving increasing attention. A recent study on the European domain shows negatively biased winter temperatures in the North for 33 CMIP5 GCMs [76] compared to ground observations from ECAD [77]. Positively biased summer temperatures are observed in the East and Central Europe. The GCM ensemble mean bias is approximately $-1°C \pm 9°C$ during winter months and $0.5°C \pm 6°C$ during summer months. Similar trends are found for the Northern Eurasia where the winter and summer periods show the largest biases [78]. Small improvements have been made since CMIP3 GCMs [79]. A full description of biases in climate models is provided in the Supplemental Information Section 7.1.

Table 1.1: Overview of the climate models along with the available pathways in this project.

GCMs	RCMs	Climate Pathways			
		Historical	RCP26	RCP45	RCP85
ICHEC-EC-EARTH	HIRHAM5	x	x	x	x
	RACMO22E	x		x	x
	RCA4	x	x	x	x
MOHC-HadGEM2-ES	RACMO22E	x	x	x	x
	RCA4	x	x	x	x
MPI-ESM-LR	CCLM-8-17	x		x	x
	RCA4	x	x	x	x
IPSL-CM5A-MR	RCA4	x		x	x
CERFACS-CNRM-CM5	RCA4	x		x	x

1.6 Structure

The remainder of this collection summarises a selection of four studies that were conducted during the full project period along with their associated supplemental information.

Chapter 2 is built around the research paper: "*21st century climate change impacts on key properties of a large-scale renewable-based electricity system*".

Chapters 3-5 describe my research related to the heating sector. Chapter 3 is built around the research paper: "*Estimating country-specific space heating threshold temperatures from national consumption data*".

Chapter 4 is built around the research paper: "*Impact of climate change on the cost-optimal mix of decentralised heat pump and gas boiler technologies in Europe*".

Chapter 5 is built around a research paper with the preliminary title: "*Techno-economic benefits of a fully coupled European electricity and heating system in a 21st century climate*".

Chapter 7 is the supplemental information for Chapter 2. In the former, the interested reader can find in-depth material on methods and extended results.

Chapter 8 is the supplemental information for Chapter 3. In the former, the interested reader can find plots of the gas and electricity data that were used in this study along with additional results.

Chapter 9 is the supplemental information for Chapter 4. In the former, the interested reader can find in-depth material on methods and extended results.

Part I

CHAPTER 2

21st century climate change impacts on key properties of a large-scale renewable-based electricity system

Article

This chapter is based on the research paper:
Kozarcanin, Smail; Liu, Hailiang; Andresen, Gorm Bruun (2019). *21st Century Climate Change Impacts on Key Properties of a Large-Scale Renewable-Based Electricity System*. Joule, 3(4), 992-1005.

Project Dissemination

The project has been published in the form of a peer-reviewed research article in Joule. An extended supplemental material has been published alongside the article for the interested reader. The wind and solar power potential and electricity consumption time series have been published in Mendeley. Several news magazines as, e.g., New Scientist, The Verge, Eurekalert and others have covered this study.

Author Contributions

S. Kozarcanin was responsible for managing and coordinating the research activities and performed the formal analysis and investigation. S. Kozarcanin wrote the original draft, visualised the data and performed the editing in the review process. H. Liu co-authored the chapter on electricity consumption in the supplemental information. Associate professor G. B. Andresen stands behind the original concept.

Highlights

- Climate change shows impacts on large-scale metrics of a European electricity system.
- Largest climate impacts are observed within fully wind-dominated electricity systems.
- 6 high-resolution CMIP5 GCMs under the forcing of three IPCC RCPs have been used.
- State-of-the-art wind and solar capacity factors and electricity demand data were used.

Summary

Falling prices and significant technology developments currently drive an increased weather-dependent electricity production from renewables. In light of the changing climate, it is relevant to investigate to what extent climate change directly impacts future highly weather-dependent electricity systems. Here, three IPCC CO_2 concentration pathways were used for the period 2006-2100 with six high-resolution climate experiments for the European domain. Climate data are used to calculate bias-adjusted 3-hourly time series of wind and solar generation and temperature-corrected demand time series for 30 European countries using a state-of-the-art methodology. Weather-driven electricity system analysis is then applied to compare five key metrics of highly renewable electricity systems. It is found that climate change changes the need for dispatchable electricity by up to 20%. The remaining key metrics, such as the benefit of transmission and storage as well as requirements for balancing capacity and reserves, change by up to 5%.

Context & and Scale

Globally, electricity production from wind and solar sources is increasing significantly. The increase is primarily driven by lower costs and by political efforts to mitigate climate change. Climate change, however, may radically change the weather that drives these sources of renewable energy. It is found that the impact of climate change on a future highly renewable European electricity system is up to 20% for a few key metrics when compared to corresponding numbers for a historical climate scenario. In most cases, however, the relative impact is

an order of magnitude smaller. The level of impact is, in general, smaller than corresponding differences from one weather year to another and also compared to differences between system designs, e.g., with different levels of international power transmission lines or different mixes of wind and solar generators.

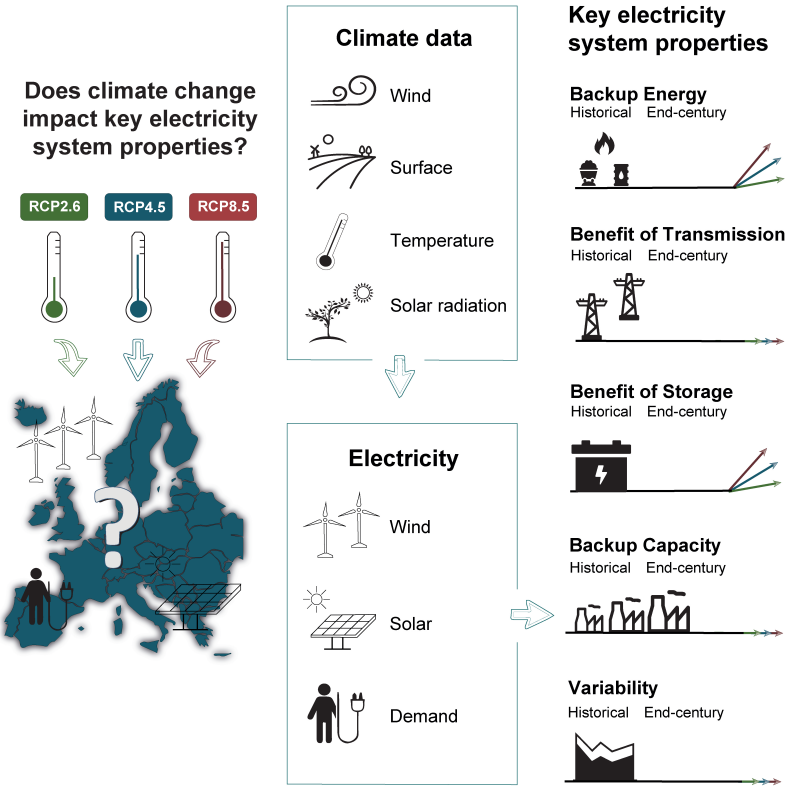

Figure 2.1: Wind and solar sources currently drive an increased weather-dependent electricity production because of decreasing costs and efforts to mitigate climate change. Unfortunately, some degree of climate change appears to be unavoidable. Different projections of climatic outcomes over the 21st century were used to assess how important key metrics of a highly renewable electricity system are affected by climate change.

2.1 Introduction

The global climate is currently undergoing vast changes, primarily due to anthropogenic emission of heat-trapping gases into the atmosphere [80]. As a consequence, the global average surface temperature has increased since the 1960s by approximately 0.2 °C per decade. A similar rate of temperature increase is projected to occur during the first half of the 21st century [81] and, at present, the changing climate is showing global impacts on natural and human systems. In this work, the focus is on the impacts of a changing climate on the dynamics of a future, highly renewable, large-scale electricity system for Europe.

Research on the impacts of climate change on large-scale electricity systems is in its infancy, and few studies have been performed in this field [82]. For an aggregated European energy system, outweighing demand-side impacts to the supply side have been found, based on the Prospective Outlook for the Long-term Energy System model (POLES) [83]. Because of global heating, the cooling demand increases while the heating demand decreases [83]. More specifically, a decreasing need for heating in central and northern Europe have been found based on the SRES A2, A1B, and B1 emission scenarios [84]. Southern Europe experiences a large increase in cooling demand, which in turn overcomes the decrease in heating demand [84]. This finding is in agreement with a study on Germany and Austria for the last quarter of the 21st century [85]. The spatial distribution of the heating and cooling needs are further reflected in increasing needs for electricity in southern Europe and decreasing needs in northern Europe [86]. Individual country studies on Norway [87], Finland [88], Slovenia [89], Austria [90], and Switzerland [91] agree upon the latter findings. The heating degree days have shown to decrease significantly, especially over Scandinavia and European Russia when using the representative concentration pathway scenarios (RCP) 4.5 and RCP8.5 [92]. For identical projections, the cooling degree days are increasing, especially over the Balkans and the Mediterranean region.

By using the SRES A1B emission scenario, negligible changes have been found in the wind power potential over the Baltic Sea and the surroundings [93, 94]. Similar results are found for Europe as a whole by using the RCP4.5 and RCP8.5 emission scenarios [95], for the UK [96], for Norway based on 10 climate experiments [87] and for Germany by using the RCP2.6 and RCP8.5 emission scenarios for the period 2031-2060 [97]. Moreover, increasing wind correlation lengths have been discovered along with increasing wind power generation in the same regions of Europe by using the RCP8.5 emission scenario [98]. A decreasing

wind power potential over the Mediterranean area have been found by using the SRES A1B and A2 emission scenarios [93, 99] along with decreasing correlation lengths [98]. For an aggregated EU27, a slight increase in the wind power production have been found until mid-century, based on the SRES A1B and E1 emission scenarios [83]. For a wind-dominated European energy system under the impact of the RCP8.5 emission scenario, increasing needs for conventional power and storage are found in most of the central, north, and Northwest areas [100], with a more homogeneous wind power generation [101] at the end of the 21st century. A decreasing solar power generation have been projected in the Scandinavian area with slight increases over southern Europe by using the RCP4.5 and RCP8.5 emission scenarios [102]. This corresponds with increased means of solar irradiation along with increased solar correlation length in large parts of southern Europe [98]. The opposite behaviour is observed for the northern parts of Europe [98]. For an aggregated EU27, an increasing amount of solar photovoltaic (PV) generation is found [83]. Based on 44 electricity scenarios for Europe, large penetrations of wind and solar power have been found to emit the least CO_2 within the ensemble of scenarios and, as a consequence, contribute the most to climate change mitigation [103].

A new addition to the existing literature emanates from the investigation of the key infrastructure metrics of a fully connected, highly renewable European electricity system by using the latest generation of climate projections provided by the Intergovernmental Panel on Climate Change (IPCC) [15]. The climate data used in this study originate from six combinations of four RCMs (regional climate models), downscaling three CMIP (coupled model inter-comparison project) phase 5 [61] GCMs (global climate models) under the forcing of IPCC RCPs. This study utilises only a subset of the GCMs that are available in the ensemble of CMIP5 GCMs. Former studies evaluate the climate model performance of capturing, e.g., storm track densities, temperatures, or precipitations, by using a large ensemble of GCMs and show acceptable agreements among a majority of the GCMs, including the ones adapted in this work [76, 104].

In order to represent a broad range of climate outcomes, three scenarios, RCP2.6 [46], RCP4.5 [49], and RCP8.5 [56], have been implemented into the global climate models. RCP2.6 is a climate projection that provides the necessary steps consistent with the goals of the 2015 Paris agreement, which aims at keeping long-term global temperature increases below 2 °C. In particular, there is an urgent need for both short and long-term action in reducing the CO_2-emission, as explained in detail in the Emission Gap Report 2017 [105]. RCP4.5 is highly influenced by high CO_2-emission cost policies, while RCP8.5 has no climate

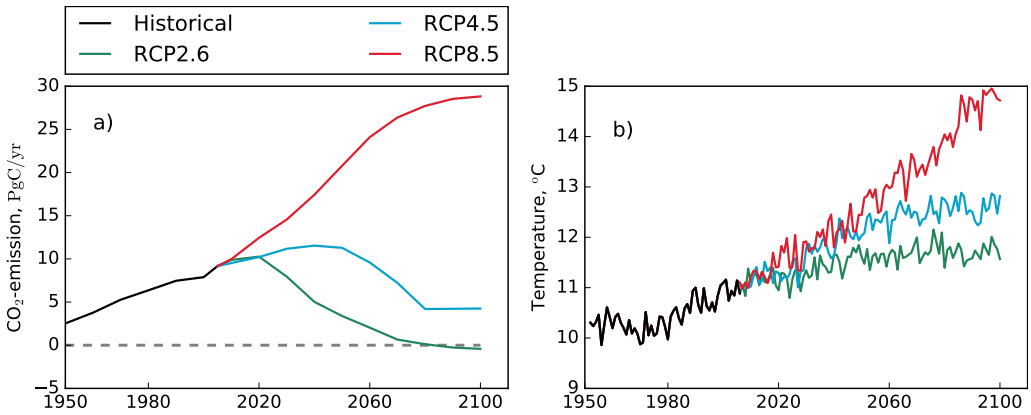

Figure 2.2: **RCP key metrics.** Panel a: CO_2 emission as a function of model year for the various projections of climate outcomes. Panel b: Average near surface temperature over Europe for the regional climate model HIRHAM5-EC-EARTH as a function of model year for identical pathways. Black, green, blue and red projections represent the historical, RCP2.6, RCP4.5 and RCP8.5 pathways.

policies implemented. The underlying assumptions of the pathways result in CO_2-emission as shown in Figure 2.2a. RCP2.6 and RCP4.5 show decreasing projections of CO_2-emission during the 21st century, while RCP8.5 leads to an increased projection that stagnates at the end of the century. For further information on the pathways, refer to Section 1.5. These projections are reflected in the European average temperature, e.g., the RCM HIRHAM5 [43], downscaling the global climate model ICHEC-EC-EARTH [44], from now on denoted as HIRHAM5-EC-EARTH, shown in Figure 2.2b. Based on the emission scenarios, 3-hourly data on climate variables with a 0.11° x 0.11° spatial resolution have been fostered on behalf of the EURO-CORDEX project [70, 106]. These data are used to calculate the time series of wind and solar power generation as well as climate-corrected electricity demand time series from which the final results are derived. Figures 2.3b-d exemplify the 2080-2100 model time span average near-surface temperature over Europe for the future emission scenarios based on the climate model HIRHAM5-EC-EARTH. Figure 2.3a represents the absolute temperature of the historical period 1986-2006. The most extreme temperature increases reach values of greater than 6 °C.

In the present study, the main source of error originates from the performance of the GCMs that provide the boundary conditions for the RCMs [107]. It is also known that biases might occur during the downscaling from GCM to RCM because of a change in the temporal resolution [108]. Various studies have en-

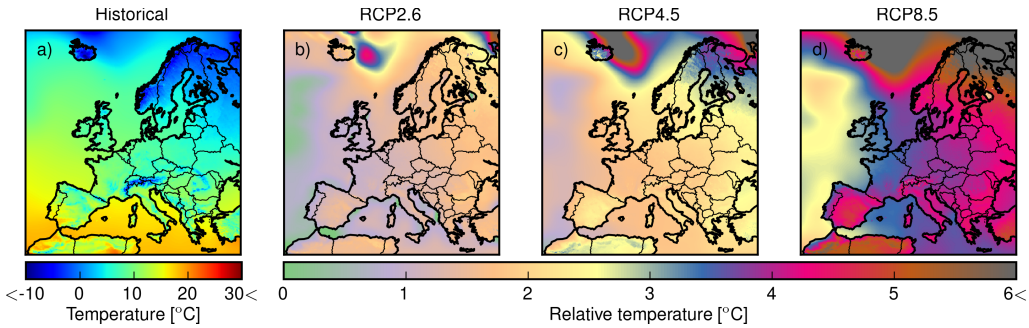

Figure 2.3: **20-Year Average Values of the Near-Surface Temperature**. The 2 meter surface temperature is based on the latest generation of IPCCs climate projections, RCPs, for the climate model HIRHAM5-EC-EARTH. Panel a: Average absolute temperature for a historical period ranging from 1986 to 2006 along with a unique color bar. Panels b-d: Temperature increase at the end of the century during 2080-2100 according to scenarios b: RCP2.6, c: RCP4.5, and d: RCP8.5 relative to the historical period, sharing one color bar.

gaged in tracking the evolution of CMIP5 GCMs and their predecessor CMIP3 GCMs by comparison to observed data, satellite data, or reanalysis. In Supplemental Information Section 7.1, biases in the wind speed, temperature, global radiation budget, and cloud cover projections are detailed as these are crucial for our study.

Although improvements are evident in the prediction of climate variables, there is still a need for more attention in this field. A detailed description of biases within the RCMs is omitted as the GCM errors propagate through the downscaling. However, the errors introduced in the downscaling should not be neglected.

In this work, the combined errors from GCMs and RCMs are partially taken into account by evaluating the results on data from six different combinations of GCM and RCM models. Relatively small deviations are observed between these independent datasets, which leads to the conclusion that model-specific biases are not a major source of error. However, biases that are similar for all model combinations cannot be excluded.

2.2 Experimental procedures

This section describes the electricity system modelling approach, data conversion and calibration procedures, and the electricity system key metrics. For a formal definition of these quantities, see Supplemental Information Section 7.2.

Weather-driven electricity system modelling

Weather-driven electricity system modelling was introduced for the first time in 2010 [109]. It is a type of top-down analysis that is particularly useful for isolating and understanding the impact of weather dynamics on an electricity system with a large penetration of variable sources, e.g., wind and solar. In addition to Europe, this type of modelling approach has previously been applied to model large-scale electricity systems in the US [110] and China [111]. But unlike most technology-rich bottom-up models, it is not well suited for determining, for example, the fuel mix of conventional dispatchable production units or to include political aspects of energy system design decisions. Further restrictions of identifying cost-optimised solutions or planning technology-based taxes, subsidies, or standards would emerge consequently. However, before addressing these issues, it is important to quantify how impactful climate change is on the important electricity system key metrics since changes in these will also change the boundary conditions for more detailed design problems. In this way, differences in key metrics for different future climate scenarios indicate that more than one end-point solution must be considered when planning the pathway from the present-day electricity system to a highly renewable system, as studied here. Similarity between the key metrics, on the other hand, indicates that the end-point solution is likely to be independent of the climate outcome. In this paper, a simplified large-scale European electricity system was implemented, of which the supply side consists solely of wind and solar power generation as well as a generic dispatchable power source, e.g., dammed hydro power or gas turbines. The demand side consists of national electricity demand. This type of electricity system aggregates the country-wise wind and solar power generation profiles into system-wise profiles. The same applies for the electricity consumption profiles. The effect of power transmission was introduced after the development of the original modelling framework [112, 113].

The effect of climate change enters the modelling via the weather-dependent wind and solar generation time series as well as the temperature-dependent part of the electricity demand. State-of-the-art methodology has been used to convert

raw wind and solar climate data into 3-hourly country-wise wind and solar capacity factor time series. For the wind capacity factors, an optimised Gaussian convolution is applied to the original wind power curve in the conversion process [36]. This has been shown to compensate well for the limited spatial and temporal resolution of the climate model data. 44 The solar conversion includes solar position geometry, calculation of direct, diffuse, and reflected irradiance on a tilted surface, a model for the photovoltaic panels that include temperature-dependent efficiency and inverter losses. In this case, an optimised Weibull curve is used to correct the model output. In both cases, the free model parameters are determined individually for each country and each climate model such that the relative entropy between the time series and an already bias-corrected reference, provided by Renewables.ninja [37, 39], is minimised for the historical period 1986-2006; see Supplemental Information Section 7.2. Hourly country-wise electricity consumption profiles have been provided by the European Network of Transmission System Operators for Electricity (ENTSO-e) [40]. These have been corrected for effects of heating and cooling by using the degree-day method; see Supplemental Information Section 7.2.

In the work presented here, wind and solar generator capacities have been scaled such that the EU-wide average generation over the historical period matches the average demand for electricity. This choice has previously been shown to describe the dynamics of a highly renewable electricity system well [109]. Because of the state of fluctuating weather events and electricity consumption behaviour, the generation and load profiles differ in most time steps. This difference is referred to as the generation-load mismatch, which is defined formally in Supplemental Information Section 7.2. For high renewable penetrations, the generation-load mismatch means that a surplus of the VRE will sometimes be available. This surplus may be either transported to other locations, used by new flexible consumption, stored for later use, or simply curtailed. At other times, VRE generation is lacking, and an ancillary system must balance the difference between supply and demand, e.g., by a combination of conventional power plants, dispatchable renewable electricity such as dammed hydropower, and electricity storage systems. Variations in instantaneous generation-load mismatch across the continent drive the transmission of renewable surplus to regions with a deficit. Furthermore, the maximum negative values of the mismatch describe the need for dispatchable power capacity, and variations in the mismatch describe the need for on-demand flexible reserves.

Key metrics

The above considerations give rise to five key metrics that describe a highly renewable electricity system. These are all described formally in Supplemental Information Section 7.2 and summarised here. The first key metric is the average dispatchable electricity. This metric quantifies the amount of energy delivered by dispatchable generators such as biomass, gas, or coal-fired power plants for a fixed wind and solar penetration. It is a good indicator of the utility value of the VREs, i.e., the amount of VRE that can directly cover the demand [114].

Generally, the useful electricity can be increased by means of geographical dispersion, e.g., by combining national systems to smooth out variations in both demand [115] and renewable generation [116]. This effect is measured with the second metric, which is defined as the absolute difference between balancing electricity required with and without unlimited transmission in a European power grid. This metric is called the absolute benefit of transmission, in contrast to the relative benefit of transmission [116]. In this paper, the required transmission capacities are not detailed but note that many other studies find that it is cost efficient to build enough to harvest most of this benefit [116, 117]. The third key metric provides a measure of the short-term benefit of storage. This key metric is defined as the absolute difference in the dispatchable electricity calculated with and without a 24-h average of the generation-load mismatch. This key metric is presented only for an unlimited transmission scenario, but a limited transmission scenario introduces no considerable differences for this metric. The reason is that the short-term benefit of storage primarily measures daily smoothing of the generation-load mismatch, whereas the benefit of transmission measures smoothing on the synoptic scale.

The three first metrics are concerned with the need for dispatchable electricity, which is closely related to, e.g., CO_2-emission, fuel consumption, and VRE curtailment. The fourth and fifth key metrics indicate what is required to stabilise an electricity system based on VREs and to maintain the security of supply. The fourth metric is measured by the maximum dispatchable capacity required during low VRE and high-demand periods. A number of studies show that VRE provides only very limited firm capacity [113]. However, firm capacity is not a good key metric, as it does not capture the correlation between VREs and demand. The fifth and final key metric is the 3-hourly short-term variability of the balancing time series. This measure was shown to be a good proxy for the need for on-demand reserve capacity [118]. The variability is largely caused by mesoscale turbulence patterns that have been shown to describe the spatio-temporal

characteristics of wind and solar power generation well [119]. This means that there is a direct relation between the 3-hourly values used here down to time scales of approximately 10 minutes, where small-scale turbulence changes the scaling.

The effects of many types of extreme weather conditions are implicitly captured by the key metrics that are calculated from the 3-hourly generation-load mismatch. For instance, an extended period of very hot weather in the RCP8.5 scenario would increase the use of dispatchable electricity and capacity as electricity demand for cooling would increase and the performance of solar panels would decrease compared to the historical scenario. Likewise, strong storms would cause wind turbines in areas with wind speeds exceeding, typically, 25 m/s to cut out abruptly, causing an increased short-term variability as well as increased needs for dispatchable electricity and capacity.

2.3 Results and discussions

End-of-century climate impacts

Initially, results based only on the climate model HIRHAM5-EC-EARTH are presented. Toward the end, the robustness of the results are presented by comparing similar findings from all six climate models. However, throughout the analyses all six climate models have been treated identically.

Except for a few cases, the different climate scenarios show a limited impact on the five key metrics of a highly renewable European electricity system. This is illustrated in Figure 2.4, where the key metrics are shown as a function of the wind-solar mix for the end of the century period 2080-2100, where all RCPs are most developed. A difference between average values for different climate scenarios is observed and is smaller than the corresponding annual variation (one sigma) in nearly all cases. In other words, annual variations within a given climate change scenario are larger than the difference between scenarios. This indicates that it is more important to incorporate existing inter-annual variation in long-term electricity system design decisions [120] compared to including the effect of climate change. Furthermore, a paired t-test reveals that, in most cases, the null hypothesis of no difference between the historical and the future 20-year mean values of the key metrics cannot be rejected (95% confidence). To some extent, this finding is related to the choice of generator capacities relative to demand because a decrease in demand happens to be balanced by an independent decrease in consumption. This is evident from Table 2.1, where it can be seen that both annual demand and wind and solar generation are decreasing slightly in the future scenarios. Furthermore, a t-test shows that, at a 95% significance level, the annual demand and annual solar capacity factors can both be considered different for the different climate change scenarios in nearly all cases. Test results for the wind capacity factors, on the other hand, are inconclusive. The magnitude of the effect of climate change on electricity demand is similar to the impact on the supply side. However, the inter-annual variability of the demand is smaller by about an order of magnitude, as can be seen in Table 2.1. The limited demand-side impact is primarily explained by the relatively low level of electrified heating and cooling in Europe. Should a larger share of the heating demand be electrified in the future, as suggested by several studies [121, 122, 123], then the effect of climate change on the demand side would increase accordingly [86, 124]. All test scores, mentioned above, are listed in the Supplemental Information Section 7.4.

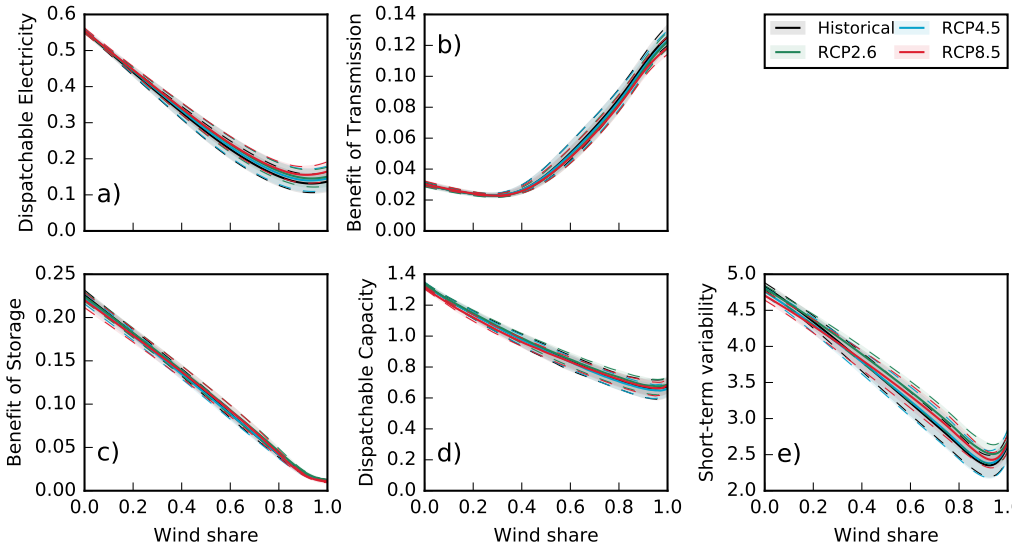

Figure 2.4: **Key Metrics as a Function of the Wind-Solar Mix for the Historical and End-of-Century Periods**. The historical period covers 1996-2006 (black), and end-of-century period covers 2080-2100 for the RCP2.6 (green), RCP4.5 (blue), and RCP8.5 (red) pathways. A wind-solar mix equal to zero represents a solar-only electricity system, and a wind-solar mix of one represents a wind-only electricity system. The averages of the annual values are indicated with fully drawn lines, and the corresponding ranges (one sigma) are shown with dashed lines. All key metrics are unitless, as described in the Experimental Procedures. Panel a: Dispatchable Electricity, b: Benefit of Transmission, c: Benefit of Storage, d: Dispatchable Capacity, e: Short-term variability.

The estimates of the difference between the climate change scenarios can also be compared to the difference between systems with different wind-solar mixes within a scenario. This comparison reveals to what extent it is more important to choose the right wind-solar mix independently of RCPs or whether it is most important to design the electricity system for the right RCP.

For the dispatchable electricity key metric, shown in Figure 2.4a, the largest difference between climate scenarios are found for a wind-solar mix of 1.0. The RCP8.5 scenario has an average value of 0.17, while the corresponding number for the historical period is 0.14, i.e., a difference of 0.03. The minimum dispatchable electricity is achieved for a wind-solar mix of about 90%. If the system is designed without storage, minimum surplus variable renewable electricity (VRE) occurs at the same mix, but if long-term storage is included, the minimum of surplus moves to a wind-solar mix of about 60% [114]. From Figure 2.4a, a corresponding change in the average dispatchable electricity of approximately 0.1 for all climate scenarios is found.

Table 2.1: **20-year average values of the normalised wind $\langle W \rangle_{20yr}$ and solar $\langle S \rangle_{20yr}$ power and electricity consumption $\langle L \rangle_{20yr}$ for the European domain.** One sigma standard deviations are shown after each value. All values have been normalised to the corresponding values calculated for the historical period.

	Historical	RCP2.6	RCP4.5	RCP8.5
$\langle W \rangle_{20yr}$	1.00 ± 0.03	0.98 ± 0.02	0.99 ± 0.04	0.96 ± 0.03
$\langle S \rangle_{20yr}$	1.00 ± 0.01	0.99 ± 0.02	0.98 ± 0.02	0.97 ± 0.03
$\langle L \rangle_{20yr}$	1.000 ± 0.005	0.995 ± 0.003	0.992 ± 0.005	0.986 ± 0.003

For each of the key metrics, the absolute value at a given wind-solar mix as well as, e.g., the location of minimum and maximum values, can be compared to the difference between climate scenarios.

For all climate scenarios, the dispatchable electricity peaks for a solar-dominated system at slightly more than half the electricity consumption. This is explained by the day-night pattern in which little dispatchable electricity is needed during the daytime and full dispatchable electricity is needed for the nighttime. On the other hand, the production of wind power during both day- and night time reduces the need for dispatchable electricity to about 15% of the annual demand. These findings are in agreement with earlier work based on historical data [114]. As stated above, the largest difference between climate scenarios occurs for wind-dominated systems, where the absolute value is also lowest. In this case, the dispatchable electricity may change by up to 20% as an effect of climate change. Such a change may have a significant impact on decisions depending on, e.g., fuel needs and levelised cost of electricity from both dispatchable sources and VREs.

The benefits of transmission, Figure 2.4b, and short-term storage, Figure 2.4c, exhibit opposite behaviours in the sense that the former grows with an increasing wind-solar mix and the latter declines. This is because both are highly dependent on the coupled spatial and temporal correlation lengths of the wind speeds and solar irradiance [125]. The high correlation lengths of the solar irradiance due to the systematic variability of the sun's position in the sky give rise to low transmission benefits and high short-term storage benefits. Because of the simultaneous production of PV power over large areas, minor needs for transmission are present for a dominant solar share, whereas the day-night cycle allows storage to cycle relatively often [126]. For a large wind share, on the other hand, the smaller wind-speed correlation length of approximately 600-1,000 km and the related synoptic time scale of about 1 week lead to increasing transmission ben-

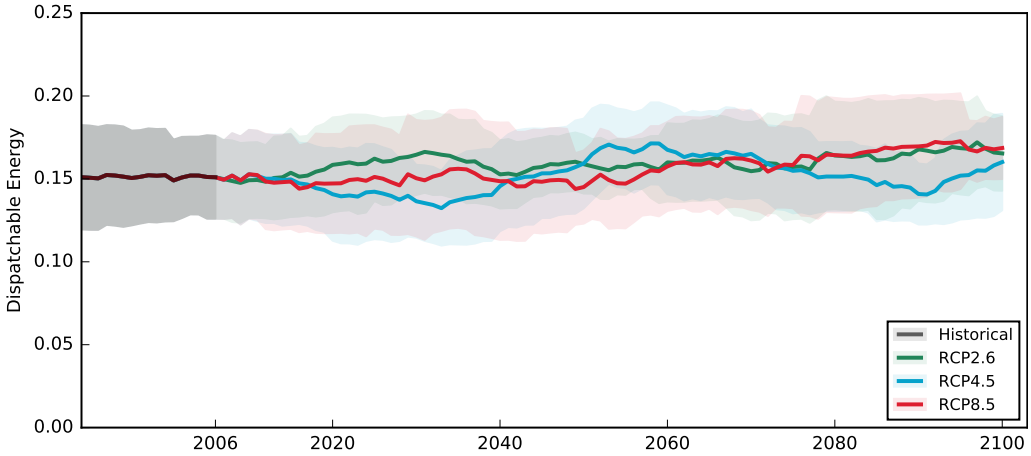

Figure 2.5: **Evolution of the dispatchable electricity as a function of model year for the climate model HIRHAM5-EC-EARTH.** The historical period covers 1996–2006 (black) and the future scenarios RCP2.6 (green), RCP4.5 (blue) and RCP8.5 (red) covers the years 2006–2100. The wind-solar mix is 0.8. The 20 year averages of the annual values are indicated with fully drawn lines, and the corresponding ranges of the one sigma standard deviation are shown with shaded areas.

efits and lower short-term storage utilisation. In both cases, the largest absolute difference between climate scenarios occurs where each of the metrics peak. As a result, the impact of climate change is limited to less than 5% here. This means that for a large-scale electricity system, major design decisions related to international transmission and storage are not strongly affected by climate change. At a finer spatial resolution, some changes in the spatio-temporal correlations are expected [100, 101].

The short-term variability, Figure 2.4e, shows higher values for low solar shares. This behaviour is due to stronger intra-day temporal variations in the solar irradiance compared to temporal variations in the wind speeds. This is further reflected in the dispatchable capacity, Figure 2.4d. In both cases, the maximum differences between climate scenarios are all limited to less than 3% of the corresponding absolute value. The dispatchable capacity describes the maximum power required to offset calms in weather-based generation, and the short-term variability is a proxy for the reserves required on standby to compensate intra-day weather variations. Climate change is often said to result in more erratic weather [127], but the key metrics show that for large-scale electricity networks, the size for both long-term and short-term reserves remains largely unchanged. This is likely due to the fact that extreme situations also occur in the 20-year historical period, albeit not as often.

Climate impacts during the century

A number of studies focus on the end of the century period alone. However, the evolution of the key metrics throughout the century was also explored. In the following, the focus will be on dispatchable electricity for a wind-solar mix of 0.8, shown in Figure 2.5. Similar results can be found for the other key metrics in the Supplemental Information Section 7.4. For this case, a gradual transition from the historical reference period toward the end of the century was not found. Instead, the trajectories of the RCPs change over time such that, e.g., the 20-year average values of each RCP cross the other trajectories multiple times. This means that the general conclusions about the relative importance of climate change on the electricity system, drawn above for the end of the century period, also hold for the transition, and it is not possible to regard specific numerical differences between RCPs as the product of a gradual evolution toward a stable climatic endpoint. Rather, the 20-year averages are not stable to an extent where they can be regarded as different between RCPs. A longer time window could be used instead. However, since the climate is changing over the course of the century, see Figure 2.2, long periods do not represent a stable climatic situation.

Ensemble of climate models

Above, results based on the HIRHAM5-EC-EARTH climate model were discussed. Now, the five other combinations of regional and global climate models included in the study are studied in order to establish to what extent the results are in agreement across the models. In general, identical numerical results for all models were not found despite the fact that all time series have been bias adjusted on the same historical period against the same reference. However, the overall findings remain, independently of the models. Figure 2.6 shows a comparison of the five electricity system key metrics for the different models in the historical period as well as in the end-of-century period for the RCPs. In most cases, the 20-year average values fall between the first and the third quartile of the annual variation, which means that the difference between individual RCMs is smaller than the annual difference within a given RCM. For the variability, this is not the case. The main reason for this is that the wind and solar time series are bias adjusted such that the distribution of instantaneous values matches the reference. However, the variability depends on the correlation between consecutive hours. This difference is not directly subject to correction, which means that models are likely to behave more differently on this parameter. Identical key metrics are also shown for the reanalysis Renewables.ninja [37, 39] time se-

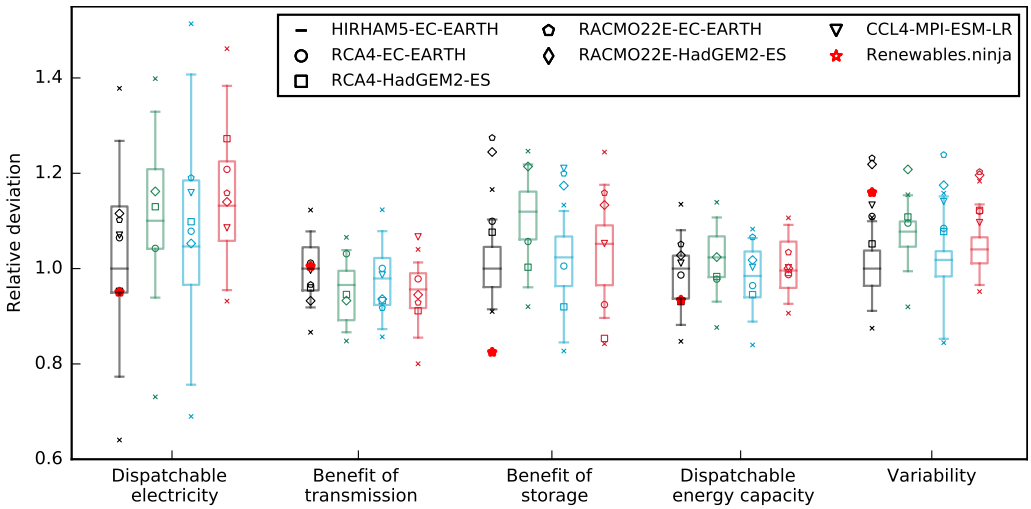

Figure 2.6: **Key metrics for six regional climate models from the EURO-CORDEX project.** These are compared for the historical period 1986-2006 (black) and end of the century 2080-2100 for the RCP2.6 (green), RCP4.5 (blue) and RCP8.5 (red) scenarios. Annual values for the HIRHAM5-EC-EARTH model are indicated as box plots. The 5% and 95% quantiles of each key metric are marked by "x". For the remaining models, only the median values of the annual means are shown. The red star shows the key metrics for the Renewables.ninja reanalysis time series. All key metrics are normalised to the median of the respective metric in the historical period of the HIRHAM5-EC-EARTH model.

ries as a red star. Here, conclusion similar to that of the climate models was observed. This reflects the adequacy of bias-corrected climate data in terms of use for power system analysis.

2.4 Conclusion

The different climate change scenarios show a modest impact on the key metrics that are representing the gross properties of a highly renewable European electricity system. On the supply side, both wind and solar power generation are affected in a way that generally reduces performance slightly as their average electricity output decreases and their variability increases with an increasing effect of climate change. Consequently, the most extreme impacts of climate change are observed within fully wind-dominated electricity systems. In this regime, the dispatchable electricity changes up to 20% of the historical values. Changes in the benefit of transmission and benefit of storage stay below 5% of historical values. Changes in the short-term variability stay below 3%.

An important consequence of these findings is that for most of the key metrics that are studied in this work, it is not required to take into account the effect of climate change on the VREs wind and solar when designing gross properties of future highly renewable electricity systems. However, other properties, e.g., siting of renewable generators and selection of conventional generators, are not studied in this work, and the impact of climate change remains inconclusive. The need for dispatchable electricity is influenced by climate change, in some cases, depending on the VRE composition in the electricity system.

In designing a future highly renewable electricity system that is robust against climate change, it is most important to focus on reaching a mixture of wind and solar power generation that minimises the need for dispatchable electricity as the effect of climate change simulated by typical GCMs has a modest impact on the gross design properties of future highly renewable electricity systems. This suggests that, to first order, the gross character of highly renewable power system design solutions is not strongly affected by differences in climate produced by the current generation of GCMs under different IPCC RCP scenarios. Further investigations, however, are required to understand the quality of GCM representation of climate change in key meteorological properties and their impact on power system design in more sophisticated modelling frameworks.

This modelling approach is easily adaptable to model large-scale features of highly renewable electricity systems in other parts of the world. Should a stronger sector coupling, in particular between the heating, cooling, and electricity sectors, become a reality, the demand-side impact of climate change would increase beyond what has been discussed in this study.

This study was published by using six independent climate models, but three more models were added to the ensemble at a later stage and the study was re-evaluated. Equivalent to Figure 5 in the main article, I present a new figure, Figure 2.7, which shows equivalent results, but now with nine climate models. This lead to an identical conclusion as for the main article and therefore strengthening the initial results.

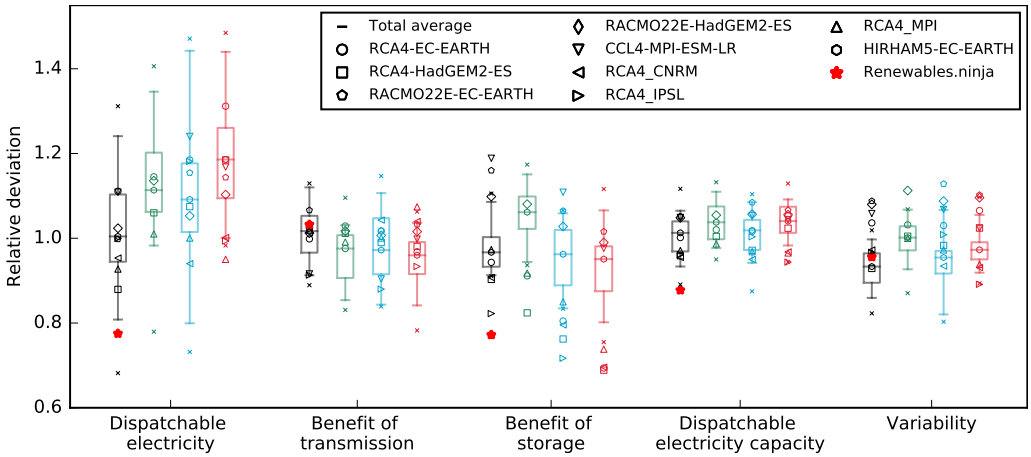

Figure 2.7: **Impact of climate change on key metrics that describe a highly renewable electricity system**. This figure is an expansion of Figure 5 in the main article by adding three more climate models. "The key metrics are compared for the historical period 1986-2006 (black) and end-of-century 2080-2100 for the RCP2.6 (green), RCP4.5 (blue), and RCP8.5 (red) scenarios. Annual values for the HIRHAM5-EC-EARTH model are indicated as boxplots. The 5% and 95% quantiles of each key metric are marked with an 'x'. For the remaining models, only the median values of the annual means are shown. The red star shows the key metrics for the Renewables.ninja reanalysis time series. All key metrics are normalised to the median of the respective metric in the historical period of the HIRHAM5-EC-EARTH model" [Verbatim from the caption of Figure 5 in the main article]. This figure was presented at the 5th international conference on smart energy systems.

Acknowledgement

The authors wish to express their gratitude to O.B. Christensen and F. Boberg from the Danish Meteorological Institute for their contribution to understanding the climate outcomes, for proofreading the final manuscript, and for supplying data from the regional climate model HIRHAM5. G. Nikulin from the Swedish Meteorological and Hydrological Institute is thanked for supplying data from the regional climate model RCA4. E. van Meijgaard from the Royal Netherlands Meteorological Institute is thanked for his thorough reading of the final manuscript on climate information and for supplying data from the regional climate model RACMO22E. P. Lenzen from the German Climate Computing Center is thanked for supplying data from the regional climate model CCLM4. Parts of the EURO-CORDEX climate data have been acquired via ESGF data nodes. Thanks to M. Victoria for a thorough proof reading. Thanks to Dr. I. Staffell for fruitful discussions. Thanks to Professor M. Greiner for fruitful discussions. Sincere thanks to M. Zvonic for providing valuable graphical inputs to the graphical abstract. Thanks to M.S. Hansen for her diligent proofreading of this paper. Thanks to H. Søndergaard for giving graphical inputs to supplemental figures. Finally, thanks to Aarhus University Research Foundation (AUFF) for funding S.K. with funding number AUFF-E-2015-FLS-7-26. H.L. acknowledges support from China Scholarship Council with grant number 201607940005 and Idella Foundation Denmark with grant number 29392. G.B.A. was funded by the RE-INVEST project, which is supported by the Innovation Fund Denmark under grant number 6154-00022B.

Author Contributions

Original: G.B.A. developed the original concept, supervised the project, and contributed to the writing. S.K. administrated the project, performed the scientific investigation, wrote the majority of the paper, including the Supplemental Information (apart from Chapter 4), and performed data validation and visualisation. H.L. wrote Chapter 4 in the Supplemental Information and provided data on electricity consumption.

Revised: G.B.A. and S.K. contributed equally to the revision and editing processes. S.K. performed all further analysis and visualisation of data. H.L. revised Chapter 4 of the Supplemental Information.

Declaration of Interest

The authors declare no competing interests.

Article History

Received: October 29, 2018
Revised: December 11, 2018
Accepted: January 30, 2019
Published: March 6, 2019

Part II

CHAPTER 3

Estimating country-specific space heating threshold temperatures from national consumption data

Article

This chapter is based on the research paper:
Kozarcanin, Smail; Andresen, Gorm Bruun; Staffell, Iain (2019). *Estimating country-specific space heating threshold temperatures from national gas and electricity consumption data*. Energy and Buildings, 199, 368-380.

Project Dissemination

The project has been published in Energy & Buildings. It has been presented at the Imperial College Centre for Energy Policy and Technology (ICEPT) book club and at several other conferences.

Author Contributions

S. Kozarcanin was responsible for managing and coordinating the research activities and performed the formal analysis and investigation. S. Kozarcanin wrote the original draft, visualised the data and performed the editing in the review process. Associate professor G. B. Andresen, Dr. I. Staffell and S. Kozarcanin developed the original concept. Associate professor G. B. Andresen and Dr. I. Staffell supervised the project.

Highlights

- National heat demand must be modelled since granular data are not widely available.
- This can be modelled with heating degree-days, but comfort temperatures must be known.
- Heating threshold temperatures range from 10-19 °C among the European countries.
- The results corresponds well to existing studies and national laws for nine countries.
- The methodology proves to be robust against daily, weekly or monthly data.

Summary

Space heating in buildings is becoming a key element of sector-coupled energy system research. Data availability limits efforts to model the buildings sector, because heat consumption is not directly metered in most countries. Space heating is often related to weather through the proxy of heating degree-days using a specific heating threshold temperature, but methods vary between studies. This study estimates country-specific heating threshold temperatures using widely and publicly available consumption and weather data. This allows for national climate and culture-specific human behaviour to be captured in energy systems modelling. National electricity and gas consumption data are related to degree-days through linear models, and Akaikes Information Criteria is used to define the summer season in each country, when space heating is not required. It is found that the heating threshold temperatures computed using daily, weekly and monthly aggregated consumption data are statistically indifferent. In general, threshold temperatures for gas heating centre around 15.0 ± 1.7 °C (daily averaged temperature), while heating by electricity averages to 13.4 ± 2.4 °C. No evidence of space heating during June, July and August is found, even if heating degree-days are present.

3.1 Introduction

Two thirds of the energy consumed in north European homes is for space heating, compared to just around a third in the US and China [128, 129, 130]. In 2015, the European heating sector accounted for more than 50% of the final energy demand of 6110 TWh/year [41]. Together, the production of electricity and heat accounted for approximately 30% of total CO_2-emission, with heat production accounting for more than half of this share [131]. Decarbonising the energy sector and space heating in particular, is therefore central in limiting global warming. Former studies have shown that the combined impact of climate change on weather-dependent electricity generation and demand is negligible [132, 133]. It is further shown that most key properties of large-scale renewable-based electricity system are robust against climate change [132]. The electricity sector is therefore already being decarbonised, most efficiently by increasing the share of renewables. However, heat does not have the same rate of technology innovation, clean options are not reducing rapidly in cost [29, 134], and so progress is very slow [30]. Natural gas, fuel oil and coal-fired boilers are the main source of heat production for the majority of European countries [135], and relatively few countries (primarily the Nordic countries) have a significant share of lower-carbon options.

The decentralised nature of heating means that data on consumption are not readily available. Unlike electricity, heat does not need to be monitored at high time-resolution to maintain system stability, and the prohibitive cost of heat meters means they are not becoming widespread, as are electric smart meters. This lack of data is a key gap for energy systems modellers, as the difficulty of decarbonising heat, and possible synergies between flexible heating load and intermittent renewable generation rise up the research agenda [136].

This research seeks to support future studies on energy system research and climate change mitigation by proposing a new framework for improving the accuracy and ease with which country-wise energy consumption for space heating can be estimated based on underlying weather data. The focus lays on space heat demand (as opposed to water heating and cooking), as space heating is the majority of final energy demand, and is the one, which depends on external conditions such as weather. The theory of heating degree-days is frequently used in the literature as a best proxy for estimating the space heating requirements [111, 137, 138]. Such an analysis can be empirically rigorous, relying on historic temperature data. However, it also relies critically on the threshold temperature below which heating is required, and this is often based on generic approxima-

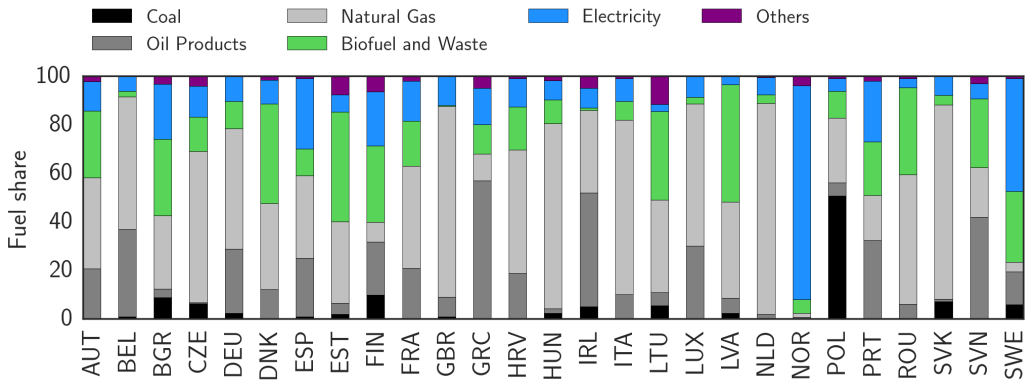

Figure 3.1: **Fuel shares of the final energy demand for the countries included in this study.** The plot is based on data compiled from [31, 141, 142]. Switzerland (CHE), Bosnia & Herzegovina (BIH) and Serbia (SRB) are excluded due to missing data. Countries are referred to by their three-letter ISO codes.

tions, which appear to have no empirical basis [139, 140]. This threshold will influence the temporal distribution of the heating degree-days.

Through careful investigation of the temporal characteristics of space heat demand and their correlation to weather data, this result allows for a new understanding of the energy demand for space heating. Therefore, the novelty of this research is to present a new state-of-the-art method that is based on the combined effect of using gas and electricity demand profiles along with weather based data for estimating the country-wise unique heating threshold temperatures along with determining the heating seasons. Alongside the newly proposed method, new country-wise heating threshold temperatures and heating seasons for a majority of the European countries were calculated and presented. These results are, to the best of our knowledge, the first to be derived empirically from historic data, giving a methodology that can be replicated globally. The threshold temperatures are then used to allocate the temporal distribution of the heating degree-days. For the purpose of this study, only the major fuel source used by a country is necessary, which is either gas or electricity with a few exceptions, as seen in Figure 3.1. In this work, a region is defined to be a country of Europe, but the method is designed to work for regions of arbitrary size as, e.g., cities. Other heating sources as, e.g., oil, coal or biomass, or direct heat consumption are as well straight forward applicable to this method. The method can also be used to calculate the cooling threshold temperatures for regions of interest.

In the literature, studies most commonly assume an identical threshold temperature when estimating the heat demand for multiple countries. Heat Roadmap Europe [41] adapts results from Eurostat [139], where the heating threshold temperature is defined as 15 °C. Stratego on the other hand uses 16 °C for five EU countries [143]. Odyssee uses 18 °C [144]. IEA uses 65 °F = 18.3333 °C [140]. Stratego defines, furthermore, heating seasons differently for the five nations while Odyssee defines a common heating season from October to April for all nations.

A considerable amount of literature has been published on estimating the energy consumption for space heating, using a diverse range of methods. Among these, a machine learning technique have been used for time ahead energy demand prediction for building heating systems [145]. A novel approach for which RGB video cameras are used as sensors for measuring personalised thermoregulation states, which can be used as indicators of thermal comfort [146]. A hidden Markov model (HMM) based learning method along with infrared thermography of the human face have been used in an attempt to capture personal thermal comfort [147]. A D-vine copula method have been used to capture the building heating needs with historical data on German household heating consumption and the respective building parameters [148]. A Modelica library was introduced in an attempt to build a control system of building energy systems [149]. Principal component and cluster analysis have also been used to create an energy classification tool in an attempt to assess the energy savings in different buildings [150]. Several studies have also explored the use of weather-based data for estimating heat or gas demand profiles, which is a well-recognised practice dating back several decades [151, 152]. It has been applied to multiple case studies for gas demand estimation [153, 154] or for heat demand estimation [137].

Two primary data sources are adapted to make this study possible: 1. temperature profiles from a global reanalysis weather model, and 2. data on the national gross consumption of electricity and gas for each country. The choice of data is first of all reflected by the amount of gas and electricity, 43% and 12%, respectively, of the final energy demand that is used for heating purposes for the EU [41]. Secondly, the availability of granular data on the consumption makes this study possible. Few of the European countries cover the majority of their heat demand by other fuels such as coal or oil products, as shown in Figure 3.1. For these fuels, granular data is not available. Further restrictions are introduced by the gas consumption profiles, as these are only available for all countries with a

monthly resolution and not separated into heating and non-heating sub sectors. Therefore, as a best proxy for the gas consumed in space heating processes the difference in the total gas consumption and gas consumed for electricity generation is explored. Gas consumed for power generation is significant, because gas prices vary from summer to winter relative to coal, and electricity demand increases in winter. Process heating is to a high degree weather independent and thereby not significant for the approximation. Hot water demand and cooking are as well weather independent and so insignificant for this study. Electricity consumption profiles, on the other hand, are typically available with hourly resolution at country level.

Initially, the methods section is presented. Here, the theory of degree-days is introduced followed by a model for space heating along with a method to estimate the national-wise heating threshold temperatures. Next, the Akaike's Information Criteria is presented and used to determine the summer season for each nation. Finally, a procedure is presented for the bias adjustment of the temperature data. This section is followed by a description of the energy data that is used in this work. Towards the end, the results and discussions section is presented. The paper ends with the conclusions and the bibliography. Additional information is available in the Supplemental Information Section 8.

3.2 Experimental procedures

The degree-day method

The demand for space heating can be related to the outside air temperatures by means of the heating degree-day method [155, 156], as explained in the following text.

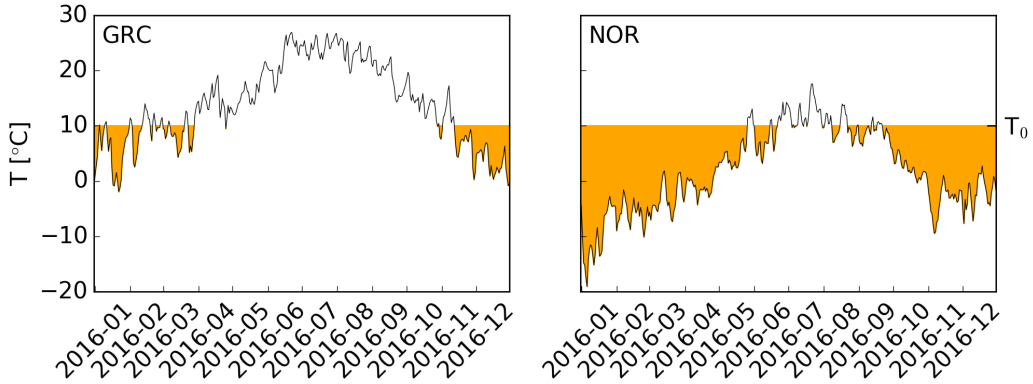

Figure 3.2: **Daily averaged temperatures for Greece and Norway in 2016.** The yellow filled area represents the amount of heating degree-days for a heating threshold temperature of 10°C.

Heating degree-days, HDD, are calculated as the integral of the positive difference between a threshold temperature, T_0, and the daily average outside temperature, T, as illustrated in Figure 3.2 for Norway and Greece. It is clear that Norway exhibits more heating degree-days due to its high latitudes, where temperatures are lower during the year. Greece, on the other hand, has longer summer periods with no heating degree-days.

The accumulated heating degree-days, $\mathrm{HDD}_{\Delta,x}$, over a time period, Δ, (e.g. a single day, a week or a month) and for a grid location, x, are related to the threshold temperature as:

$$\mathrm{HDD}_{\Delta,x} = \int_{\Delta} (T_{0,x} - T_x(t))_+ \, \mathrm{d}t$$

It is assumed that a single threshold temperature, $T_{0,x}$, is used for all grid locations in the set of grid locations, X, within a country. The choice of $T_{0,X}$ is not unique and can be chosen according to the region or study [156]. $T_x(t)$ denotes the time dependent bias adjusted temperature profile at grid location, x.

The procedure for the bias adjustment is detailed in Section 3.2. $(T_{0,x} - T_x(t))_+$ is defined positive or zero as:

$$(T_{0,x} - T_x(t))_+ = \begin{cases} T_{0,x} - T_x(t) & \text{if} \quad T_{0,x} > T_x(t) \\ 0 & \text{if} \quad T_{0,x} \leq T_x(t) \end{cases}$$

It is assumed that all individuals have an identical desire for space heating, and so the heat demand is proportional to the population density. The national population-weighted heating degree-days, $\mathrm{HDD}_{\Delta,X}$, are then calculated as:

$$\mathrm{HDD}_{\Delta,X} = \frac{1}{p_X} \sum_{x \in X} p_x \cdot \mathrm{HDD}_{\Delta,x}$$

where p_x and p_X denote the gridded and total population of a country, respectively.

Space heat modelling

The total heat demand, L^{heat}, is the sum of the demand for space heating, $L^{\text{space heat}}$, and hot water use, $L^{\text{hot water}}$:

$$L^{\text{heat}} = L^{\text{space heat}} + L^{\text{hot water}}$$

Hot water consumption is generally constant throughout the year [157], and so assumed to be independent of the ambient temperature. Therefore, it is not treated further in this paper. $L^{\text{space heat}}$, on the other hand, is assumed to be linearly dependent on the heating degree-days. In the literature, the energy demand for space heating is generally considered to be proportional to the heating degree-days [111, 138]. For a country and a time period, it takes the form:

$$L_{\Delta,X}^{\text{space heat}} = p_X \cdot L_{0,X}^{\text{space heat}} \cdot \mathrm{HDD}_{\Delta,X} \cdot \Theta_X \tag{3.1}$$

where, $L_{0,X}^{\text{space heat}}$ is a constant equal to the average space heating demand per capita per degree-day in a country X. $\Theta_X \in [0,1]$ is a binary indicator function that defines the heating season. $\Theta_X = 1$ represents winter months where space heating is required. Summer months are represented as $\Theta_X = 0$, for which space heating is not required.

In the following section a method is presented that can be used to determine the country-specific heating threshold temperature, $T_{0,X}$, and a method to determine the country-specific heating season, Θ_X.

Threshold temperatures for space heating

Ideally, the heating threshold temperature should be determined by comparing the heating degree-days directly to a corresponding time series of the heat demand. Since heat demand data is not widely available, except for cities with well monitored district heating networks [158], the following analysis is based on country aggregated gas consumption data, L_X^{gas}, or electricity consumption data, L_X^{el}. This method can also be applied to actual heat demand data. Data on gas and electricity consumption is available for all European countries, as described in Section 3.2, as well as many other countries. An example of gas and electricity consumption along with monthly aggregated heating degree-days for France is shown in Figure 3.3.

Gas and electricity are typically converted using boilers, resistance heaters or heat pumps, which operate with comparable efficiency over the year (given that most heat pumps in Europe are ground source rather than air source) [29]. Referring to Equation 3.1, this motivates the following model for the gas or electricity consumption as a function of heating degree-days:

$$\hat{y}_{X,\Delta}(t;T_{0,X}) = \beta_{0,X} \cdot \mathrm{HDD}_{X,\Delta}(t;T_{0,X}) + \beta_{1,X} \tag{3.2}$$

where $\hat{y}_{X,\Delta}(t;T_{0,X})$ is the modelled consumption for gas or electricity, summed over a period, Δ, and evaluated at time, t. $\beta_{0,X}$ and $\beta_{1,X}$ are model parameters that are assumed to be independent of both time and temperature. $\beta_{1,X}$ defines the consumption of gas or electricity that cover all domestic energy demand apart from space heating. $\beta_{0,X}$ defines the consumption of gas and electricity that is used for space heating alone in units of Watt-hours (Wh) per heating degree-day. This parameter is dependent on the culture-specific requirements for thermal comfort and on the thermal insulation of buildings. It can therefore be viewed as a thermal performance factor of the building envelope. Finally, only $\mathrm{HDD}_{X,\Delta}$ is assumed to depend on T_0. Note that this relation only applies in the case of $\Theta_X = 1$ (winter months).

The model parameters, $\beta_{0,X}$ and $\beta_{1,X}$, as well as the best choice of $T_{0,X}$ for a country are determined by minimising the root mean square of the errors be-

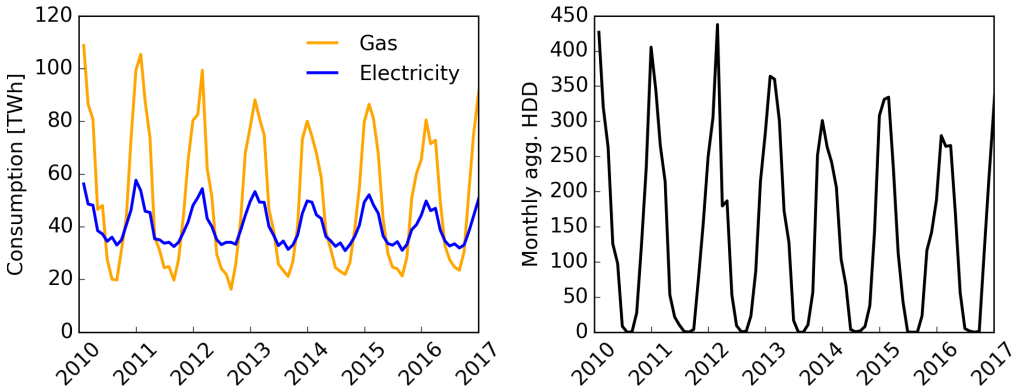

Figure 3.3: **Gas and electricity consumption and heating degree-days**. Monthly aggregated gas consumption (orange), electricity consumption (blue) and heating degree-days (black) for France during 2010–2017. The heating degree-days are calculated by using a space heating threshold temperature of 15 °C.

tween the modelled consumption, $\hat{y}_{X,\Delta}$, of gas or electricity and the corresponding measured consumption, $y_{X,\Delta}$ as:

$$\min_{T_{0,X},\beta_{0,X},\beta_{1,X}} \quad RMSE = \sqrt{\frac{1}{n}\sum_{t}\left(\hat{y}_{X,\Delta}(t;T_{0,X}) - y_{X,\Delta}(t)\right)^2}$$
$$\text{s.t.} \quad 5 \leq T_{0,X} \leq 25$$

where n is the sample size. In the following analysis, independent values for $T_{0,X}$ are calculated for each year of data, and then a median is taken to calculate a single value along with the 25th to 75th percentile significance range. The optimal values of $\beta_{0,X}$ and $\beta_{1,X}$ relate to the energy mix and population of a country. These are not discussed further in this study.

Heating seasons

During summer months when space heating is turned off, both the gas and electricity demand is assumed to be independent of the heating degree-days. A constant summer demand for a country, $\beta_{1,X}$, is then the simplest model that describes this relationship. Thus, Equation 3.2 is extended in the following way:

Winter model:

$$\hat{y}_{X,\Delta}(t;T_{0,X}) = \beta_{0,X} \cdot HDD_{X,\Delta}(t;T_{0,X}) + \beta_{1,X}$$

Summer model:

$$\hat{y}_{X,\Delta}(t) = \beta_{1,X}$$

To make a self-consistent determination of the model parameters, an initial guess is undertaken in which the three warmest months: June, July and August are used to determine the single free parameter, $\beta_{1,X}$, of the summer model and November-March the resulting winter model free parameters, $T_{0,X}$ and $\beta_{0,X}$. Then, all months are classified by using the newly acquired heating threshold temperature, $T_{0,X}$, and Akaike's Information Criterion (AIC), as described below. The model parameters are then recalculated by using the new classification for the winter and summer months. This process may be repeated until model parameters and classification reach convergence, which usually happened after a single repetition.

The Akaike's Information Criterion, AIC [159] is a well-recognised procedure for model selection, which takes both descriptive accuracy and parsimony into account. The objective of the AIC model selection is to quantify the information lost when the probability distribution associated with a model is used to represent the probability distribution of the data. The classification is then performed by choosing the model with the lowest expected information loss, and, thus, the lowest AIC value [159]. The AIC for a model m is defined as:

$$\mathrm{AIC}_{m,X} = -2\log(L^{\max}_{m,X}) + 2F_m + \frac{2F_m(F_m+1)}{n-F_m-1} \tag{3.3}$$

$L^{\max}_{m,X}$ represents the maximum likelihood value for a model and country, while F_m represents the degrees of freedom for a model. n_m represents the amount of data points for a model. $L_{m,X}$ is shown in Equation 3.4. $\sigma^2_{m,X}$ can be estimated by its maximum likelihood estimator $\hat{\sigma}^2_{m,X}$. A maximisation of $L_{m,X}$ rewards accuracy, leading to lower AIC values while more free parameters penalises the lack of parsimony and leads to higher AIC values. The third term in Equation 3.3 is a modification [160], which is recommended if $\frac{n_m}{F_m} < 40$ [161].

$$L_{m,X} = \left(2\pi\sigma^2_{m,X}\right)^{-\frac{n}{2}} \exp^{-\frac{1}{2\sigma^2_{m,X}}\sum_t\left(\hat{y}_{m,X,\Delta}(t)-y_{X,\Delta}(t)\right)^2} \tag{3.4}$$

Table 3.1: **AIC scores for the summer and winter model classifications for heating by gas in Hungary**. Each score is followed by the associated weight of evidence in parentheses.

HUN	Jan	Feb	Mar	Apr	May	Jun
Winter:	52.04 (1.0)	47.82 (1.0)	45.35 (1.0)	41.89 (1.0)	36.08 (0.43)	34.21 (0.02)
Summer:	82.58 (0.0)	78.39 (0.0)	72.53 (0.0)	56.54 (0.0)	35.54 (0.57)	26.72 (0.98)
	Jul	Aug	Sep	Oct	Nov	Dec
Winter:	34.37 (0.02)	31.45 (0.01)	39.36 (0.06)	41.18 (1.0)	43.08 (1.0)	47.08 (1.0)
Summer:	26.64 (0.98)	22.90 (0.99)	33.97 (0.94)	62.14 (0.0)	71.46 (0.0)	79.47 (0.0)

It is also important to address the weight of evidence of choosing the model with the lowest AIC. The Akaike weight of evidence, $w_{m,X}(\mathrm{AIC})$, [161] is defined as:

$$w_{m,X}\left(\mathrm{AIC}_{m,X}\right) = \frac{\exp^{-\frac{1}{2}\Delta_{m,X}\mathrm{AIC}}}{\sum_{m=1}^{M}\exp^{-\frac{1}{2}\Delta_{m,X}\mathrm{AIC}}}$$

where $\sum_{m,X} w_{m,X}\left(\mathrm{AIC}_{m,X}\right) = 1$. $\Delta_{m,X}\mathrm{AIC} = \mathrm{AIC}_{m,X} - \min\left(\mathrm{AIC}_{M,X}\right)$ and M denotes the ensemble of possible models.

In general, a preferred model is accepted if the ratio of the weights of evidence exceeds 2 [162], alternatively, an ensemble average of models is recommended. In this work, the AICs are respected regardless of the evidence ratio but in cases of a low evidence ratio, extra attention is paid to the classification. These issues arise mostly in spring and autumn, where the outdoor temperatures vary significantly.

Figure 3.4 exemplifies the method, described above, for the case of using gas for heating in Hungary. Test data belonging to each month (shown with black) is classified into either of the two classes. January to April are classified as winter months with high weights of evidence, as seen in Table 3.1. May is classified as a summer month, but with a very weak weight of evidence and the model selection is indecisive. June to September are classified as summer months. October to December are classified as winter months with strong weights of evidence. The classification of September shows the importance of a summer model. For this month the national gas consumption show no significant relation to the heating degree-days and so gas is not used for heating purposes.

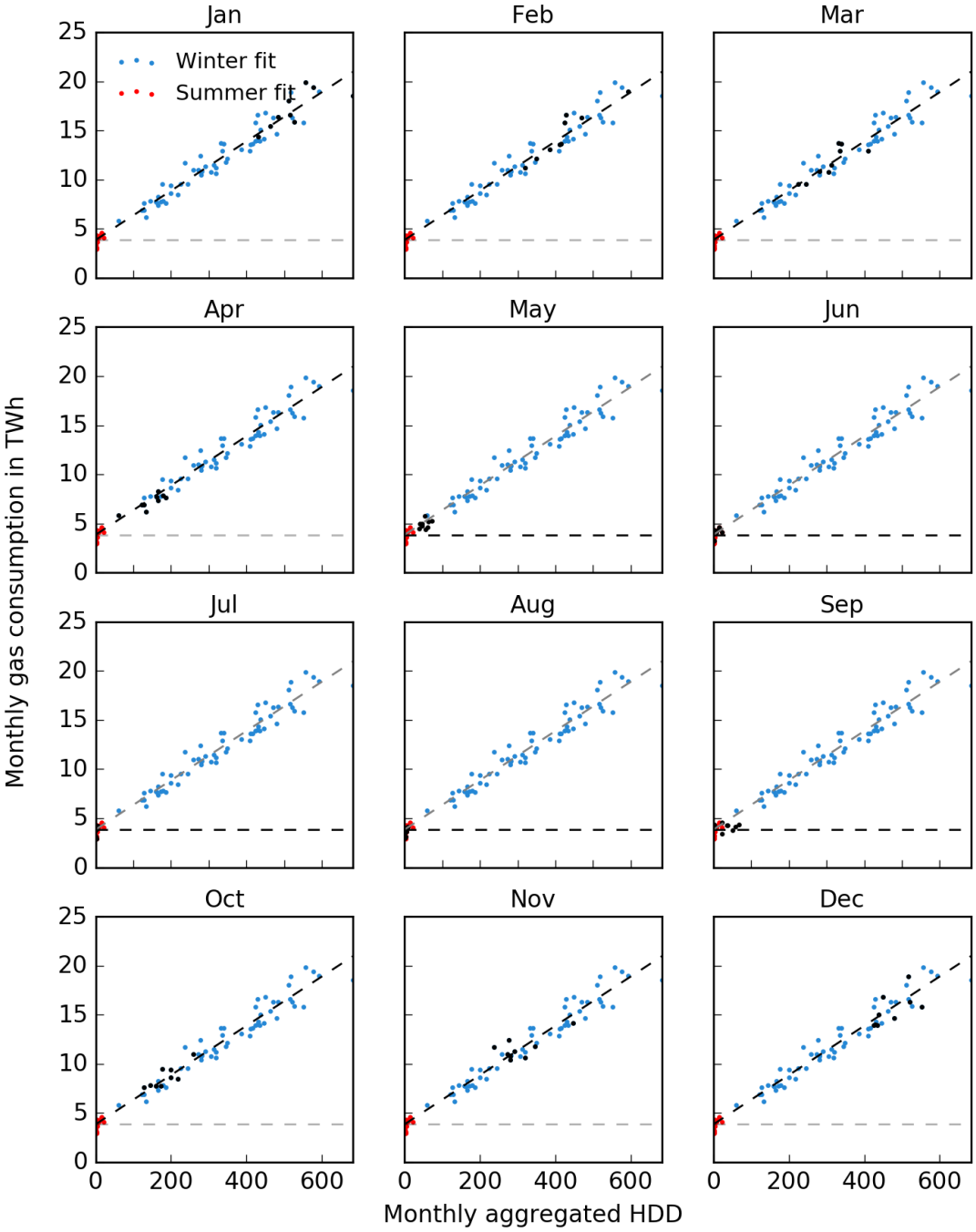

Figure 3.4: **Monthly gas consumption as a function of monthly aggregated heating degree-days for Hungary**. Winter (blue) and summer (red) classes with monthly data (black) to be classified for Hungary. The data spans the years from 2009 to 2018. The winter class is trained by the blue coloured data while the summer class is trained by the red coloured data.

Bias adjustment of temperature profiles

This section presents a simple method that can be used to bias adjust any temperature data. In this study, a best representation of real temperature data is important for a correct estimation of the heating degree-days.

The reanalysis air temperature data comes from the Climate Forecast System Reanalysis (CFSR) data set, which is supplied by the National Center for Atmospheric Research (NCAR) [163]. This data covers the entire globe from 1979 to present and is updated on a monthly basis. The spatial and temporal resolution covers Europe with 0.312° and 1 hour, respectively. The main advantage of using global reanalysis data is a high availability in all locations, consistency across many decades, and preservation of correlations between different weather fields relevant for energy system analysis, e.g. temperature, wind, solar and precipitation data.

Temperature data based on direct measurements comes from the European Climate Assessment (ECAD) who as well provides an interpolation in space [164]. The data set covers Europe for the period 1950–2017 with a spatial and temporal resolution of 0.5° and 1 day, respectively. The data covers various time periods depending on the mast operation span. In a simple bias correction procedure, the CFSR reanalysis temperature data was compared to the ECAD air temperature measurements in all grid locations, x, and with a daily resolution. ECAD air temperature measurements were interpolated in space by the "nearest neighbour" method to meet the resolution of CFSR.

In a linear regression, as in Equation 3.5, the ECAD temperature data set acts as a predictor variable while the CFSR temperature data set acts as the response variable. The least square estimators α_0 and α_1 denote, as usual, the gradient and offset, respectively. The system of linear equations is solved for every grid cell, x, contained within the set of grid cells X. The bias adjusted CFSR temperature profiles are finally calculated as:

$$T_x^{adj}(t) = \frac{1}{\alpha_{0,x}} T_x(t) - \frac{\alpha_{1,x}}{\alpha_{0,x}} \tag{3.5}$$

where $t \in [0;1826]$ denotes the day number in the period from 01/01/2011 to 31/12/2015. The corrections are summarised in Figure 3.5. In general, the corrections are relatively small, and the most extreme bias correction parameters are observed in sparsely populated mountainous regions as, e.g. the Alps, Sierra Nevada, Sierra Blanca and the West chain of the Norwegian mountains.

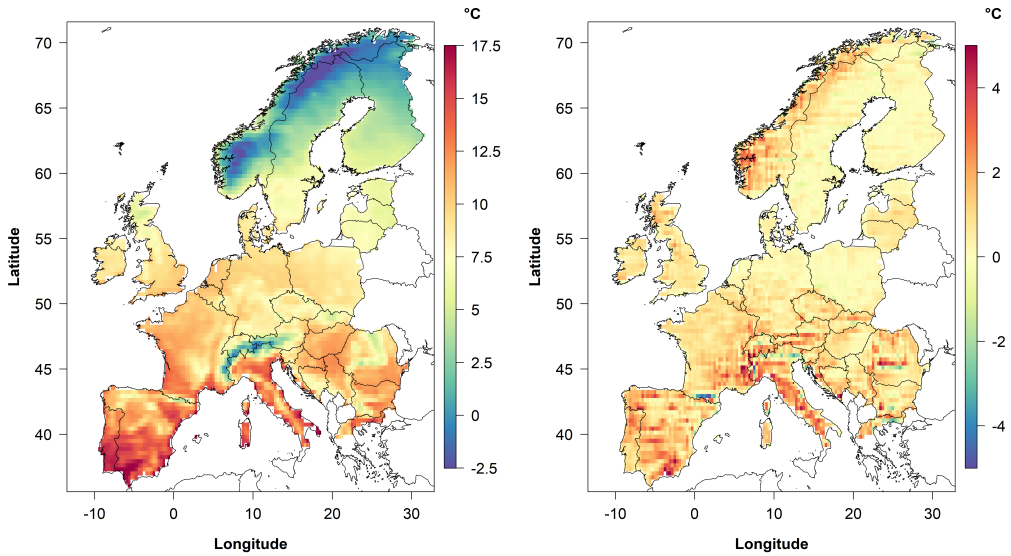

Figure 3.5: **Upper plot: Spatial distribution of the uncorrected average temperatures from 2005-2010. Lower plot: Spatial distribution of the average temperature correction.**

Energy data

Acquisition of energy consumption data varies significantly between energy sectors and countries, and nationwide data on energy use with high granularity are generally not available. This data gap introduces a serious weakness for energy system research. In the following detailed information is provided on the data that is used in this study.

Electricity consumption data

National electricity consumption profiles with hourly resolution were acquired from the European Network of Transmission System Operators for Electricity, (ENTSO-E). The data covers the period 2006-17 [40] (See also Figures 8.1 and 8.2 from the Supplemental Information). Data from 2009 and earlier is limited to the member TSOs of the Continental Europe region. Data from 2010 and on includes all ENTSO-E members. National data for the UK [28], France [165] and Denmark [166] were obtained separately to correct for gaps and inconsistencies in the ENTSO-E data.

Gas consumption data

Data on electricity production from gas is available through the ENTSO-E transparency platform with daily resolution [40]. From this, the amount of gas that was used to produce electricity is estimated with a conversion efficiency of 51.5%. Total national gas consumption with monthly resolution is available through Eurostat from 2008 to 2018 [167] (See also Figures 8.3 and 8.4 from the Supplemental Information). This covers all end-uses, including consumption by the gas sector it self, but excludes export. End use consumption includes the residential, service, industrial and agriculture sectors. Data on gas entering and exiting a country is metered by the national gas TSOs with a daily resolution and made available through the ENTSO-G transparency platform from earliest September 2013 [168]. National gas consumption with daily resolution is then estimated for a few countries by the difference in the amount entering and existing gas combined with gas storage data from AGSI [169]. The UK national gas consumption excluding the share of gas used in electricity production was provided by the UK TNO. Danish total gas consumption was provided by Energinet [168].

3.3 Results and discussions

Initially, results from a first analysis is presented where the iterative procedure (described in Section 3.2) has been used to estimate the threshold temperatures and the corresponding heating seasons for all countries. For this, exclusively monthly aggregated gas and electricity consumption data were used. In both cases, the iteration converged after the first cycle. Next, the resulting classification is adopted and used to recalculate the threshold temperatures by using weekly and daily gas and electricity consumption data. This allows for an assessment of the influence of data granularity.

Heating threshold temperatures

Figures 3.6 and 3.7 show the median score of the yearly threshold temperatures which were computed by using daily, weekly and monthly aggregated gas and electricity consumption data, respectively. Nine yearly values of the threshold temperature allows for a determination of the corresponding $[q_{25\%}, q_{75\%}]$ uncertainty ranges for the monthly Eurostat gas consumption data and ENTSO-E electricity consumption data. In the following, the focus is on results computed by using monthly aggregated consumption data.

From Figure 3.6 it is clear that the estimated threshold temperatures by using Eurostat (black) and ENTSO-G (red) gas consumption data are not significantly different within the Eurostat uncertainty range. Threshold temperatures for Norway and Portugal are not shown as by classification no space heat demand is covered by gas. For Norway, this is in agreement with radical changes in the Norwegian energy system with a ban of using gas for domestic heating by 2020. Results for Spain, Greece, Lithuania and Romania appear with substantial 25th to 75th percentile uncertainties. These are not unexpected as for these countries, gas covers a minor share of the final energy demand (Figure 3.1) and, consequently, no penetrative relation might be developed to the weather. There are, however, other possible explanations as, e.g., data quality or quantity. In the case of heating by electricity, a majority of the countries show unstable threshold temperatures along with extensive 25th to 75th percentile range. As for heating by gas, these results could have impacts from several sources. A few countries as Finland, France, Norway and Sweden show valid results with small error scores.

Heating threshold temperatures that are based on monthly consumption data have been summarised in Table 3.2. Results are not presented where a fuel type

covers less than 15% of the final heating demand, as below this, the relationship between fuel consumption and heating degree-days (Equation 3.2) lost statistical significance. Because of missing gas demand data for Bosnia & Herzegovina and Serbia the heating threshold temperatures for heating by gas cannot be estimated. Moreover, the missing fuel shares for these countries (as shown in Figure 3.1) makes the presence of the heating threshold temperatures for heating by electricity in Table 3.2 indecisive. However, for the sake of completeness of Table 3.2 , it is chosen to present these as special cases. A few countries hold a heating threshold temperature for both fuel types. It is clear that threshold temperatures for heating by electricity are smaller in comparison to heating by gas. It is difficult to explain this result, but it might be related to that electricity is a more expensive source of heating in countries for which gas is the predominantly heating source. Therefore, electricity could be used as a supplementary for gas during extreme temperature drops. In general, the ensemble of country-wise threshold temperatures for heating by gas average to 15.0±1.7 °C (1 sigma standard deviation). The electricity values average 13.4±2.4 °C. A graphical overview of the country-wise heating threshold temperatures for heating by gas and electricity is provided in Figure 3.8.

The need for space heating is determined by the difference between ambient air temperature and the desired indoor temperature, and how well the building is insulated. The latter can be measured by the building U-value [170, 171], which is a thermal transmittance coefficient that measures the rate of heat transfer through the building's fabric in units of W/m^2K. From the EC buildings database for U-values [172], it is clear that the Nordic countries, with a few exceptions, hold the lowest building U-values compared to the rest of the European countries. This suggests that the national building standards could explain the lower heating threshold temperatures for the Nordic countries as well-insulated buildings can maintain a comfortable temperature from passive and solar gains at lower outdoor temperatures. The human relationship between temperature and comfort may also explain some of the differences. For example, personal comfort desires or personal incomes hold an important role in this relationship. In general, it is difficult to assign any specific explanation for the variance in the national threshold temperatures and there might, however, be other possible explanations. In conclusion, the need for space heat is controlled by the indoor temperatures, which in turn is dependent on the indoor and outdoor environments of the building.

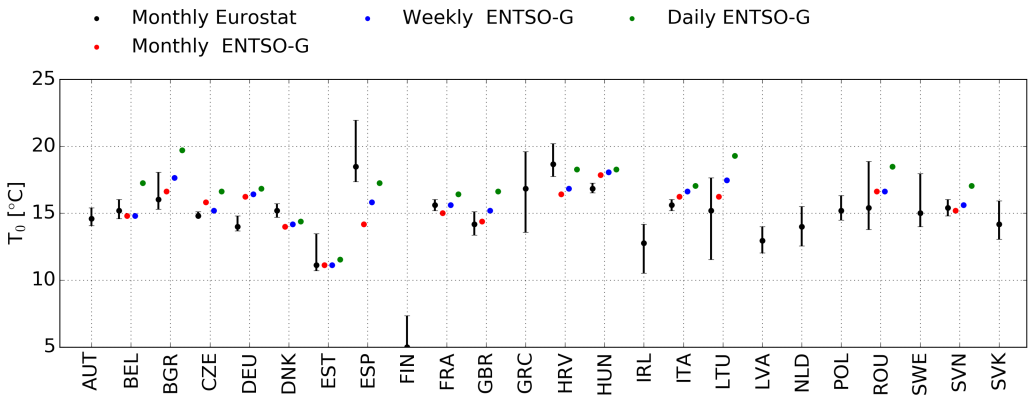

Figure 3.6: **Median of the yearly heating threshold temperatures calculated by using Eurostat gas demand data with monthly resolution (black) and ENTSO-G gas demand data with monthly (red), weekly (blue) and daily (green) resolutions.** Threshold temperatures for Denmark and UK were recalculated by using data from national sources, as explained in Section 3.2. $[q_{25\%}, q_{75\%}]$ uncertainty ranges are provided for the monthly Eurostat gas consumption data. Switzerland, Serbia and Bosnia & Herzegovina are not shown due to missing data. Norway and Portugal are not shown as heating by gas is classified as non-existing for these countries.

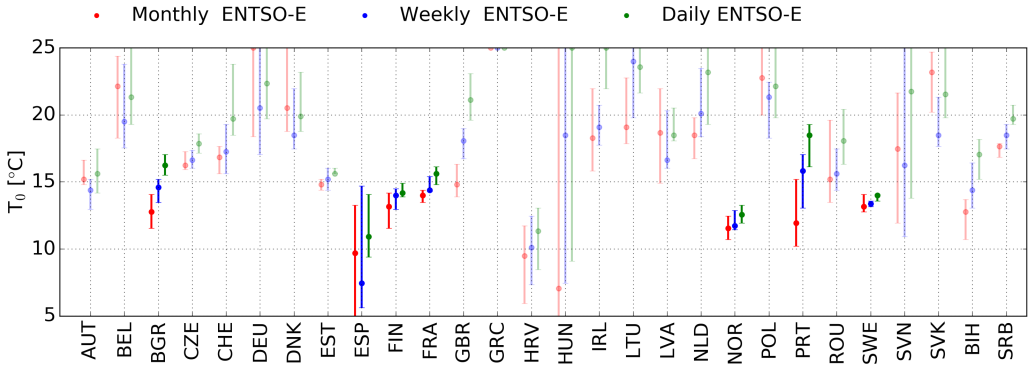

Figure 3.7: **Median of the yearly heating threshold temperatures by using ENTSO-E electricity consumption data with daily (black), weekly (blue) and monthly (red) resolutions.** $[q_{25\%}, q_{75\%}]$ uncertainty ranges are provided for the case of all data resolutions. Countries of which the final heat demand is covered by less than 15% by electricity are shown with faint colors. Results for all countries apart from Denmark, France and UK were obtained by using electricity consumption data provided by ENTSO-E. Results for France, Denmark and UK were obtained by using data from national sources, as explained in Section 3.2. Italy is not shown as heating by electricity is classified as non-existing.

Table 3.2: **Heating threshold temperatures for heating by gas and electricity with 25th to 75th percentile uncertainty ranges**. The results are based on monthly consumption data. n.a denotes either a fuel type share that is below 15% and the results cannot be trusted, or missing consumption data and the results cannot be obtained.

	Electricity	**Gas - Eurostat**
Country	$T_0\,[q_{25\%}, q_{75\%}]$ °C	$T_0\,[q_{25\%}, q_{75\%}]$ °C
AUT	n.a.	14.59 [14.08, 15.41]
BEL	n.a.	15.20 [14.59, 16.02]
BGR	12.76 [11.53, 14.08]	16.02 [15.31, 18.06]
CZE	n.a.	14.80 [14.80, 15.10]
CHE	16.84 [15.61, 17.65]	n.a.
DEU	n.a.	13.98 [13.67, 14.80]
DNK	n.a.	15.20 [14.69, 15.71]
EST	n.a.	11.12 [10.71, 13.47]
ESP	9.69 [5.00, 13.27]	18.47 [17.35, 21.94]
FIN	13.16 [11.53, 14.18]	n.a.
FRA	13.98 [13.47, 14.39]	15.61 [15.20, 16.02]
GBR	n.a.	14.18 [13.37, 15.10]
GRC	n.a.	16.84 [13.57, 19.59]
HRV	n.a.	18.67 [17.76, 20.20]
HUN	n.a.	16.84 [16.53, 17.24]
IRL	n.a.	12.76 [10.51, 14.18]
ITA	n.a.	15.61 [15.20, 16.02]
LTU	n.a.	15.20 [11.53, 17.65]
LVA	n.a.	12.96 [12.04, 13.98]
NLD	n.a.	13.98 [12.55, 15.51]
NOR	11.53 [10.71, 12.45]	n.a.
POL	n.a.	15.2 [14.49, 16.33]
PRT	11.94 [10.20, 15.20]	n.a.
ROU	n.a.	15.41 [13.78, 18.88]
SWE	13.16 [12.76, 14.08]	n.a.
SVN	n.a.	15.41 [14.80, 16.02]
SVK	n.a.	14.18 [13.06, 15.92]
BIH	12.76 [10.71, 13.67]	n.a.
SRB	17.65 [16.84, 17.86]	n.a.

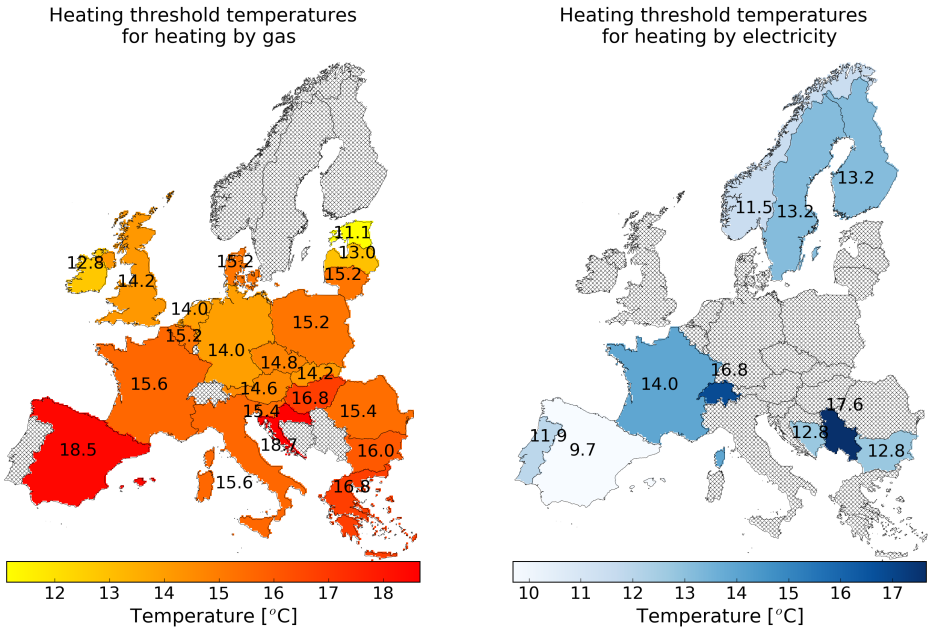

Figure 3.8: **Estimated heating threshold temperatures for heating by gas and electricity**. Left figure: Estimated heating threshold temperatures by using gas consumption data. Right figure: Estimated heating threshold temperatures by using electricity consumption data. Hatched areas indicate either missing data and no results can be computed or a poor relation between energy consumption and outside ambient temperature.

Non-heating summer seasons

Table 3.3 presents a 10 year average (2008-2017) of monthly aggregated heating degree-days for each country. Enveloped values represent the summer seasons for which space heating is usually not required, since the heat absorbed during daylight hours is enough to keep the buildings warm during colder periods. The binary indicator function, Θ_X, takes a values of zero for the enveloped months and one for the rest. Countries for which threshold temperatures are available for both heating by gas and electricity, the minimum required heating season is shown. It is clear that all countries exhibit a summer period from June-August. Apart from this, the classification shows a spread in the summer months, which mostly depends on the geographical location of the countries. As could be expected, South European countries usually hold longer summer periods without heating while the Northern countries tend to have shorter summer periods.

Daily and weekly aggregated gas and electricity consumption data that belong

Table 3.3: **Results of the AIC classification procedure**. Each number denotes the monthly averaged heating degree-days from 2008 to 2017. These are calculated by using the heating threshold temperatures that are presented in Tab. 3.2. Enveloped values denote the classified summer months.

Country	Jan	Feb	Mar	Apr	May	Jun	Jul	Aug	Sep	Oct	Nov	Dec
AUT	482	406	315	171	78	26	13	15	62	181	287	431
BEL	366	317	264	161	75	19	4	4	33	119	224	328
BIH	380	309	226	95	33	4	1	0	22	96	180	333
BGR	502	386	304	163	53	8	1	1	28	147	250	422
CHE	556	496	426	292	188	92	59	65	153	272	390	520
CZE	503	416	325	173	71	16	3	5	51	187	292	437
DEU	401	344	274	147	58	12	1	2	31	134	241	351
DNK	427	393	355	229	110	29	2	3	34	147	255	365
EST	474	416	372	206	56	5	0	0	13	140	241	363
ESP	175	152	106	46	14	1	0	0	1	13	78	156
FIN	620	536	497	326	136	37	4	11	74	264	368	507
FRA	356	311	247	150	70	16	3	4	28	104	211	320
GBR	301	270	248	171	90	26	5	5	26	90	193	270
GRC	287	234	194	92	17	0	0	0	3	41	112	236
HRV	523	438	349	202	100	24	6	6	72	209	318	471
HUN	521	414	309	144	50	7	1	1	39	178	302	465
IRL	225	204	197	135	65	15	2	2	16	62	152	207
ITA	287	241	173	74	22	4	2	2	10	49	134	259
LTU	595	493	428	245	87	25	2	7	68	254	340	480
LVA	519	436	375	199	55	8	0	0	26	184	274	401
NLD	335	299	247	141	61	11	0	1	14	88	192	290
NOR	440	393	350	221	107	33	8	11	47	172	281	391
POL	521	434	362	200	83	22	4	7	61	208	306	444
PRT	73	62	31	10	1	0	0	0	0	0	23	64
ROU	530	417	305	140	42	6	1	2	32	161	275	451
SRB	507	400	300	144	55	10	2	2	37	164	279	448
SVK	507	410	317	155	58	13	4	6	48	178	284	447
SVN	486	411	312	157	63	11	3	4	52	176	282	441
SWE	500	442	397	248	109	26	2	7	49	196	304	429

to the winter classified months have been used to recalculate the heating threshold temperatures for the daily and weekly time resolutions. The results are shown in Figures 3.6 and 3.7, respectively. For both consumption types, the statistical similarity in threshold temperatures for each individual country provide a robust indication of the adequacy of using less granular data for estimating the threshold temperatures. On the other hand, it is clear that the threshold temperatures increase with increasing data granularity.

In the following, the significance of reaching country specific heating threshold temperatures and summer seasons is presented. As a case study, results for Great Britain are used but an identical analysis can be performed for each individual country by utilising the heating degree-days in Table 3.3. For Great Britain, October averages to 90 heating degree-days, and is classified as a winter month, while May, which as well averages to 90 heating degree-days, is not. Contrary to May, the winter classified October is explained by an existing relation between gas consumption and heating degree-days. On the other hand, the AIC evidence ratio for May is below 2 and, thus, more years of consumption data would be needed to fully justify this classification. A similar classification is shown for Hungary for May and September, as shown in Figure 3.4. Similar cases appear for Denmark, Estonia, Greece, Romania, Switzerland and Bosnia & Herzegovina, as shown in Table 3.3. These issues arise mostly during autumn and spring where the monthly temperature differences exhibit large variances over the years.

Average heating degree-days that are calculated by using a threshold temperature of 14 °C, 16 °C and 18 °C for Great Britain are shown in Figure 3.9. The summer season is shown by a depreciation of heating degree-days from May to October. It is clear that a 2 °C increase in the threshold temperature introduce a significant difference in the accumulated heating degree-days over a year. The most striking result, which emerges from the classification, is the extreme change in the seasonal pattern of the heating degree-days.

Quantitative measures of the heating degree-days are shown in Table 3.4 for six case studies. In the most extreme scenario, case study (c) overestimates the heating degree-days by approximately 93%, which is almost a doubling in comparison to case study (d). For a fixed average space heat demand per capita per space heat heating degree-day, $L_{0,\mathrm{GBR}}^{\text{space heat}}$, GBR, the energy demand for space heating, Equation 3.1, is consequently overestimated by identical shares. These results suggest that the current estimations of the energy demand for space heating

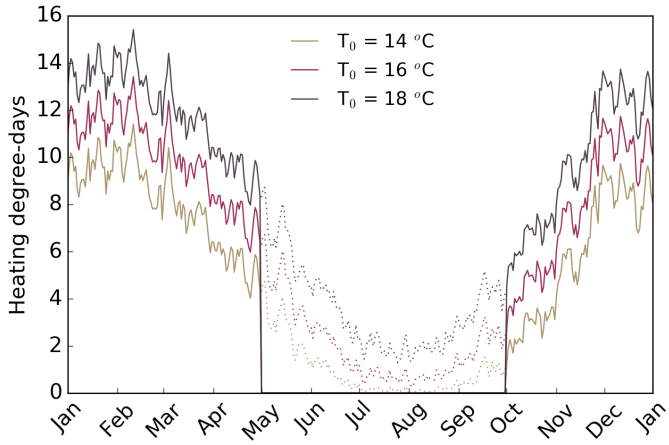

Figure 3.9: **Daily averaged heating degree-days over 10 years for Great Britain**. These are calculated with heating threshold temperatures, T_0 = 14°C (yellow), T_0 = 16°C (red) and T_0 = 18°C (black). Fully drawn lines illustrate the heating degree-days during winter months as a result of the classification. Dotted lines illustrate summer months for which space heating is not needed and has to be removed.

in various projects might be highly over or underestimated for some countries. This might introduce further changes as, e.g., the estimation of CO_2-emission, technology choice for heating or peak demand estimation. On the other hand, a yearly fixed energy consumption for space heating will be distributed differently according to the seasonal distribution of heating degree-days.

Table 3.4: **Overview of the yearly aggregated heating degree-days for six case studies of Great Britain denoted by a)-f)**. Previous studies have used threshold of 15°C, 16 °C, 18 °C or 18.33°C across all countries.

	With summer season	**Without summer season**
$\boldsymbol{T_0}$ **= 14°C**	a) 1654	d) 1510
$\boldsymbol{T_0}$ **= 16°C**	b) 2235	e) 1927
$\boldsymbol{T_0}$ **= 18°C**	c) 2896	f) 2350

Figure 3.10 illustrates the synergy between the monthly averaged air temperature measurements (blue curve), the threshold temperatures (red dashed line) and the classified summer seasons (hatched area) for Greece, Italy and Norway. From these figures, it is clear that the monthly averaged temperatures fall below the heating threshold temperature outside the hatched area, which indicates that space heating is needed. Figures for all countries, for which air temperature

measurements are available, can be seen in the Supplementary Information Figures 8.5-8.7.

Country-wise verification

Denmark has no heating season defined by law. 54% of the end-use heat demand is provided by district heating [173] which dominates the Danish heat production. During summer time, the district heating utilities mainly deliver hot water. A similar summer season is determined in this work with a heating threshold temperature of 15.20 [14.69, 15.71] °C. A similar finding was presented by [158].

Czechia has a legally defined heating season that lasts from September 1st to May 31st [143]. If the daily average outside temperature is below 13 °C then the district heating utilities start to deliver heat. An identical heating season is determined by this work with a threshold temperature of 14.80 [14.80, 15.10] °C. A possible explanation for this discrepancy is that our results covers the complete heating production by electricity and gas while 13 °C only refers to district heating.

Great Britain has no heating season provided by law but a typical heating season starts by October 1st and ends at April 30th and is further restricted with a day time peak temperature being 16 °C or lower for a few consecutive days [143]. An identical heating season is proposed in this study with a threshold temperature of 14.18 [13.37, 15.10] °C which is conductive with 16 °C daytime and 9 °C night temperatures. A threshold temperature of 13 °C is proposed by the [174] based on qualitative surveys.

Germany has no legal heating season, but the German Tenants Association, [175] , states the heating season typically runs from October 1st to April 30th. This gives a heating season that is two months shorter than found in this work, which is explained by the threshold temperatures. The Association of German engineers, VDI2067, estimate a German heating threshold temperature of 12 °C, whereas a threshold of [13.67, 14.80] is presented by this study.

Finland also has no heating season defined by law. An accepted heating threshold temperature is 12 °C from autumn to December and lowers to 10 °C during the spring [176]. Here, a value of 13.16 [11.53, 14.18] °C is proposed to be used from September through to May.

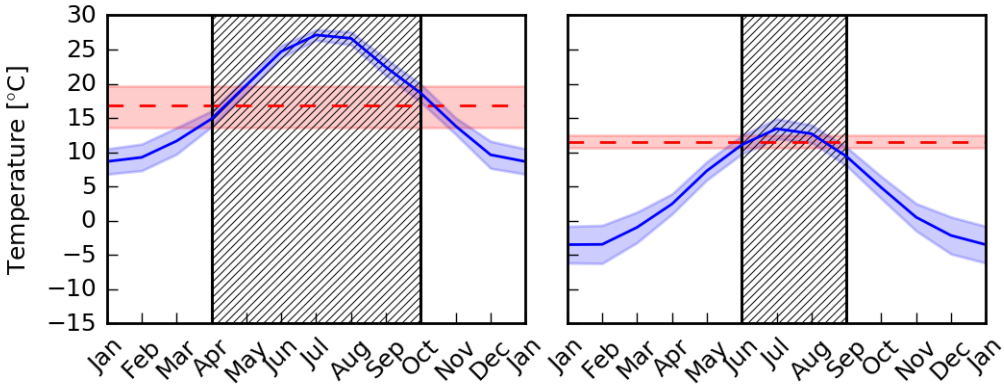

Figure 3.10: **Monthly averaged temperatures from 2008 to 2017**. Blue full drawn curves show the monthly averaged temperatures with 1 sigma uncertainty ranges (shaded blue regions), heating threshold temperatures (red dashed lines) with $[q_{25\%}, q_{75\%}]$ uncertainty ranges (shaded red regions) and classified summer season (black hatched areas) for Greece (upper figure), Italy (central figure) and Norway (lower figure)

Italy has several heating seasons defined by law depending on six different climatic zones from the mountainous North with a colder climate to the flat South with a temperate climate [143]. October 15th is the earliest date at which heating is permitted and lasts at most to April 15th. A national-aggregate heating period is found to run from October 1st to March 31st with a threshold of 15.61 $[15.20, 16.02]$ °C.

Croatia has a typical heating season to range from September 15th to May 15th. The heating season is in this study proposed to start at September 1st and last to April 30th with a heating threshold temperature of 18.67 $[17.76, 20.20]$ °C.

Romania's district heating utilities begin to operate by law if the outside average temperature reaches 10 °C or lower for three consecutive days, and no later than November 1st. Heat delivery stops, by law, if the daily average temperature exceeds 10 °C for three consecutive days and not earlier than April 15th. In this work, the overall heating season is found to start from October 1st and last to March 31st with a heating threshold temperature of 15.41 $[13.78, 18.88]$ °C.

Spain holds heating threshold temperatures from 13 to 14.8 °C depending on the region [177, 178]. In this work, 9.69 $[5.00, 13.27]$ °C is found for electricity use and 18.47 $[17.35, 21.94]$ °C for gas use.

3.4 Conclusion

This study was undertaken to design a new method to determine the national energy demand for residential and commercial space heating with better than annual resolution. Furthermore, the study was designed to work for any given country based on its historic fuel consumption and weather data. In doing so, a new method is proposed to determine a consistent empirically-derived national-wise heating threshold temperature which can be used to determine the national aggregated heating degree-days. Secondly, the extent of a winter period is determined for which space heating is required. This is represented by a binary indicator function taking only values of zeros and ones. The final energy demand for space heating is then a function of the newly acquired heating degree-days and the binary indications. As a case study, these methods have been applied to the majority of European countries, using data on national aggregated heating degree-days along with national demand for gas and electricity. The following conclusions can be drawn:

The country specific heating threshold temperatures for heating by gas range from 11.12 °C to 18.67 °C with a country ensemble mean of 15.0 ± 1.7 °C (1 sigma standard deviation). The electricity values range from 9.69 °C to 17.67 °C with a corresponding ensemble mean of 13.4 ± 2.4 °C. This suggests that the currently used threshold temperatures might be overestimated by approximately 5 °C for some countries in the literature.

It is found that the newly empirically-derived country-wise heating threshold temperatures and the estimated summer seasons make considerable differences to the temporal allocation of the heating degree-days. Based on an in-depth case study of Great Britain, it is found that previous studies might have overestimated the annually accumulated heating degree-days by up to 93%. With our newly proposed heating threshold temperature of 14 °C excluding the May-September summer season, the heating degree-days reach an annually accumulated value of 1510 degree-days for Great Britain. In contrast, by using 18 °C including the summer season as, e.g., in the Odyssee project, the alternative value reaches 2896 degree-days. The heating threshold temperatures given in the literature are often not unique for countries and so a direct comparison between the existing values and the results of this study is difficult to make and should be done with care.

The heating threshold temperatures were computed by using daily, weekly and monthly aggregated data and shown to be marginally different within 25th to

75th percentile significance range. This provides a good indication of the adequacy of using monthly aggregated data for such an application.

The heating threshold temperatures tend to increase with increasing temporal resolution of consumption and weather data.

Based on the AIC classification theorem, the European countries exhibit a summer period of at least June, July and August where space heating is not required. South European countries exhibit longer summer periods, up to a maximum of 7 months for Portugal.

Ultimately, heterogeneous threshold temperatures were found for space heating across neighbouring countries in Europe, which suggest that the threshold temperatures cannot be extrapolated to neighbouring countries. Therefore, this study excels from the standard practice of using a blanket, even arbitrary value, such as 16 °C or 18 °C across multiple countries which over-simplify and misrepresent the true nature and scale of national space heating demand. If an unrepresentative heating threshold temperature is used then the seasonal behaviour of the heat demand becomes incorrect.

Some limitations of this study need to be considered. Firstly, the lack of data for national gas consumption specifically for space heating purposes adds a layer of complexity, as the end-uses of space heating, water heating, cooking and other industrial processes cannot be disentangled. Gas consumed for electricity generation could be estimated, but consumption data would also be useful for this purpose. ENTSO-G and other authorities could consider increasing the transparency of data reporting to aid further research on heating demand. Secondly, this study did not evaluate data on coal and oil consumption, which was not found at monthly or better resolution. This may prove important for countries such as Poland and Greece, and would further enhance results. Thirdly, countries with various climatic areas and a diverse terrain might hold different threshold temperatures in different regions, as might countries with large socio-economic differences between regions. Assessing sub-regions of countries would require more granular data on electricity and gas demand than is currently made openly available, but would be an interesting future topic for research.

Acknowledgement

Thanks to Aarhus Universitet Research Foundation for funding S. Kozarcanin with funding number AUFF-E-2015-FLS-7-26. I. Staffell acknowledges the Engineering and Physical Sciences Research Council for funding the IDLES project (EP/R045518/1). G. B. Andresen was funded by the RE-INVEST project, which is supported by the Innovationsfonden under grant number 615400022B .

Declaration of Interest

The authors declare no competing interests.

Article History

Received: January 28, 2019
Revised: July 1, 2019
Accepted: July 4, 2019
Published: July 4, 2019

CHAPTER 4

Impact of climate change on the cost-optimal mix of decentralised heat pump and gas boiler technologies in Europe

Article

This chapter is based on the research paper:
Kozarcanin, Smail; Hanna, Richard; Gross, Robert; Staffell, Iain; Andresen, Gorm Bruun. *Impact of climate change on the cost optimal mix of decentralised heating in Europe*. The manuscript is uploaded to arXiv and submitted for publication to Energy Policy.

Project Dissemination

The project has been presented at the Imperial College Centre for Energy Policy and Technology (ICEPT) book club and at other conferences.

Author Contributions

S. Kozarcanin was responsible for managing and coordinating the research activities and performed the formal analysis and investigation. S. Kozarcanin wrote the original draft and visualised. R. Hanna provided the political assessment in Section 4 in collaboration with R. Gross. Associate professor G. B. Andresen, Dr. I. Staffell and S. Kozarcanin developed the original concept. G. B. Andresen and I. Staffell supervised the project.

Highlights

- Increasing global warming decreases the need for space heating.
- Current climatic conditions favour gas boilers and heat pumps.
- Climate change makes heat pumps more cost competitive and gas boilers less.
- Heat policies in Europe are broadly consistent with cost-optimal technologies.
- In several countries, cost-optimal technologies and real deployment do not match.

Summary

Residential demands for space heating and hot water account for 31% of the total European energy demand. Space heating is highly dependent on ambient conditions and susceptible to climate change. A techno-economic standpoint is adopted and used to assess the impact of climate change on decentralised heating demand and the cost-optimal mix of heat pump and gas boiler technologies. Temperature data with high spatial resolution from nine climate models implementing three Representative Concentration Pathways from IPCC are used to estimate climate induced changes in the European demand side for heating. The demand side is modelled by the proxy of heating-degree days. The supply side is modelled by using a screening curve approach to the economics of heat generation. A decrease of about 16%, 24% and 42% in the space heating demand in low, intermediate and extreme global warming scenarios. When considering historic weather data, a heterogeneous mix of technologies are cost-optimal is found, which depends on the heating load factor (number of full-load hours per year). Increasing ambient temperatures toward the end-century improve the economic performance of heat pumps in all concentration pathways. Cost optimal technologies broadly correspond to heat markets and policies in Europe, with some exceptions.

4.1 Introduction

Energy consumption for space heating is by far the most important end-use in the European (EU28) residential heating sector with an estimated share of 52% in 2015 [41]. Space heating is strongly temperature dependent and mostly consumed during cold winter seasons [179]. Heating systems are therefore designed to meet peak demand during cold winter periods, but for long-term design decisions, it is necessary to focus on long-term changes in the climate. Depending on the degree of climate change in the future, it is believed that the peak demand for space heating might change significantly. Given these points, the principal aim of this study is to analyse the 21st Century climate change impact on the selection of cost-optimal, decentralised heating technologies for different locations in Europe. Decentralised heating is defined as all heating systems installed on a per-building basis. This means that the focus is not on large-scale centralised heating systems such as combined heat and power plants or other district heating facilities. This paper draws upon climate affected temperature data from the newest simulations carried out in the framework of the CMIP (Coupled Model Inter-comparison Project) Phase 5 [61, 180] and the EURO-CORDEX project [70, 72]. Data from nine climate models from a combination of 4 regional climate models, RCM, downscaling 5 global climate models, GCM, under the forcing of the latest generation of climate projections provided by the Intergovernmental Panel on Climate Change, IPCC [15] are used. For this study, data with the best available resolutions is used, which is 3hr in time and 0.11° × 0.11° in space for Europe. A full description of the climate data is provided in Section 1.5 and a full description of biases in climate models is provided in the Supplemental Information Section 7.1. An overview of the models in use is presented in Table 1.1.

A fundamental impact on the selection of heating technologies, that to the best of the authors knowledge has not been studied in detail, is the impact of local climates on the cost-optimal design of decentralised heating systems. Throughout this article, *system design* refers to the cost-optimal selection of decentralised heat generating technologies. Spatial variations in the ambient temperatures fluctuate heterogeneously from the oceanic to the mainland climates of West and East Europe, respectively, and from the cold northern to the warmer southern climates. Climate change is furthermore expected to introduce long term and heterogeneous temperature anomalies across Europe. Whereas hot water demand is relatively constant throughout the year and between years [157], the energy consumed for space heating will therefore fluctuate more wildly and be subject to long-term trends that are currently not well understood.

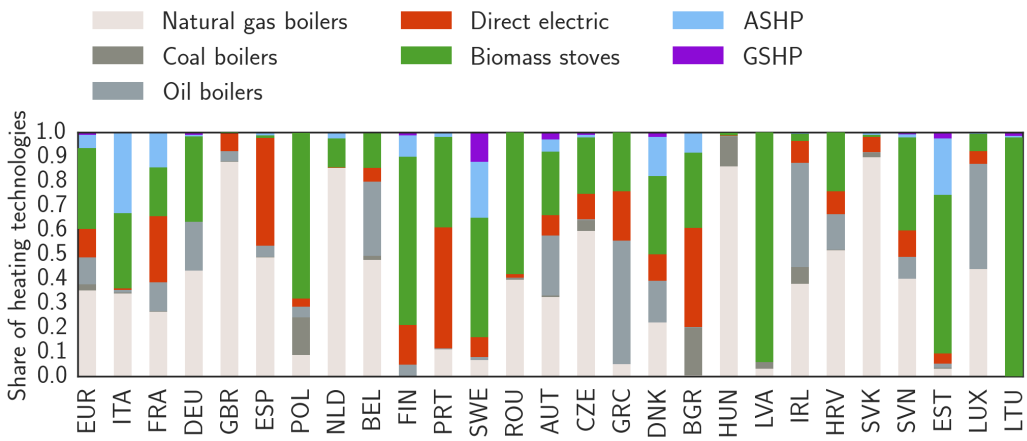

Figure 4.1: **Shares of the installed stock of heating technologies across the European countries in 2012**. The x-axis lists the countries, referred to by their three-letter ISO codes. Data from [31].

A secondary aim of this paper is to evaluate the fit between cost-optimal technologies for decentralised heating and heat policies in Europe. Actual deployment of heating technologies in different countries may not necessarily reflect which technologies are most cost-optimal in a given location. The purpose of this policy assessment is to identify where policy intervention might be required to achieve lower cost outcomes, while contributing to overall efforts to decarbonise heating.

Figure 4.1 illustrates the current technology shares that are responsible for delivering the decentralised heat for a majority of the European countries. The European average bar shows that fossil fueled boilers dominate the heat generation, followed by biomass fueled technologies. Heat pumps are relatively new technologies compared to boilers and consequently hold a minor share of the total installed technology stock. On the other hand, heat pumps are gaining more attention with 99% of the units installed after 2002 while 42% of the fossil fuel boilers were installed previous to 1992 [31]. The large increase in the penetration of heat pumps in European homes has been motivated by various policy and regulatory drivers such as subsidies and carbon taxes, building regulations, improved technical standards and information dissemination [32, 33].

The focus of this paper is on the European aggregated space heat demand and used to examine the extent to which it changes under the impact of global warm-

ing. Then the consequent changes in the CO_2-emission are estimated. To isolate the effect of climate change, an unchanged stock of national heat generating technologies throughout the 21st Century is assumed. For each 144 km^2 grid cell, defined by the spatial resolution of the climate data, a cost-optimal technology for a historical time frame 1970-1990 and for an end-century time frame 2080-2100 is mapped, and compare the differences. The demand and supply sides are modelled as highly temperature dependent. The heat demand is modelled through the heat load factor, which most commonly is determined as the fraction of the yearly averaged heat demand to the maximum. For the supply side, a simplified techno-economical standpoint of heat generation is used. Initially, policy decisions are excluded but a section is devoted to a policy assessment of the results. The application of state-of-the-art technical procedures combined with the large ensemble of highly granular climate data, that support the analyses, is considered as novel to existing literature. In summary, this approach provides new and more robust results that quantify the change in space heat demand throughout this century.

A limited amount of research has been devoted to this field, all with a focus on historical heating systems. Heat load capacity factors have been calculated for 80 locations in Europe for a historical time frame spanning the years 1981-2000 [181]. Under historical weather conditions that are typical to the European region, the seasonal performances of six heating system configurations have been investigated and finds that these are sensitive to the selection of electricity and gas driven heat pumps [182].

This paper is structured as the following: Section 2 presents the methodologies of this paper. Results are presented in Section 3. Current policies on decentralised heating in Europe along with future prospects are presented in Section 4 along with the study limitations. Conclusions and policy implications are presented in Section 5. Finally, a nomenclature is added in Section 6.

4.2 Experimental procedures

This section is devoted to a qualitative description of the methods that are used in this work. A detailed derivation of the mathematical formulations can be found in the Supplemental Information Section 9.1.

Technology and price assumptions

Inspired by Figure 4.1, the following listed technologies compose the ensemble of the decentralised heat generating technologies in this study:

Electricity driven air source heat pumps (ASHP) draw heat from the ambient air to supply hot water and space heating through hydraulic based water systems. Air source heat pumps require only an outdoor and indoor unit and are therefore easy to retrofit into existing houses. A limited amount of equipment and installation procedures give this technology an economic advantage compared to ground source heat pumps. On the other hand, the large temperature fluctuations between the external heat collector (source temperature) and the output at home (sink temperature) throughout the year, especially in winter periods with high heat demand and low ambient temperatures, challenge their efficiency, denoted by the Coefficient Of Performance (COP). In this work, the temporally- and spatially-explicit COP values are calculated and based on the prevailing air and soil temperature, with a sink temperature of 55 °C [29]. Full details are given in the Supplemental Information Section 9.2.

Electricity driven ground source heat pumps (GSHP) are identical to the previous, but draws heat from the soil instead, which offers a substantially higher yearly averaged COP. Temperature measurements from existing boreholes in Denmark show that at a depth of 20 meters, the ground temperatures have settled, i.e., become seasonally independent [183]. In this work, the ground temperatures are estimated as an average of 20-year air temperatures. The resulting values correspond to temperatures at a depth of approximately 50 meters below ground, depending on soil type and geographical location [183]. The higher capital investments of ground source heat pumps are compensated by the lower running costs compared to air source heat pumps.

Air-to-air heat pumps with auxiliary electricity driven boilers (A2A+EB) is a hybrid system that consists of an electric boiler for hot water supply and an air-to-air heat pump that draws heat from the ambient air and supply heat through air exchangers. Air-to-air heat pumps have the lowest capital investments of all the heat pumps. Furthermore, air-to-air heat pumps utilise a lower sink temperature, which in this work is assumed to be 30 °C [29]. This increases the COP further, and consequently reduces the running costs by around 20% when compared to underfloor heating operating at 40 °C which is typical for GSHP [29]. Since air-to-air heat pumps cannot provide hot water they have to be installed alongside a hot water technology, which is assume to be an electricity driven

boiler. The combined technology efficiency will then be reduced. The share of each technology is determined by the individual shares of space heat and hot water demand to the total amount.

Natural gas fired boilers are assumed to cover both the hot water demand and space heat with hot water circulating through radiators. This technology has a very low capital cost but a relatively high running cost.

Oil fired boilers are identical to the previous but fired with oil.

Biomass boilers cover both the space heat demand and hot water by connection to radiators. The boiler is assumed to be automatically stocked. These types of boilers most commonly utilise wood pellets as fuel, which leads to the expensive fuel price in Table 4.1.

The stock of coal fired boilers has reduced heavily since 1992 with 58% of all units being installed before 1992 and 12% after 2002 [31]. Currently, coal fired boilers comprise only 2% of the total heating technology stock in Europe [31]. The decreasing trend is mainly believed to be a result of aggressive CO_2 and air quality policies in the European countries. As a result, coal fired boilers are excluded in this study.

Technologies such as fossil fuel driven boilers are very mature and possess relatively small price variability. Technologies such as heat pumps are still relatively new to the market and therefore subject to significant price variability between manufacturers and countries, and uncertainties in the future cost reductions and learning rates. These are mostly related to overcoming technological barriers, future markets and the technology demand [184]. Upper and lower bounds of these uncertainties are presented in Table 4.1 for all technologies that are included in this study.

In Table 4.1 the technology properties and prices for retrofit into existing single family houses are summarised. As the focus of this paper is on the impact of climate change on heating across a continent, rather than modelling the bespoke heating mix in individual countries, all prices are excluding national taxes and levies, and assumed to be constant across regions. This allows for a direct measure and comparison of the impact of climate change across regions and time. Furthermore, this procedure reduces uncertainties related to national policies on tax regulations. For the same reasons, infrastructure constraints such as

the absence of gas distribution networks in many countries and the inability of electricity distribution networks to meet large demands for heating from other countries are ignored, which is discussed further in Section 4.4.

Heat load factors

The heat load factor, HLF, denoted as μ, is defined as the unitless ratio of the residential heat demand, L^{Total}, to the maximum possible output of heat, P^{Total}, over a given time period, Δ, as:

$$\mu = \frac{L^{\text{Total}}}{P^{\text{Total}} \cdot \Delta} \tag{4.1}$$

The decentralised nature of heating means that data on consumption is not readily available and therefore not applicable. Known to the literature, the theory of heating degree-days is most frequently used as a best proxy for modelling the variations in the day-to-day heat demand. The heating degree-days are calculated by using national temperature profiles. In this study, the 3-hourly temperatures are averaged into daily values, to emulate a night storage since the daily averaged value is higher than night-temperatures but lower than day-temperatures. The theory of the heating degree-days and its application to approximate L^{Total} is described formally in the Supplemental Information Section 9.1. The maximum output of heat, P^{Total}, depends on the cold extreme temperature, as described in the Supplemental Information Section 9.1.

As stated previously, the heat load factors are determined as the fraction of the yearly averaged heat demand to the peak. Thus, large heat load factors are common in cold climates due to long running hours, but also in mild climates where hot water demand dominates the heat load. High load factors are consistent with a reduction in the overall cost per kWh of heat generated, since fixed expenses would be spread across more units of energy generated, hence the cost per unit of generation is reduced. Technologies with low marginal costs such as heat pumps prove as economically favourable in these circumstances. On the other hand, warmer climates tend to decrease the heat load factors, as peak hours deviate considerably relative to the base load hours. Technologies with low capital investments would serve as economically favourable in these conditions.

Table 4.1: **Technology costs and properties.** The *unperturbed* pricing scheme consists of installation, equipment and maintenance costs along with the uncertainty ranges that are prepared from Energinet [184]. Since Energinet does not provide an underlying distribution for each uncertainty range, a conservative approach is taken and assumes that all installation, equipment and maintenance costs are uniformly distributed. This means that these expenses are equally likely to occur within a specific uncertainty range. Electricity and gas prices excluding taxes and levies are prepared from the Eurostat database [185, 186]. Oil prices are prepared from the IEA database [187]. Biomass prices (wood pellets) are prepared from the Cross Border Bioenergy project [188]. The uncertainty range of fuel costs, σ, is defined according to a Gaussian distribution with a spread of 20% of the fuel price [189]. A price variation of about ±20% is well represented by the coefficient of variation seen across annual-average gas and power prices in Europe over the last two decades [185, 186]. Technology properties are prepared from Energinet [184]. "t" denotes that the efficiency of heat pumps (COP) is temperature dependent.

	Boilers			**Heat pumps**			**Biomass stoves**
	Gas Fired	Oil Fired	Electricity Driven	Air to Air (A2A)	Air to water (ASHP)	Ground to Water (GSHP)	
Unperturbed pricing scheme							
Installation Cost [€/kW]	100 [93, 148]	100 [80, 140]	50 [30, 70]	75 [50, 83]	304 [240, 480]	420 [350, 560]	118 [40, 200]
Equipment Cost [€/kW]	170 [157, 252]	230 [187, 326]	50 [30, 70]	225 [150, 250]	456 [360, 720]	780 [650, 1040]	472 [160, 800]
Maintenance Cost [€/kW/yr]	17 [14, 22]	14 [13, 18]	7 [5, 10]	22 [17, 25]	24 [19, 30]	24 [19, 30]	25 [16, 27]
Fuel Cost [€/MWh]	45 ± σ	64 ± σ	127 ± σ	127 ± σ	127 ± σ	127 ± σ	51 ± σ
Technology properties							
Installed Capacity [kW]	10	10	10	10	10	10	10
Lifetime [yr]	20	20	20	12	18	20	20
Discount rate [%]	4	4	4	4	4	4	4
Efficiency [%]	97	95	100	t	t	t	88

Techno-economic standpoint of heat generation

In a simplified approach to the economics of heat generation, only the most significant costs and properties of decentralised technologies are included. Firstly, capital investments are included which are fixed, one time expenses, made up of equipment and installation costs. Equipment expenses cover the machinery including environmental facilities, whereas installation expenses cover engineering, civil works, buildings, grid connection, installation and commissioning of equipment [184]. A yearly fixed maintenance expense is added. It includes all costs that are independent of how the technology is operated [184]. Finally, marginal costs are included, which primarily depend on the technology operation time. Small scale effects such as the decrease in efficiencies or increase in maintenance expenses as a function of time are ignored. All technology properties and prices are formally introduced in Section 4.2.

The hourly accumulated cost, $X^{TOT}_{x,\theta}$, for a technology, θ, depends linearly on the heat load factor, μ_x, at each grid location, x, as:

$$X^{TOT}_{x,\theta} = X^{CAP}_{\theta} + \mu_x \cdot X^{OP}_{x,\theta} \tag{4.2}$$

A detailed review of the capital and marginal expenses, X^{CAP}_{θ} and $X^{OP}_{x,\theta}$, respectively, is conducted in the Supplemental Information Section 9.1. In this work, it is chosen to set the installed capacity to 10 kW for all technologies to scale the total cost to an appropriate value for a typical household. The capacity is kept fixed throughout the grid cells. However, the choice of capacity will not affect the results of this study as it is chosen to be identical for all technologies, see the Supplemental Information Section 9.1 for further details.

Example of an application

The heat load factor, μ_x, is calculated at first for each grid location, x, as shown in Equation 4.1. The heating expenses are then calculated for each technology, θ, and each grid location, x, by using Equation 4.2. The data covers a modelling time span of 20 years, since 20 years define the approximate extent of a climatic period and the typical lifespan of a heating technology. Figure 4.2 shows the accumulated expenses as a function of the heat load factor, μ, for the grid cell of southern Stockholm, Sweden. This is termed in the screening curve for heating technologies, analogous to the screening curves used for comparing electricity generation costs [190]. In the case of oil and biomass boilers, high fuel prices and low efficiencies result in large operational expenses, which make

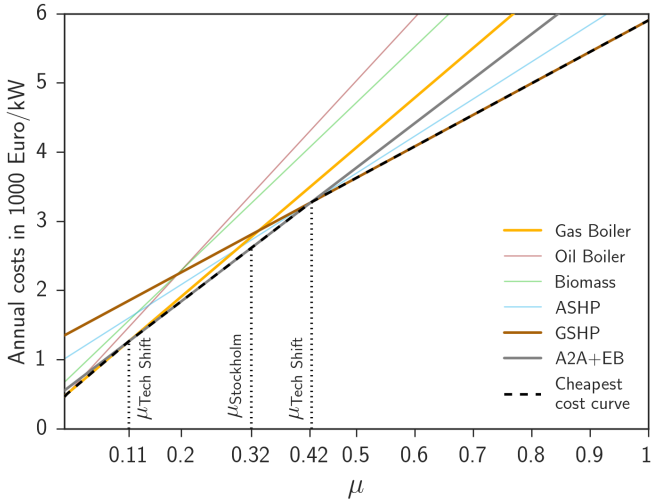

Figure 4.2: **A screening curve showing annual cumulative heating costs**. These are shown in 1000 Euro/kW as a function of heat load factors, μ, for the grid cell of southern Stockholm. $\mu_{\text{Tech Shift}}$ defines the heat load factor for which two technology crossing points occur. $\mu_{\text{Stockholm}}$ defines the heat load factor for Stockholm, Sweden.

these technologies highly uncompetitive. On the other hand, high COPs of heat pumps compensate for their high capital investments, which make these technologies competitive to gas boilers at high values of μ.

For Stockholm, the optimal technologies consist of gas boilers, air-to-air heat pumps with auxiliary electricity driven boilers and ground source heat pumps. For heat load factors below 0.11, gas boilers would serve as the cost-optimal choice for heating purposes. Since heat load factors never reach this domain it stays as non-applicable. For heat load factors between 0.11 and 0.42, air-to-air heat pumps with auxiliary electricity driven boilers would serve as a cost-optimal choice. Finally, for heat load factors above 0.42, ground source heat pumps would be cost-optimal. The heat load factor of southern Stockholm, $\mu_{\text{Stockholm}}$, equals 0.32, for which air-to-air heat pumps with auxiliary electricity driven boilers would serve as cost-optimal. This procedure is repeated for each of the 412 x 424 grid locations in the data set and for all of the nine climate models.

4.3 Results

Impact of climate change on the heating degree-days

Initially, results that show the extent to which the European heating degree-days change under the impact of global warming are presented. The gridded temperature profiles, $T_x(t)$, have been weighted according to the population density in each grid cell [191]. The population weighted temperature profiles are used to calculate the heating degree-days, which have been aggregated by summing over all grid-cell values within a country. The weighting is especially important for the Nordic countries as, e.g, Norway, where the sparsely populated areas in the north, otherwise, would contribute significantly to the aggregation. Figure 4.3 presents the yearly aggregated heating degree-days for Europe from 1970 to 2100 for each of the three projections of climatic outcomes, RCP2.6, RCP4.5 and RCP8.5. Each yearly result is composed of a climate model ensemble average and shown relative to the corresponding 1970 value. A 10 year moving average (full drawn curves) is used to highlight the long-term trends over annual fluctuations. It is clear that all climate change pathways result in a decreasing trend in the heating degree-days, with magnitudes being specific to the climate conditions of each RCP. The year of 2100 in RCP8.5 shows a decrease of approximately 42% in comparison to 1970, which is a consequence of almost 5 °C temperature increase in the business-as-usual scenario. Corresponding values for RCP2.6 and RCP4.5, are 16% and 24%, respectively. The uncertainties stay below ±8% of the ensemble average for all RCPs, which provides a strong evidence of agreement among the ensemble of climate models. The temperature data have been bias adjusted as explained in [179].

To estimate the resulting change in the CO_2-emission from space heating, a fixed national stock of heating technologies throughout the century is assumed in order to remove the effect of technological change and to isolate the effect of climate change. Based on 2015 values, the production of electricity and heat in the EU28 accounted for approximately 30% of total CO_2-emission, with heat production accounting for more than half of this share [192]. Altogether, a decrease of 42% in the heating degree-days for RCP8.5, leads to a decrease of 12.5% in the CO_2-emission. For RCP2.6 and RCP4.5 the respective values are 4.8% and 7.2%. In the following, the focus is on the supply side of heat, in a search for the cost-optimal technologies to cover the changing demand throughout the 21st Century.

For the remainder of the results section the focus is on each grid location sepa-

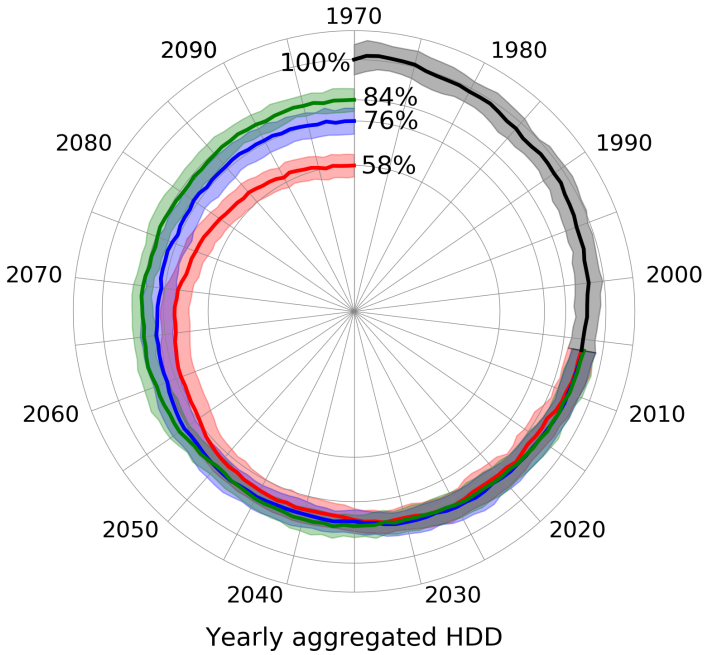

Figure 4.3: **10 year moving average of the yearly aggregated heating degree-days**. Full drawn curves shows the heating degree-days for each of the three projections of climatic outcomes, RCP2.6 (green), RCP4.5 (blue) and RCP8.5 (red). Each yearly result is composed of a climate model ensemble average and shown in percent of the corresponding 1970 value. $\pm 1\sigma$ standard deviations are shown with shaded regions.

rately rather than a country aggregation. For each location, a cost-optimal heating technology is found by following the procedure explained in Section 4.2. Initially, results are presented that are based on a predefined reference period for the ICHEC-EC-EARTH HIRHAM5 climate model. Equivalent results are afterwards presented for all climate projections and climate models, but during the analysis, all data has been treated equivalently.

Cost-optimal heating technologies in a historic time frame

The unperturbed cost assumptions, presented in the first four rows of Table 4.1, are subjected to uncertainties that strongly reflect the maturity of the technologies. These will naturally propagate into output uncertainties, meaning that the selection of cost-optimal technologies might be as uncertain as the input prices, which they are subjected to. In order to assess the robustness of the se-

lection of cost-optimal technologies, the optimisation process, as explained in Section 4.2, has been run with 100 Monte Carlo trials for the pricing scheme. Each pricing scheme consists of a random perturbation of the unperturbed installation, equipment, maintenance and fuel prices subjected to their respective uncertainty ranges.

The results of the optimisation processes are presented on the radar chart in Figure 4.4a for all pricing schemes. Each plot shows the normalised number of grid cells (proportional to land area across Europe) for which a technology serves as a cost-optimal, i.e., sum of the technology shares for a single plot is 100%. It becomes clear that each individual pricing scheme defines a unique technology distribution, resulting in a highly cost-sensitive outcome of the optimisation. The *unperturbed* pricing scheme, as presented in Table 4.1, has a tendency towards single technology dominance, i.e., gas boilers serve as cost-optimal in all grid locations, as shown with blue in Figure 4.4a. This results from a combined effect of the range of possible fuel prices, which is larger than the diversity in heat load across grid cells and the substantially lower gas boiler prices compared to the costs of the remaining technologies. A detailed discussion on the single technology dominance is provided in the Supplemental Information Section 9.2. Focusing briefly on the end of century climatic periods, it is found that the *unperturbed* pricing scheme leads to an identical technology distribution as for the historical period, for all projections of climatic outcomes. This is an important issue to address, as with this pricing scheme, the impact of climate change will not show its potential significance in the selection of technologies. The significance of climate change is therefore clarified by selecting a pricing scheme that to a high degree defines a balanced distributions of technologies. The selection is based on minimising the sum of squares of the difference between a technology share, θ_i, and the maximum appearing technology share, $\theta_{\max,i}$, as shown in Equation 4.3, which leads to the *balanced* pricing scheme, presented in Table 4.2. The *balanced* pricing scheme is classified as a unique outcome of the perturbation process, where the gas boiler expenses increase significantly compared to the respective increase in heat pump expenses, which gives heat pumps an economic benefit. The red plot in Figure 4.4a illustrates the resulting technology share by using the *balanced* pricing scheme. Gas boilers cover 59% of Europe whereas ground source heat pumps cover 26% and the hybrid of air-to-air heat pumps and auxiliary electricity driven boilers cover 15%.

$$\min_{\theta} \sum_{i} \left(\theta_i - \theta_{\max,i}\right)^2 \tag{4.3}$$

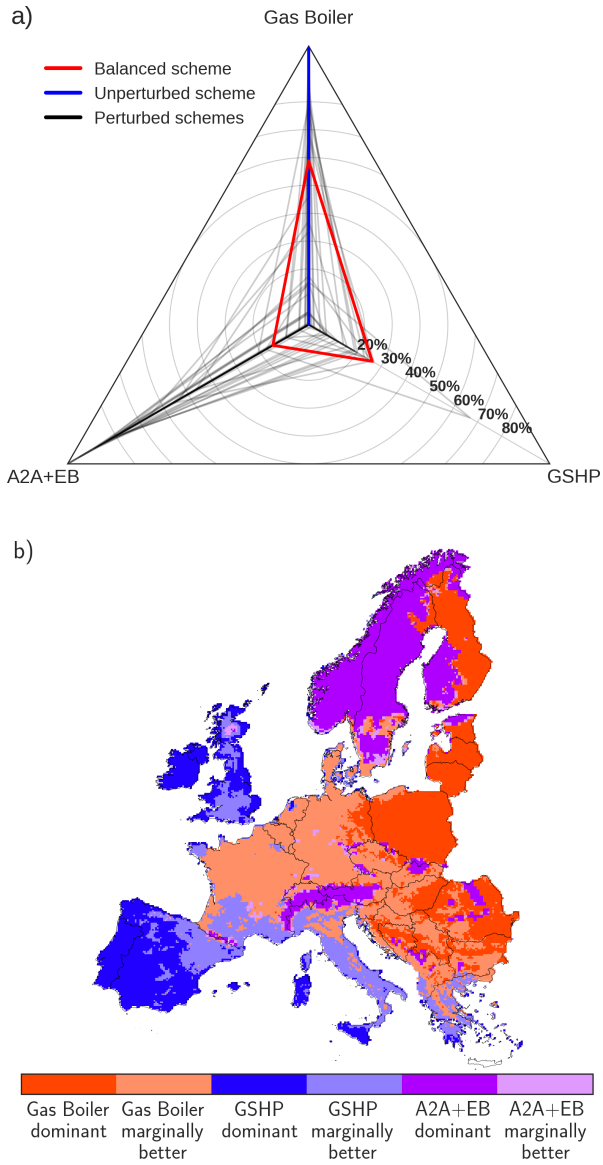

Figure 4.4: **Panel a: Cost-optimal technology distributions based on the ICHEC-EC-EARTH HIRHAM5 climate model.** Blue line is a result of the *unperturbed* pricing scheme. Shown with red is the resulting technology distribution by using the *balanced* pricing scheme. Black curves show technology distributions from 99 perturbed pricing schemes (see Equation 4.3). **Panel b: Spatial distribution of technologies resulting from the *balanced* pricing scheme, which is summarised with red in Panel a.** GSHP denotes ground source heat pumps. A2A+EB denotes the hybrid of air-to-air heat pumps with auxiliary electricity driven boilers.

Table 4.2: **The *balanced* pricing scheme, which is designed to enforce a balanced distribution of technologies across Europe**. The technology properties remain unchanged during the perturbation process, as presented in Table 4.1.

	Boilers			**Heat pumps**			**Biomass stoves**
	Gas Fired	Oil Fired	Electricity Driven	Air to Air (A2A)	Air to water (ASHP)	Ground to Water (GSHP)	
Balanced pricing scheme							
Installation Cost [€/kW]	117	99	64	65	347	443	84
Equipment Cost [€/kW]	200	293	48	194	520	824	336
Maintenance Cost [€/kW/yr]	18	17	7	21	24	24	23
Fuel Cost [€/MWh]	65	80	144	144	144	144	59

Oil and biomass boilers, and air source heat pumps are not economically viable for all pricing schemes and therefore not considered further. For most of these technologies, this is explained by a combination of high oil, biomass and electricity prices and low technology efficiencies. The unexpected outcome that air source heat pumps serve as economically unfavourable, can be justified by the technology COP that to a high degree determines the operational expenses. The empirical equations for the COPs, as presented in the Supplemental Information Section 9.2, are highly dependent on the heat source and sink temperatures. Soil temperatures are in general higher and more uniform over the the winter heating season compared to air temperatures. Ground source heat pumps therefore offer higher COPs over the year compared to air source heat pumps for any given sink temperature. Again, this reflects purely techno-economic potential, and does not consider geological or social barriers to uptake, especially the significant disruption caused by retrofit installations [29]. Depending on the hot water to the space heat ratio, the combined technology efficiency of air-to-air heat pumps with auxiliary electricity driven boilers will lower accordingly.

The spatial distribution of the cost-optimal technologies, resulting from the *balanced* pricing scheme, is shown in Figure 4.4b. This reflects where technologies would be best placed throughout Europe if there were homogenous prices, policies and public attitudes towards each - which is not the case in reality. The difference between the present-day distribution of technologies and this figure shows the impact of non techno-economic considerations on heating choice. The "marginally better" category defines a ±5% region around the intersection point of two cost curves, which defines an indecisive region where either of the technologies can provide a cost-optimal option for heating. The "dominant" category defines the outside region. Each technology is therefore subjected to one of the two categories:

Marginally better:

$$\mu_{\text{Tech Shift, x}} - 0.05 < \mu_x < \mu_{\text{Tech Shift, x}} + 0.05$$

Dominant:

$$\mu_{\text{Tech Shift, x}} - 0.05 \geq \mu_x$$

$$\mu_{\text{Tech Shift, x}} + 0.05 \leq \mu_x$$

where $\mu_{\text{Tech Shift, x}}$ defines the heat load factor at the intersection point of two

cost curves at a grid location, x, as shown in Figure 4.2. Interestingly, the historical time frame does not illustrate an expected north-south dipole, but a split for which heat pumps are dominating the coastal areas, and gas boilers the mainland areas. This result is partially explained by the Köppen–Geiger climate classification system for Europe [193] and partially by the assumption of constant hot water use across Europe, as detailed in the following.

The cold oceanic climate of West Europe results naturally in a large heat consumption throughout the year that, as a result, increases the heat load factor to a value of 0.5, depending on the grid location. Ground source heat pumps serve as cost-optimal in these regions, as a result of their relatively low operational expenses at high heat load factors. Air-to-air heat pumps with auxiliary electricity driven boilers serve as cost-optimal in Scandinavia. This is a result of the low hot water to space heat ratio in cold climates, which in turn limits the decrease of the combined technology efficiency. Contrary to North-West Europe, the tempered Mediterranean climate results in a decreased energy consumption for space heating. The hot water to the space heat ratio increases therefore significantly, which results in increased heat load factors. As for the West European areas, technologies with low operational expenses for high heat load factors serve as economically favourable. On the other hand the increased hot water to space heat ratio, decreases the combined efficiency of the air-to-air heat pumps with auxiliary electricity driven boilers, which makes this technology economically unfavourable in temperate climates. The overall cold winters and hot summers in the East European mainland result in low heat load factors. As a result, gas boilers become economically favourable.

From this point, the paper will only discuss results that are based on this pricing scheme, which is referred to as the *balanced* pricing scheme.

End-of-century projections

Figure 4.5 shows the spatial distribution of cost-optimal technologies resulting from the *balanced* pricing scheme. These are now shown for the three end-of-century time periods defined to span the years 2080–2100 for all of the climate projections. Historical results are added for easy reference. The most striking observation to emerge is the large increase in the attractiveness of heat pumps towards continental Europe, as a result of changing climatic conditions. This is the product of many interlinked factors, considering that climate change affects both the supply and demand side simultaneously. However, the main effect

is observed on the supply side, because of increasing heat pump COPs due to increasing winter temperatures. Another contributing factor might be the increasing heat load factors that emerge as a result of a fixed hot water use and a decreasing demand for space heat. For Scandinavia, the hot water to space heat ratio increases significantly due to a decreased need for space heating. As a result, the combined efficiency of air-to-air heat pumps with auxiliary electricity driven boilers decreases and therefore makes this technology economically unfavourable and out-priced by gas boilers.

Climate model ensemble average

Finally, in Figure 4.6 the results of Figure 4.5 are summarised for all climate models. The bars illustrate the climate model ensemble average of the population weighted technology distributions, for each individual country. The categories of dominance, "marginally better" and "dominant" have been merged in this figure. The errorbars denote the respective 25th and 75th percentiles. The bars are ordered according to descending shares of ground source heat pumps in the RCP8.5 end-of-century time frame. It is clear that the heating infrastructure for the far west and far south countries is largely unaffected by the climate induced weather changes. This can be seen from the largely unaffected shares of ground source heat pumps for the different climate periods. The robustness of this result is confirmed by the small uncertainties, illustrating a high agreement among climate models. Norway and Sweden make a sharp transition from air-to-air heat pumps with auxiliary electricity driven boilers to a mixture of gas boilers and ground source heat pumps, also confirmed by the high agreement among the climate models. The Baltics, including Finland make a transition from air-to-air heat pumps with auxiliary electricity driven boilers towards strong gas boiler dominance with high agreement across models. For the remaining countries, it is clear that a higher degree of climate change, suggests a transition from gas boilers to ground source heat pumps. These results come with relatively large uncertainties, which results in a fluctuating degree of technology transition among the climate models. In general, it is observed that a higher degree of global warming tends to increase the stock of heat pumps towards the mainland of Europe. On the other hand, this trend is difficult to compare between the climate projections because of different underlying assumptions from the Integrated Assessment Modelling.

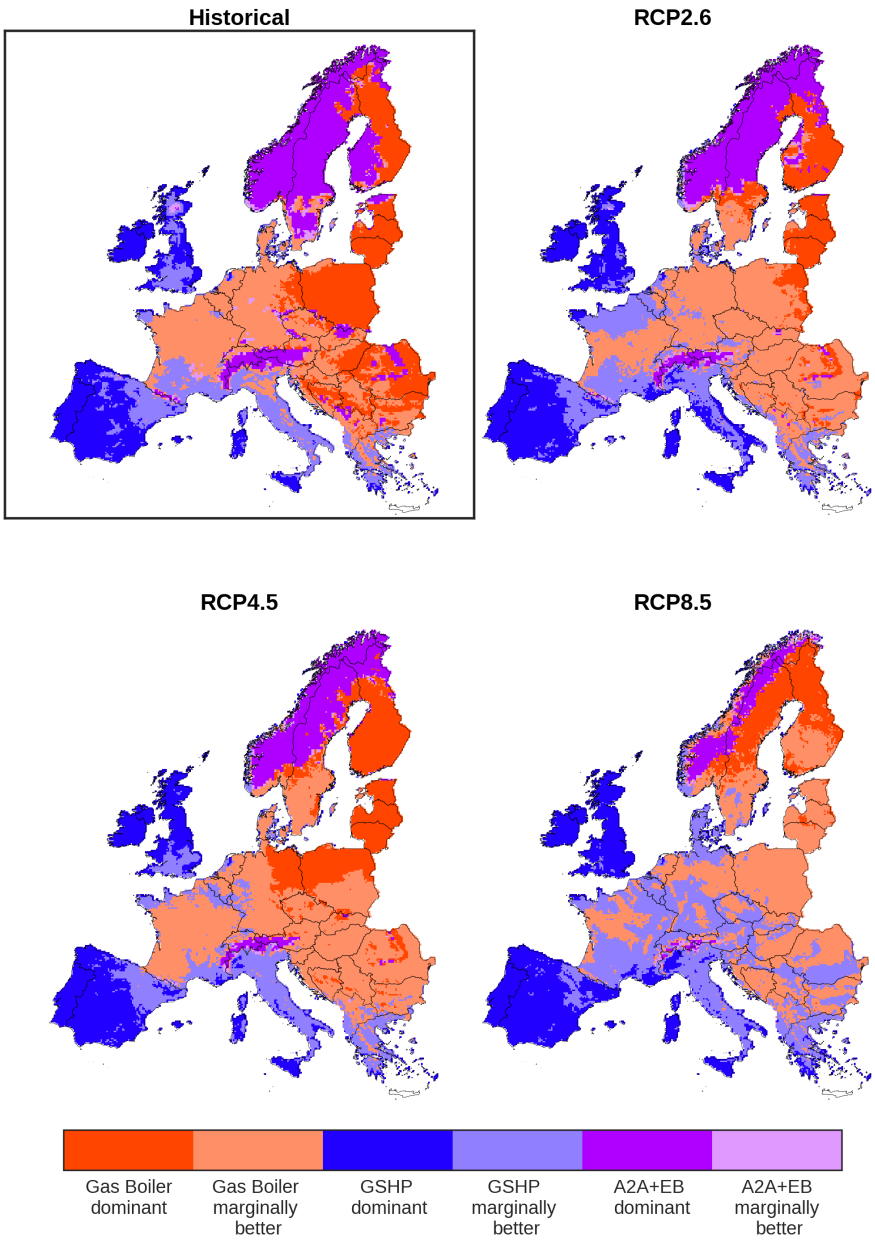

Figure 4.5: **Spatial distributions of the cost-optimal heating technologies by using the *balancing* pricing scheme**. The historical period is defined to span the years 1970–1990. RCP2.6, RCP4.5 and RCP8.5 spans a climatic period from 2080–2100. GSHP denotes ground source heat pumps and A2A+EB denotes the hybrid technology of air-to-air heat pumps with auxiliary electricity driven boilers.

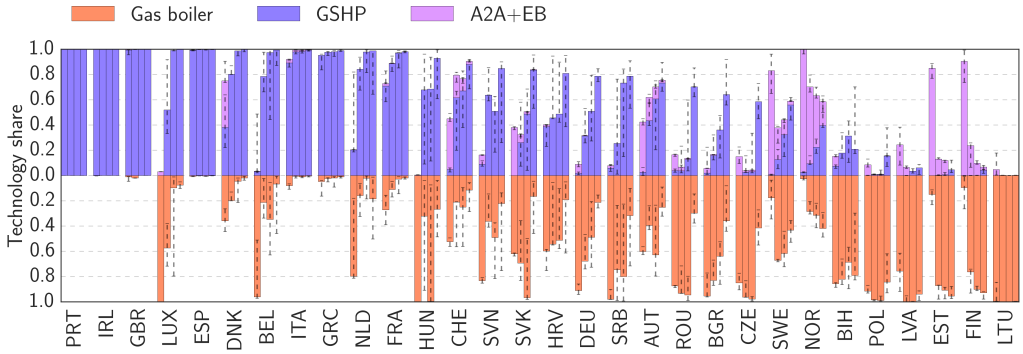

Figure 4.6: **Climate model ensemble average of the population weighted shares of the national technology distribution**. For each country the order of bars represent results from the historical, RCP2.6, RCP4.5 and RCP8.5 climate projections. Error bars illustrate the respective 25th and 75th percent quantiles. The shares of gas boilers and heat pumps have been separated for the matter of visualisation. The y-axis illustrates therefore the same quantity but in separate directions. GSHP denotes ground source heat pumps and A2A+EB denotes the hybrid of air-to-air heat pumps with auxiliary electricity driven boilers.

4.4 Discussions

Current status of heat policies in Europe affecting the stock of heating technologies

This paper finds that across Europe as a whole, space heating demand declines by 16% to 42% under different climate change projections from 1970 to 2100. This is consistent with other studies where a decreased heating demand in Europe have been observed across an ensemble of Earth System Models under RCP4.5 and RCP8.5 [194]. Similarly, a 37% decrease in residential heating demand have been found by the period 2071-2100, compared to 2010, based on five global climate scenarios [195]. In section 4.4, the focus is on general policy implications in particular relating to the flexibility of existing heat policy frameworks to adapt to reduced heating loads given more stringent building regulations and climate change.

The second part of this analysis points to different zones of Europe where heat pumps or gas boilers may be more or less optimal in cost or performance terms given projected temperature increases to the end of the century. In general, ground source heat pumps are shown to be more economically optimal in western and southern Europe, whereas gas boilers are more optimal in eastern Europe and some Nordic countries.

In this section, the numerical findings on cost-optimal decentralised heating technologies under climate change projections are compared with the current state of policies, national policy strategies and technological deployment in different European countries. Cost-optimal technologies have been found for the period 2080-2100, and it is argued that current heat policies and longer-term strategies for heat decarbonisation, for example to 2050, are relevant to the interpretation of these findings. Although the European stock of heating technologies will have undergone several replacement cycles by the late 21st Century, there are important sources of path dependency and lock-in that have led in particular to increasing returns to adoption of incumbent heating technologies such as natural gas boilers in the UK, or biomass-based district heating in Sweden [196]. Without policy intervention to address these, there is a risk that existing, incumbent heating technologies and linked infrastructures are self-perpetuating, limiting opportunities for and slowing the deployment of alternative decentralised heating technologies such as heat pumps. In addition, it would be advantageous to support learning and cost reduction of heat pumps [197] through policies to support their increased installation in regions where

they are likely to become more cost-optimal under climate change in the longer term.

It is found that in general, national heat policy outcomes and intentions align reasonably well with cost-optimal technologies as indicated by the model used in this work. However, there are also important mismatches between cost-optimal technologies and their real-world deployment. These mismatches are at least partly a product of the presence or absence and balance of policies which support or hinder the deployment of heat pumps or gas boilers. It is argued that policy makers should be mindful of which technologies are most economically optimal in particular regions both currently and under projected climate change, in order to deliver cost-optimal policy outcomes.

Another focus of this section is on national-scale policies in order to understand variation between countries. Nevertheless, a number of EU heat pump support policies have been implemented and are interconnected with some national policies. For example, the EU Renewable Energy Directive in 2009 officially recognises heat pumps as a renewable energy technology [198]. It sets out a minimum efficiency level needed to produce renewable heat from electrically-driven heat pumps, equivalent to a seasonal performance factor (SPF) of over 2.88 [199]. This Directive also contributed to quality assurance in Europe by requesting that member states should introduce or have in place certification schemes for installers of heat pumps by 2012 [198, 200]. In 2016, the European Commission published the first EU Heating and Cooling Strategy [201]. This strategy was endorsed by the European Parliament, which also proposed that subsidies supporting fossil fuel heating should be phased out [202].

Policy frameworks and changes in heating demand

The findings of this study point to lower heating demand with increased global warming. Heating demand is also expected to fall further through the 21st Century based on EU-wide and national efforts to tighten building standards. Policies and regulations promoting building energy efficiency are relatively recent and will take time to address around three quarters of the European building stock which is considered to be energy inefficient [203]. There are significant challenges with reducing heat loss from buildings and replacing old, inefficient heating appliances, and these challenges vary across different sectors, e.g. service buildings, public buildings, problems with split incentives in privately-rented homes, industry [201, 204].

In Europe, mandatory standards at an EU and national level have resulted in increased thermal efficiency of new and refurbished buildings, and greater use of more efficient heating appliances such as condensing boilers and heat pumps, leading to decreasing heat demand at an individual building level [205, 206, 204]. There is significant potential for this trend to continue with further replacement and renovation of existing buildings, particularly since the average number of new dwellings built every year from 2000 to 2012 represented just 1% of the EU housing stock [206]. In 2016 in the EU, heating consumption per m^2 was 68% of the level of heating demand in 1990. However, overall heating consumption only declined by 4% due to the increase in building floor area over this period [205].

The Energy Performance of Buildings Directive was introduced in the EU in 2010 and stipulates minimum energy efficiency standards for building renovations, while also requiring new buildings to consume close to zero energy from the end of 2020 [203]. The Energy Efficiency Directive (2012) further requires EU member states to produce a long-term strategy for investing in improving the energy performance of existing residential and commercial buildings after 2020. This should include action plans for reducing heating and cooling demand and undertaking deep building renovations typified by 60% or greater energy efficiency improvements. These regulations are technology neutral and therefore allow flexibility to achieve stipulated energy savings with a diversity of highly-efficient, decentralised heating technologies [203].

Similar mandates have also been enacted at a national level in Europe. For example, Germany introduced the Energy Efficiency Ordinance to implement the European Energy Performance of Buildings Directive. In the Netherlands, progressively stronger energy efficiency standards have resulted in decreasing heat demand. France introduced the Régulation thermique in 2012, requiring all new buildings (constructed from 2013 onwards) to meet a maximum level of primary energy consumption meaning that direct electric heating could not be used in new buildings [204].

Technology support policies: southern and eastern Europe

The findings in Section 4.3 indicate that ground source heat pumps are favourable under the end-of-century scenario in southern European countries with a Mediterranean climate such as Spain, Portugal, Italy and Greece. However, there ap-

pears to be relatively limited policy support for heat pumps in these countries, where the majority of sales are for air-to-air heat pumps which can provide both heating and cooling [202, 207]. In Portugal, there has been an absence of national incentives for heat pumps [207]. In Spain, reversible air-to-air heat pumps are mainly used for cooling; gas boilers are more likely to be used for space heating [34]. Small air-to-air heat pumps may be combined with electric heating to provide both heating and cooling in some Mediterranean coastal zones of Spain. Italy has made tax reductions available for the installation of heat pumps on the condition that high seasonal performance factors are achieved [32, 208]. There have also been information dissemination activities - the Gruppo Italiano Pompe di Carole is a group of manufacturers which promotes heat pumps through exhibitions, seminars and training courses [34].

Most homes in Greece use diesel heating oil for space heating, while electricity, natural gas and biomass provide less than 12% of total space heating each [209]. The installed capacity of ground source heat pumps in Greece has experienced a rapid growth in the last two decades, from 0.4 $MW_{thermal}$ in 1999 to 135 $MW_{thermal}$ in 2014 [210]. This is a result of several factors, including rising oil prices compared to electricity prices, higher public awareness of ground source heat pumps and legislation introducing a licensing process for installations. In recent years, the development of the ground source heat pump market has been adversely affected by the economic crisis and an inactive construction industry [210].

The results show gas boilers to be optimal in eastern Europe particularly under RCP2.6 and RCP4.5, see Figure 4.6. There is uneven agreement between this finding and the direction of heating policies in different eastern European countries. Following the decline of communism, many eastern and central European countries began to shift away from expensive and poorly maintained district heating systems towards individual household heating technologies [211, 212]. In Poland, coal is the dominant fuel for heating, and therefore a transition to gas heating and/or heat pumps would help to improve air quality and achieve decarbonisation. 40% of Poland's 13 million houses use individual coal boilers or furnaces for space heating [34, 202], while coal-fuelled district heating supplies space heating to approximately a further 30% of total dwellings [202, 213]. Around two thirds of the 2 million gas boilers installed in Polish houses are used only as a supplementary heat source in cold periods [34]. Despite a lack of specific policy support for heat pumps from the Polish state, sales of heat pumps grew to over 20.000 per annum by 2015 [33, 34, 202].

Heat pump sales in Slovakia have been constrained by the presence of a dense gas network [34]. There were no investment subsidies for heat pumps prior to 2015, and retrofitting heat pumps to buildings with existing gas connections is an unattractive investment; most market potential for heat pumps is in the new build sector. In the Czech Republic, the findings reveal ground source heat pumps as economically favourable in RCP8.5 (although gas boilers are more cost-optimal in the other projections). Investment subsidies were introduced in the Czech Republic in 2014 and support ground source and air source heat pumps which achieve a minimum efficiency standard [34].

Technology support policies: northern and western Europe

The findings in this study show that ground source heat pumps are more cost-optimal in western Europe even under moderate temperature increases, but less optimal in northern Europe. In a number of western and northern European countries, a combination of policies have been effectively implemented to stimulate the take-up of heat pumps, including policies to raise technical standards, promotion and information campaigns and investment subsidies [32]. Up-front grants have been provided in Austria for consumers to switch from fossil fuel heating to heat pumps which achieve minimum performance standards based on the seasonal performance factor [214]. In Denmark, an information campaign was followed by a subsidy scheme in 2010 to promote the replacement of dilapidated oil heaters with energy efficient heat pumps [215]. A subsidy scheme in Sweden from 2006 to 2010 made up-front grants available for households to switch from oil heating to heat pumps, district heating or biomass. The entire budget for this subsidy was used up after the first year of the scheme, with heat pumps being the most popular replacement for oil heating [204, 216].

Long-term stability of policy support has been an important success factor for substantial deployment of heat pumps in countries such as Sweden, Switzerland and Austria, since this increases industry and consumer confidence [32]. Carbon and fuel taxes represent further instruments capable of incentivising the switch from fossil fuel heating to low carbon alternatives. Carbon taxes have been adopted, in particular, by northern European countries since the early 1990s, including Finland, Norway, Sweden and Denmark [217]. Sweden has the highest carbon tax in Europe, which has been increased threefold since 1991 [218]. Separate taxes have also been applied on natural gas heating and heating oil. Energy and carbon taxes in Sweden have helped to encourage the substitution

of oil boilers with heat pumps [204, 216].

In Germany, where 54% of households are connected to the gas grid [32], there were over 700.000 heat pumps in operation in 2015 [202]. This is consistent with cost-optimal technologies indicated for this country in Figure 4.6: principally gas boilers in RCP2.6 and RCP4.5, and a mixture of heat pumps and gas boilers in RCP8.5. Heat pumps have replaced some gas boilers in Germany, but this is largely restricted to new build homes: the share of heat pumps' contribution to primary heating energy increased from 1% of new build homes in 2000 to 27% in 2017. The equivalent share for natural gas declined from over three quarters of new homes in 2000 to 39% in 2017 [219].

A combination of building regulations and investment subsidies have helped to increase the proportion of heat pumps providing heating in new build houses in Germany [204]. The Market Incentive Programme (MAP) for renewable heat has made investment grants available since 2008 for the installation of ground-source and air-to-water heat pumps, linked to minimum seasonal performance factors [33, 204]. Higher investment grants are available for ground source heat pumps (given their higher up front costs) in comparison to air source heat pumps. This policy is in line with the numerical model output which shows ground source heat pumps as economically favourable in Germany under higher temperature increases, see Figure 4.6. While MAP also offers higher grants for heat pumps installed in existing homes compared to new builds, the share of heat pump sales to the retrofit sector has still been decreasing in recent years. This illustrates that increasing the portion of renewable heat in the existing housing stock continues to be a key priority [204].

The results indicate that combined air-to-air heat pump/electric boiler systems are cost-optimal in Norway and Sweden under moderate temperature increases, see Figure 4.6. In Norway, electricity price rises and investment subsidies for end users have stimulated the uptake of heat pumps [204]. A subsidy programme for householders was introduced in 2003 which covered 20% of the initial costs for installing air-to-air heat pumps, although this subsidy has since ended [204, 220]. In 2015 there were approximately 750.000 heat pumps installed in a third of all households in Norway [221]. In Sweden, over half of heat pump sales in buildings in 2016 were for reversible air-to-air heat pumps, which can operate in conjunction with direct electric heating in existing homes [202, 207, 222]. Swedish building regulations requiring greater energy efficiency and lower heating demands in new buildings have contributed to the increas-

ing dominance of air-to-air heat pumps compared to ground source heat pumps since 2005 [33].

Prospects for heat pumps: lessons from countries with natural gas heating

In this paper, a cost-optimal distribution of decentralised heating technologies for Europe is presented. The analysis does not reflect how country to country possibilities for shifting to a more optimal mix of heating technologies are constrained by path dependency and lock-in to existing heating infrastructure. Selection and replacement of heating technologies is dependent upon contingent factors such as the coverage and extent of gas networks, and availability of local natural resources for fuels and energy sources [32, 196, 204].

Policy support aimed at achieving a transition from gas boilers to heat pumps is challenging in countries such as the Netherlands and the UK where gas heating is dominant. Both countries have made very limited progress in substituting gas heating for lower carbon alternatives. The numerical findings show that ground source heat pumps are a definitively cost-optimal solution in the UK, see Figure 4.6. However, the UK has a low uptake of heat pumps compared to many northern and western European countries. In part this is due to path dependent developments that led to the emergence of gas central heating as an affordable, convenient and familiar technology for UK household consumers, which provides high levels of thermal comfort [196]. There is also a lack of continuous, coordinated policies on technical standards and promotion of heat pumps in the UK, leading to poor consumer awareness and low confidence in the technology [32, 223]. In order to help meet the 5th carbon budget [224], the UK's Committee on Climate Change has set a target for at least 2.5 million heat pumps to be installed in UK homes by 2030, compared to a total stock of approximately 160.000 in 2016 [225].

In contrast to the UK, the Netherlands has ambitious long-term policy targets to phase out the contribution of natural gas to its heat supply. Figure 4.6 suggests that in the Netherlands, heat pumps are cost-optimal under climate change scenarios. On other hand, approximately 85% of dwellings in the Netherlands use natural gas for space heating [202]. The dominance of natural gas as a heating source was cemented after the discovery of extensive local gas reserves in the Groningen gas field in 1959 [204]. Earthquakes in 2012 caused by gas extraction from the Groningen gas field led to public protests and the government therefore decided to reduce gas production [226]. Depletion of the gas field is also expected, so that the Netherlands is likely to become a net importer of natural

gas from 2030 to 2035 [227]. Energy security concerns over the potential future need to import Russian gas, in addition to climate policy, have also motivated long-term national goals to seek low carbon alternatives to natural gas [204].
The 2050 Dutch Energy Agenda implies that most of the country's 6 million homes currently heated with natural gas will need to be disconnected from gas supply by 2050 [202, 228]. This is based on a long-term target to reduce CO_2-emission from the residential and commercial heating sector by 80-95% by 2050 [228]. The Dutch government has indicated that electrification could be central to plans to phase out natural gas heating, and have stated that energy efficiency, heat pumps and district heating would be three key elements to a low emission building sector. Strategic decisions will need to be made about the future of the existing gas grid, in terms of whether it could be utilised as a carrier for alternatives to gas such as hydrogen and green gas, or whether it might need to be decommissioned and replaced [204].

Study limitations

The analyses of this paper are subject to a number of limitations. The main limitation deals with the assumption of constant fuel and technology related prices across regions and time. As previously stated, this is a simple approximation which leads to an unrepresentative picture of the real world. However, this is necessary for performing an objective study of the influence of climate change, separate from the political and personal drivers, and thus answer the research questions of this work.

Secondly, the optimisation was limited to only consider cost constraints. Other important subjects to constrain are the different projections of RCP related CO_2-emission. This limitation suggests that results belonging to otherwise low or negative CO_2-emission scenarios as, e.g., for the end-of-century RCP26 pathway, should be interpreted with caution. An in-depth analysis of the cost-optimal design decisions, including CO_2-emission constraints, would additionally require a coupling to the electricity sector. Such an extensive work require a study on its own.

Then, this study is limited to only consider decentralised heating technologies, such as small scale fossil fueled boilers or heat pumps. Large-scale centralised technologies, such as district heating, are also important to consider, but these are subject to different economic and political considerations, and thus cannot be thought of as a like-for-like replacement for existing heating systems in all

countries of Europe. This study can be extended to include these by assigning heat transportation to densely populated areas as, e.g., cities or suburbs.

A fourth limitation is the relatively low number of climate models that are used to acquire the results. To the best of the authors' knowledge no other climate affected data exists with higher data granularity. If applicable, an identical analysis can be performed by including more climate data.

The results do not consider the practicality of deploying technologies in different countries or locations given the relative coverage of gas or electricity networks, natural resource endowments, and the origins of path dependencies in incumbent heating systems. Therefore, in some countries or areas, certain heating technologies, even though being cost-optimal, might not be physically feasible to install because of the lack of distribution networks to meet the large demands for heating [229].

Additionally, this analysis does not account for the costs of network infrastructures (also given their local availability) required to operate the heating technologies, i.e. gas and electricity networks. It is recognised that network costs may vary significantly by location or depending on energy sources and vectors used to achieve heat decarbonisation [230], and this could have a significant impact on the results in terms of overall system and end user technology costs. Also, location-specific barriers to technology uptake are not considered, such as lack of suitable building types or land availability for ground source heat pumps in urban areas. Together, these constraints could have a significant impact on results, and are recommended as areas for further study.

4.5 Conclusions and policy implications

This study set out to determine the cost-optimal design decision for decentralised heating in European homes. With fixed costs, the climate is allowed to determine the most economical heating technologies over a timespan of 20 years in a historical period defined to span the years 1970-1990 and for three end-of-century time periods defined to span the years 2080-2100. Bias-adjusted high resolution temperature data from 9 combinations of 5 global climate models downscaled by 4 regional climate models under the EURO-CORDEX project, have been adapted to model the heat demand and supply side. Due to transparency issues on actual heat consumption data, the theory of heating degree-days is used as a proxy for the variations in the day-to-day heat demand over 20 years. Notwithstanding the impact of policies or consumer preferences, it is shown that the climate holds a vital role in the cost-optimal design of decentralised heating infrastructures in Europe.

It is found that climate change introduces a decreasing demand for space heating. This demand is estimated to decrease by approximately 42%, 24% and 16% in 2100 for the RCP8.5, RCP4.5 and RCP2.6 climate projections, respectively, compared to the corresponding value in 1970. Peak heating demand may have been overestimated in the UK for example [231], and can also be expected to reduce with the implementation of tighter building energy efficiency standards and a more thermally efficient European building stock by later in the century. In Europe, current EU and national heat policies and regulations do not appear to be future-proofed to account for potential long-term changes in heat demand, and how these changes might affect the optimal mix and economics of decentralised heating technologies. It is recommended that similar to EU mandates for energy efficiency in buildings, it is important that heat policy frameworks take a flexible and technology neutral approach that allows for uncertain changes in heat demand due for example to climate change, energy efficiency policies, or increased electrification of heating. The calculation in the EU Renewable Energy Directive, which stipulates a minimum SPF for heat pumps to be considered a form of renewable energy [199], may also need to be revised to account for the impact of lower end-use heating load on heat pump performance.

Climate change and cost-optimisation suggest a shift in the decentralised heating infrastructure from gas boilers to ground source heat pumps, for a majority of the European countries. This is driven by the two main factors. Firstly, climate change will increase ambient temperatures and thus improve the efficiency of heat pumps. Secondly, the diminishing need for space heating means the year-

round demand for hot water becomes more important, increasing the utilisation of heating technologies through the year, thus benefiting heat pumps with their high upfront, but low ongoing, costs. For many countries this is in correspondence with aggressive policies on increasing penetrations of heat pumps. The far west and far south European countries are subjected to a high heat load factor, for which ground source heat pumps serve as economically favourable. As for the UK, there is a comparatively low uptake of heat pumps, where key barriers to further uptake are a lack of policy continuity and co-ordination and low consumer confidence and awareness. On the other hand, the Netherlands is developing ambitious long-term policies to increase the penetration of heat pumps. Portugal, Spain, Italy and Greece lack policy support for heat pumps, where the majority of sales are for reversible heat pumps which provide both heating and cooling. Aggressive policies for substantial deployment of heat pumps are evident in countries such as Sweden, Switzerland and Austria. For Switzerland, this is in correspondence with a higher penetration of ground source heat pumps at the end-of-century time frames in all RCPs. Climate conditions in Sweden and Austria lead to a marginal increase in the penetration of ground source heat pumps, while gas fired boilers take the largest technology share. High carbon taxes in Finland, Norway, Sweden and Denmark are used to pursue a decrease in the use of fossil fuel heating technologies. Only for Denmark do the climate conditions align with these policies. The continental climate across eastern Europe leads to a robust choice of gas boilers as the cost beneficial choice of heating in all RCPs.

Despite the findings suggesting a wider deployment of ground source heat pumps, the majority of heat pump sales in Europe over the last decade have been for air source heat pumps and in particular reversible air-to-air heat pumps which can provide both heating and cooling [202, 207]. Air source heat pumps tend to be cheaper and easier to install than ground source heat pumps, and have benefited from technical improvements, which have raised their efficiency and increased their suitability to perform effectively in a wider range of climatic conditions and building types [202].

In general, ground source heat pumps are used to a greater extent in countries with colder climate zones, e.g., Nordic countries, where the heat source temperature needs to be more stable, although reversible air-to-air heat pumps still have the highest share of heat pump sales in these countries over the last ten years [202]. Reversible air-to-air heat pumps dominate sales in warmer, southern Mediterranean countries, where purchases of ground source heat pumps

are minimal or absent. This overall pattern is by no means universal and the country-to-country distribution of ground source versus air source heat pumps is affected by various non-climate related factors affecting consumer uptake of heat pumps, including upfront costs, building regulations, availability of sufficient space for ground source heat pump components and thermal stores, and inconvenience caused by installation [202, 232].

It is recognised that national heating policies aimed at decarbonisation should be designed with respect to a portfolio of technologies, including those not featured in this analysis, for example district heating or hydrogen. These findings should therefore not be treated as a policy prescription, and moreover the analysis focuses on the impact of climate change on technology costs and excludes a calculation of carbon intensity. This carries the consequence that under higher temperature increases, gas heating is indicated as a more optimal technology in a country such as Sweden, which has promoted deep decarbonisation of its heating sector and where the heat pump market is mature. Meeting the 1.5 °C target under the Paris Agreement and net zero emission reduction targets imply a significantly reduced or minimal role for natural gas in the energy mix. Gas heating could have a role as a bridging technology to low carbon heating for example through the use of hybrid heat pumps, whereby a heat pump operates in parallel with a gas boiler.

This study underlines the benefit of accelerating heat pump support policies in countries such as the UK and Netherlands which depend largely on natural gas heating. These countries can learn from the experience in northern and western Europe. While this study points to heat pumps being more cost-optimal in western Europe under projected climate change, heat pump markets in countries such as Austria, Switzerland, France and Germany are actually less mature than in northern Europe. Gas boilers are also identified as being more optimal in eastern Europe, where in some cases (such as Poland) there may be potential to displace more carbon intensive coal heating with natural gas heating. One of the most surprising outcomes of the study is that ground source heat pumps are identified as suitable solutions in southern Mediterranean countries. This points to a need for more coordinated policies in these countries to support heat pumps as a low carbon alternative for heating in buildings, given the current predominance of reversible heat pumps which are also used for air conditioning, and have emerged largely as a market development in the absence of specific policy assistance.

Acknowledgement

The authors wish to express their gratitude to O. B. Christensen and F. Boberg from the Danish Meteorological Institute for their contribution to understanding the climate outcomes and for supplying out data from the regional climate model HIRHAM5. G. Nikulin from the Swedish Meteorological and Hydrological Institute is thanked for supplying out data from the regional climate model RCA4. E. van Meijgaard from the Royal Netherlands Meteorological Institute is thanked for supplying out data from the regional climate model RACMO22E. P. Lenzen from the German Climate Computing Center is thanked for supplying out data from the regional climate model CCLM4. Parts of the EURO-CORDEX climate data have been acquired via ESGF data nodes. Thanks to Fabian Levihn from Stockholm Exergi for providing district heating consumption data. Thanks to Aarhus University Research Foundation for funding S. Kozarcanin with funding number AUFF-E-2015-FLS-7-26. I. Staffell acknowledges the Engineering and Physical Sciences Research Council for funding the IDLES project (EP/R045518/1). G. B. Andresen was funded by the RE-INVEST project, which is supported by the Innovation Fund Denmark under grant number 6154-00022B. R. Hanna and R. Gross were funded by the UK Energy Research Centre - Phase 3 (UK Research and Innovation Energy Programme, grant reference EP/L024756/1), the Committee on Climate Change and the Department for Business, Energy & Industrial Strategy.

Author Contributions

IS, GBA and SK designed the study. IS and GBA furthermore supervised the entire study. SK administrated the project, performed the scientific investigation, wrote the majority of the paper apart from Section 4, performed data validation and visualisation. SK wrote the supplementary information. RH produced Section 4 on the political aspects in collaboration with RG and drawing on research undertaken by RH and RG for UKERC.

Declaration of Interest

The authors declare no competing interests.

CHAPTER 5

Techno-economic benefits of a fully coupled European electricity and heating system in a 21st century climate

Article

Kozarcanin, Smail; Andresen, Gorm Bruun. *Techno-Economic Benefits of a Fully Coupled European Electricity and Heating System in a 21st Century Climate Change*. In preparation for publication in One Earth.

Project Dissemination

The project has been presented on a few occasions in-house.

Author Contributions

S. Kozarcanin was responsible for managing and coordinating the research activities and performed the formal analysis and investigation. S. Kozarcanin wrote the original draft and visualised the data. Associate professor G. B. Andresen and S. Kozarcanin developed the original concept. Associate Professor G. B. Andresen supervised the project.

Summary

Anthropogenic activities have already exposed the global climate to significant change with devastating results. Timely mitigation strategies are therefore important and can be achieved through cross-vector integration and sector coupling, but time is limited. As a first step towards a carbon neutral energy economy an investigate into sector coupling is performed by imposing additional synergy between the European electricity and heating systems. Because of uncertain outcomes of climate change, three diverse CO_2-concentration pathways from the IPCC AR5 are introduced. Three-hourly time series on the national wind and solar capacity factors, electricity and space heat consumption, which were carefully generated from an ensemble of nine climate models, are used to represent various outcomes of the European climate during the 21st Century. Through a techno-economic cost-optimisation, it is found that radical CO_2-constraints are consistent with extreme electrification, which almost doubles the system costs compared to historical standards. Carbon intensive pathways allow for fossil-fuel dominance with significant cost reductions. Independent of the concentration pathways, the costs of a flexible system coupling are comparable to that of a weak system coupling.

5.1 Introduction

It is now definite that anthropogenic CO_2-emission is the main driver in climate change [1] leading to increasingly frequent and devastating weather events around the globe. Mitigation of climate change requires therefore immediate action, which can be enforced through energy system transformation [2]. 195 member countries of the United Nations Framework Convention on Climate Change, UNFCC, [233] have recognised this issue to be the ultimate objective of international climate negotiations. Electrification of end-use sectors is currently the best known and most feasible solution for rapid decarbonisation [3, 4], but time becomes a limited factor if increasing degrees of climate change are to be avoided. Studies even suggest that the energy demand could be met with pure renewable technology [234, 235]. Electrification of the energy system can in turn provide additional flexibility, reliability and adequacy. Based on previous studies the initial hypothesis is that the design of energy systems will change from traditional fossil fuel dominance where the electricity and heating sectors are loosely coupled into a fully coupled system [236, 237]. It is expected that a change in the cost-optimal system design will influence the energy system transformation in the direction of the cost-optimum over a period of about 30 years. Thus the real-world system is expected to drift towards the cost optimum, but not to closely resemble it, e.g., due to technology lock-in.

Given this, the benefits of imposing additional synergy between the European electricity and heating systems are analysed and compared to the alternative of maintaining today's pure system coupling, which to some extent might perform equally well. However, mitigating climate change is a global collective work, which today is one of the most difficult social challenges [238], and so it becomes important to consider a diverse range of climatic outcomes. Information on long-term projections of climatic outcomes for the continent of Europe are contained within the Representative Concentration Pathways [15], RCP, provided by the Intergovernmental Panel on Climate Change [239], IPCC, on a yearly time scale from 2000-2100. The transition towards net-zero carbon emission is represented by the reconstructed concentration pathway 2.6, or RCP2.6 [46], which closely resembles the 2015 Paris Agreement [8] to keep the global average temperature increase below 2 °C and pursue efforts to reduce the limit to 1.5 °C. Additionally two reconstructed concentrations pathways are implement, RCP4.5 [49] and RCP8.5 [56], which contain intermediate and relaxed CO_2-emission targets, respectively. Previous work has shown that the variable renewable power production and power consumption change by up to 5% compared to historical levels as a consequence of a changing climate [132]. On the

other hand, climate change is expected to strongly influence the heating sector via the temperature dependent heat demand [240], and the final systems may be quite different in different climates. With this in mind, a techno-economic cost optimisation is applied for the capacity investments and dispatch of energy producing technologies for each climatic pathway through a new power system optimisation framework for simulating and optimising modern power systems, PyPSA, [241].

Initially, a loosely coupled electricity and heating system is designed that serve as a base-line scenario. Methanisation is the only technology linking the individual systems, as shown in Figure 5.1. The produced methane can be used in all gas-fired technologies. Combustion of pallets and gas are the only ways of heat generation. The more sophisticated strong coupling, as shown in Figure 5.2, includes heat pumps, electricity driven boilers and cogeneration of power and heat. Detailed descriptions of the systems are supplied in the Methods section. The electricity node is connected to a large-scale transmission system, which consists of a network of 30 nodes each representing a country of Europe with 50 cross border AC and DC transmission lines operated by members of the European Network of Transmission System Operators, ENTSO-E. Such a network was first time introduced in 2010 [109] and modified hereafter [112] and later commonly used in the literature [132, 242, 243].

Each node is supplied with a carefully generated 3-hourly, national aggregated, time series on the wind and solar power potential, electricity and heat consumption covering the years from 2000 to 2100. The time series have been generated on the grounds of cutting edge climate change affected weather data [132, 240, 179]. Weather data has been supplied from fours regional climate models, RCM, downscaling five CMIP5 global climate models [61, 180], GCM, forced by the different climatic pathways provided by the IPCC. This results in nine high resolution climate models. The data is a final product of the EURO-CORDEX project [70] and comes with a temporal and spatial resolution of 0.11° x 0.11° and 3-hours, respectively. Such granularity is important for capturing regional and temporal weather differences for energy system analysis. Climate change data with this granularity is suitable for energy system research where extreme events such as cold winters with low winds are captured [132].

Modelling all sectors of the energy system with highly granular data is computationally demanding and previous studies have either focused on a few demand sectors or sacrificed the granularity [237]. The large ensemble of climate models

in this study adds up to 11200 model years with a real simulation time of about 30 days. This study illustrates the importance of early decision making if the global average temperature increase is to stay below catastrophic levels.

Although a technical assessment of energy system transformations is used, improved political actions, better economical management or behavioural changes have to be considered as well and improved [244, 245]. This gap between science and policy has to be addressed and improved. So far a limited amount of studies have reported detailed research on the impact of climate change on sector coupled energy system transformations for climate change mitigation [2, 246]. In general, studies mainly focus on individual sectors as, e.g., heating, electricity, agriculture, etc. or various political assessments. In one study, transport electrification was introduced to assess the necessary transitions of energy systems for the transport sector by using the MESSAGE integrated assessment modelling framework [247]. Several studies argue for an energy system transition towards a higher consumption of biomass for energy production [248]. Higher penetrations of nuclear [249] and hydro power [250] are options discussed as well as an energy system transformation towards a low carbon future. Few studies focus on a transition from high intensity fossil fuel technologies such as, e.g., coal plants to lower intensity fossil fuels as, e.g., gas plants. The effect of natural gas on the CO_2-emission is not based on the difference between the emission factors of, e.g., gas and of coal, but on the emission factor of gas relative to that of a broader basket of energy technologies [251]. Political actions are as well key elements for energy system transitions. In this regard, a framework of how to diagnose possible obstacles for climate change mitigation has been provided [252].

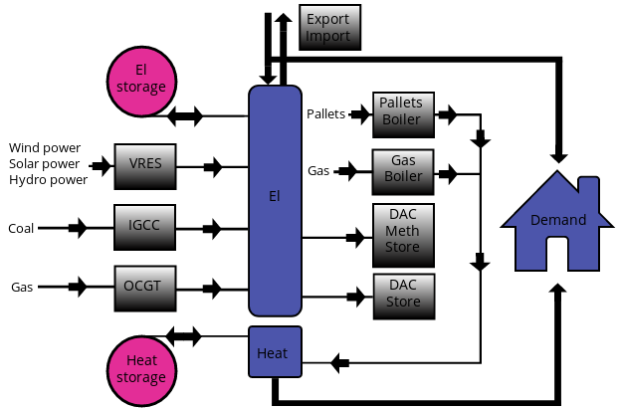

Figure 5.1: **Weak system coupling**. Renewable electricity sources (or RES) along with coal and gas fired power plants (Integrated Coal Gasification Combined Cycle, IGCC and Open Cycle Gas Turbines, OCGT) are suppliers of electricity. Heat is supplied by combustion of pallets and gas in boiler technologies. Methanisation is the only technology linking the electricity and heating systems. Hot water, electricity and gas storage facilities add flexibility to the system.

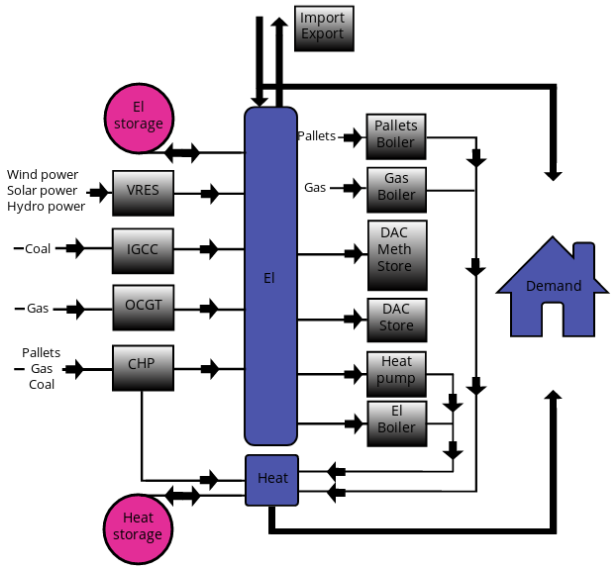

Figure 5.2: **Strong system coupling**. Renewable electricity sources (or RES) along with coal and gas fired power plants (Integrated Coal Gasification Combined Cycle, IGCC and Open Cycle Gas Turbines, OCGT) are suppliers of electricity. Cogeneration of power and heat (or CHP) supplies both electricity and heat through combustion of gas, coal and pallets. Heat is supplied by combustion of pallets and gas in boiler technologies. Methanisation, heat pumps and electricity driven boilers allow for further synergies between the individual systems. Hot water, electricity and gas storage facilities add flexibility to the system.

5.2 Experimental procedures

Energy system design

Wind, solar and hydro electricity capacities represent the primary power production. The generated electricity is used to cover whole or in part the electricity demand or to feed the bridging technologies. Renewable power production is to a large extent weather dependent, and issues of intermittency enforces the use of flexible power plants as OCGT and IGCC. The role of these is to support renewable power production in meeting the electricity demand. Decentral combustion of pallets and gas are the main sources of heat production. In RCP2.6, as the only negative emission scenario, direct air capture, DAC, is used to capture a portion of carbon from the air that corresponds to the negative emissions. The captured carbon is then stored and not used in any chemical processes. DAC appears therefore as exogenous to the model. The radical assumption of using DAC was chosen because other sources could not be guaranteed [237]. In low emission scenarios as RCP2.6 and RCP4.5, methanisation, which includes both DAC and chemical processes, is used to counter balance CO_2-emission from conventional power and heat generation. The generated methane is then reused in gas fired technologies. IPCC has, controversially, assumed systems mainly based on conventional technologies as coal, gas and biomass fired power plants as well as nuclear energy. For the low emission scenarios, most of the former are equipped with carbon capture and storage, CCS. However, many studies of low emission systems conclude that energy systems based on variable renewable energy generation, e.g., wind and solar, are more cost efficient and more technically feasible than the alternatives. E.g. CCS does not work well yet at large scale. In addition, decreasing costs of wind and solar energy are currently making them competitive with conventional energy generation whereas a conventional plant equipped with CCS will naturally always be more expensive than a conventional plant on its own. As a consequence some cost scenarios will naturally predict increasing wind and solar generation even in the absence of political and economical instruments that target low CO_2-emission.

Finally, decentralised heat pumps have gained significant political and economical attention in Europe during the past decade. These have shown to benefit from the increasing global temperatures throughout the 21st Century, and that they will dominate the cost optimal generation of heat among decentralised electricity driven technologies [240]. This makes heat pumps central in defining a separation between the week and strong coupled energy systems. Electricity driven boilers are introduced to compete with heat pumps. Cogeneration of

electricity and heat, CHP, have gained significant potential in energy systems. Although CHP plants hold a large share of the energy production in the Nordic countries [253], the remainder of European countries fall severely behind [254]. This gives CHP a central place in defining the difference in the strong and weak coupled systems. Electricity hot water and gas storages are introduced for both system types.

Production system optimisation

During the past few decades numerous models on energy systems have emerged. A majority of these are not adequate to deal with modelling of modern energy systems [255]. Therefore a new power system optimisation framework for simulating and optimising modern power systems – Python for Power System Analysis, PyPSA, [241] is adopted. PyPSA include features as vRES, non-vRES technologies, various forms of storage or sector coupling etc. Since PyPSA is designed to scale well with large networks and long time series it is well-suited for this analysis. A complete overview of how PyPSA excels from the remainder of energy system models is provided in [241]. Here, only the main components are describe. PyPSA solves a linearised optimal problem subject to a minimisation of the overall system cost.

Renewable generator capacities are all subject to optimisation, though with an upper capacity limit that is country specific. Conventional generators, storage capacities, heat generation capacities and transmission capacities are all as well subject to optimisation. Electricity and heat demand along with the hydroelectricity capacities are not subject to optimisation.

The optimisation objective function is given as:

$$\min_{F_l, G_{n,r}, g_{n,r,t}, H_{n,s}, h_{n,s,t}, f_{l,t}} \Big(\sum_{l} c_l F_l + \tag{5.1}$$

$$\sum_{n,r} c_{n,r} G_{n,r} + \sum_{n,r,t} o_{n,r} g_{n,r,t} \tag{5.2}$$

$$\sum_{n,s} c_{n,s} H_{n,s} + \sum_{n,s} \hat{c}_{n,s} E_{n,s} + \sum_{n,s,t} o_{n,s} h^{+}_{n,s,t} \Big) \tag{5.3}$$

where Equation 5.1 describes flow cost minimisation, Equation 5.2 heat and power production cost minimisation and Equation 5.3 storage cost minimisation. In this minimisation $c_{n,r/s}$ and $o_{n,r/s}$ defines the fixed and marginal cost in a

node n of a certain generator technology r or storage technology s. c_l defines the fixed cost of a cable l. F_l denotes the cable capacities on each cable. $G_{n,r}$ denote the generator capacities at each node. The generator capacity is further split into power and heat technologies. The dispatch energy at time t is denoted by $g_{n,r,t}$. $H_{n,s}$ and $G_{n,s}$ defines the storage unit power capacities and energy capacities, respectively, for a storage technology s. Finally, $h^+_{n,s,t}$ defines the positive part of the storage dispatch.

The objective function is supported by the following constraints for the dispatch of generators and storage. The dispatch of generators is constrained by their generator capacities and an upper and lower time-dependent availability $g^u_{n,r,t}$ and $g^l_{n,r,t}$, respectively as:

$$g^l_{n,r,t} \cdot G_{n,r} \leq g_{n,r,t} \leq g^u_{n,r,t} \cdot G_{n,r} \qquad \forall n, r, t \tag{5.4}$$

where $g^l_{n,r,t}$ and $g^u_{n,r,t}$ equals 0 or 1, respectively for a fully flexible generator. The dispatch of storage units is similarly constrained by a lower and upper availability $h^u_{n,s,t}$ and $h^l_{n,s,t}$, respectively as:

$$h^l_{n,s,t} \cdot H_{n,s} \leq h_{n,s,t} \leq h^u_{n,s,t} \cdot H_{n,s} \qquad \forall n, s, t \tag{5.5}$$

where $h^l_{n,s,t}$ is negative while $h^u_{n,s,t}$ is positive due to charging and discharging of the storage. The energy levels $e_{n,s,t}$ of all storage units are similarly constrained as:

$$e^l_{n,s,t} \cdot E_{n,s} \leq e_{n,s,t} \leq e^u_{n,s,t} \cdot E_{n,s} \qquad \forall n, s, t \tag{5.6}$$

where $e_{n,s,t}$ is defined in great detail in [241]. The cable flows $f_{l,t}$ are optimisation variables but do not appear in the objective function. The flows are as well constrained by an upper and lower availability $f^u_{l,t}$ and $g^l_{l,t}$, respectively as:

$$f^l_{l,t} \cdot F_l \leq f_{l,t} \leq f^u_{l,t} \cdot F_l \qquad \forall l, t \tag{5.7}$$

CO_2-emission constraints

CO_2-emission enters the techno-economic cost-optimisation as constraints and clearly, as shown in the upper plot of Figure 5.3, these represent a broad range of climate projections. IPCC provides information on CO_2-emission on smaller spatial scales such as the world economic regions. However, an aggregate for the

individual continents as Europe is not available. Therefore, the CO_2-emission accounted for by the European power and heating sectors have to be estimated. This is done in two steps. Firstly, these are approximated by the OECD90 (UNFCCC Annex I countries) total CO_2-emission. This allows for a downscaling of the world wide CO_2-emission to only consider constraints available for the OECD90 countries, which in turn account for a majority of the European countries. Secondly, the OECD90 CO_2-emission take into account emissions by fossil fuel burning (liquid, gas and solid fuels), industry (combustion and process emissions [256]) and transportation (bunker fuels) (RCP Database v2.0.5 [257]). The emissions are then rescaled to align the historical values of European electricity and heating sector CO_2-emission provided by odyssee [144]. The result is shown in upper plot in Figure 5.3. Due to missing projections of historical CO_2-emission model data, only 5 years were available for the comparison. This approximation separates the electricity and heating CO_2-emission from the remaining sectors, removes non-European countries from the OECD90 and adds missing European countries. To the best of the authors knowledge, this is a state-of-the-art approximation of the CO_2-emission accounted for by the European electricity and heating sectors throughout the 21st Century and no other approximations are available in the literature. The bottom plot of Figure 5.3 shows the respective temperature increases for Europe in the different projections.

These constraints are implemented as:

$$\sum_{n,r,t} \frac{1}{\eta_{n,r}} w_t \cdot g_{n,r,t} \cdot e_r \leq CO_2^u \leftrightarrow \mu_{CO_2} \tag{5.8}$$

where CO_2 constraints are introduced by an upper limit for CO_2-emission CO_2^u. e_r denotes the specific emissions of the technology fuel r and technology efficiency η. w_t is a weighting that can be introduced. μ_{CO_2} defines the shadow price of this constraint.

Energy-demand mismatch

Equating the energy and demand assures that all demand $d_{n,t}$ will be satisfied either by generators and storage or flows $f_{l,t}$ as:

$$\sum_r g_{n,r,t} + \sum_s h_{n,s,t} + \sum_l K_{n,l} \cdot f_{l,t} = d_{n,t} \leftrightarrow w_t \cdot \lambda_{n,t} \qquad \forall n,t \tag{5.9}$$

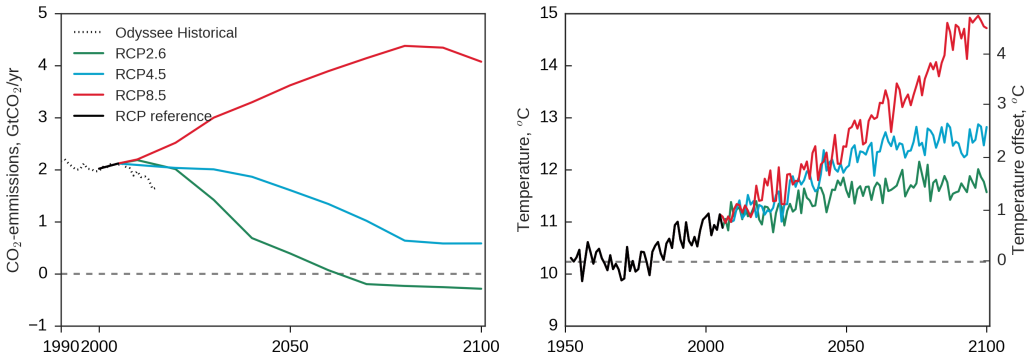

Figure 5.3: **Important reconstructed concentration pathway metrics**. Upper plot: Annual CO_2-emission accounted for by the European electricity and heating sectors (EU28 + Norway and Switzerland). Full drawn curves illustrate emissions provided by the IPCC. The historical, RCP2.6, RCP4.5 and RCP8.5 projections are shown with black, green, blue and red curves, respectively. The black dotted curve shows CO_2-emission accounted for by the European electricity and heating sectors provided by odyssee. Lower plot: Yearly average European temperatures calculated from the climate model ICHEC-EC-EARTH HIRHAM5 [43, 44].

where $K_{n,l}$ is the incidence matrix of the network. $\lambda_{n,t}$ is the marginal price at each bus and guarantees energy conservation at each node by implementing Kirchoff's current law. Kirchoff's voltage law is implemented as well as:

$$\sum_l C_{l,c} \cdot x_l \cdot f_{l,t} = 0 \qquad \forall c, t \tag{5.10}$$

where c defines each independent cycle which is expressed as a direct combination of cables l by a matrix C_{lc}. x_l is the reactance of cable l.

Data

Power production data

The conversion and validation procedures of climate data into country specific wind power potential (capacity factors) follow a state-of-the-art method [132] and so only a summary is provided here. The time series of national wind power potential was constructed by using climate model specific 10m wind speeds. These were extrapolated to the turbine hub height by using climate model specific surface roughness lengths. Since the initial time series several improvements have been made. 1) National wind power potential is now split into onshore and offshore potential. 2) Previously, a single wind power curve have been used to represent the conversion procedure regardless of the turbine

properties. The improved version utilise a range of wind power curves, now depending on the wind turbine capacity [258]. The wind power potential is validated according to already bias-corrected time series [37].

The conversion and validation procedures of the national solar power potential are equally presented in [132]. Climate model specific temperature data along with the incoming and outgoing solar radiation was used in the conversion procedure. The REAtlas [36] was used to model the solar geometry, account for diffused radiation, efficiency loss due to temperature and inverter losses. The validation of the the solar power potential is performed by comparing to already bias-corrected time series [38].

The upper limits of the onshore and offshore wind power and solar power generator capacities are fixed to the national specific usable areas. For example, wind farms are not placed in highly populated areas such as urban areas and solar PV panels are not build in highly overgrown areas such as forests. [243] provide a detailed overview of the capacity layouts for the renewable power production.

Hydroelectricity generators are fixed to their current national capacities. These are divided into reservoir and run-of-river generators with river inflow, and pumped hydro storage as pure storage units. These are then concatenated in time to cover the model time span from 2000 to 2100. [243] details the underlying assumptions of the hydroelectricity generators.

Heat production data – COP

Heat production by heat pumps are governed by the heat pump Coefficient of Performance, COP, which defines the ratio of the heat output to the amount of electricity input. The COP is strongly temperature dependent and therefore fluctuates accordingly on intra and inter-annual time scales. National-wise COP time series have therefore been generated by using climate model specific temperatures. The COPs are calculated by using two empirical formulations [29, 240], which separates defrost operations at temperatures below 5 °C. A sink temperature of 55 °C is used [29]. The heat pumps are assumed to be air-source heat pumps that cover both space heating and hot water demand. These are favoured due to their straight forward retrofit installations in already existing buildings.

Electricity consumption data

The preparation of electricity demand data is presented in great detail in [132] and so a summary is provided here. National hourly electricity consumption from 2006-2015 was provided by the European Network of Transmission System Operators for Electricity, ENTSO-E, [40]. In order to remove the inter-annual trends the time series was detrended linearly to represent a constant inter-annual consumption. As the main goal of this work is to assess the impact of climate change on the energy system, any human impacts from the electricity consumption are avoided. The inter-annual time series is therefore concatenated to meet the time span from 2000–2100. The electricity consumption was then corrected for impacts from electrified heating and cooling by using the theory of degree-days.

Heat consumption data

The decentralised nature of heating means that data on consumption is not readily available and therefore not applicable. The theory of degree-hours is most frequently used as a best proxy for modelling the variations in the day-to-day heat demand. For every country, a time series of the heating degree-hours is developed by using national specific heating threshold temperatures and heating seasons [240, 179]. For Luxembourg the heating threshold temperature is defined to be 17 °C. The country specific heating threshold temperatures allow the national climate and culture-specific human heating behaviour to be captured in the calculation of the heating degree-hours. Furthermore, national non-heating periods allow for a more realistic representation of the intra-annual allocation of the heating degree-hours.

The heating degree-hours are straightforwardly converted into national heat demand by multiplying with country specific values of the energy demand for space heating and hot water use. Estimated values of the national energy consumption for space heating and hot water demand was obtained from the Heat Roadmap Europe project [41]. Table 5.1 provides an overview of the heating degree-hours, space heating and hot water demand in units of $\frac{kJ}{HDH \cdot cap}$ and $\frac{kJ}{hours \cdot cap}$, respectively. Data for Norway, Switzerland, Serbia and Bosnia & Herzegovina are not available and average values of neighbouring countries are used instead.

Prior to the calculation of the heating degree-hours, the temperature data was

bias corrected by comparing to temperature ground measurements provided by the European Climate Assessment (ECAD) who provide an interpolation in space [132, 164]. National temperature profiles are population weighted [191] to avoid strong impacts from sparsely populated areas as, e.g., northern Scandinavia [240].

This study, as the only in the literature apply a consistent method to model the national day-to-day variability in the heating requirements for all European countries by making use of country specific heating threshold temperatures and heating seasons.

Table 5.1: **Overview of the national population, heating degree-hours and space heat and hot water demands**. Space heat demand is provided in units of $\frac{kJ}{HDH \cdot cap}$ while hot water demand is provided in units of $\frac{kJ}{hours \cdot cap}$. HDH denotes the heating degree-hours and cap denotes the population.

Country	Population	heating degree hours	Space heat demand	Hot water demand
AUT	8557761	56770	500.92	475.42
BIH	3819684	37443	252.20	168.14
BEL	11183411	39733	798.83	455.67
BGR	7112641	45119	216.51	219.55
CHE	8238610	78408	706.51	431.22
CZE	10777060	55573	407.54	427.09
DEU	82562004	43755	690.70	618.22
DNK	5661723	46409	619.28	616.98
EST	1280227	42602	673.26	288.90
ESP	47199069	15256	494.45	500.65
FIN	5460592	69247	629.31	368.77
FRA	64982894	35274	685.85	289.64
GBR	63843856	33400	617.39	522.68
GRC	11125833	27682	377.55	295.50
HRV	4255374	60672	326.28	299.38
HUN	9911396	55390	423.61	277.80
IRL	4726856	21899	1088.55	434.71
ITA	61142221	29354	742.96	385.81
LTU	2998969	59968	278.24	287.77
LUX	543261	65192	782.69	529.53
LVA	2031361	48501	515.21	364.15
NLD	16844195	34204	766.69	392.80
NOR	5142842	51625	576.48	482.61
POL	38221584	58529	339.39	250.52
PRT	10610014	7307	520.07	348.60
ROU	21579201	48768	213.80	175.21
SRB	9424030	54860	252.20	197.39
SWE	9693883	56687	480.86	462.09
SVN	2079085	54083	384.19	415.09
SVK	5457889	53672	333.04	293.66

Pricing

Fixed technology and fuel costs along with technology properties throughout the century are assumed. The key problem with this approach is the misrepresentation of the real world fluctuations in prices and properties. Nevertheless, this approach is necessary in order to convey the research questions of this study. The reason of using constant prices is to enforce an objective study of the influence of climate change on future energy systems, separate from political and personal drivers.

Tables 5.2–5.6 provides an overview of the technology prices and properties. As the focus of this paper is the impact of climate change on the technology-mix on a European scale, rather than modelling the technology mix on country scale, the prices are excluding national taxes and levies, and assumed to be constant across Europe. This procedure reduces uncertainties from national policies on taxes and levies.

Table 5.2: **Fuel types.** Pallets are assumed to be carbon neutral by means of the biomass-carbon cycle.

Fuel	CO_2 intensity tCO_2/MW_{th}	Fuel price €/kW_{th}
Gas[1]	0.19	21.6
Coal[1,2]	0.36	8.4
Pallets[3]	0.00	51

[1] Schröder et al. [DIW Data Documentation, 259]

[2] Natural Resources Canada [Natural Resources Canada, 260]

[3] Cross Border Bioenergy/European Biomass Association [Cross Border Bioenergy/European Biomass Association, 188]

Table 5.3: **Power producing technologies.** From left: Lifetime in years, overnight expense in €/kW$_{el}$, fixed and operational maintenance expense in percent of the overnight expense and efficiency.

Technology	Lifetime Yr	Investment costs €/kW$_{el}$	FOM %	η
Wind[1] onshore	25	1182	2.96	1
Wind[1] offshore	25	2506	3.19	1
Solar[3]	25	575	2.5	1
Hydro[1]	80	2000	1	0.9
ROR[1]	80	3000	2	0.9
PHS[1]	80	2000	1	0.74
OCGT[1,4]	30	400	3.75	0.39
IGCC[1,4]	40	1450	3.75	0.45

[1] Schröder et al. [DIW Data Documentation, 259]
[3] Vartiainen et al. [The true competitiveness of solar PV, 261]
[4] Danish Energy Agency and Energinet.dk [DEA, 262]

Table 5.4: **Decentral conversion technologies.** From left: Lifetime in years, overnight expense in €/kW$_{el}$, fixed and operational maintenance expense in percent of the overnight expense and efficiency.

Decentral Technologies	Lifetime Yr	Investment costs €/kW$_{th}$	FOM %	η
Gas boilers[5]	20	175	2	0.9
Pallet boilers[4]	20	590	1	0.88
Air source[5,6] heat pumps	20	1050	3.5	t
Power to gas[5,7] (DAC + methanation)	25	500	3	0.6
DAC[5,7]	25	200	3	0.4

[4] Danish Energy Agency and Energinet.dk [DEA, 262]
[5] Palzer [PhD Thesis, Fraunhofer 263]
[6] Palzer and Henning [264]
[7] Fasihi et al. [265]

Table 5.5: **Central conversion technologies.** From left: Lifetime in years, overnight expense in €/kW$_{el}$, fixed and operational maintenance expense in percent of the overnight expense, electric efficiency, power-to-heat ratio of CHP plants in back-pressure operation and the specific electrical power loss.

Central technologies	Lifetime Yr	Investment costs €/kW$_{el}$	FOM %	η^{el}	α	ξ
CHP gas[8]	25	900	3	0.55	1.7	0.15
CHP coal[8]	40	1900	3	0.46	0.75	0.15
CHP pallets[8]	25	2000	3	0.46	0.75	0.15

[8] Dahl et al. [189]

Table 5.6: **Storage technologies.** The investment cost of the water tank storage is 860€/m^3. By using 40K temperature difference and 1.17 kWh/m^3/K it approximates to 18 €/kWh.

Technology	Lifetime Yr	Investment costs	FOM %	η
Battery storage[9]	15	145 €/kWh	0	1
Battery inverter[9]	20	310 €/kW$_{\mathrm{el}}$	3	0.81
Decentral water tank storage[10,11]	20	18 €/kWh	1	τ = 3 d
Decentral water dis/charging[10]				0.81

[9] Budischak et al. [266]
[10] Henning and Palzer [267]
[11] Gerhardt et al. [268]

5.3 Results and discussions

Initially, the overall system costs for the end-century of all climate pathways are presented. Although the system costs misrepresent the real world price fluctuations, they onset a central discussion on the potential influence of global parameters such as the weather year and CO_2-constraints on the prices. Then the underlying energy system transformations that lead the overall system costs are discussed. To this end, the focus is on a single climate model, ICHEC-EC-EARTH [44] HIRHAM5 [43], but strive that during this time all the other climate models have been treated equally.

Energy system transitions

The total system costs are presented in Table 5.7 in the form of climate model ensemble averages along with the corresponding 1σ standard deviations. The total system cost is defined as a summation of all node-individual costs. Two major results can be extracted from this table: 1) Independent of the climate pathways (Historical, RCP2.6, RCP4.5 or RCP8.5), the strong coupling introduce lower system costs, which is reasoned by the enhanced flexibility of technology selection and 2) Independent of the system coupling (weak or strong), the end-century of RCP2.6 is associated with the highest system cost, increasing by more than 100% compared to historical values. The end-century of RCP4.5 results in the second most expensive system followed by the end-century of RCP8.5. Two global attributes of the energy systems are driving the system costs: 1) The weather, which is determined by the input data and 2) The CO_2-constraints. The potential effect of each is evaluated in an upcoming section, but first the energy system transitions leading to these system costs are discussed.

Figure 5.4 illustrates the energy flow for each climate pathway in terms of sankey diagrams. Each sankey diagram show the energy flow of the aggregated European energy system and is not country-specific. The left and right columns present the weak and strong system coupling, respectively. The rows represent the different pathways in the following order: Historical, RCP8.5, RCP4.5 and RCP2.6. Focusing initially on the historical period, a moderate system change when transforming towards a strong coupling is observed. In the latter, CHP plants cover a moderate share of the energy production by replacing the inefficient coal plants for electricity production and 20% of the heat production initially generated by gas boilers. This reduces the system efficiency by almost 50% and therefore lowers the system cost, as seen in Table 5.7. The reduction

Table 5.7: **Total system costs.** Model average of the total system costs in billion EUR per year with 1σ standard deviations. The upper half shows the system costs from the weakly coupled system and lower half shows similarly for the strongly coupled system. The historical column represents model year 2000 and the RCP columns represent the model year 2100.

historical	**rcp26**	**rcp45**	**rcp85**
	Weak system coupling		
223 ± 7	453 ± 16	253 ± 14	169 ± 8
	Strong system coupling		
189 ± 7	418 ± 18	228 ± 10	141 ± 7

amounts to 30 billion EUR per year which is 15% of the weak system cost.

Because of system similarities, our next focus is on the end-century of RCP8.5, shown in the second row of Figure 5.4. RCP8.5, as the only pathway, leads to a reduced system cost compared to historical values. The system costs reduce by 25% in both the weak and strong coupled systems relative to historical values. The cost reduction is first and foremost regulated by the lower heat demand leading to a lower heat production, which is discussed in detail for all climate pathways by [240]. Secondly, the reduced emission constraints allows coal plants to replace the more expensive renewable capacities for electricity production. The new system comes with a significantly increased energy loss, exclusively reasoned by the ineffective coal plants. Identical to the historical period, the transition towards a strong coupling introduces a large share of CHP plants, which replace the coal plants for power production and a significant share of heat production by gas boilers. This comes with a total system cost reduction of 17% relative to the weak system costs.

A system transition towards the end-century of RCP4.5, reveals a clear change in the composition of energy producing technologies even though the energy demand stays relatively unchanged. This modification is predominantly justified by the moderate CO_2-constraints for the end-century of RCP4.5, as will be discussed in detail in the following section. RCP4.5 is the first pathway that introduce radical changes to the traditional energy systems by deviating from fossil-fuel domination, but comes with an increasing cost of 7% and 20% for the weak and strong system couplings compared to the historical values. In general, coal fired technologies are eliminated while gas fired technologies are exposed to significant capacity reductions, which in turn reduces the system loss. The

power is mainly provided by renewable capacities and covers the electricity demand along with the power supply for the methanisation process. Methanisation is used to stabilise the system emissions to meet the overall emission constraints. The generated methane is already included in the left drawn gas store, but shown explicitly in the right side of the sankey diagram in order to illustrate the magnitude. The heat demand is met by decentralised boilers burning excavated gas, methane (generated by the methanisation process) and wood pallets. Although pallets are expensive they come with the benefit of being CO_2-neutral. The system composition for the strong coupling is slightly modified by replacing pallet boilers with heat pumps and electric boilers which in turn increases the renewable power production. This transition reduces the system cost by 6% compared to the weak system cost.

Finally, the extreme CO_2-constraints at the end-century of RCP2.6 enforces an energy system transition similar to the end-century of RCP4.5, but with a more aggressive approach. This results in a system cost increase of more than 100% for both system couplings, respectively. It is clear that reaching a stable future with stable global temperatures requires a costly system transformation. In this case, the increased renewable capacities along with increasing use of expense pallets for heat production are the main drivers for the increased system cost. Direct air capture, DAC, is introduced and used to capture a portion of the atmospheric carbon that corresponds to the negative emission. As for RCP4.5 where methane was used to subsidise the heat generation, in this case the gas store to left in the sankey diagram consist solely of methane that is generated by the methanisation process. The strong coupling is not significantly different from the weak coupling in terms of the technology composition. As for the RCP4.5, the transition towards a strong coupling reduces the system cost by 5%.

In conclusion, it is evident that focusing on reaching a strong system coupling would give financial benefits of about 15% for the RCP2.6 and RCP4.5. With the current emerging policies and efforts on climate change mitigation, it is likely that the end of the 21st Century would experience a climate that is well-defined by the RCP2.6 or RCP4.5 pathways or a mixture of these. In this regard, it is far more important to focus on keeping the current coupling between the electricity and heating sectors and focus more on the transition towards a renewable dominated system, as in the end-century of RCP2.6 and RCP4.5, rather than focusing on reaching a strong coupling. RCP8.5 shows the benefit of a strong coupling with a system cost reducing of 25%. However, this is an extremely unlikely pathway for the end-century and should not be considered in detail.

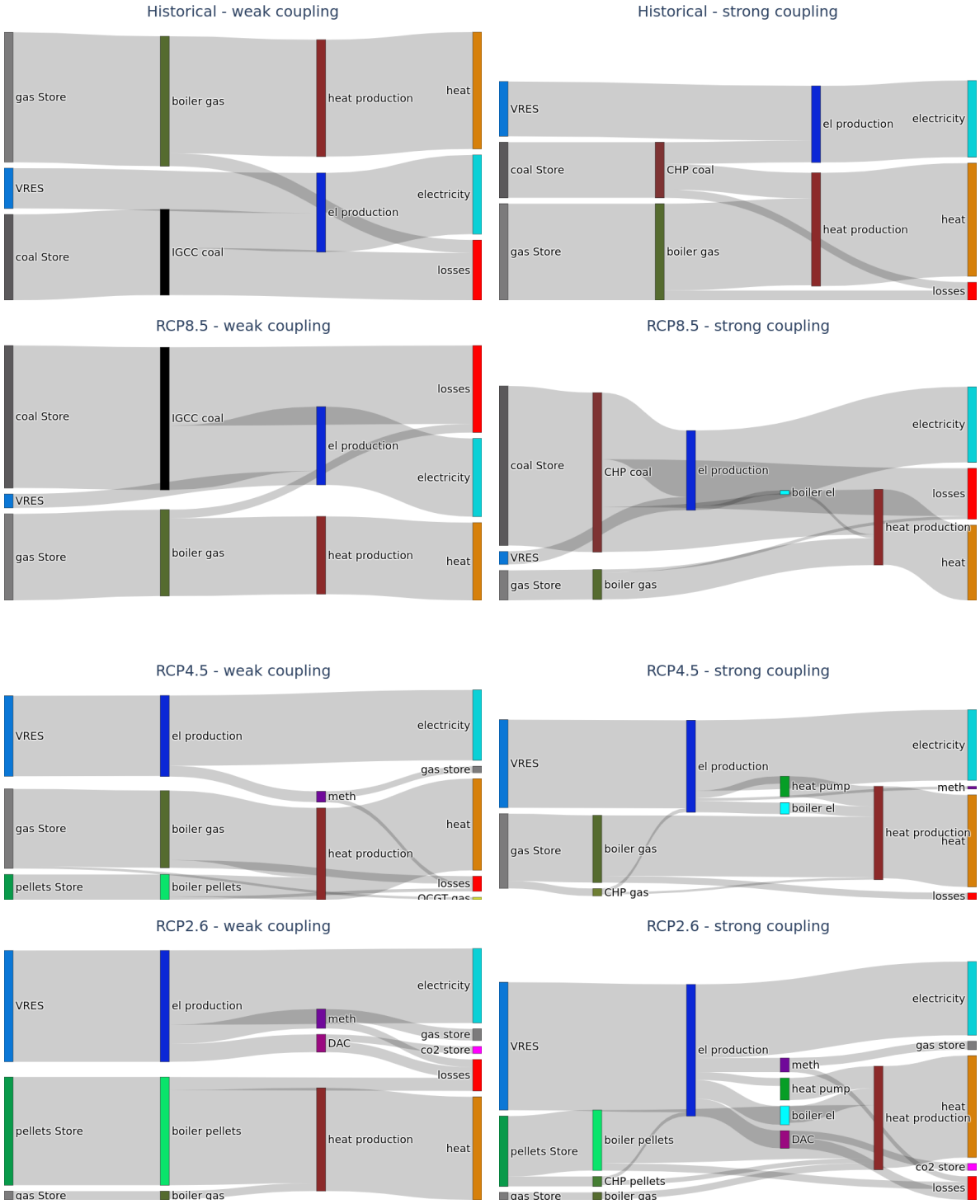

Figure 5.4: **Sankey diagrams illustrating the energy flow**. Left and right columns show the energy flow in the weak and strong coupled systems, respectively. The first, second, third and fourth rows illustrate the energy flow in cost-optimal energy systems that are subject to climate conditions from the historical period and to the end-of-century in the RCP8.5, RCP4.5 and RCP2.6 pathways.

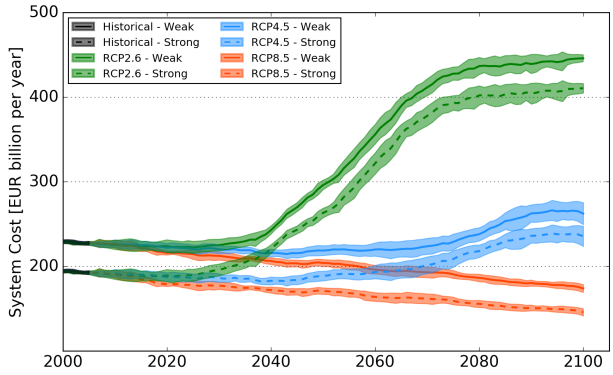

Figure 5.5: **Average system costs in EUR billion per year**. Climate model ensemble average of the total system costs as a function of model year. Shaded regions represent the climate model 1σ ensemble standard deviation. The dashed and fully drawn curves represent the strong and weak system couplings, respectively. Black, green, blue and red plots represent results from the historical, RCP2.6, RCP4.5 and RCP8.5 climate pathways, respectively.

Expanded system costs

In the previous section, system costs for the years of 2000 and 2100 were discussed. In Figure 5.5 these are expanded and present similar values for all model years. Small standard deviations illustrate a strong agreement among climate models. A 10 year moving average is used to highlight the long term trends over annual fluctuations. Certainly, the different climate pathways evolve differently throughout the 21st Century. RCP8.5 distinguishes from RCP2.6 and RCP4.5 as the only pathway with system costs lower than present values. The climate pathways RCP2.6 and RCP4.5 distinguish them selves from RCP8.5 already previous to 2020.

Weather vs. CO_2-constraints

This section is devoted to an assessment of the potential influence of the weather and CO_2-emission constrains on the energy system costs. The focus is again on the years 2000 and 2100 as in Table 5.7. The logic behind this assessment is explained by using the historical time frame (year of 2000) as an example. To assess the impact of CO_2-constraints on the system costs, the weather year of 2000 is kept fixed, but exposed to the CO_2-constraints from the remaining climatic pathways. Oppositely, to assess the impact of weather, the CO_2-constraint are fixed to the year of 2000 and expose the weather of the remaining climatic pathways to this constraint. This procedure is done for all possible combinations. The results are shown in Table 5.8. Each of the three sections are made up of em-

phasised diagonal and off-diagonal values. Values from Table 5.7 are shown in the diagonal of Table 5.8 and emphasised with bold. As an example, 223 billion EUR is the system cost for a weak coupling in a historical weather year and with a historical CO_2-constraint. Just below, 469 billion EUR is the system cost for a weak coupling in a historical weather year but now with a RCP2.6 end-century CO_2-constraint.

In this discussion, the focus is only on the weak system coupling, the upper section of Table 5.8, but identical statements can be pursued for the strong system coupling. By fixing the CO_2-constraint as, e.g., for the historical time frame as in the first row, it is clear that the system cost decreases depending on the weather of each pathway. This decrease is either governed by the electricity or the heating sector. In evaluating the potential influence of each, similar results are presented for a pure electricity sector at the bottom of Table 5.7. It is clear that for fixed CO_2 constraints the system costs change at most by 2%, which clearly rules out any impacts from the electricity sector. This is a robust result that directs the focus away from the electricity sector and onto the heating sector. This result is well-aligned with previous studies [132, 240]. In conclusion, the system costs are to a high degree independent of the electricity sector, but partially governed by the changing heat demand due to temperature increases.

Oppositely, by fixing the weather year as, e.g., in column 1, the impact of the CO_2-constraints on the system costs is assessed. It is clear that, for a fixed pathway, the system costs fluctuate severely. These change significantly, which gives a robust indication of the substantial impact of CO_2-constraints on the system costs. In this case, it is also important to notice the identical fluctuations for the pure electricity system.

In conclusion, the change in system costs for a transition towards the end-century of each pathway is governed by the decreasing heat demand and changing CO_2-constraints. The shares of each fluctuate according to the pathway. The increasing system costs for the end-century of RCP2.6 is strongly affected by the significant decrease in CO_2-emission. A 16% decrease in the heat demand holds an insignificant share in the system price. A moderate decrease in the CO_2 constraints at the end-century of RCP4.5 governs the moderate increase in the system costs. The 24% decrease in the heat demand has a moderate share in the system costs. The system cost for the end-century RCP8.5 is equally regulated by the increasing CO_2-constraints and the 42% decrease in the heat demand.

Table 5.8: **Total system costs.** Model average of the total system costs in billion EUR per year with 1σ standard deviations. The upper half shows the system costs from the weakly coupled system and lower half shows similarly for the strongly coupled system. The "Historical" panes represent the model year of 1990 and the "rcp" panes represent the model year of 2100. cProj (the columns) defines the climate projection and year from where weather data has been used. co2 (the rows) defines the climate projection and year from where co2 constraints have been used.

co2 \ cProj	**historical**	**rcp26**	**rcp45**	**rcp85**
		Weak system coupling		
historical	**223 ± 7**	219 ± 6	200 ± 7	174 ± 8
rcp26	469 ± 10	**453 ± 16**	415 ± 15	353 ± 27
rcp45	300 ± 15	292 ± 14	**253 ± 14**	209 ± 14
rcp85	217 ± 8	210 ± 2	193 ± 6	**169 ± 8**
		Strong system coupling		
historical	**189 ± 7**	185 ± 5	167 ± 6	143 ± 7
rcp26	432 ± 13	**418 ± 18**	381 ± 16	321 ± 29
rcp45	265 ± 16	260 ± 14	**228 ± 10**	190 ± 13
rcp85	180 ± 7	176 ± 3	162 ± 6	**141 ± 7**
		Electricity only		
historical	**98 ± 1**	99 ± 1	98 ± 1	98 ± 1
rcp26	178 ± 4	**179 ± 612**	180 ± 5	178 ± 6
rcp45	115 ± 2	117 ± 4	**117 ± 2**	115 ± 3
rcp85	95 ± 2	93 ± 2	91 ± 1	**93 ± 2**

Sensitivity analysis

Optimising energy systems through a cost-minimisation exposes the modelling procedure to a significant weakness that is subject to the cost assumptions. These might change over the course of the future and the current assumptions might therefore become unrepresentative of future energy systems. In this study, the robustness of the results is assessed through a sensitivity analysis on the input parameters.

To this end, 100 perturbed pricing schemes were generated on the basis of Monte Carlo trials of the initial fuel and investment cost assumptions, which are shown in Tables 5.2 – 5.6. The perturbed prices are subject to a random selection from a normal distribution with a mean and standard deviation equal to the unperturbed price and 10% of the unperturbed price, respectively. This ensures a rep-

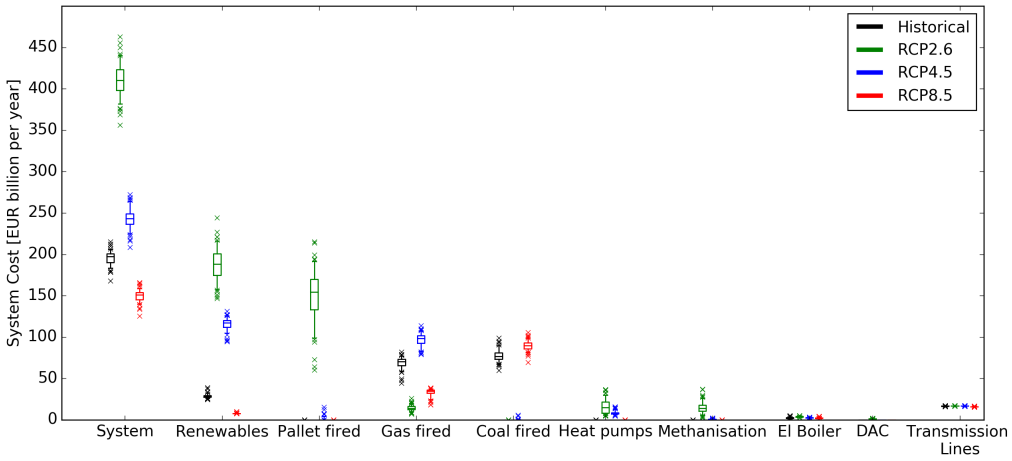

Figure 5.6: **Price sensitivity of the individual components of the fully coupled system design**. The *System* category shows the sensitivity of the full system. The *Renewables* category shows the sensitivity of all renewable capacities combined. The *Pallet, Gas and Coal fired* categories combine all related technologies and show their sensitivity. The *Heat pumps* category shows the sensitivity of of heat pumps. Finally, the *Methanisation* category shows the sensitivity of the methanisation processes. The black, green, blue and red colors illustrate the historical period, and the end-century of the RCP2.6, RCP4.5 and RCP8.5 pathways. The boxes in the plots show the 25% and 75% quantile. The center line shows the median. The whiskers show the minimum and maximum values.

resentative sample of many combinations of perturbed cost assumptions. The strong coupling is used as a case-study because of the larger ensemble of technologies. Furthermore, the sensitivity analysis is only applied to the historical period for the model year 2000 and for all pathways at year 2100.

The results are shown in Figure 5.6 as box plots. The total system costs are shown in the *System* category while the remaining categories show the costs of grouped system components. It is observed that the total system costs (most left category) in the historical and end-century of RCP8.5 stay relatively unaffected by a change in the input prices. Oppositely, the system cost at the end-century of RCP2.6 and RCP4.5 are subject to some price fluctuation. From the *Gas Fired* category, it is clear that the total cost of gas related components stay relatively unaffected, independent of the climate pathways. Because of strong CO_2-emission constraints, coal is not consumed in the RCP2.6 and RCP4.5 pathways. For the historical period and the end-century of RCP8.5, the cost of coal related components stay as well unaffected. Costs related to pallet combustion and renewable power production change significantly as a function of input prices. This indi-

cates that cost competition between pallet fired technologies and power driven technologies may appear. Finally, it is observed that although the costs of the individual system components may change significantly depending on the input prices, the total system costs are affected to a lower extent.

5.4 Conclusion

It is found that transitions from the current traditional fossil fuel dominated energy systems towards the end-century in each of the potential climatic outcomes are strongly affected by the weather and constraints on CO_2-emission.

Our modelling of a cost-optimal European energy system reveals an intense use of conventional power capacities for energy production. About 20% - 50% of the power production is delivered by coal power plants and co-generation of power and heat while the remaining is provided by renewable capacities. All heat production is delivered by gas boilers or co-generation of power and heat. This comes with a total system cost between 189 $\pm$ 7 and 223 $\pm$ 7 billion Euros per year for the strongly and weakly coupled systems, respectively. Such systems are furthermore found to be impassive towards fluctuating price assumptions.

Relaxed CO_2-constraints at the end-century of RCP8.5 allows for additional energy production by CO_2-intense power capacities compared to traditional systems - especially by coal fired technologies. Increasing global warming reduces the need for space heating by about 45% compared to historical values and thereby reduces the need for heat generation. Taken together, these factors contribute to a lowering of the system cost by 25% compared to the similar for the traditional system. This type of transition comes with the disadvantage of designing highly inefficient systems caused by the increased use of ineffective conventional power capacities. On the other hand, this makes the system less susceptible towards price fluctuations. Although, this system design is an interesting case study, it is very extreme and unlikely scenario of global warming.

The end-century of RCP2.6 and RCP4.5 lead to significantly different system design decisions compared to the end-century of RCP8.5. An energy system transition towards any of these pathways requires a substantial increase in renewable power capacities to replace the conventional energy production. Moderate CO_2-constraints in RCP4.5 still allows for heat production by gas consumption, but the emissions have to be stabilised by methanisation. Heat production is subsidised by pallet boilers, which are assumed to be CO_2-neutral, heat pumps and electric boilers. The full electricity demand is exclusively provided by renewable capacities. Such a system reduces the energy loss by a factor of 2 but increases the system cost between 7% and 20% compared to traditional values. This system is subject to a higher degree of variability of the total system costs.

The end of century in RCP2.6 is subject to the most intense CO_2-constraints and

thereby eliminating conventional technologies altogether. Gas fired technologies are still available but consumes methane provided by methanisation. This system requires direct air capture technologies to capture a portion of the atmospheric carbon that corresponds to negative emission. A major share of heat demand is provided by expensive biomass combustion. Taken together, this radical energy system transition comes with an increased system cost of more than 100% compared to traditional values.

CHAPTER 6

General Conclusion

This dissertation is the final product of a three-years Ph.D. project, outlining my research into the impacts of climate change on the European electricity and heating systems. It consists of four research chapters, each representing a study that is either published, submitted for review or in preparation. Climate science enters this project as a result of using a range of climate projections to represent diverse, but plausible outcomes of the 21st century climates. These were provided by the Intergovernmental Panel on Climate Change in their latest assessment report. The World Climate Research Programme has developed high-resolution weather data with built-in information on climate change from these projections. In continuation of the aforementioned projects, I have applied cutting-edge procedures to develop 3-hourly state-of-the-art energy system related time series, which represent the national averaged wind and solar power potential, national aggregated electricity and heat consumption and national averaged coefficient of performance of heat pumps. Weather data from nine climate models have been used to generate nine independent datasets, which span the years from 1970 to 2100. These data form the foundation of this project and are used in all analyses.

In the first analysis, I show that independent of the level of climate change, power production from wind and solar sources and power consumption change at most by 5% compared to historical levels. This study also revealed that today's design of a highly renewable European electricity system might perform equally well at the end of this century as of now and that it is more important to design future electricity systems with a focus on the inter-annual weather vari-

abilities rather than climate change. This is an important result for this project, as it implies that the coupling to other sectors is to a large extent unaffected by changes in the variable renewable electricity production and the electricity consumption. These conclusions are based on analyses of five important metrics that describe a highly weather dependent electricity system.

Turning to the heating sector, it becomes evident that a lack in monitoring the historical energy consumption for space heating results in a significant shortage of open-available data that can be used in research. Estimates that fit the requirements of this project are as well not available. To this end, I have developed a coherent method that can be used for this purpose. As a case study, the method was applied to generate national space heat consumption time series for the European countries. By taking the national temperature and primary energy consumption into consideration, the method showed to improve the modelling of space heating to a great extent compared to existing results.

In the third analysis, I am investigating into the impact of climate change on the European space heat consumption and into the cost-optimal options for decentralised heat generation. In contrast to the electricity system, the demand and supply sides of the heating sector are both significantly affected according the degree of climate change. Energy demand for space heating decrease by up to 40% compared to historical levels. Heat pumps are becoming more economic viable and more widespread in Europe. These results indicate that the design of future cost-optimal heating systems look very different from the design of today's systems. As a consequence, the benefits of a strong coupling between the electricity and heating systems might look very different in the different outcomes of climate change. An assessment into the related policies reveals that in many countries aggressive policies have to be implemented in order to meet the results of this study.

The core topic of this project deals with an investigation into the extent to which a stronger synergy between the European electricity and heating systems proves beneficial compared to a weakly coupled system. I reveal that, independent of the climate projections, a strongly coupled electricity and heating system reduces the system cost by 10% and increases the system efficiency by 50% compared to its loosely coupled counterpart. From an economic standpoint, the benefits of a fully coupled system are rather small. The energy efficiency increases on the other hand significantly. This is reasoned by the use of more energy efficient technologies in the strong coupling. Independent of the system

coupling strengths, climate change has a significant impact on the cost-optimal design of future energy systems. The total system costs fluctuate from below 30% for the most extreme climate projection to above 90% for the least extreme projection compared to a historical reference point. These changes are driven by strong impacts of a changing climate and changing CO_2-emission constraints within the different climate projections. Strict emission constraints allow only for expensive renewable technologies, biomass combustion and methanisation facilities to operate, while the opposite allows for the cheaper options of fossil fuel driven technologies.

The aim of this project was to provide more insight to the impact of climate change on the European electricity and heating systems. This study makes several noteworthy contributions to the existing literature and extends our knowledge within this field. In the following, I summarise each contribution to the literature in a few sentences. 1) Variable renewable power production and consumption are hardly affected by a changing climate. 2) Space heating is significantly affected according to the degree of climate change. 3) Modelling the energy consumption for space heating by incorporating the weather and primary fuel consumption has shown improvements compared to the existing literature. 4) Heat pumps become more economic viable and more widespread in Europe with an increasing degree of climate change. 5) Independent of the climate outcomes, modest cost-benefits are observed for a strongly coupled European electricity and heating system compared to the weakly coupled counterpart. Climate change has on other hand a significantly higher impact on the costs of designing future coupled systems compared to historical reference values.

Appendix

CHAPTER 7

21st century climate change impacts on key properties of a large-scale renewable-based electricity system

The material in this chapter is the Supplemental Information (SI) for the paper *21st Century Climate Change Impacts on Key Properties of a Large-Scale Renewable-Based Electricity System*. The material is not intended for the regular reader, but only for other researchers, with special interests. Section 1 provides a general overview of the climate models that are used in this work along with a short description on their numerical biases. Section 2 presents the electricity system modelling and system key metrics. In section 3 the underlying procedures of the data conversion and validation processes are explained along with the results. Section 4 presents the methods of correcting the electricity consumption profiles for impacts from electrified heating and cooling along with the results. The methods of sections 2, 3 and 4 are straight forward applicable to other studies. In Section 5, the statistical test that is used for this work is presented. Section 6 presents additional results to the main article.

7.1 Extended introduction

In this section, the climate models are introduced and how they assist research on climate change. The need for climate models is explained at first and followed by a description of biases that might be introduced due to the underlying climate assumptions. A short technical description of the local and global models that are used in this work is presented. After that, the latest generation of IPCC's climate projections are explained. In the last section, the data that is available for this study is presented.

The need for climate models

Studies on the impact of climate change on human and natural systems are highly dependent on state-of-art mathematical models of climate projections. These are most commonly built upon assumptions on the average concentrations and emission of heat trapping gases in the atmosphere. The need for information on climate change is necessary in order to perform timely mitigation strategies. So far, synoptic scale climate models succeed in representing trends of large scale weather changes but lacks in describing these on the meso or lower spatial scales. Meso scale models with high accuracy of prediction are important due to climate weirding, which is a term that describes how climate change may cause local weather to become more unpredictable and extreme in addition to general increase in average temperature [269, 270]. Regional and global climate models are a set of models describing the past and present climates on the meso and synoptic scales, respectively. Below, the most common climate models known to the literature are described.

General circulations models or global climate models, GCM, are a class of complex mathematical representations of the coupling between atmospheric and oceanic global climate models, AGCM and OGCM, respectively. AGCM's consist of a dynamical core which solves the equations of fluid motion for e.g. surface pressure along with other variables as solar radiation, velocity or the temperature. Apart from atmospheric components the AGCM's usually contain a model representing the land surface. Examples of AGCM's common to the literature are the Integrated Forecasting System, IFS, made available by the European Centre for Medium Range Weather Forecasts ECMWF, the ECHAM6 developed at the Max Planck Institute MPI or the Hadley Atmospheric Model 3 HadAM3 available from the Hadley Centre. OGCM's model the oceans with fluxes imposed from the atmosphere and may as well contain sea ice models.

Examples of OGCM's are the Nucleus for European Modelling of the Ocean NEMO, the Max Planck Institute ocean model MPIOM or the Hadley Oceanic Model 3 HADOM3. AGCM's and and OGCM's can be coupled forming AOGCM's here after denoted as GCM's.

Most of the current GCM's run with a spatial resolution of $1°$ which corresponds to approximately $110\,\mathrm{km}$ over Europe. These large scale grid cells are able to cover vastly differing areas from high mountains to flat coasts. In order to understand the outcome of future climate projections on smaller scales a down scaling from the GCM's to regional climate models RCM's is needed. A technique used most commonly is dynamical down scaling, DD, in which outputs from the driving models, GCM's, are used as forcing data to provide boundary and initial conditions for the RCM run [271, 272]. In this regard, the large scale information from the GCM's are contained within the RCM domain. The RCM run is hereby able to simulate meso scale properties on a finer domain. Throughout this work this process will be referred to as "RCM run GCM forcings". This method has so far been used in a variety of projects as the Ensembles-based predictions of climate changes and their impacts ENSEMBLES [273], the Regional Climate Model Inter-comparison Project RMIP [274], the North American Regional Climate Change Assessment Program NARCCAP [275], the Prediction of Regional scenarios and Uncertainties for Defining European Climate change risks and Effects PRUDENCE [276], the Europe–South America network for climate change assessment and impact studies CLARIS [277], and A COordinated Regional climate Downscaling EXperiment CORDEX [70, 106] which is used in this work. The CORDEX experiment provides data with spatial resolution of $0.11°$ or $0.44°$ corresponding to approximately $12\,\mathrm{km}$ or $50\,\mathrm{km}$ in Europe, respectively. The standard temporal resolutions are $3\,\mathrm{hr}$, $6\,\mathrm{hr}$, $12\,\mathrm{hr}$, monthly.

Biases in global climate models

Although successive research within climate modelling provides comprehensive knowledge on the climate there is still a need for more attention in this field. Below a brief discussion on biases is presented that are evident within the climate variables that are important for this study.

The North Atlantic eddy-driven jet stream was investigated with 11 CMIP5 GCMs by evaluating the jet latitudes and wind speeds in a historical run from 1980-2004 [278]. Compared to reanalysis, typical biases between $1°$ and $2°$ are observed in the latitude mean seasonal cycle anomaly for a majority of the GCMs.

The corresponding seasonal amplitude variations reach up to $\pm 10^\circ$ for a few GCMs, which is an over or underestimation of about 5° compared to reanalysis. But compared to identical CMIP3 GCMs, it is an improvement [279]. In addition, a slight poleward shift in the jet stream was shown under the IPCC RCP4.5 and RCP8.5 induced global warming during the end of the century [278]. This is further confirmed for 26 CMIP5 GCMs under the IPCC RCP8.5 emission scenario, which shows a poleward jet shift of approximately 2° in the Southern Hemisphere and 1° in the North Atlantic and North Pacific [280]. In all GCMs, the mean seasonal anomaly bias for the jet stream wind speeds is overestimated for the winter months while the opposite is the case for summer months. A majority of the GCMs are overestimating the corresponding amplitudes [278]. The jet wind speed biases are smaller in the CMIP3 GCMs compared to the CMIP5 GCMs [279].

The GCM cloud simulations, which most directly affect the solar energy yield calculated in our study, remain the major source of inaccuracy in climate predictions. Total amount of cloud cover, amongst other climate variables, in 27 CMIP5 GCMs was evaluated by comparing to satellite data covering the years 1986-2007 [281]. It is shown that the linear correlation coefficient of the GCM wise 20 year annual average of the total cloud amount ranges from 0.11 to 0.83 with a root mean square error of 10% to 23%. For CMIP5 experiments, the IPCCs Fifth Assessment Report AR5 [282] presents a difference of 2% to 3% in regional changes of cloud fractions for the years 2081–2100 under the RCP4.5 emission scenario. For the RCP8.5 emission scenario, a difference of 5% to 6% is presented.

The global radiation budget biases that are most strongly influenced by clouds are the incomming radiative shortwave flux at the surface along with the outgoing flux at top of the atmosphere and the reflected flux. For a number of CMIP5 GCMs, regional biases were found to range from $-25\,\mathrm{Wm}^{-1}$ to more than $30\,\mathrm{Wm}^{-1}$ for the incomming flux compared to EBAF-Surface flux radiation product for a time period 2000-2010 [283]. The multimodel global area average bias is reduced by 30% compared to CMIP3 GCMs. Similar findings are evident for the regional outgoing flux as well as reflected flux with an improvement of the multimodel global area average bias with a factor of 2 compared to CMIP3 GCM. With these consideration in mind, it is evident that CMIP5 GCMs have improved since phase 3, although room for further improvement remains. In this work, the compensation for static biases in the solar energy yield as explained in the methods section.

In the present study, surface air temperatures are used to adjust the electrical demand for changes in heating and cooling needs. The GCM ability to accurately replicate this field is receiving increasing attention. A recent study on the European domain shows negatively biased winter temperatures in the North compared to ground observations [76, 77]. Positively biased summer temperatures are observed in the East and Central Europe for 33 CMIP5 GCMs. For the total European domain, the GCM ensemble mean bias is approximately $-1\,^{\circ}\mathrm{C} \pm 8\,^{\circ}\mathrm{C}$ during winter months. The corresponding values for summer months are $0.5\,^{\circ}\mathrm{C} \pm 6\,^{\circ}\mathrm{C}$. Similar trends are found for Northern Eurasia where the winter and summer periods show the largest biases [78]. Small improvements has been made since CMIP3 GCMs [79].

Global and regional climate models

EC-EARTH [44] is a coupled global climate and earth system model that was developed on the basis of the numerical weather prediction model, NWP, of the European Centre for Medium-Range Weather Forecasts, ECMWF. The components of EC-EARTH consist of ECMWF's atmospheric model IFS, a land model H-TESSEL [284], an oceanic circulation model NEMO [285] and a sea ice model LIM [286]. The Integrated Forecasting System IFS cycle31r1, utilises the 3-dim Navier Stokes equations and uses a spectral method to compute the dynamics of the atmosphere in each grid-point. A complete description of the IFS specific cycle31r1 can be found on the website of ECMWF. This model includes Observation Processing [287], Data Assimilation [288], Dynamics and Numerical Procedures [289], Physical Processes [290], The Ensamble Prediction System [291], Technical and Computational Procedures [292] and the Wave model [293]. Minor changes to the physics parametrisations evolving from a set of later ECMWF cycles has been utilised in order to optimise the model for climate simulations. IFS and H-TESSEL are coupled to NEMO and LIM2 by the Ocean Atmosphere Sea Ice Soil version 3, OASIS [294].

The Hardley Global Environment Model 2 - Earth System, HadGEM2 [63], is a coupled earth system model based on a two stage development from its predecessor HadGEM1 [295] along with additional improvements as described in [296]. The components of the HadGEM2 model consist of a land surface exchange scheme MOSES II [297], a large-scale hydrology module LSH [298] which is based on the TOPMODEL approach [299], a river scheme based on the TRIP model [300], an improved representation of the aerosols [301], an atmospheric chemistry component based on the UK Chemistry and Aerosols model UKCA [302], a terres-

trial carbon cycle component which is developed on the basis of the TRIFFID dynamic vegetation model [303] and a soil carbon model RothC [304], and an ocean carbon cycle component [63].

The Max Planck Institute Earth System Model MPI-ESM-LR is a coupled earth system model which consists of the atmospheric circulation model component ECHAM6 [305] which is development from its predecessor ECHAM5 [306, 307]. A land vegetation model JSBACH [308] and an ocean-sea ice component MPIOM [309] is implemented as well. The coupling of the atmospheric and oceanic models is done by OASIS as in EC-EARTH.

HIRHAM5 [43] is a regional atmospheric climate model developed on the basis of the dynamics used in the High Resolution Limited Area Model HIRLAM7 [310] and the physical parametrisation schemes from the global climate model ECHAM5 [306, 307]. The set of HIRLAM models are numerical short-range weather forecasting systems developed by the international HIRLAM program and used for weather forecasting by numerous meteorological institutes as DMI, FMI, KNMI, met.no, INM and SMHI. ECHAM5 is a general atmospheric circulation model developed on the basis of the dynamics from ECMWF operational forecast model cycle 36 and a comprehensive parametrisation package developed at Hamburg. The full summary of changes of the model cycles of ECMWF can be seen on the website of ECMFW.

The set of regional climate models *RCA* are initially based upon the numerical short-range weather forecasting system HIRLAM [311]. The latest release of the RCA models, RCA4 [74], includes both physical and technical upgrades in respect to RCA3 [73]. RCA3 performed substantially well over Europe due to incorporated European climate parametrisations and compensating errors. The focus of RCA4 was to create a model that is usable in any domain worldwide without the need for retuning. In RCA4, the physical parametrisation was improved by including a new global physiography data base amongst other physical parametrisations.

RACMO2.2 is the latest release of its family of RACMO2 [75] regional climate models in which the dynamics has not been changed since its predecessor RACMO2.0 [312]. Certain physics are changed as a new physics package emanating from ECMWF cycle 31r1 has been used.

The *climatic version of the COSMO model, CCLM,* is a non-hydrostatic regional climate model developed by the Climate Limited-area Modelling-Community, the

CLM-Community, which became the regional community model for the German climate research in 2005. CCLM is based upon its predecessor Local Model, LM, of the German Meteorological Service.

7.2 Extended experimental procedures

Electricity system modelling

The electricity system network topology is composed of 30 nodes with 50 interconnecting links as seen in Figure 7.1. Each node, n, represents a country of Europe. All nodes are supplied by a wind and solar power generation time series, $G_n^W(t)$ and $G_n^S(t)$, and an electricity demand time series $L_n(t)$. The country-wise total renewable electricity generation, $G_n^R(t)$, is given in terms of the total wind, $G_n^W(t)$, and solar, $G_n^S(t)$, power generation as:

$$G_n^R(t) = \gamma_n \left(\alpha_n G_n^W(t) + (1-\alpha_n) G_n^S(t) \right) \langle L_n \rangle_t \tag{7.1}$$

where $\langle\rangle_t$ denotes the time average. The wind-solar mix, α_n, and renewable penetration, γ_n, are defined as:

$$\alpha_n = \frac{\langle G_n^W \rangle_t}{\langle G_n^R \rangle_t} \quad \text{and} \quad \gamma_n = \frac{\langle G_n^R \rangle_t}{\langle L_n \rangle_t}$$

α_n allows for a any desired mixture of wind and solar power within the total renewable generation. γ_n allows for any share of renewable power to cover the demand. $\alpha_n = 1$ represents a pure wind dominating electricity network while $\alpha_n = 0$ represent complete solar domination. The instantaneous mismatch between the renewable electricity generation and the electricity demand

$$\Delta_n(t) = G_n^R(t) - L_n(t) \tag{7.2}$$

is in most instances non-zero as a consequence of fluctuating weather and consumption [109] in the search for an optimal mixture of wind and solar power in electricity systems. The more advanced electricity system modelling includes a balancing response [113], $B_n(t)$, between renewable power and demand along with a power transmission response [112], $P_n(t)$. Equation 7.3 defines the nodal balancing equation that has to be fulfilled by all nodes at all time steps:

$$\Delta_n(t) = B_n(t) + P_n(t) \tag{7.3}$$

The instantaneous mismatch has to be balanced by power generation or by curtailing renewable power and/or by the means of power transmission response.

Two extremes of nodal coupling are defined. In the first, a limited power transmission introduces nodal independence. The power transmission response, $P_n(t)$, is consequently zero for all nodes at all time steps:

$$P_n(t) = 0 \quad \forall n, t,$$

From Equation 7.3 it is evident that each node has to sustain its own power balancing either by subsidising with dispatchable power or curtailing renewable power. In the second approach, infinite transmission capacities introduce full nodal coupling. The countries are forced to synchronise their electricity system balancing response relative to their mean load [113] as:

$$B_n(t) = \frac{\langle L_n \rangle}{\Sigma_k \langle L_k \rangle} \Sigma_m \Delta_m(t)$$

Fixed installed wind and solar capacities

The already presented electricity system modelling approach has to be extended in order to ensure fixed wind and solar capacities, K_n^W and K_n^S, for all climate simulations. In the current approach, the installed wind and solar capacities fluctuate in time and space according to weather fluctuations presented by the wind and solar capacity factors, $CF_n^W(t)$ and $CF_n^S(t)$, as shown by Equation 7.4. Nodal wind and solar capacities that are fixed in time are then defined by taking an average of the reference/historical, ref, capacity factors from 1986-2006 for the HIRHAM5-EC-EARTH climate model as shown in Equation 7.5.

$$K_n^W(t) = \frac{\gamma_n \alpha_n \langle L_n \rangle_t}{CF_n^W(t)} \quad \text{and} \quad K_n^S(t) = \frac{\gamma_n (1-\alpha_n) \langle L_n \rangle_t}{CF_n^S(t)} \tag{7.4}$$

$$K_{n,ref}^W = \frac{\gamma_{n,ref} \alpha_{n,ref} \langle L_{n,ref} \rangle_t}{\langle CF_{n,ref}^W \rangle} \quad \text{and} \quad K_{n,ref}^S = \frac{\gamma_{n,ref} (1-\alpha_{n,ref}) \langle L_{n,ref} \rangle_t}{\langle CF_{n,ref}^S \rangle} \tag{7.5}$$

$\alpha_{n,ref}$ and $\gamma_{n,ref}$ are assumed to be fixed at 0.8 and 1, respectively, as these values minimise the need for dispatchable power [114]. Future wind and solar power generation, $G_{n,scen}^W$ and $G_{n,scen}^S$, for any time period, $scen$, are defined as:

$$G_{n,scen}^W(t) = K_{n,ref}^W \cdot CF_{n,scen}^W(t) \quad \text{and} \quad G_{n,scen}^S(t) = K_{n,ref}^S \cdot CF_{n,scen}^S(t)$$

The newly acquired wind-solar mixture, $\alpha_{n,scen}$, and the renewable penetration, $\gamma_{n,scen}$, are defined as:

$$\alpha_{n,scen} = \frac{\langle G_{n,scen}^W \rangle}{\langle G_{n,scen}^W \rangle + \langle G_{n,scen}^S \rangle} \quad \text{and} \quad \gamma_{n,scen} = \frac{\langle G_{n,scen}^W \rangle + \langle G_{n,scen}^S \rangle}{\langle L_{n,scen} \rangle}$$

and the total renewable electricity generation is defined as:

$$G^R_{\text{n, scen}}(t) = G^W_{n,scen}(t) + G^S_{n,scen}(t)$$

$G^R_{n,scen}(t)$ replaces $G^R_n(t)$ in Equation 7.2. $L_n(t)$ is replaced by $L_{n,scen}(t)$. The electricity demand profile is corrected for impacts from electrified heating and cooling as explained in Section 7.2.

Key metrics

The dispatchable electricity, $G^B_n(t)$, is extracted from the system balancing response and is defined as:

$$G^B_n(t) = -\min(B_n(t), 0)$$

For an aggregated network topology, the dispatchable electricity is normalised to the total system-wise load and defined as:

$$G^B = \frac{\sum_n \langle G^B_n(t) \rangle_t}{\sum_n \langle L_n(t) \rangle_t}$$

The benefit of transmission, β_T, is defined as the absolute difference of the system-wise backup power, G^B, for zero and infinite transmission, T_0 and T_∞, respectively, as:

$$\beta_T = G^B(T_0) - G^B(T_\infty)$$

The benefit of storage, β_S, is defined as the absolute difference of the system backup power, G^B, when calculated by using the original generation-demand mismatch, $\Delta_n(t)$, and a 24-hour running average, $\Delta^{\text{smoothed}}_n(t)$, as:

$$\beta_S = G^B(\Delta_n(t)) - G^B(\Delta^{\text{smoothed}}_n(t))$$

The dispatchable capacity, κ^B, defines the amount of dispatchable electricity that can be produced at each time step as:

$$0.99 = \int_0^{\kappa_n^B} p_n \left(G_n^B \right) dG_n^B$$

where p_n denotes the probability. By using a 100% quantile of the dispatchable energy would over estimate the need for backup energy as these events are rare and occur only in few hours during a year. A 99% quantile is around half as large. The total system-wise value is a summation over all nodes as:

$$\kappa^B = \sum_n \kappa_n^B$$

The system-wise variability is defined as:

$$\sum_n std_t \left(G_n^B(t) - G_n^B(t+1) \right) / K^{W+S}$$

where std_t denotes the standard deviation in time. K^{W+S} denotes the system-wise installed wind and solar capacities.

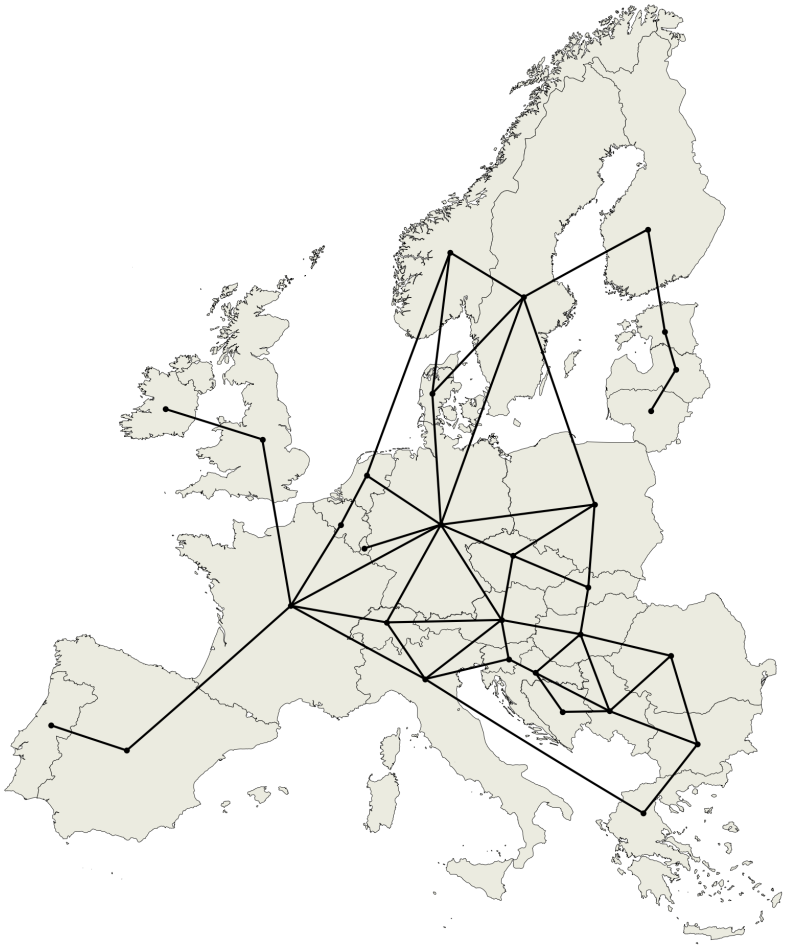

Figure 7.1: Network topology of the European electricity system

Conversion and validation of energy system related data

Known to the literature, climate models tend to over or underestimate their data output with different local biases around the globe [313, 314, 315]. Climate model data is applicable to studies as energy system modelling, but requires calibration in order to meet the weather events for the region of interest. Climate data is used to produce wind and solar capacity factor profiles for the different countries of Europe. The time series calibration is then performed on the capacity factors due to their direct use in the electricity system. These are calibrated according to already bias adjusted wind and solar capacity factor time series provided by the Renewables.ninja [37, 39]. Renewables.ninja provide hourly wind capacity factors for the EU-28 plus Norway and Switzerland simulating the present-day fleet of wind farms and hourly solar capacity factors for the EU-28 plus Norway and Switzerland, simulating the present-day fleet of PV farms. The capacity factors are calibrated within the reference/historical period ranging from 1986 to 2006. The acquired biases are then applied to all future time periods.

Wind speed to wind power conversion

In this section, the conversion process of the wind speeds into wind capacity factors is presented. To represent the current country-wise installed wind capacities, the equivalent amount of 3.6MW SIEMENS SWT 107 turbines are placed at the nearest grid points according to their real sites [35]. Figure 7.3 shows the real turbine distribution across Europe.

The full conversion procedure is composed of a wind speed extrapolation process and wind speed to wind power conversion process, as shown in Figure 7.2.

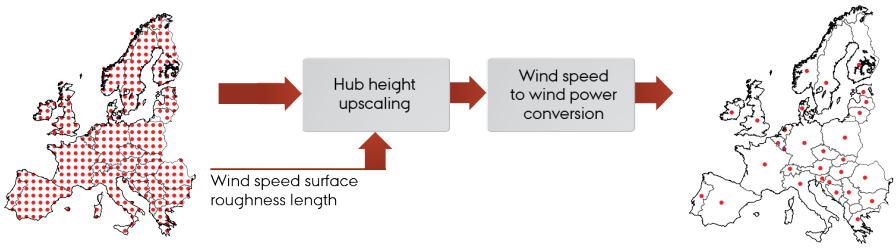

Figure 7.2: Schematic presentation of the wind speed to wind power conversion procedure.

This is performed in each grid cell followed by a country-wise aggregation. The 10 m wind speeds have been extrapolated to meet the wind speeds at the turbine hub height of 90 m. Vertical extrapolation of wind speeds is most commonly described by a logarithmic scaling law in planetary boundary layers, see Equation 7.6, and treats the vertical variation of the mean wind speed, u, as a function of the height, h, above the ground, the surface roughness length, z_0, and the 10 m wind speeds, $u_{10\,\mathrm{m}}$ [316]

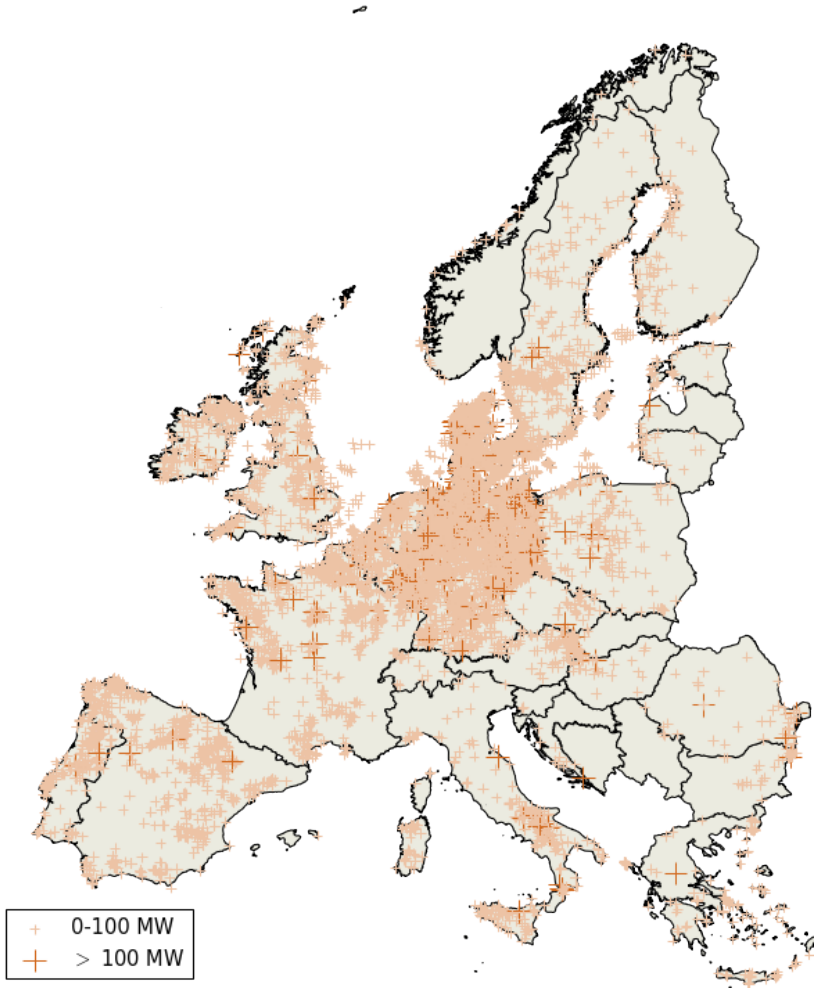

Figure 7.3: Wind turbine/fleet sites positioned according to the wind database [35]

$$u(h) = u_{10m} \cdot \frac{\ln \frac{h}{z_0}}{\ln \frac{10\text{m}}{z_0}} \tag{7.6}$$

The extrapolated wind speeds are converted into wind power by a smoothed version of the original wind power curve, shown as the dashed and full drawn curves, respectively, in Figure 7.4. Essentially, turbines assigned to one grid cell are not all affected by the same wind speeds. Furthermore, the turbines may not perform as specified by the manufacturer or some turbines could be out of operation due to maintenance. To take all effects into consideration a simple heuristic smoothing function [36], is applied to the original wind power curve. The smoothed power curve, P_{smooth}, has been calculated for all wind speeds, v_0, below the cut-out speed as the convolution:

$$P_{smooth}(v_0) = \eta \int_0^\infty P_0(v)\text{Ker}(v_0, v - \Delta v)dv \tag{7.7}$$

$$\text{Ker}(v_0, v - \Delta v) = \frac{1}{\sqrt{2\pi}\sigma_0} e^{-\frac{1}{2}\left(\frac{(v_0 + \Delta v - v)}{\sigma_0}\right)^2}$$

The integral of the kernel is normalised to unity and its functional form is a Gaussian curve with a standard deviation, σ_0, and a mean value, $v_0 + \Delta v$. The smoothing parameters, Δv and σ_0, determine the shape of the smoothed power curve. Δv determines a simple offset in the power production while σ_0 determines the smoothing degree of the original power curve. The country-wise wind power generation time series have been normalised to the maximum installed wind power capacity. This normalisation provides the wind capacity factors which have to be corrected for the bias that appears within the climate models. The country-wise smoothing parameters are determined during the bias adjustment as explained in the following section.

Wind power calibration

The optimisation problem in Equation 7.8 determines the smoothing parameters by minimising the Kullback-Leibler (KL) divergence between the Renewables.ninja and climate model capacity factors. The KL-divergence is a well known non-symmetric measure of the difference between two probability distributions. It measures the information lost, when in this context, the climate data capacity factor profiles are used to approximate the Renewables.ninja profiles.

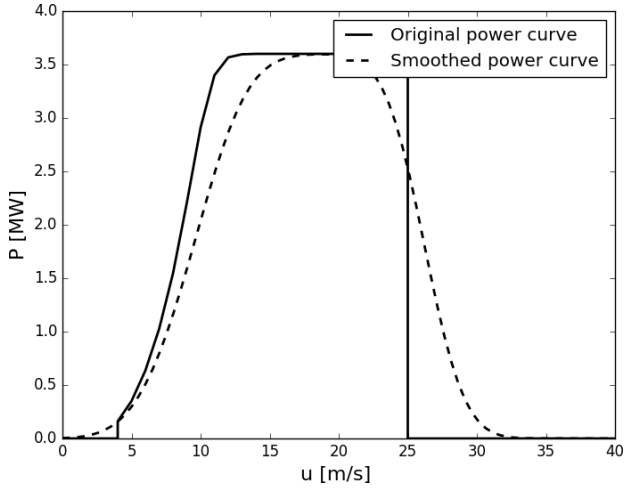

Figure 7.4: Wind power curves for the Siemens SWT 107 3600kW turbine. The full drawn curve represents the original power curve and the dashed curve represents the smoothed power curve for $\sigma_0 = 2.29$ and $\Delta v = 1.27$.

In Equation 7.8, $CF^W_{\mathrm{R,q}}$ represents a certain quantile, q, of the Renewables.ninja capacity factor time series while $CF^W_{\mathrm{C,q}}$ represents the same quantile for the climate model time series. The set of σ_0 and Δv that leads to the lowest KL-divergence are then fixed as the final smoothing parameters an applied to the original wind power curve. This optimisation is performed for each country in all climate models. The optimised wind power curve is then used in the conversion process for all future periods.

$$\begin{aligned} \text{minimise} \quad & D_{\mathrm{KL}} = \sum_q CF^W_{\mathrm{R,q}} \ln\left(\frac{CF^W_{\mathrm{R,q}}}{CF^W_{\mathrm{C,q}}(\sigma_0, \Delta v)}\right) \\ \text{subject to} \quad & 1 \leq \sigma_0 \leq 10 \\ & -2 \leq \Delta v \leq 10 \end{aligned} \tag{7.8}$$

Wind power calibration results

Figures 7.5 to 7.10 show the resulting D_{KL} from each minimisation step in Equation 7.8 as heat maps for all climate models: HIRHAM5-EC-EARTH, RCA4-EC-EARTH, RCA4-HadGEM2-ES, RACMO22E-EC-EARTH, RACMO22E-

HadGEM2-ES and CCLM4-MPI-ESM-LR. D_{KL} is normalised to the maximum occurring value, 325.60, which appears for Luxembourg in the climate model RCA4-HadGEM2-ES. The black dots indicate the optimal values of σ_0 and Δv that minimises D_{KL}.

Table 7.1 summarise the resulting D_{KL} from each minimisation step in Equation 7.8. Some countries as e.g. Denmark and Germany indicate a very localised distribution of D_{KL} and small changes in σ_0 and Δv leads to prominent changes in D_{KL}. Other countries show a more smoothed distribution in which the same changes in σ_0 and Δv lead to negligible changes in D_{KL}. In general, D_{KL} for the regional climate models HIRHAM5 and RACMO22E show a more localised distribution compared to the respective countries in RCA4 and CCLM4. Wind time series for Serbia and Bosnia are not available in Renewables.ninja. To attain σ_0 and Δv for these countries the average of the neighbouring countries was applied.

Figure 7.11 show a comparison of the climate model historical capacity factors to the Renewables.ninja capacity factors as qq-plots. The wind capacity factor profiles from the different climate models compares statistically well to the Renewables.Ninja for the majority of the European countries. Few countries, as Portugal, show results that are either over or under estimating the wind power profiles, even after the bias adjustment has been performed. As a secondary result, qq-plots of the wind power increments are shown for the different countries in Figure 7.12. The method of power curve smoothing, Equation 7.7, is able to track the wind power increments to a high degree for the majority of countries.

Table 7.2 shows the average values of the wind capacity factors for the different models and countries. These are furthermore shown as bar plots for each climate model in Figure 7.13.

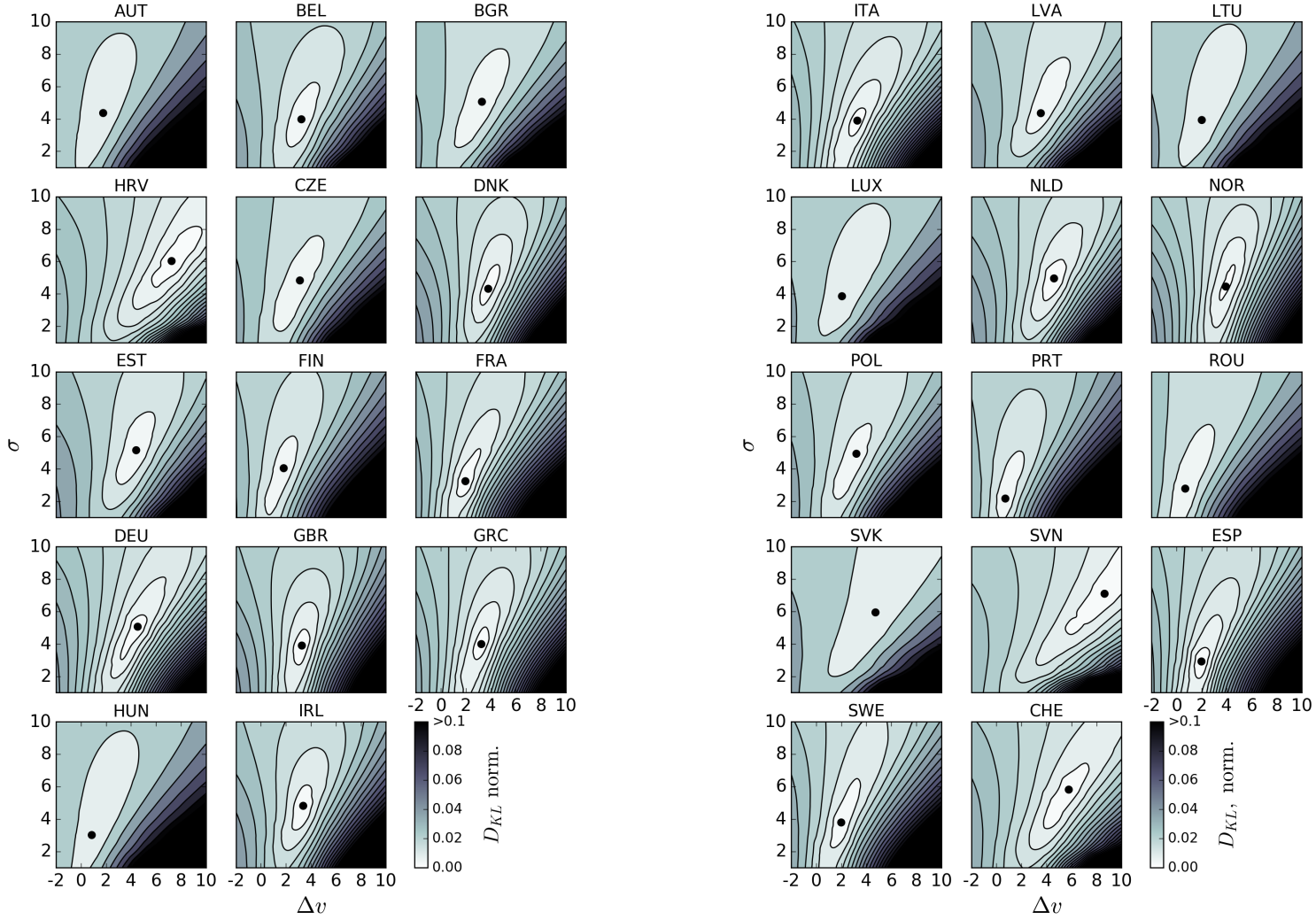

Figure 7.5: Heat maps of the resulting Kullback-Leibler divergence, D_{KL}, as a function of σ_0 and Δv for countries in the climate model HIRHAM5-EC-EARTH, normalised to the maximum occurring value 325.60. The black dots indicate the optimal values of σ_0 and Δv for which D_{KL} is minimised.

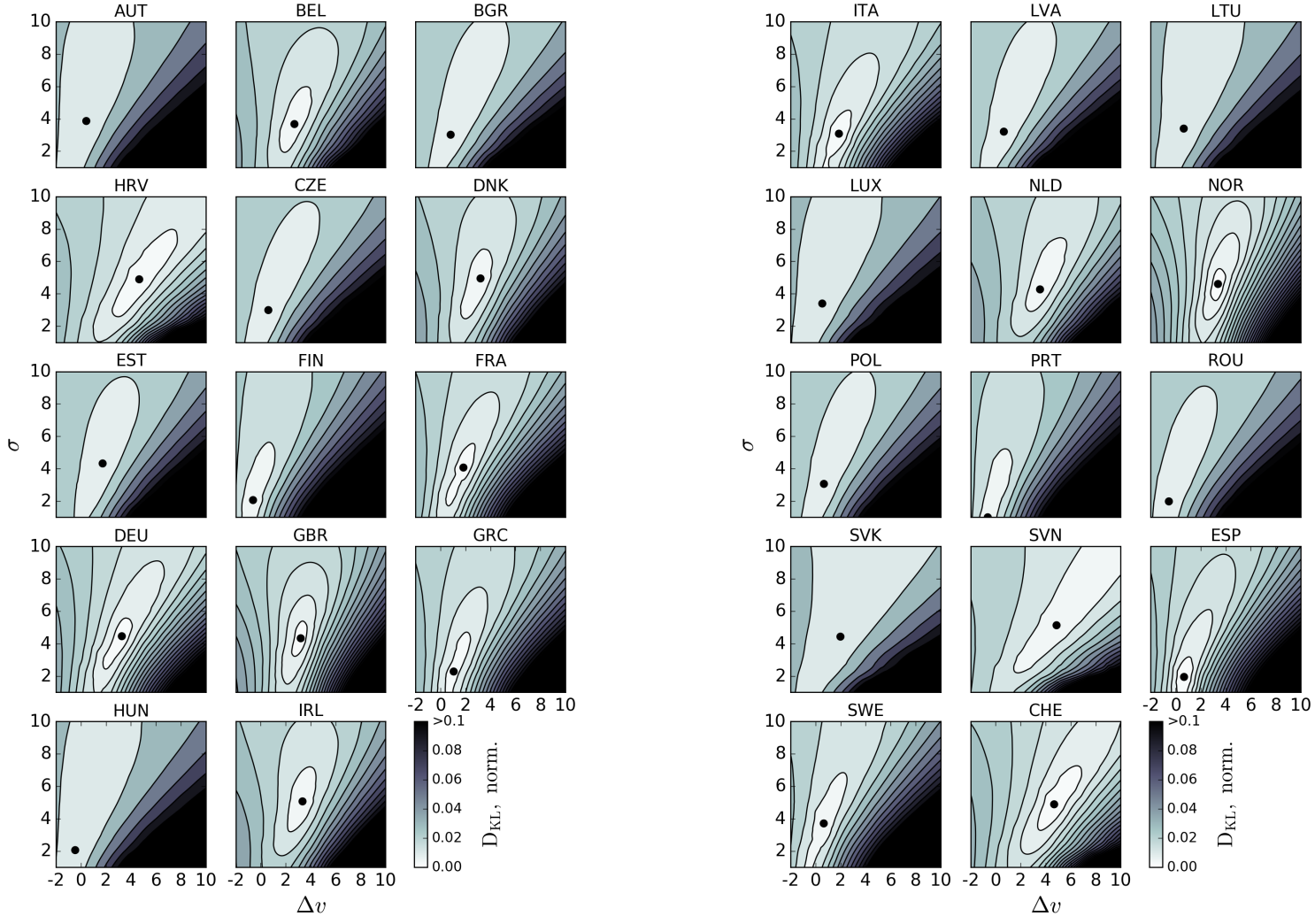

Figure 7.6: Heat maps of the resulting Kullback-Leibler divergence, D_{KL}, as a function of σ_0 and Δv for countries in the climate model RCA4-EC-EARTH, normalised to the maximum occurring value 325.60. The black dots indicate the optimal values of σ_0 and Δv for which D_{KL} is minimised.

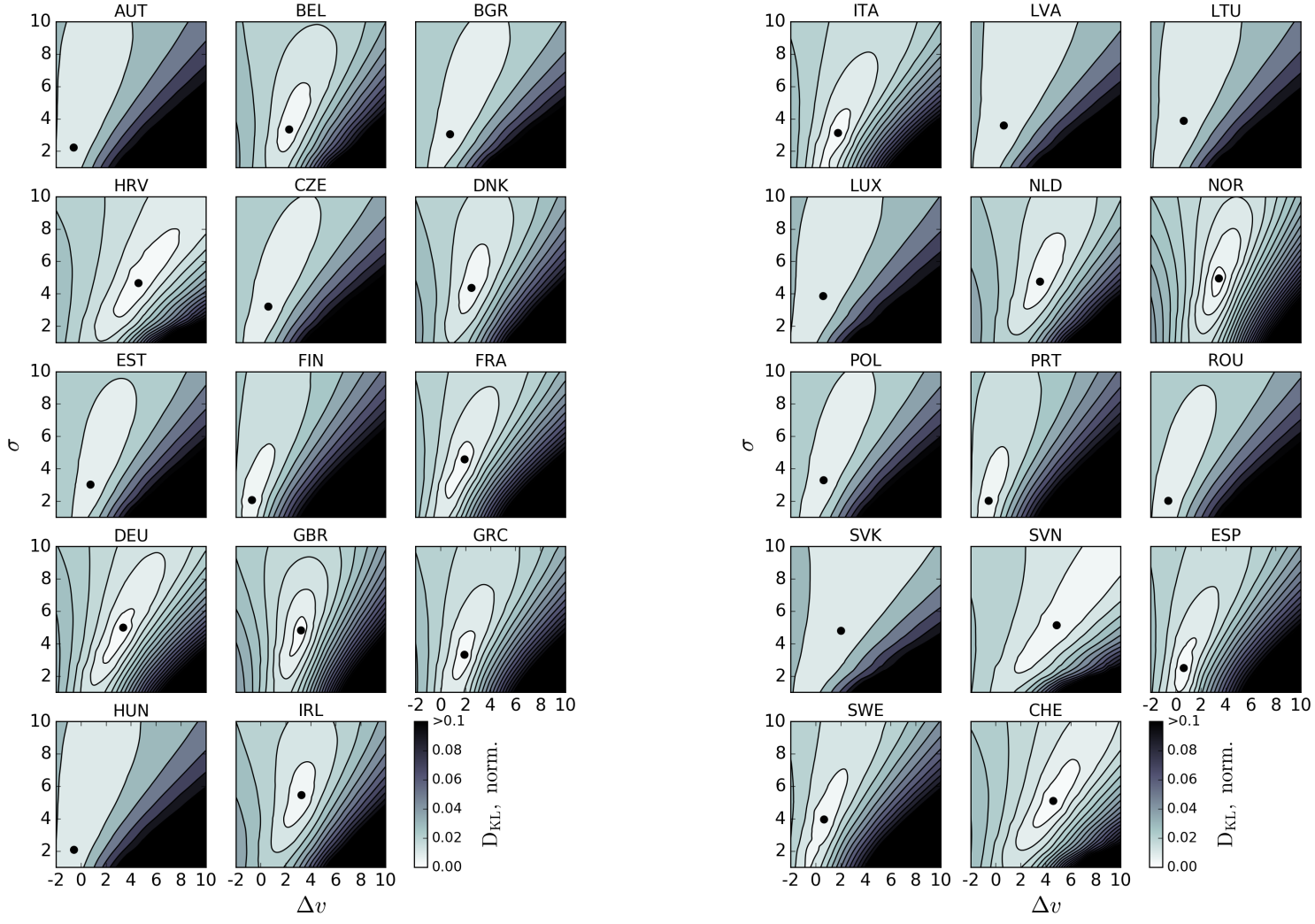

Figure 7.7: Heat maps of the resulting Kullback-Leibler divergence, D_{KL}, as a function of σ_0 and Δv for countries in the climate model RCA4-HadGEM2-ES, normalised to the maximum occurring value 325.60. The black dots indicate the optimal values of σ_0 and Δv for which D_{KL} is minimised.

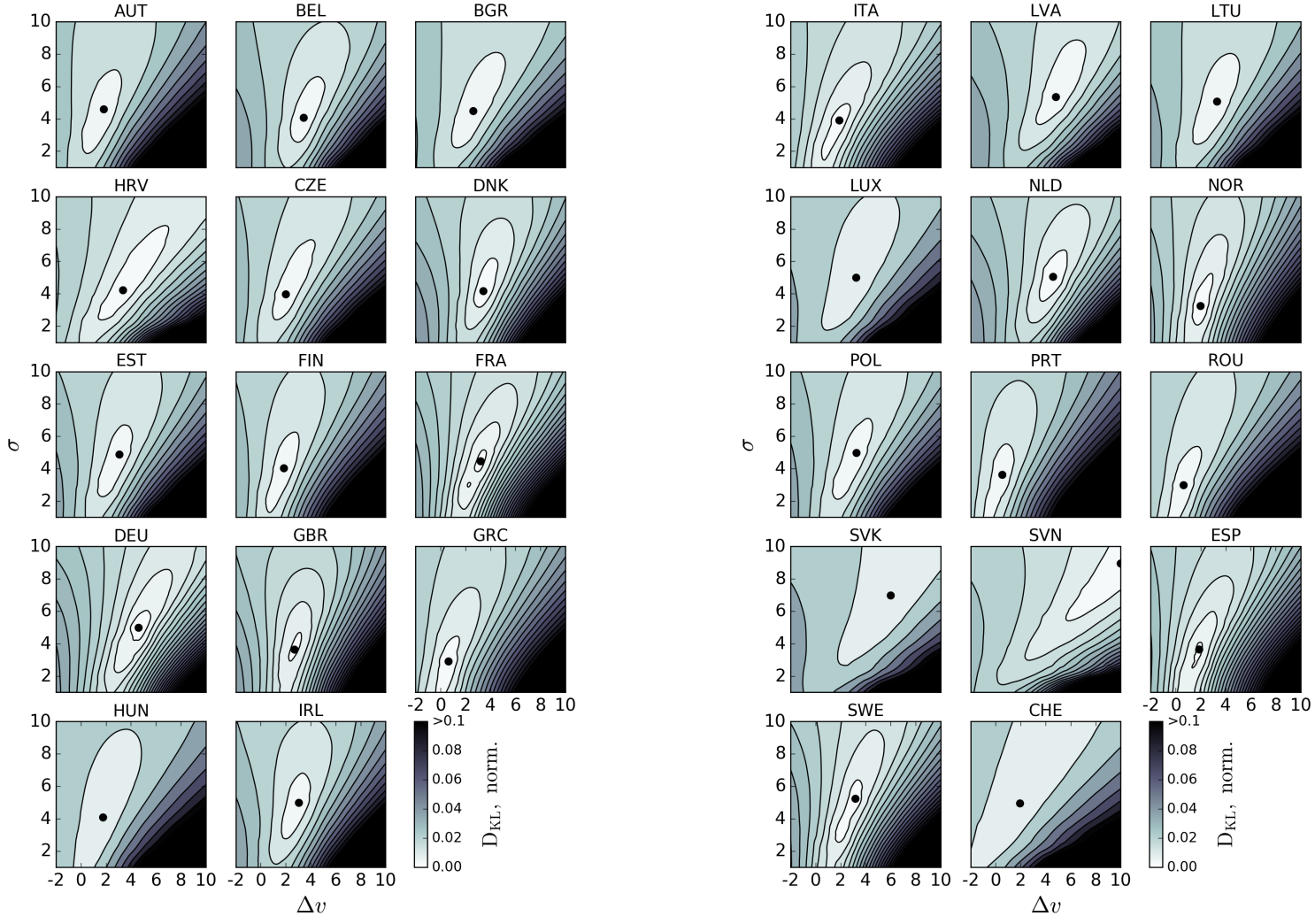

Figure 7.8: Heat maps of the resulting Kullback-Leibler divergence, D_{KL}, as a function of σ_0 and Δv for countries in the climate model RACMO22E-EC-EARTH, normalised to the maximum occurring value 325.60. The black dots indicate the optimal values of σ_0 and Δv for which D_{KL} is minimised.

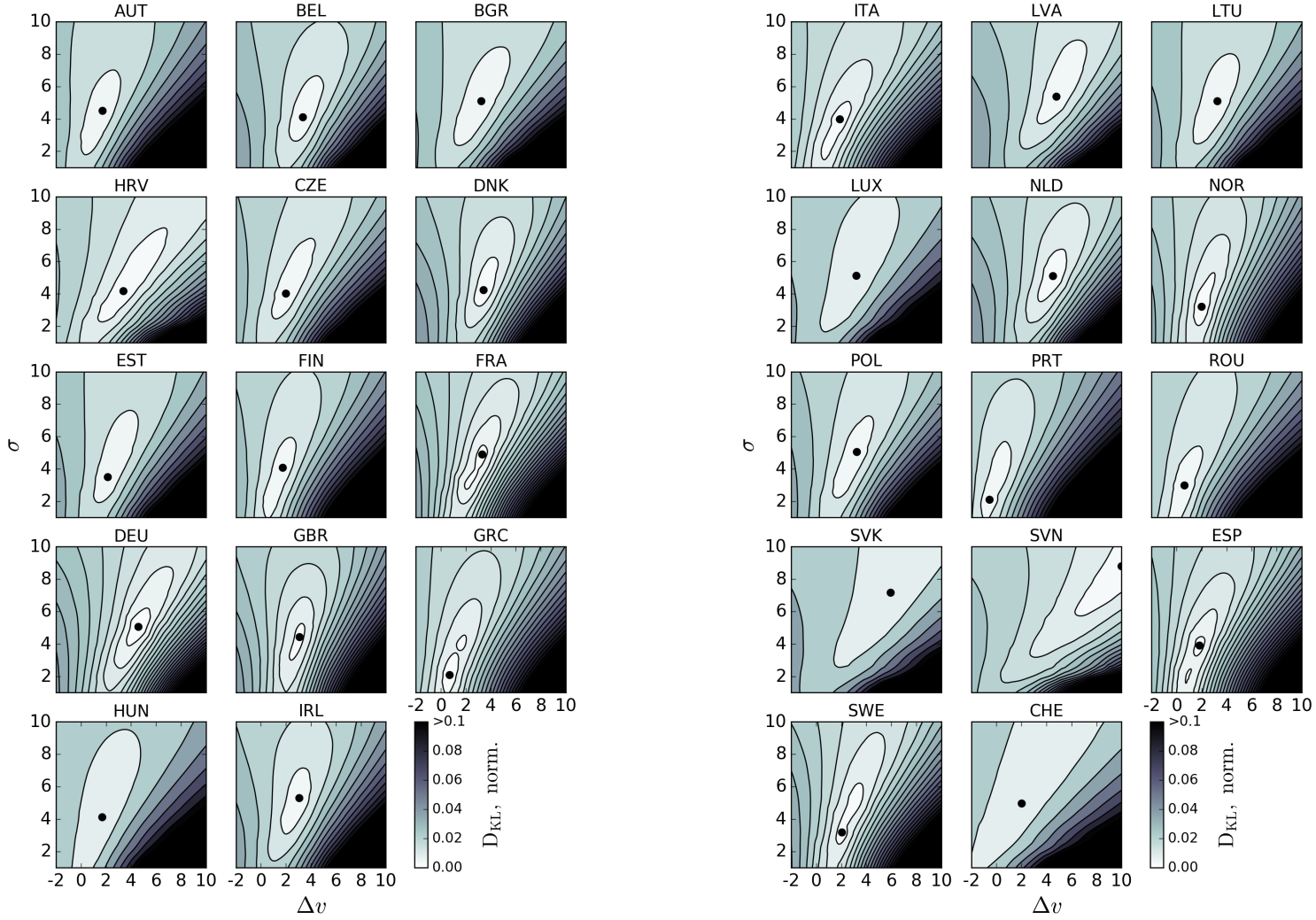

Figure 7.9: Heat maps of the resulting Kullback-Leibler divergence, D_{KL}, as a function of σ_0 and Δv for countries in the climate model RACMO22E-HadGEM2-ES, normalised to the maximum occurring value 325.60. The black dots indicate the optimal values of σ_0 and Δv for which D_{KL} is minimised.

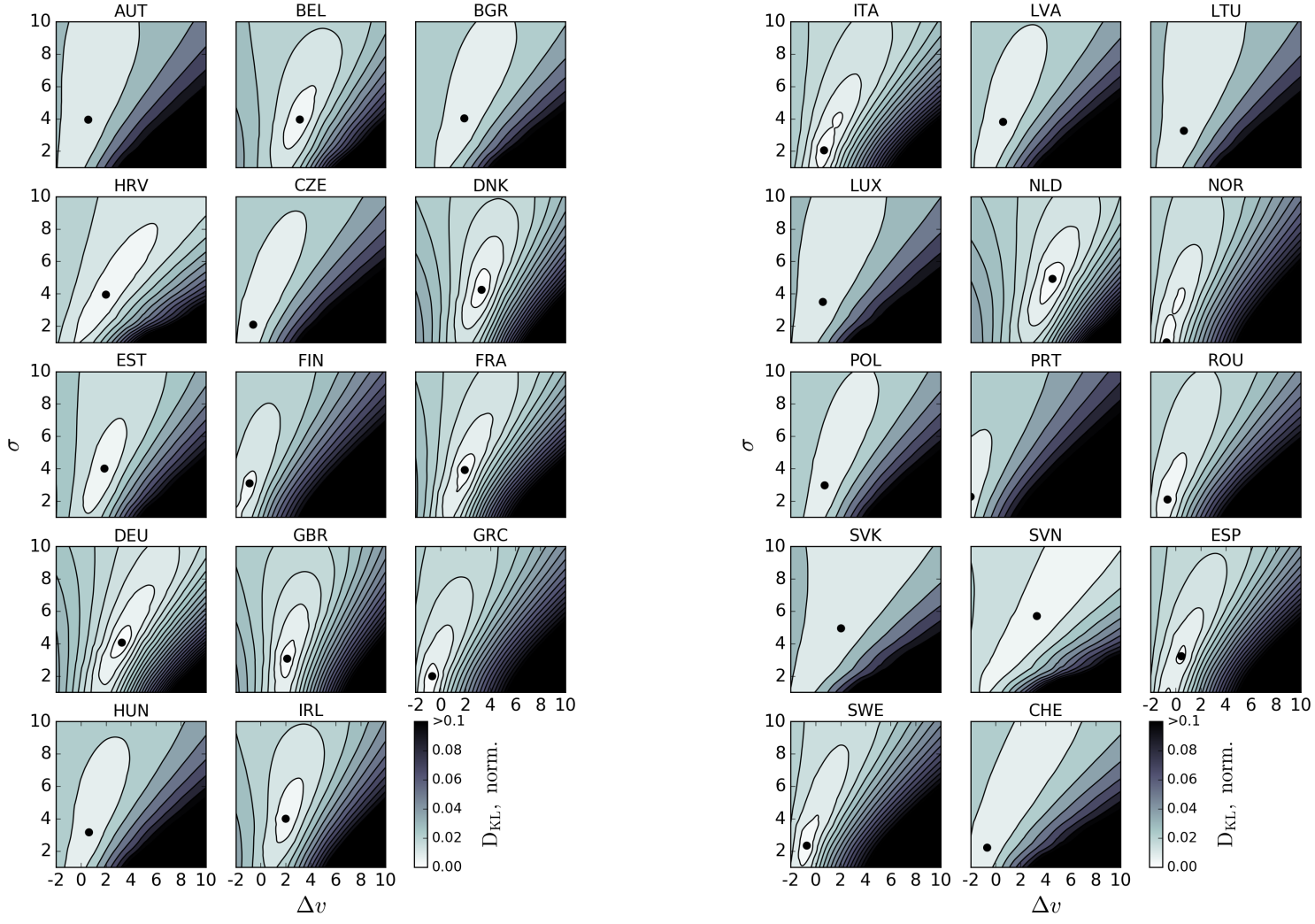

Figure 7.10: Heat maps of the resulting Kullback-Leibler divergence, D_{KL}, as a function of σ_0 and Δv for countries in the climate model CCLM4-MPI-ESM-LR, nosmalised to the maximum occurring value 325.60. The black dots indicate the optimal values of σ_0 and Δv for which D_{KL} is minimised.

Country	HIRHAM5 EC-EARTH		RCA4 EC-EARTH		RCA4 HadGEM2-ES		RACMO22E EC-EARTH		RACMO22E HadGEM2-ES		CCL4 MPI-ES-LR	
	Δv	σ_0	Δv	σ_0	Δv	σ_0	Δv	σ_0	Δv	σ_0	Δv	σ_0
AUT	1.772	4.360	0.426	3.865	-0.583	2.225	1.832	4.586	1.724	4.495	0.583	3.946
BEL	3.237	3.973	2.697	3.676	2.276	3.342	3.441	4.063	3.357	4.099	3.129	3.955
BGR	3.285	5.054	0.811	3.018	0.763	3.045	2.625	4.477	3.237	5.090	1.904	4.027
HRV	7.249	6.027	4.667	4.892	4.607	4.658	3.369	4.216	3.393	4.171	2.000	3.946
CZE	3.117	4.829	0.607	2.991	0.607	3.207	2.012	3.964	2.000	4.018	-0.607	2.090
DNK	3.790	4.315	3.201	4.946	2.480	4.360	3.429	4.162	3.417	4.234	3.285	4.243
EST	4.414	5.153	1.736	4.324	0.763	3.018	3.081	4.874	2.144	3.495	1.880	4.009
FIN	1.820	4.045	-0.619	2.063	-0.703	2.063	1.856	4.027	1.748	4.072	-0.895	3.099
FRA	1.964	3.243	1.832	4.072	1.928	4.577	3.213	4.459	3.309	4.892	1.940	3.919
DEU	4.535	5.063	3.273	4.459	3.381	4.991	4.619	4.982	4.595	5.054	3.273	4.063
GBR	3.273	3.901	3.201	4.333	3.225	4.820	2.709	3.631	3.093	4.423	2.120	3.072
GRC	3.237	3.991	1.051	2.279	1.916	3.315	0.643	2.901	0.703	2.081	-0.667	1.991
HUN	0.859	3.009	-0.462	2.054	-0.559	2.072	1.772	4.072	1.700	4.108	0.643	3.153
IRL	3.381	4.811	3.345	5.063	3.261	5.450	3.057	4.973	3.069	5.288	2.000	3.991
ITA	3.285	3.892	1.868	3.081	1.796	3.126	1.904	3.901	1.892	3.973	0.679	2.054
LVA	3.550	4.351	0.655	3.207	0.655	3.586	4.823	5.342	4.799	5.369	0.595	3.811
LTU	2.012	3.928	0.643	3.396	0.643	3.874	3.309	5.063	3.261	5.090	0.655	3.261
LUX	2.060	3.856	0.535	3.396	0.607	3.856	3.249	4.991	3.213	5.117	0.583	3.495
NLD	4.607	4.955	3.550	4.270	3.550	4.748	4.595	5.045	4.523	5.099	4.547	4.919
NOR	3.934	4.450	3.381	4.604	3.453	4.946	1.988	3.243	2.000	3.207	-0.727	1.000
POL	3.213	4.937	0.667	3.063	0.643	3.288	3.273	4.973	3.249	5.045	0.727	2.973
PRT	0.715	2.171	-0.631	1.000	-0.559	2.018	0.535	3.622	-0.547	2.099	-2.000	2.270
ROU	0.691	2.784	-0.547	1.982	-0.595	2.018	0.631	2.982	0.631	2.982	-0.655	2.099
SVK	4.739	5.946	1.988	4.432	2.036	4.793	6.012	6.973	5.952	7.162	2.036	4.946
SVN	8.643	7.099	4.871	5.135	4.883	5.135	10.000	8.946	10.000	8.793	3.297	5.703
ESP	1.988	2.919	0.667	1.946	0.643	2.495	1.880	3.640	1.832	3.901	0.450	3.225
SWE	2.000	3.784	0.655	3.703	0.679	3.946	3.189	5.225	2.060	3.171	-0.703	2.333
CHE	5.784	5.811	4.679	4.883	4.607	5.090	1.952	4.937	2.024	4.955	-0.679	2.207
SRB	1.612	3.616	-0.066	2.351	-0.130	2.378	1.676	3.844	1.856	4.060	0.631	3.093
BIH	1.612	3.616	-0.066	2.351	-0.130	2.378	1.676	3.844	1.856	4.060	0.631	3.093

Table 7.1: Optimal values of the smoothing parameters, σ_0 and Δv, for the different countries and models.

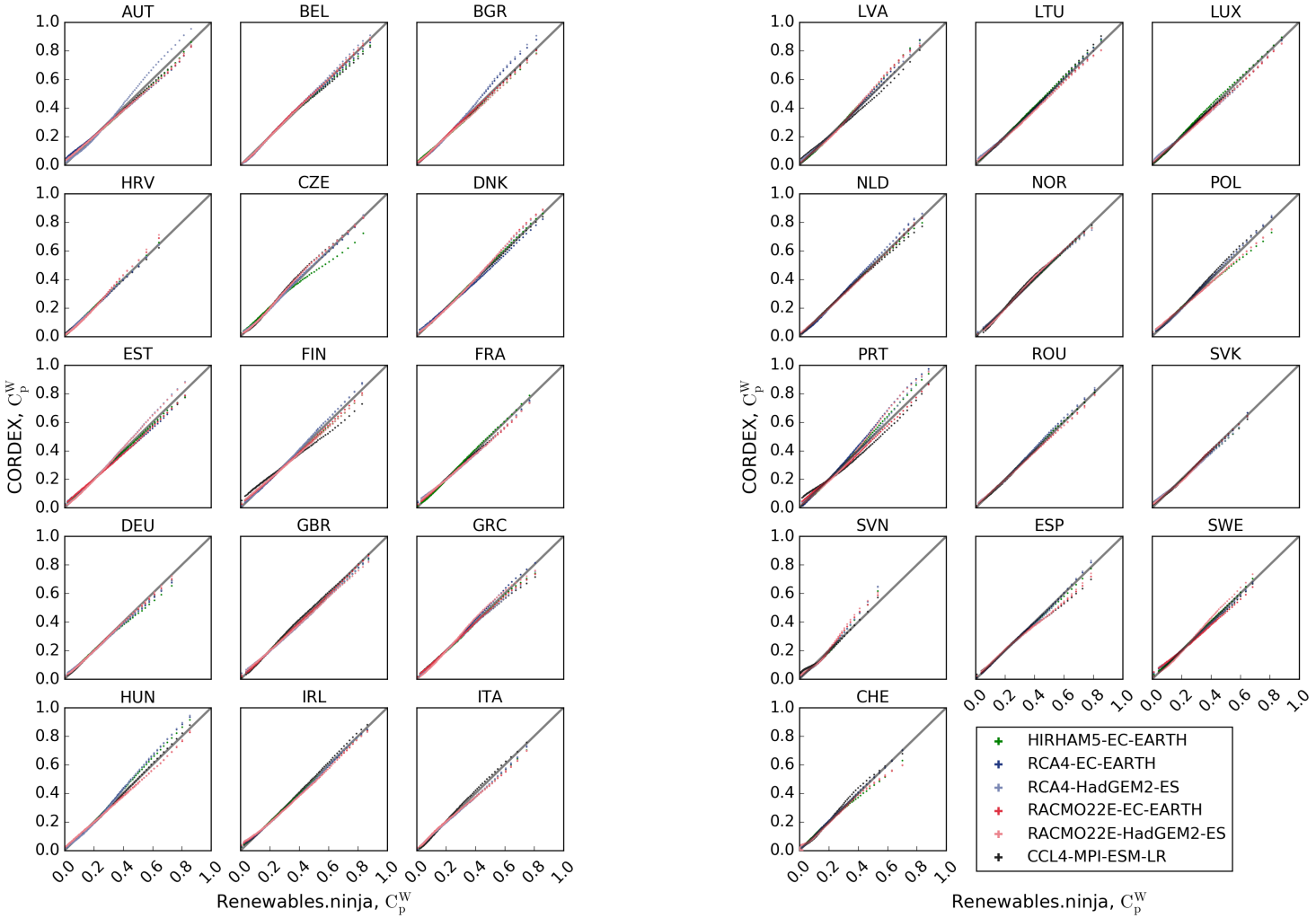

Figure 7.11: QQ plots of the Renewables.Ninja and climate model wind capacity factors. The black, green, dark blue, light blue, dark red, light red and yellow plotting represent capacity factors for all six climate models.

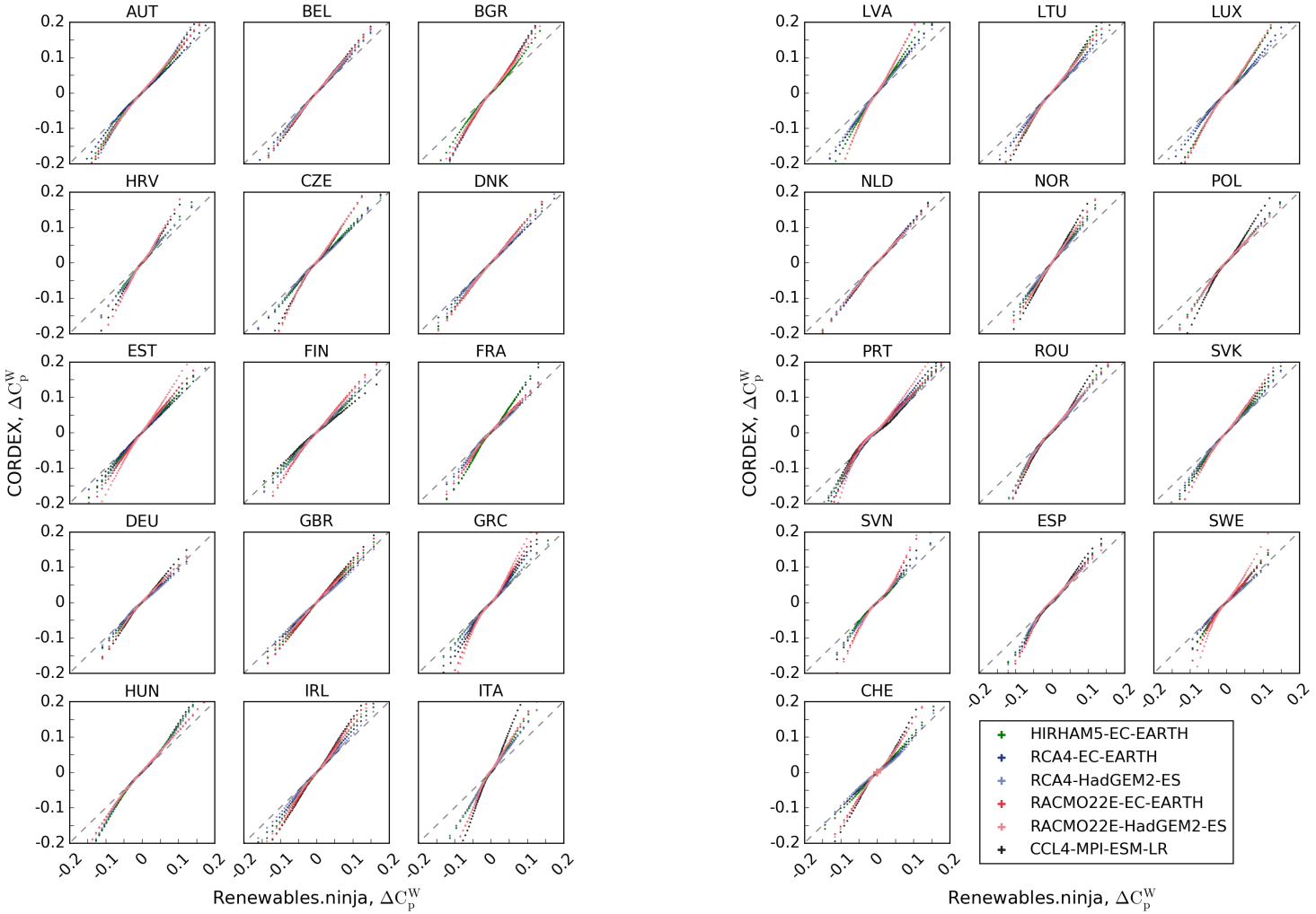

Figure 7.12: QQ plots of the Renewables.Ninja and climate model wind capacity factor increments. The black, green, dark blue, light blue, dark red, light red and yellow plotting represent capacity factors for all six climate models.

Country	**Renewables. ninja** $\overline{C_p^W}$	**HIRHAM5 _EARTH** $\overline{C_p^W}$	**RCA4 _EARTH** $\overline{C_p^W}$	**RCA4 _HadGEM2** $\overline{C_p^W}$	**RACMO22E _EARTH** $\overline{C_p^W}$	**RACMO22E _HadGEM2** $\overline{C_p^W}$	**CCL4 _MPI** $\overline{C_p^W}$
AUT	0.270	0.267	0.271	0.283	0.267	0.266	0.273
BEL	0.274	0.270	0.272	0.279	0.278	0.276	0.268
BGR	0.224	0.222	0.235	0.236	0.225	0.220	0.225
HRV	0.125	0.129	0.129	0.127	0.125	0.126	0.129
CZE	0.235	0.231	0.236	0.235	0.242	0.240	0.242
DNK	0.293	0.297	0.289	0.299	0.300	0.299	0.290
EST	0.263	0.261	0.260	0.274	0.261	0.272	0.262
FIN	0.284	0.282	0.290	0.292	0.283	0.281	0.286
FRA	0.241	0.243	0.239	0.240	0.237	0.240	0.242
DEU	0.202	0.201	0.200	0.202	0.203	0.203	0.199
GBR	0.334	0.330	0.327	0.327	0.333	0.327	0.342
GRC	0.254	0.251	0.261	0.250	0.254	0.259	0.252
HUN	0.247	0.260	0.262	0.259	0.245	0.244	0.249
IRL	0.308	0.310	0.307	0.308	0.304	0.305	0.317
ITA	0.198	0.197	0.197	0.196	0.197	0.197	0.201
LVA	0.232	0.237	0.236	0.238	0.237	0.237	0.234
LTU	0.261	0.270	0.264	0.265	0.257	0.256	0.265
LUX	0.240	0.250	0.238	0.242	0.237	0.236	0.240
NLD	0.247	0.248	0.252	0.253	0.248	0.248	0.247
NOR	0.307	0.309	0.310	0.311	0.311	0.311	0.316
POL	0.249	0.246	0.253	0.253	0.246	0.245	0.259
PRT	0.283	0.291	0.304	0.295	0.280	0.296	0.277
ROU	0.241	0.247	0.251	0.248	0.241	0.241	0.242
SVK	0.178	0.179	0.180	0.182	0.182	0.180	0.178
SVN	0.101	0.106	0.107	0.107	0.111	0.113	0.118
ESP	0.251	0.252	0.254	0.252	0.247	0.248	0.245
SWE	0.258	0.263	0.261	0.263	0.255	0.263	0.255
CHE	0.164	0.164	0.168	0.165	0.160	0.161	0.166

Table 7.2: Average capacity factors for the countries and models.

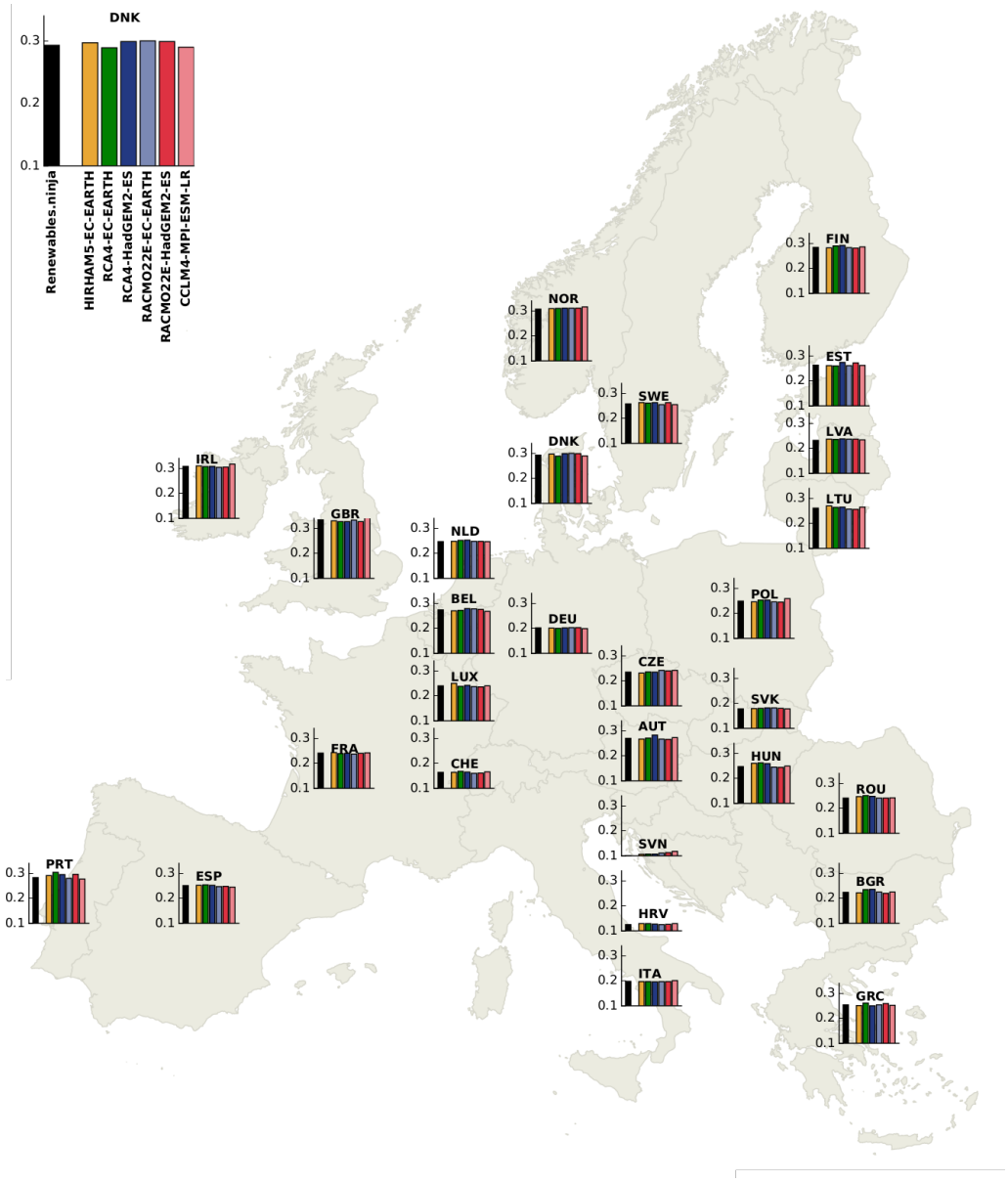

Figure 7.13: Comparison of the average wind capacity factors for the different models within each country.

Solar data to solar power conversion

The conversion procedure of solar data into solar power is shown schematically in Figure 7.14 and is implemented in the REAtlas [36]. Due to missing literature on actual PV-sites, one PV panel of type Scheuten215IG is placed in each grid cell. As for the wind power generation, this process is performed in each grid cell and followed by a a country-wise aggregation. In the first part of the conversion procedure, the fraction of diffusive radiation on a horizontal surface is calculated [317]. Here, the incoming and outgoing short wave radiation and the 2m surface temperatures are used along with the solar position. The amount of radiation hitting the horizontal surface along with the diffused radiation fraction is then used to calculate the amount of radiation hitting a tilted surface [318]. The tilted surface irradiation is highly dependent on the PV panel orientations. Due to restricted knowledge on actual orientations, azimuth angles and tilts are chosen to be Gaussian distributed in order to cover a variety of actual orientations [39]. Azimuth angles are distributed with a standard deviation $\sigma = 40$ and mean $\mu = 0$ as seen in Figure 7.15a. Panel tilts are distributed with a standard deviation $\sigma = 15$ and mean $\mu = 25$ as seen in Figure 7.15b. Finally, efficiency losses due to high temperatures are calculated [319]. The inverter efficiency during the conversion from DC to AC signals is assumed to be 90%. The country-wise aggregated solar power generation time series are nosmalised to the maximum installed solar power capacity in each country.

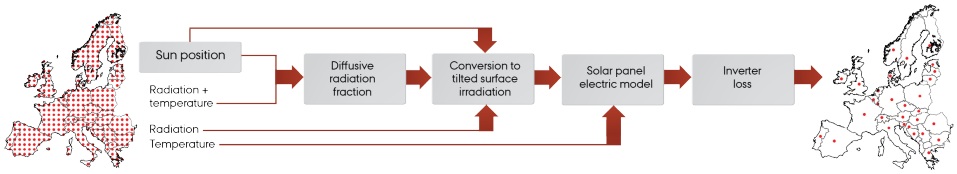

Figure 7.14: Schematic presentation of the solar variables solar power conversion procedure.

Solar power calibration

Due to several approximations in the solar conversion process the final solar capacity factors are adjusted by using the cumulative Weibull distribution as shown in Equation 7.9. The Weibull adjusted solar capacity factors, $CF_{\mathrm{C}}^{S}(t,\lambda,k)$, was separated from the initial solar capacity factors, $CF_{\mathrm{C}}^{S,pre}(t)$ by a superscript, pre. k>0 is the shape parameter or Weibull slope, and λ>0 is the scale parameter of the Weibull distribution.

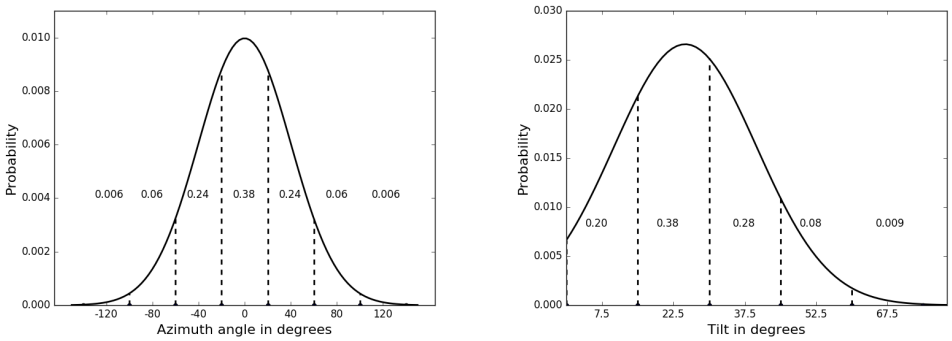

Figure 7.15: Panel a: Gaussian distribution of the azimuth angles. The values on the figure indicates the probability of a solar panel having a certain azimuth angle. Panel b: Gaussian distribution of the tilts. The values on the figure indicates the probability of a solar panel having a certain tilt.

$$CF_{\mathrm{C}}^{S}(t,\lambda,k) = 1 - \exp^{-\left(\frac{CF_{\mathrm{C}}^{S,pre}}{\lambda}\right)^{k}} \tag{7.9}$$

The optimal set of bias adjusting parameters, λ and k, are determined by minimising the Kullbak-Leibler divergence as shown in Equation 7.10.

$$\begin{aligned} \text{minimise} \quad & D_{\mathrm{KL}} = \sum_{q} CF_{\mathrm{R,q}}^{S} \ln\left(\frac{CF_{\mathrm{R,q}}^{S}}{CF_{\mathrm{C,q}}^{S}(\lambda,k)}\right) \\ \text{subject to} \quad & 0.1 \leq \lambda \leq 1 \\ & 1 \leq k \leq 3 \end{aligned} \tag{7.10}$$

The optimal set of k and λ that minimise the KL-divergence is used to Weibull adjust all future solar capacity factors.

Solar power calibration results

Results from each step of minimisation are shown in Figures 7.16-7.21 for the models HIRHAM5-EC-EARTH, RCA4-EC-EARTH, RCA4-HadGEM2-ES, RACMO22E-EC-EARTH, RACMO22E-HadGEM2-ES and CCLM4-MPI-ESM-LR, respectively. These are normalised to the maximum occurring value, 29938.81, which is for Portugal in the model CCLM4-8-17_MPI-ESM-LR. The black dots indicate the optimal values of k and λ for which D_{KL} is minimised.

Results from each step of minimisation are summarised in 7.3. Across the ensemble of models, the southern European countries show less variance in D_{KL} compared to the northern countries. As an example, small changes in k and λ leads to minor changes in D_{KL} for e.g. Finland whereas similar changes in k and λ lead to major differences in D_{KL} for Spain. This behaviour is further visualised in the qq-plots shown in Figure 7.22 comparing the solar capacity factors from Renewables.ninja and the climate models. Less good fit is seen in the capacity factors for the South European compared to the North European countries. This behaviour is further pronounced in the capacity factor increments shown in Figure 7.23. Examples of less god fits are seen for Greece amongst others, whereas fairly good fits are seen for the Norway amongst others. The mean values of the capacity factors are shown in Table 7.4. For Greece as an example, the climate models deviate between 1.7% and 5.8% compared to Renewables.Ninja. To exemplify a Northern country, the climate models show deviations from 1.1%-2.3% for Norway compared to Renewables.Ninja. The climate models RCA4-EC-EARTH and RCA4-HadGEM2-ES generally lead to the best match in the country-wise capacity factors. Figure 7.24 illustrates the solar power capacity factors as bar plots.

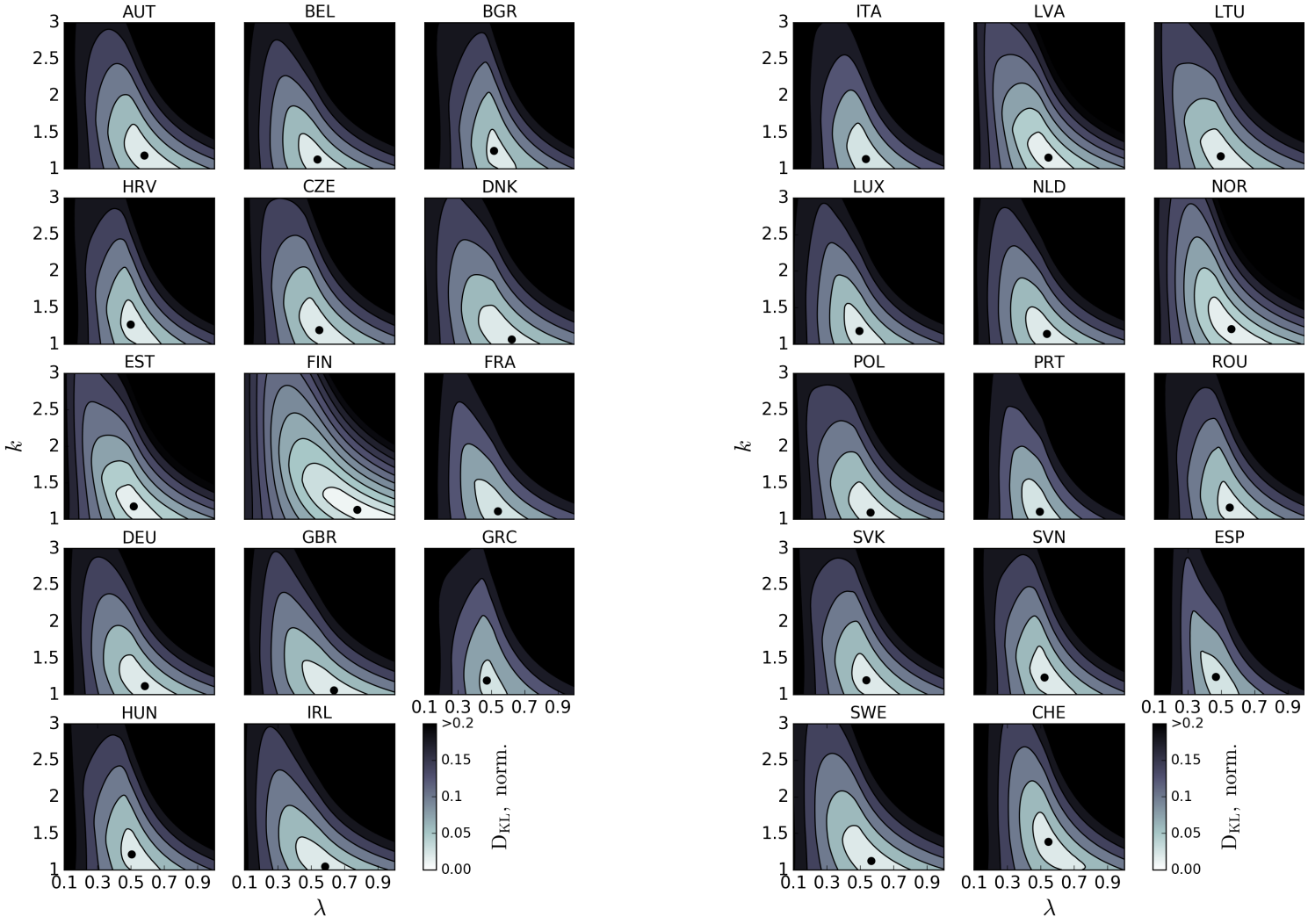

Figure 7.16: Heat maps of the resulting Kullback-Leibler divergence, D_{KL}, as a function of λ and k for countries in the climate model HIRHAM5-EC-EARTH, normalised to the maximum occurring value 29938.81. The black dots indicate the optimal values of λ and k for which D_{KL} is minimised.

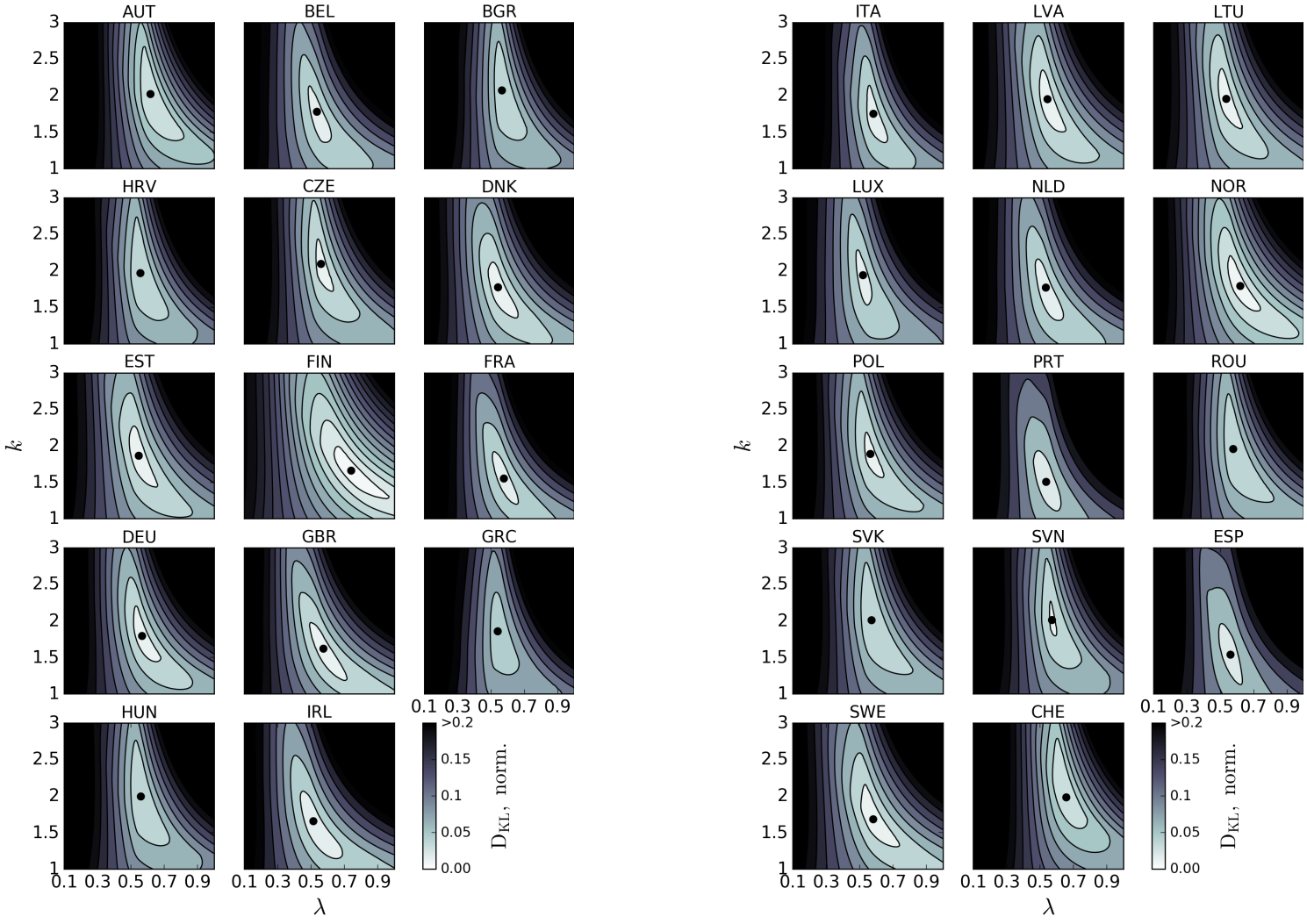

Figure 7.17: Heat maps of the resulting Kullback-Leibler divergence, D_{KL}, as a function of λ and k for countries in the climate model RCA4-EC-EARTH, nosmalised to the maximum occurring value 29938.81. The black dots indicate the optimal values of λ and k for which D_{KL} is minimised.

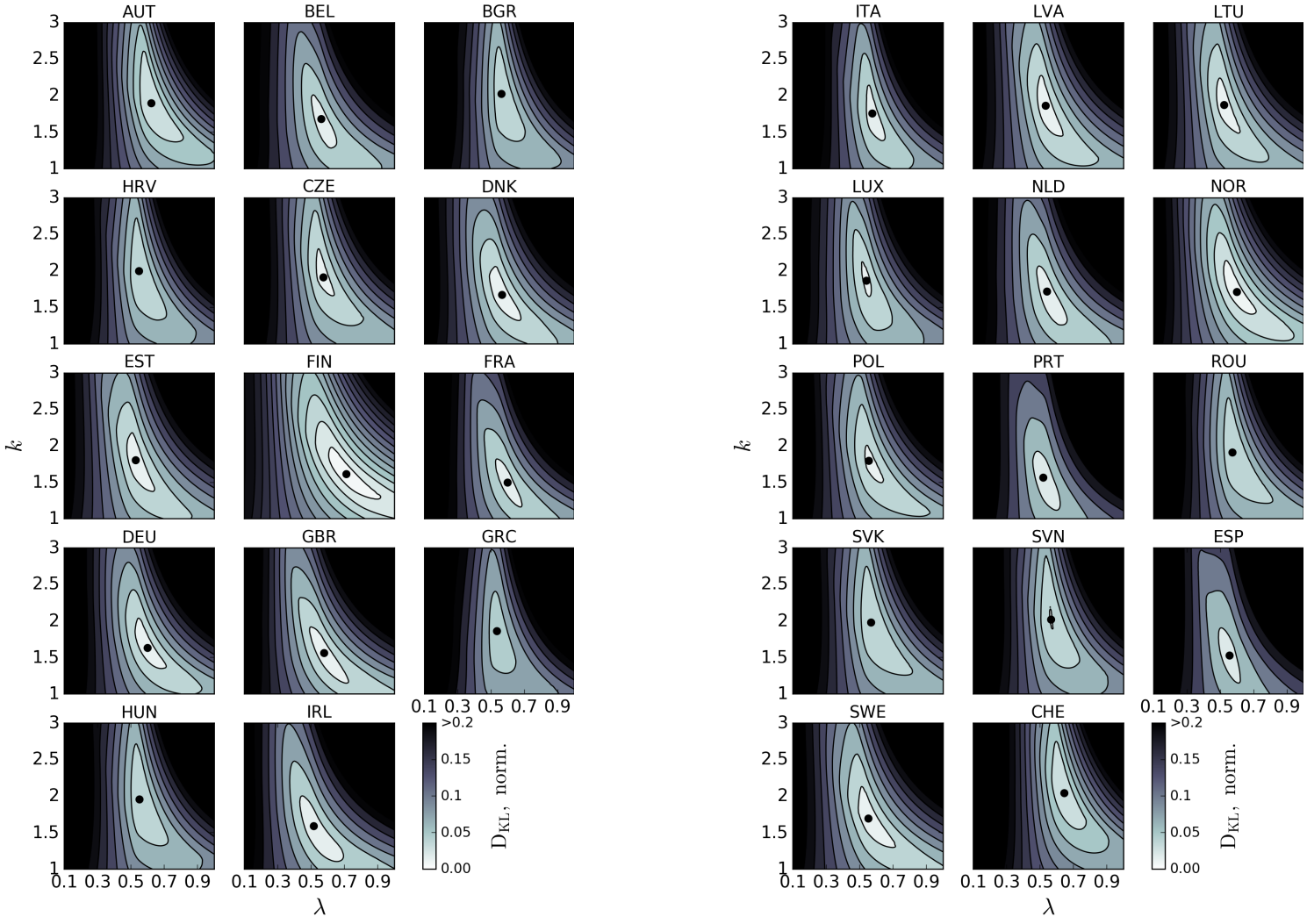

Figure 7.18: Heat maps of the resulting Kullback-Leibler divergence, D_{KL}, as a function of λ and k for countries in the climate model RCA4-HadGEM2-ES, nosmalised to the maximum occurring value 29938.81. The black dots indicate the optimal values of λ and k for which D_{KL} is minimised.

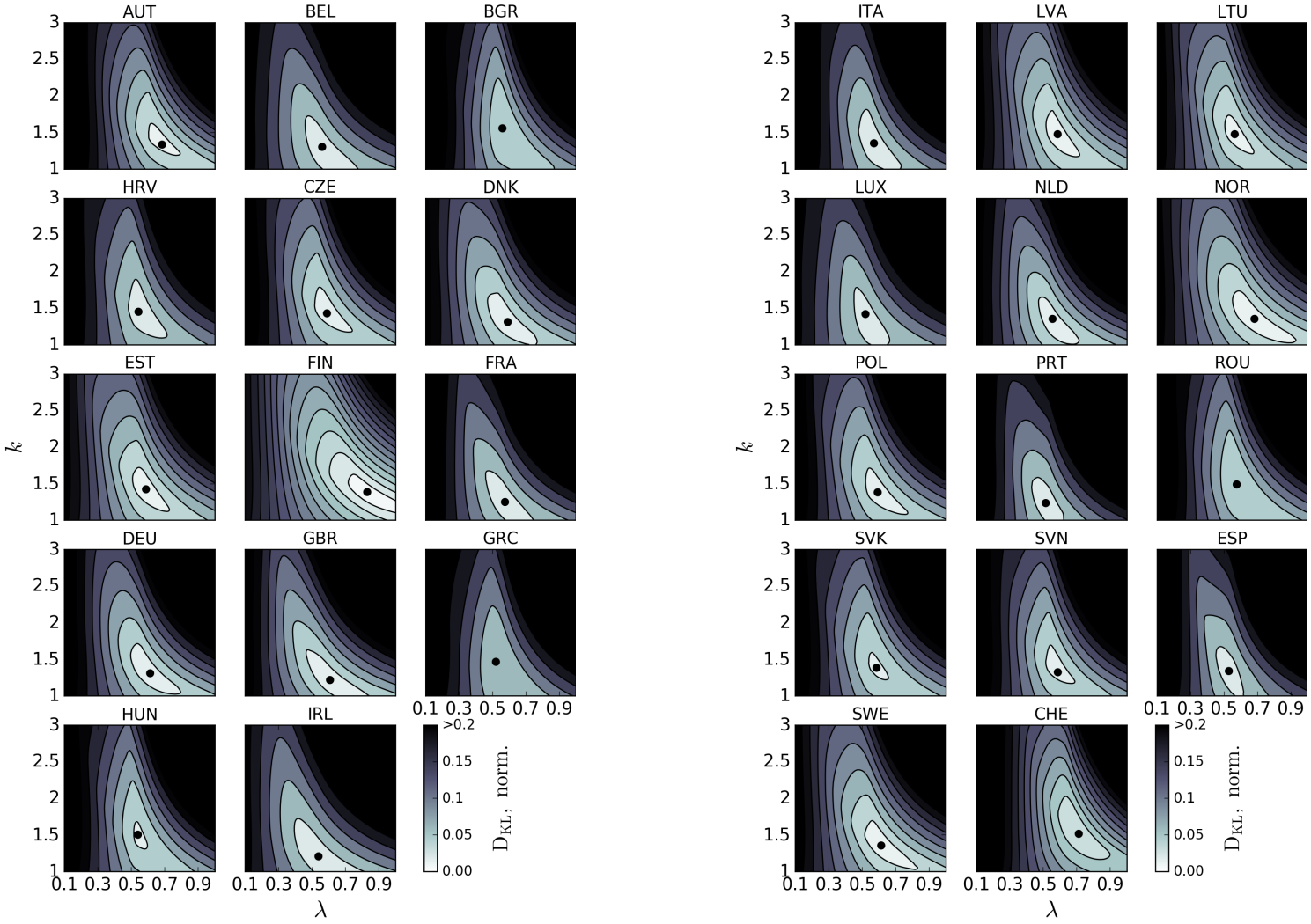

Figure 7.19: Heat maps of the resulting Kullback-Leibler divergence, D_{KL}, as a function of λ and k for countries in the climate model RACMO22E-EC-EARTH, nosmalised to the maximum occurring value 29938.81. The black dots indicate the optimal values of λ and k for which D_{KL} is minimised.

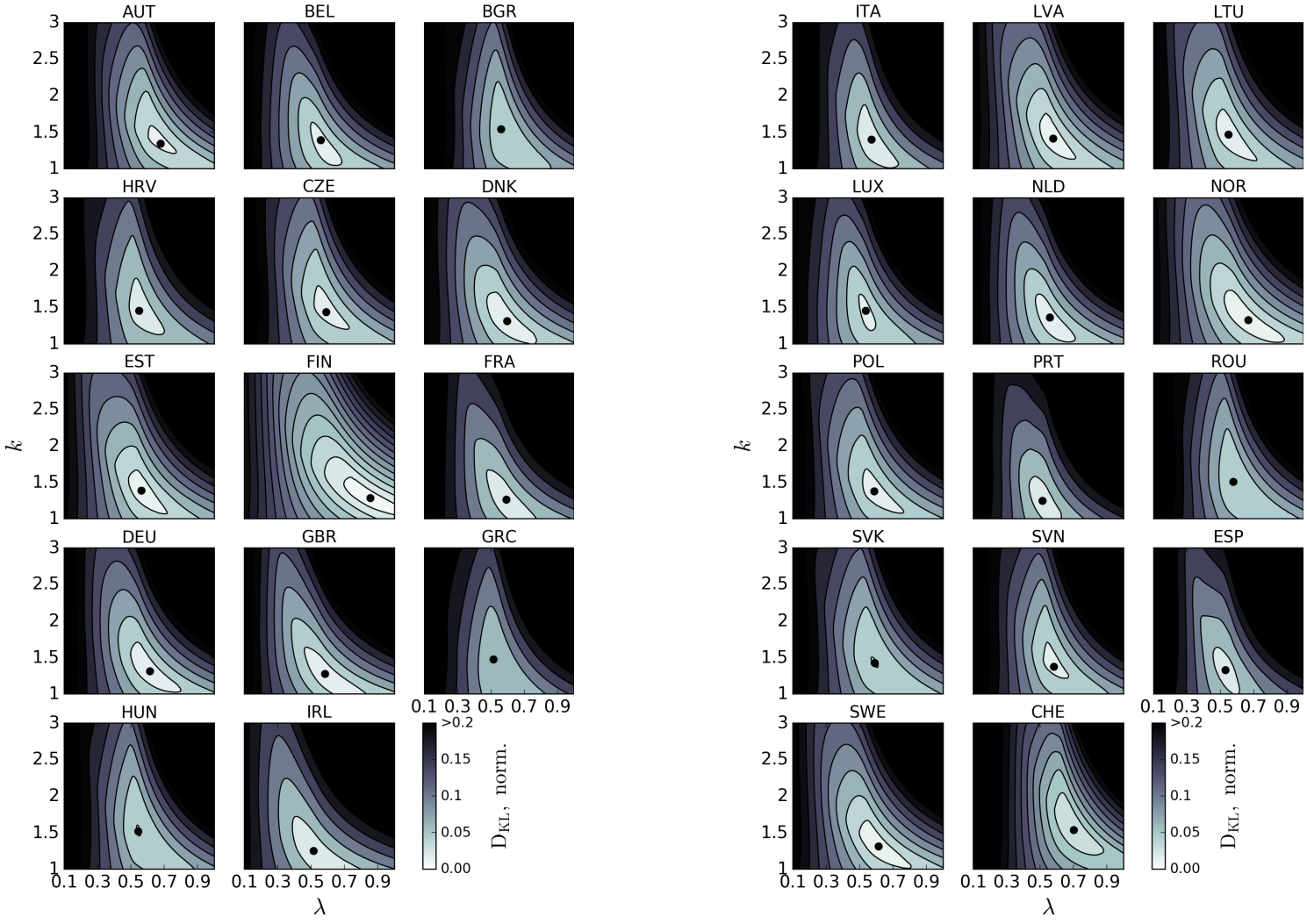

Figure 7.20: Heat maps of the resulting Kullback-Leibler divergence, D_{KL}, as a function of λ and k for countries in the climate model RACMO22E-HadGEM2-ES, nosmalised to the maximum occurring value 29938.81. The black dots indicate the optimal values of λ and k for which D_{KL} is minimised.

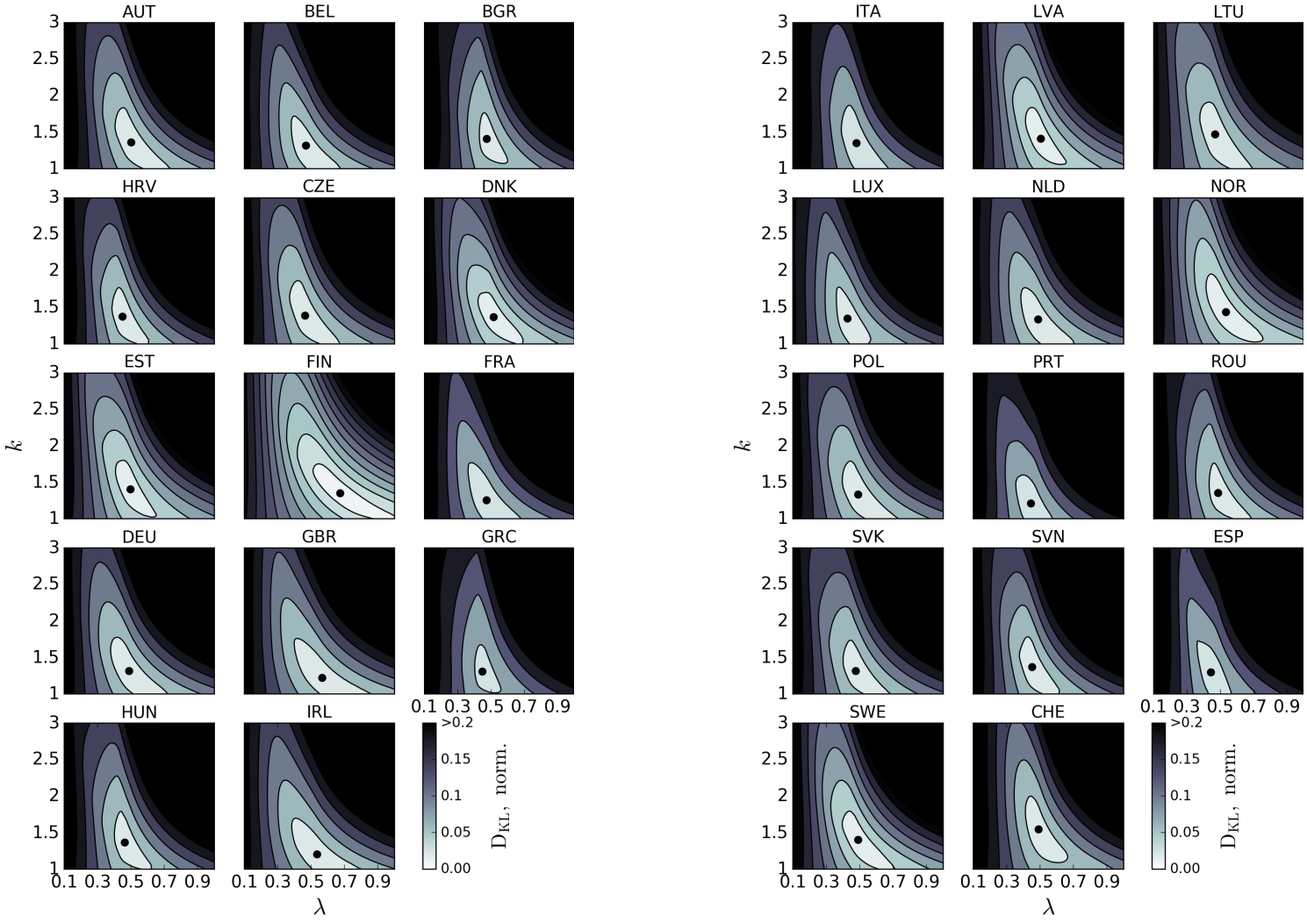

Figure 7.21: Heat maps of the resulting Kullback-Leibler divergence, D_{KL}, as a function of λ and k for countries in the climate model CCLM4-MPI-ESM-LR, nosmalised to the maximum occurring value 29938.81. The black dots indicate the optimal values of λ and k for which D_{KL} is minimised.

Country	HIRHAM5 EC-EARTH		RCA4 EC-EARTH		RCA4 HadGEM2-ES		RACMO22E EC-EARTH		RACMO22E HadGEM2-ES		CCLM4 MPI-ESM-LR	
	λ	k	λ	k	λ	k	λ	k	λ	k	λ	k
AUT	0.581	1.178	0.618	2.019	0.623	1.893	0.685	1.332	0.679	1.338	0.503	1.356
BEL	0.539	1.124	0.537	1.777	0.563	1.677	0.562	1.300	0.560	1.386	0.471	1.312
BGR	0.517	1.242	0.567	2.069	0.564	2.021	0.560	1.555	0.562	1.537	0.476	1.404
BIH	0.511	1.254	0.568	2.017	0.560	2.013	0.564	1.476	0.562	1.525	0.467	1.368
CHE	0.547	1.382	0.659	1.981	0.647	2.039	0.714	1.515	0.704	1.533	0.493	1.543
CZE	0.550	1.188	0.561	2.091	0.576	1.907	0.591	1.426	0.593	1.430	0.466	1.382
DEU	0.584	1.114	0.568	1.793	0.601	1.629	0.614	1.308	0.615	1.308	0.490	1.312
DNK	0.623	1.060	0.543	1.771	0.568	1.667	0.592	1.308	0.598	1.306	0.517	1.362
ESP	0.469	1.240	0.562	1.537	0.557	1.525	0.530	1.338	0.532	1.324	0.445	1.294
EST	0.517	1.174	0.548	1.863	0.530	1.801	0.588	1.422	0.564	1.384	0.498	1.402
FIN	0.777	1.128	0.742	1.659	0.714	1.611	0.832	1.384	0.858	1.282	0.677	1.348
FRA	0.541	1.108	0.578	1.551	0.601	1.494	0.576	1.248	0.594	1.260	0.475	1.252
GBR	0.638	1.056	0.576	1.619	0.580	1.559	0.609	1.216	0.586	1.272	0.568	1.218
GRC	0.474	1.190	0.541	1.857	0.537	1.859	0.522	1.464	0.516	1.470	0.450	1.304
HRV	0.499	1.264	0.558	1.965	0.550	1.993	0.543	1.448	0.550	1.448	0.450	1.368
HUN	0.505	1.210	0.560	1.993	0.552	1.953	0.540	1.503	0.545	1.515	0.464	1.362
IRL	0.585	1.044	0.515	1.655	0.518	1.587	0.541	1.206	0.517	1.246	0.538	1.200
ITA	0.534	1.130	0.583	1.749	0.577	1.753	0.570	1.350	0.572	1.394	0.482	1.346
LTU	0.498	1.168	0.537	1.953	0.524	1.869	0.565	1.474	0.550	1.462	0.470	1.466
LUX	0.495	1.176	0.521	1.937	0.541	1.861	0.520	1.416	0.538	1.448	0.428	1.342
LVA	0.547	1.150	0.546	1.949	0.535	1.859	0.587	1.474	0.580	1.408	0.506	1.406
NLD	0.538	1.136	0.536	1.767	0.543	1.713	0.557	1.350	0.560	1.356	0.490	1.330
NOR	0.562	1.202	0.621	1.789	0.601	1.707	0.683	1.350	0.669	1.320	0.535	1.430
POL	0.562	1.090	0.565	1.887	0.556	1.793	0.593	1.380	0.588	1.374	0.492	1.330
PRT	0.495	1.102	0.538	1.505	0.521	1.563	0.516	1.234	0.516	1.244	0.447	1.208
ROU	0.552	1.158	0.578	1.955	0.574	1.907	0.577	1.488	0.579	1.505	0.488	1.352
SRB	0.510	1.246	0.568	2.035	0.562	2.007	0.560	1.537	0.558	1.547	0.468	1.368
SVN	0.523	1.232	0.573	2.011	0.568	2.017	0.588	1.322	0.585	1.370	0.454	1.366
SVK	0.537	1.194	0.572	2.009	0.569	1.977	0.586	1.382	0.591	1.422	0.477	1.312
SWE	0.567	1.120	0.582	1.681	0.553	1.691	0.614	1.354	0.614	1.308	0.492	1.398

Table 7.3: Overview of the calibration parameters λ and k parameters for the different countries

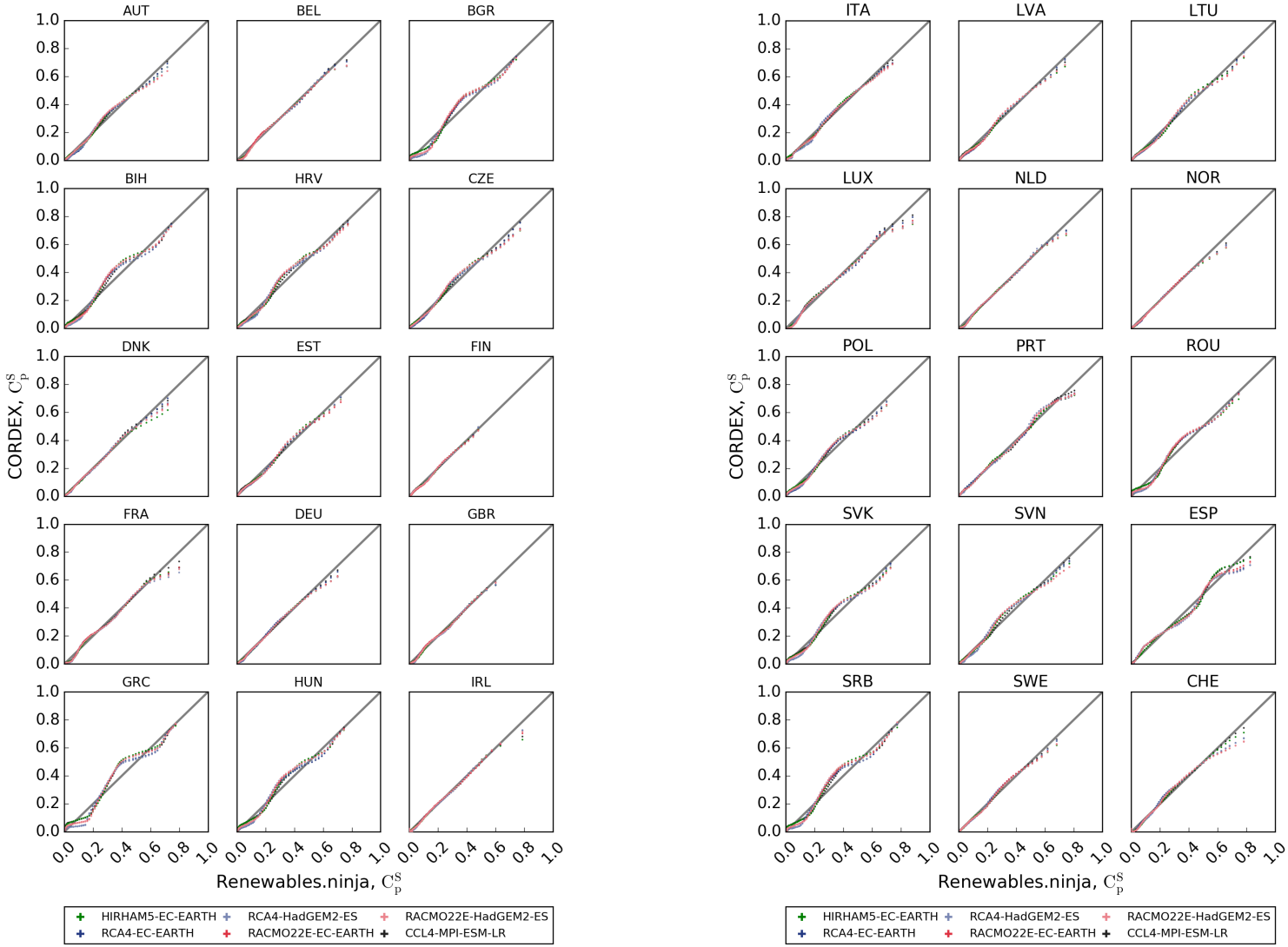

Figure 7.22: QQ plots of the Renewables.Ninja and climate model solar capacity factors. The black, green, dark blue, light blue, dark red, light red and yellow plots represent capacity factors for all six climate models.

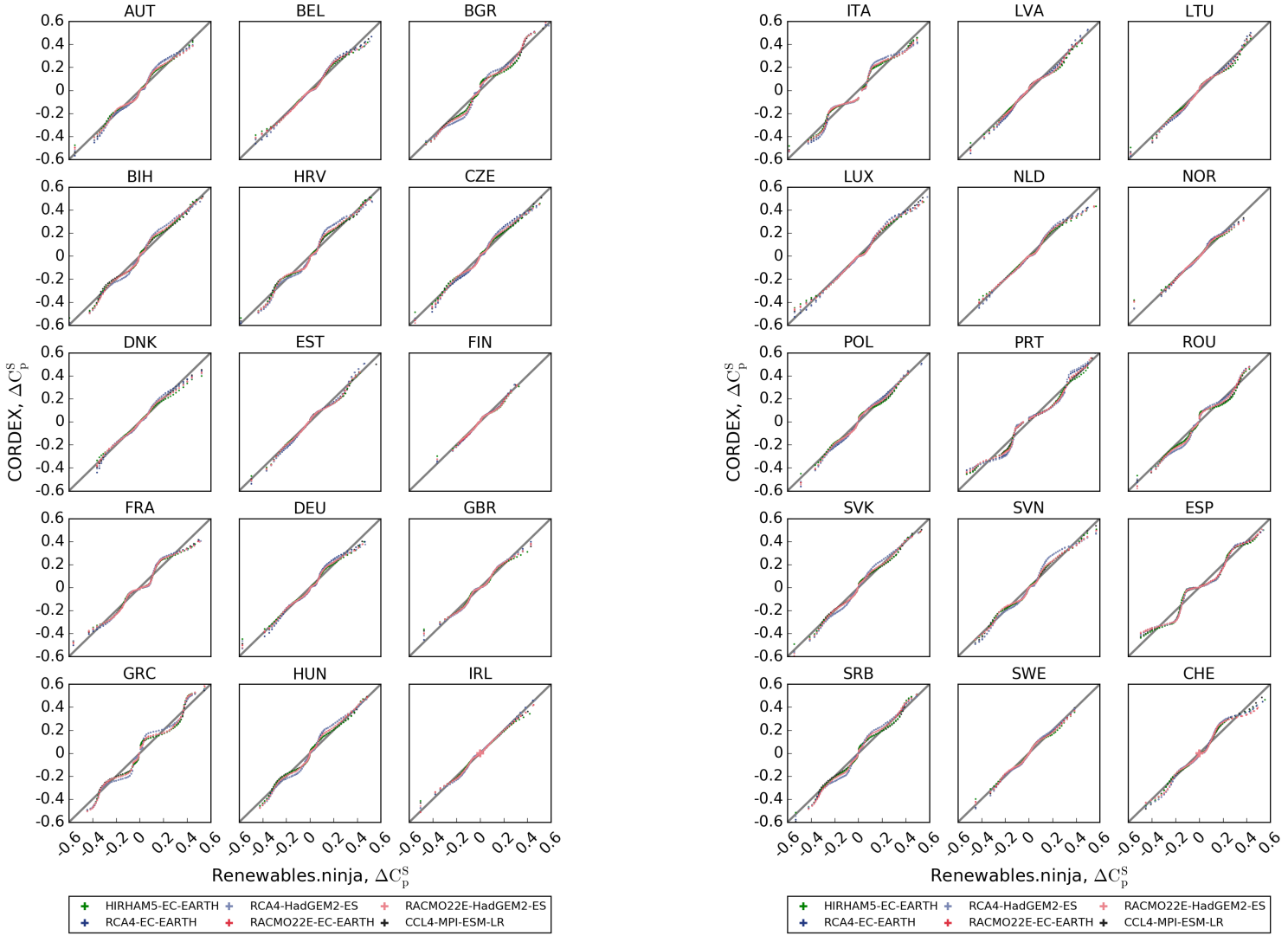

Figure 7.23: QQ plots of the Renewables.Ninja and climate model solar capacity factor increments. The black, green, dark blue, light blue, dark red, light red and yellow plots represent capacity factors for all six climate models.

Country	**Renewables. ninja** $\overline{C_p^S}$	**HIRHAM5 EC-EARTH** $\overline{C_p^S}$	**RCA4 EC-EARTH** $\overline{C_p^S}$	**RCA4 HadGEM2-ES** $\overline{C_p^S}$	**RACMO22E EC-EARTH** $\overline{C_p^S}$	**RACMO22E HadGEM2-ES** $\overline{C_p^S}$	**CCLM4 MPI-ESM-LR** $\overline{C_p^S}$
AUT	0.125	0.125	0.124	0.125	0.125	0.126	0.126
BEL	0.118	0.116	0.116	0.116	0.116	0.114	0.117
BGR	0.150	0.156	0.152	0.153	0.154	0.156	0.155
BIH	0.140	0.147	0.143	0.144	0.146	0.146	0.144
CHE	0.128	0.125	0.127	0.125	0.124	0.125	0.127
CZE	0.121	0.122	0.120	0.121	0.122	0.122	0.122
DEU	0.116	0.114	0.115	0.114	0.114	0.114	0.116
DNK	0.107	0.104	0.107	0.106	0.106	0.106	0.108
ESP	0.179	0.180	0.179	0.178	0.180	0.179	0.182
EST	0.103	0.104	0.103	0.103	0.102	0.103	0.104
FIN	0.064	0.064	0.064	0.065	0.064	0.064	0.065
FRA	0.139	0.138	0.138	0.137	0.139	0.138	0.140
GBR	0.101	0.099	0.099	0.100	0.101	0.100	0.101
GRC	0.173	0.183	0.177	0.176	0.179	0.179	0.181
HRV	0.146	0.149	0.147	0.148	0.150	0.150	0.148
HUN	0.140	0.145	0.141	0.145	0.144	0.145	0.143
IRL	0.103	0.103	0.102	0.102	0.103	0.103	0.103
ITA	0.160	0.161	0.158	0.158	0.158	0.158	0.159
LTU	0.111	0.113	0.111	0.111	0.112	0.112	0.112
LUX	0.125	0.123	0.122	0.122	0.121	0.121	0.126
LVA	0.104	0.103	0.103	0.103	0.103	0.104	0.104
NLD	0.116	0.113	0.114	0.114	0.113	0.113	0.114
NOR	0.089	0.087	0.087	0.088	0.088	0.088	0.088
POL	0.115	0.118	0.115	0.117	0.116	0.116	0.117
PRT	0.181	0.180	0.180	0.182	0.181	0.181	0.180
ROU	0.137	0.140	0.140	0.141	0.140	0.141	0.142
SRB	0.143	0.149	0.145	0.147	0.147	0.150	0.146
SVN	0.138	0.141	0.141	0.140	0.140	0.140	0.140
SVK	0.127	0.130	0.129	0.130	0.130	0.130	0.131
SWE	0.097	0.097	0.098	0.098	0.098	0.096	0.097

Table 7.4: Overview of the mean solar capacity factors for the countries and models.

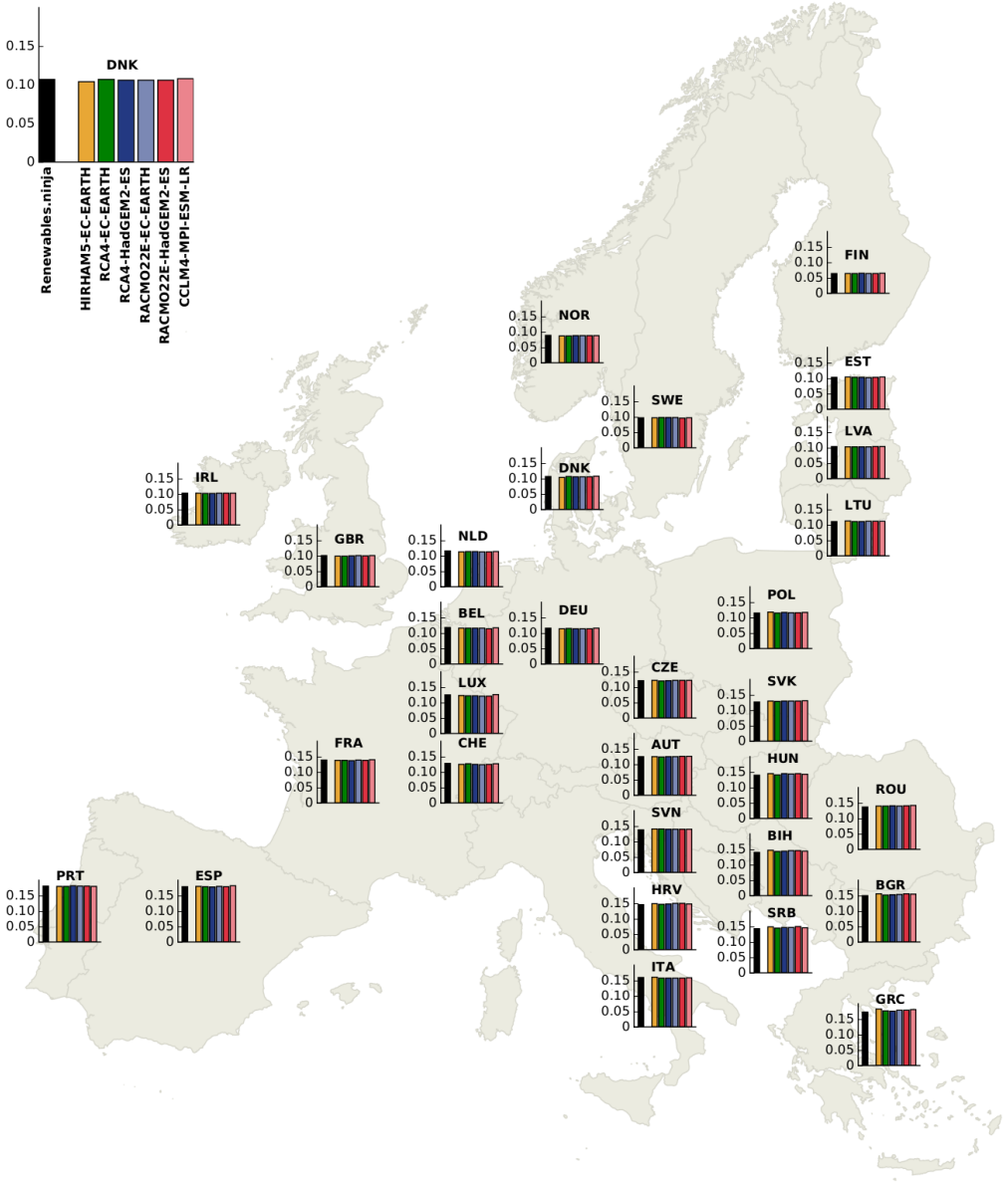

Figure 7.24: Comparison of the average solar capacity factors for the different models within each country.

Generation of future electricity load time series

Historical consumption data shows that electricity consumption is heavily dependent on the ambient temperatures due to electrification of heating and cooling. To reflect this effect, the theory of *Degree Days* is applied to estimate the future electricity demand by combining historical load and temperature data with future temperature projections from the climate models. This way, the future load time series does not only retain temporal fluctuation patterns but also reflect climate change induced heating and cooling demand variations.

As seen in Figure 1.6 the ambient temperatures show an absolute increase of 2 – 5 °C up to 2100. This can cause major impacts on the electricity usage, consequently power systems, due to less demand for electrical heating in winter and higher cooling demand in summer.

Degree Days

The theory of degree days are used to quantify the relationship between the ambient temperatures and the 3-hourly electricity consumption time series. The underlying idea, is that, when the ambient temperature increases, the electricity consumption increases as well in order to cover electrified cooling demands. Oppositely, in winters during cold days the electrified heating demand increases. In most European countries, due to its high latitudes, summer is mostly not too hot for air conditioning and more heating utilities are built for cold winters.

The mathematical formulations of the heating and cooling degree hours, $D_n^{\texttt{heating}}$ and $D_n^{\texttt{cooling}}$, are shown in Equations 7.11 and 7.12, respectively. These are formulated as the temperature exceedance over certain heating and cooling cutoff values, $T_{\texttt{cutoff}}^{\texttt{heating}}$ and $T_{\texttt{cutoff}}^{\texttt{cooling}}$, respectively.

$$D_n^{\texttt{heating}}(t) = \max\{0, \quad T_{\texttt{cutoff}}^{\texttt{heating}} - T_n(t)\} \tag{7.11}$$

$$D_n^{\texttt{cooling}}(t) = \max\{0, \quad T_n(t) - T_{\texttt{cutoff}}^{\texttt{cooling}}\} \tag{7.12}$$

$T_n(t)$ is the 3-hourly population-weighted temperature time series for a country, n. Population densities [320] are shown in Figure 7.25. The cutoff temperatures, $T_{\texttt{cutoff}}^{\texttt{heating}}$ and $T_{\texttt{cutoff}}^{\texttt{cooling}}$, equal 10 $^\circ C$ and 18 $^\circ C$, respectively, which is both empirical and supported by data.

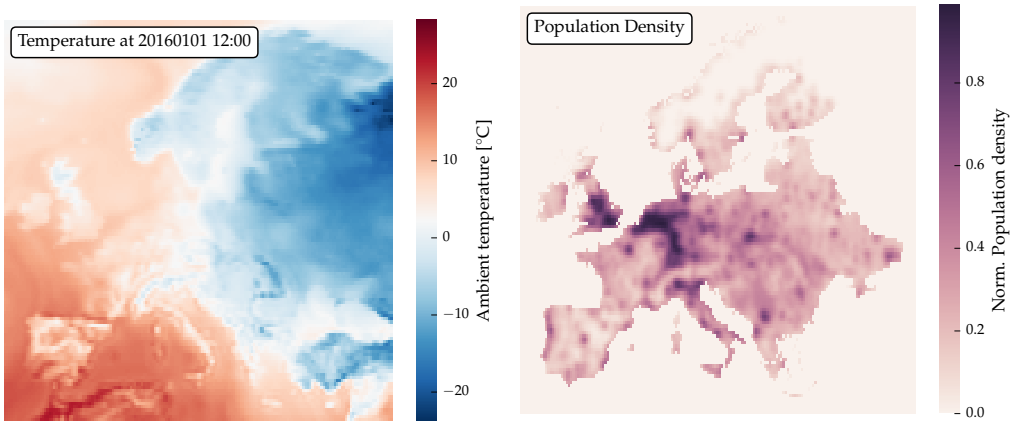

Figure 7.25: Temperature at 12 pm January 1st 2016, and population density in CFSR gridded cells.

The historical temperature is extracted from a high spatial resolution gridded hourly reanalysis dataset called Climate Forecast System Reanalysis (CFSR) [321], a product of NOAA. In CFSR, the globe is meshed into 880×1760 raster cells of the size $40 \times 40\text{km}^2$, and at the center of each, hourly temperature values from 2006 to 2015 at 2m above ground are available. The load time series, on the other hand, are hourly electricity consumption profiles for 33 European countries collected from the European Network of Transmission System Operators for Electricity (ENTSO-E).

The relation between degree hours and the electricity consumption, $L_n(t)$, is represented by a linear relation as in Equation 7.13.

$$L_n(t) = \hat{\beta}_{0,n} + \hat{\beta}_{1,n} D_n^{\texttt{heating}}(t) + \hat{\beta}_{2,n} D_n^{\texttt{cooling}}(t) \tag{7.13}$$

$\hat{\beta}_{0,n}, \hat{\beta}_{1,n}, \hat{\beta}_{2,n}$ denote the intercept and slopes, respectively, for each country. In Figure 7.27, the heating degree-day hours and the corresponding electricity consumption are shown for 33 European countries as black dots and blue lines as model fit based on the slopes and intercepts.

Scandinavian countries, like Sweden, Finland and Norway are characterised by high slopes and small intercepts. This is attributed to their high latitudes. Denmark and Iceland does not exhibit good fits as their well-established district heating utilities can meet most of the heating demand in winter. The Baltic countries, Latvia, Lithuania and Estonia exhibit good fits. As for inland coun-

tries, Austria, Poland, Czech Republic, Slovakia, Bulgaria, Romania and Serbia all fit the degree hours fairly well. The same holds true for the northern Balkans, Bosnia& Herzegovina, Croatia and Macedonia. The linear model is not able to fit the load profile for Greece and Italy, both giving almost horizontal fits in the linear regression. This is due to their low latitude and warm winters. Special attention is given to Germany and Hungary, as they are the countries which heavily rely their heating on natural gas. This constitutes approx. 40% and 70% of the demand, respectively. Hence, the electricity consumption in winter fits poorly with degree hours.

Identify heating power in historical load time series

The coefficients of the linear regression, $\hat{\beta}_{0,n}, \hat{\beta}_{1,n}$ and $\hat{\beta}_{2,n}$, are used to identify the fraction of electricity used for heating and cooling at each time step depending on the ambient temperature in that hour.

Take the example of a Nordic country as Finland, Figure 7.28 shows a clear linear fit, where the points are closely distributed around the fitting line. An intercept of 0.85 means that when temperature drops below 10 $°C$ in Finland, 15% of the load can be attributed to heating demand on average, which is called the heating power.

Given the population-weighted temperature time series and combining Equations 7.11, 7.12 and 7.13, a heating, $L_n^{\texttt{heating}}$, and cooling power, $L_n^{\texttt{cooling}}$, time series can be determined by:

$$L_n^{\texttt{heating}}(t) = \hat{\beta}_{1,n} D_n^{\texttt{heating}}(t) \tag{7.14}$$

$$L_n^{\texttt{cooling}}(t) = \hat{\beta}_{2,n} D_n^{\texttt{cooling}}(t) \tag{7.15}$$

In Figure 7.29, the time series (averaged over 3-day windows for better visualisation) of population-weighted temperatures (red), original load (blue) and base load $L_{base}(t)$ (green) is shown, which is defined by:

$$L_n^{\texttt{base}}(t) = L_n(t) - L_n^{\texttt{heating}}(t) - L_n^{\texttt{cooling}}(t). \tag{7.16}$$

It is clear that, whenever the ambient temperature drops below 10 $°C$, there are difference between the original and base load, and the lower the temperature, the greater the differences be. The same procedure was applied to 33 European countries and their base load are plotted in Figure 7.30. Resulting time series

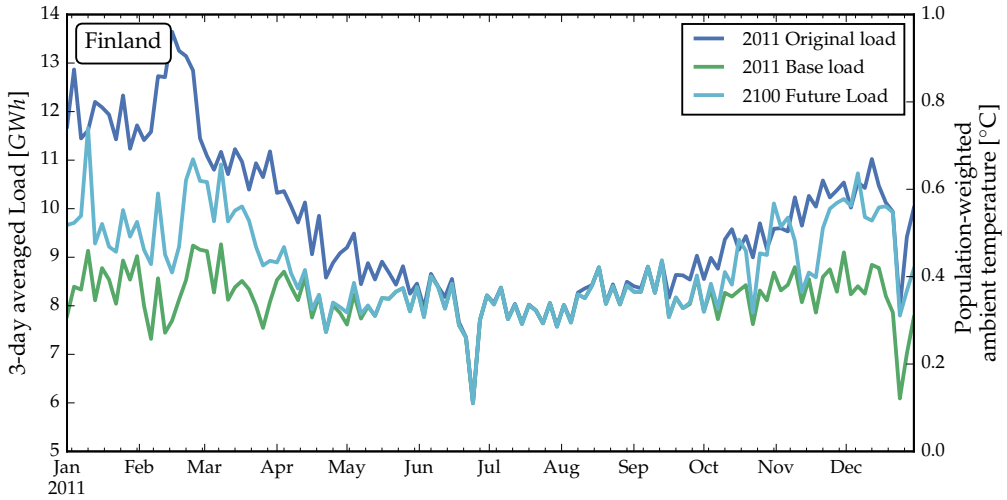

Figure 7.26: 3-day averaged 2011 historical, 2011 base and modelled future load time series for Finland.

show that, Greece and Italy are mostly affected by summer cooling demand.

Future load time series based on CORDEX temperature

By using the climate model temperatures, the future electrical heating and cooling consumption using the degree-hour theory are estimated. Then, the future load time series is determined by combining its terms $\hat{\beta}_{1,n} D_n^{\texttt{future-heating}}(t)$, $\hat{\beta}_{2,n}$, $D_n^{\texttt{future-cooling}}(t)$ and the 2011 base load:

$$L_n^{\texttt{future}}(t) = L_n^{\texttt{base}}(t) + \hat{\beta}_{1,n} D_n^{\texttt{future-heating}}(t) + \hat{\beta}_{2,n} D_n^{\texttt{future-cooling}}(t),$$

in which $D_n^{\texttt{future-heating}}(t)$ and $D_n^{\texttt{future-cooling}}(t)$ are calculated in the same way as Equations 7.11 and 7.12, except that future ambient temperature time series is used instead.

In Figure 7.26, the example of Finland is taken again to show the differences among the historical load in 2011, base load 2011 and future load in sample year 2100 in the climate projection rcp8.5 within the climate model ICHEC-EC-EARTH-HIRHAM5. It is clear that, with future temperature increases, Finland

exhibits significantly lower electricity demand in winter and summer load remains intact.

Among the 33 countries studied, the majority share the same trend as Finland, with decreased electricity demand during winter but with summer demand unchanged. Greater load drop in winter is seen in northern countries, such as the Scandinavians and the Baltic countries. Also slightly more cooling power is needed in summer for Greece and Italy due to projected higher summer temperatures. Iceland, Macedonia and Montenegro give no future load since they are not covered by this work.

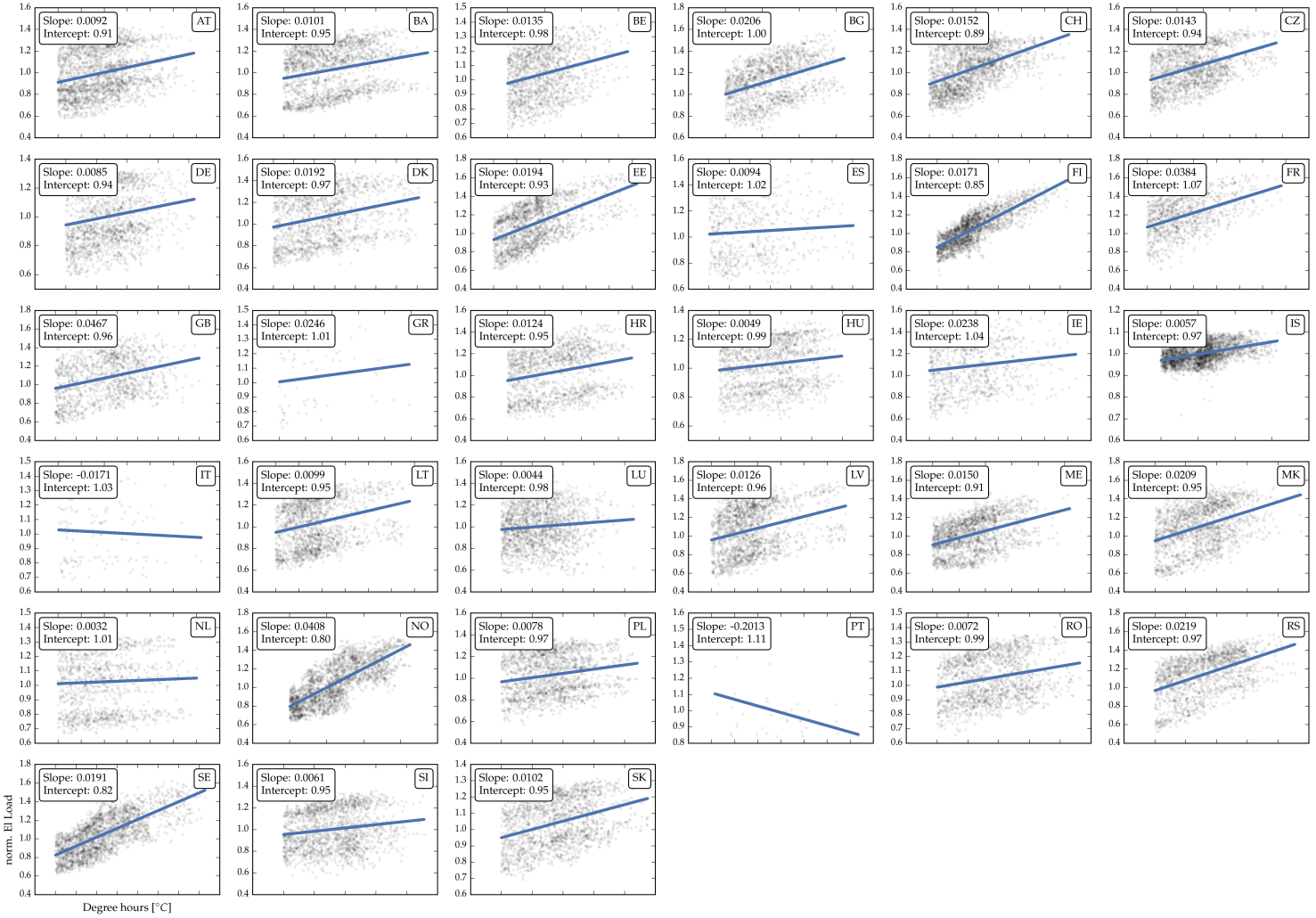

Figure 7.27: Linear relations between normalised electricity load and heating degree hours in 33 European countries.

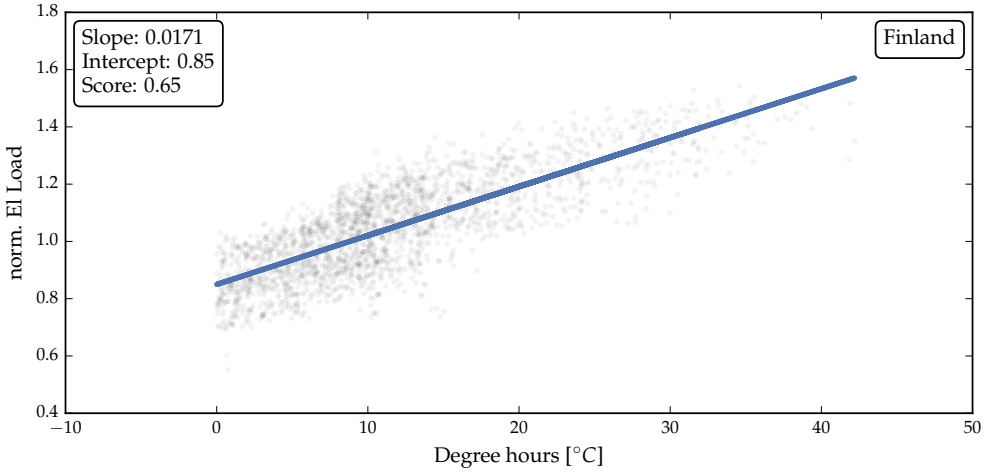

Figure 7.28: Linear relation between normalised electricity consumption and heating degree hours in Finland.

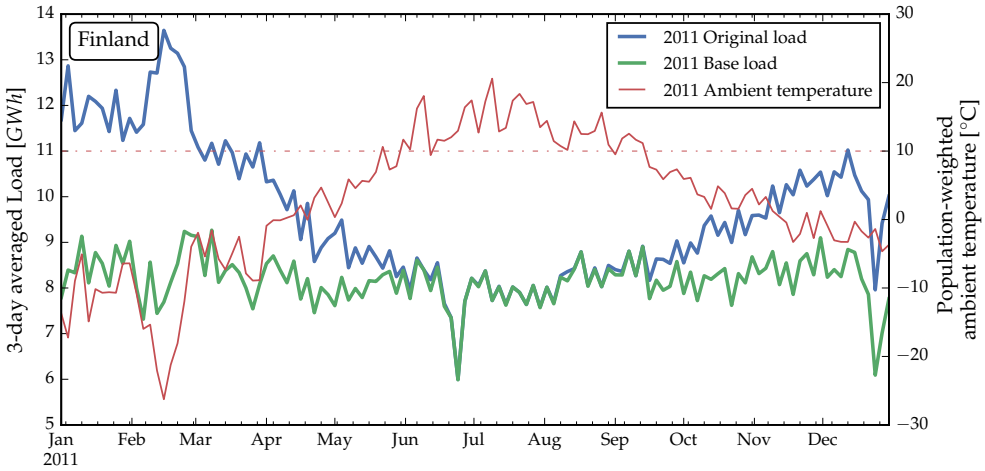

Figure 7.29: 3-day averaged electricity load, base load and population-weighted ambient temperature for Finland in 2011.

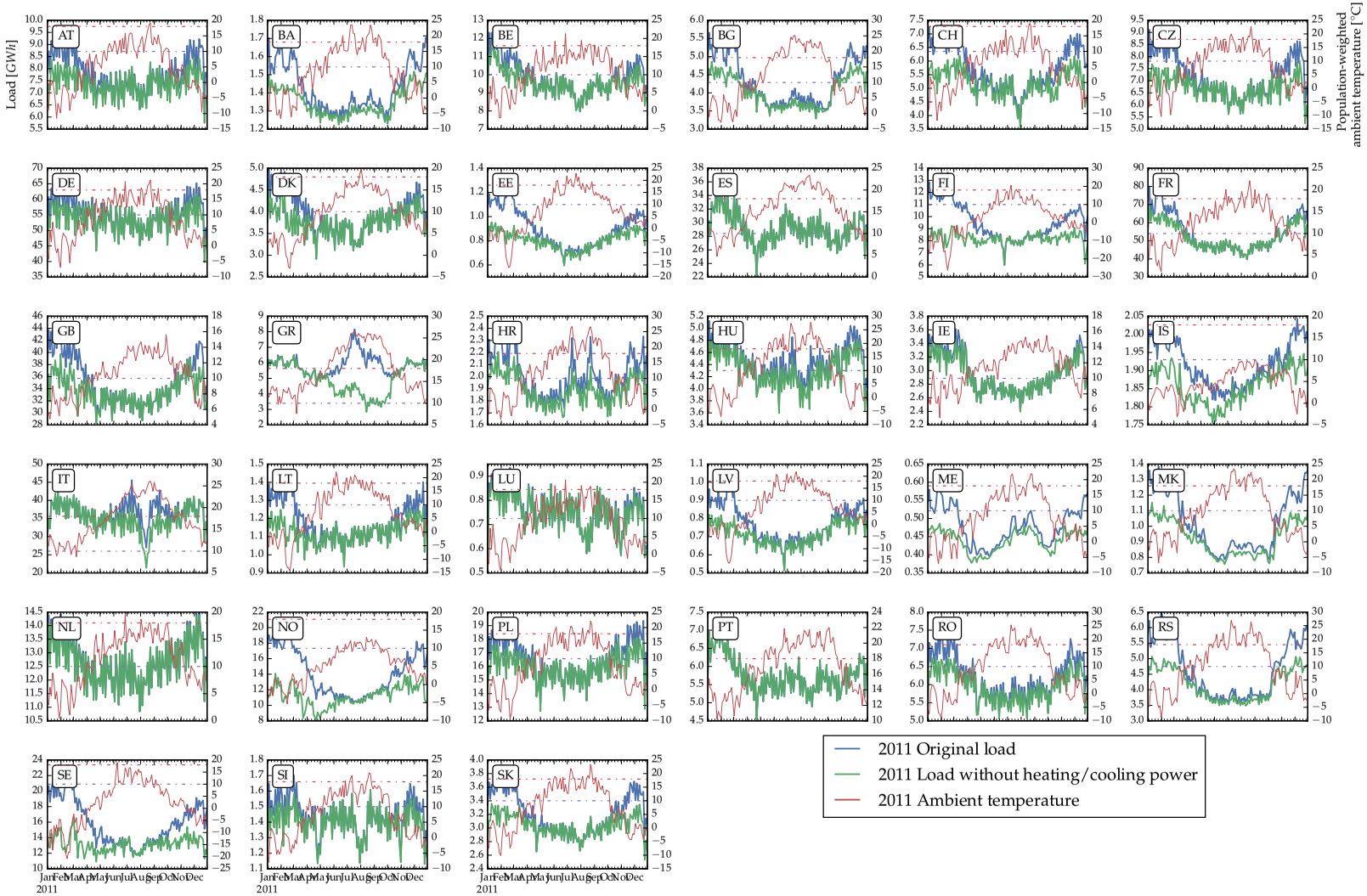

Figure 7.30: 3-day averaged electricity load, base load and population-weighted ambient temperature for 33 European countries in 2011.

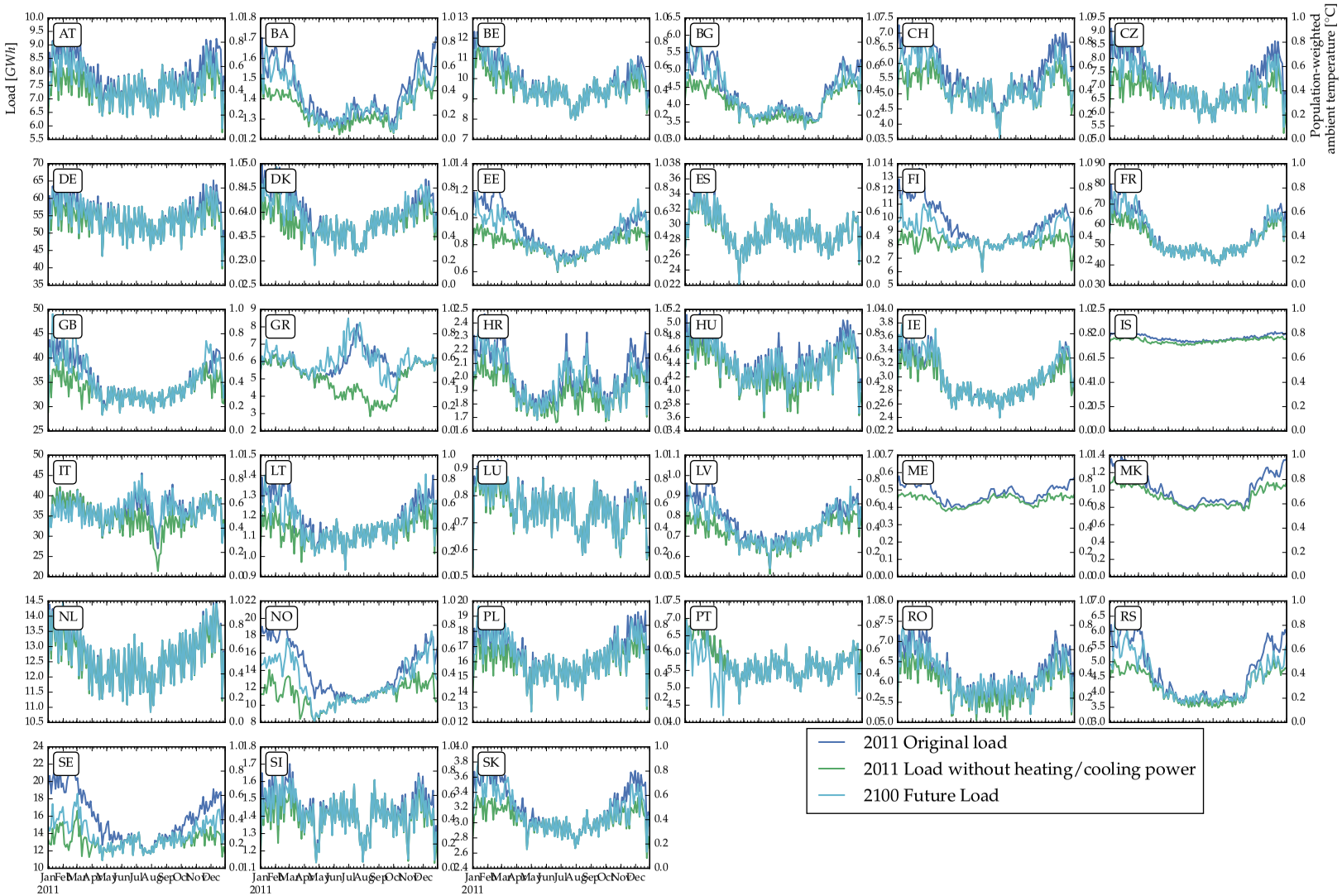

Figure 7.31: 3-day averaged 2011 historical, 2011 base and modelled future load time series for 33 European countries.

7.3 Statistical tests

To test if the key metrics for historical or/and end-of-century electricity systems are significantly different from one another the independent two-sample Welch's test [322] is evaluated in two different ways. The independent two-sample Welch's test is an extension of the Student's t-test [323]. Unlike the former, which assumes equal sample sizes and equal variance of the sample distributions, the latter is designed to deal with unequal sample sizes and data distribution variances. Although the property of unequal sample sizes is not necessary for this approach different sample variances are assumed. Welch's test statistic is calculated as:

$$t = \frac{\mu_{X_1} - \mu_{X_2}}{\sqrt{\frac{\sigma^2_{X_1}}{n_{X_1}} + \frac{\sigma^2_{X_2}}{n_{X_2}}}}$$

where the subscripts denote data samples, μ the sample mean, σ sample variance and n the sample size.

In the first approach, the corresponding p-value is estimated by simple table lookup. The degrees of freedom are approximated by the Welch-Satterthwaite equation [322]. In the second approach, bootstrapping is used with replacement on random sampling in accordance to [324]. Both test evaluations test if the mean of the populations over a time period has changed. This is observed in the t-test statistic which explores the difference in the population average.

Data samples are prepared by calculating 20 yearly averages of the key metrics for a historical period from 1986-2006 and for an end-of-century period from 2080-2100 for each of the climate models.

7.4 Additional results

In this section, additional results to the article are presented. Table 7.5 is an extension of Table 2.1 from Chapter 2, showing the average values and one σ standard deviation of the annual values for wind and solar power generation and the electric consumption for all climate models. All variables are nosmalised to the historical values in the climate model HIRHAM5-EC-EARTH. This gives an average value of 1 for all variables in the historical period within HIRHAM5-EC-EARTH. Across all climate models, the average annual wind and solar power production and electric consumption decreases slightly towards the end of the century.

Table 7.6 shows the t-statistic evaluations of the change in 20 year average populations of the wind and solar power production and the electric consumption from the different climatic periods. The p-values for the t-statistic have been evaluated by two methods as described in Section 7.3. For both evaluations of the t-statistic, the annual demand and annual solar capacity factors can both be considered different for the different climate projections due to p-value scores lower than 5% in a vast majority of the test results. The statistical difference in the wind capacity factors, on the other hand, is inconclusive when testing between the historical period and end-of-century periods. The wind capacity factors cannot be considered different in the ensemble of end-of-century periods due to high p-score values in most cases.

Figure 7.32 shows the evolution of the nosmalised wind and solar power generation and the electric consumption as a function of model year for HIRHAM5-EC-EARTH. For all variables, a slight decrease is seen towards the end of century. The one σ standard deviations for wind and solar power generation are higher compared to the respective values for electric consumption. This reflects the nature of the high variance in the wind speeds and incoming short wave radiation as a product of the climate models. The smaller standard deviations for the electricity consumption reflects a fairly stable temperature increase during the 21st century.

Table 7.7 shows similarly the t-statistic evaluations of the change in 20 year average populations of the key metrics resulting from the different climate projections. The p-values for the t-statistic have been evaluated by two methods as described in Section 7.3. The wind-solar mix and renewable penetration are fixed at 0.8 and 1, respectively. In most cases for both test evaluations, the distributions of annual scores cannot be assumed to come from different underlying

distributions due to p-value scores fairly higher than 5%. The null-hypothesis that climate change has no impact on the key metrics cannot be rejected with a 95% confidence in this case. As stated in the article, a wind solar mix of 0.8 forces high wind domination into the system and consequently results in relatively high uncertainties.

Figures 7.33 - 7.38 show the evolution of the dispactable electricity, benefit of transmission, dispatchable capacity and the short-term variability as a function of model year for the climate models. As in Table 7.7, the wind-solar mix and renewable penetration are fixed at 0.8 and 1, respectively. None of the key metrics show a gradual transition from the historical period towards the end of century. The disptachable electricity, benefit of transmission and storage, dispatchable capacity and variability does not show a gradual transition from the historical reference point and towards the end of the century for all climate models. The key metric pathways tend to cross multiple times during the model years and a diverse impact on the electricity system as a consequence of the different climate projections can be rejected.

Table 7.5: Average values and one σ standard deviation of the annual wind and solar power generation and the electric consumption values for the historical calibration period (1986-2006) and the end-of-century period (2080-2100) for all climate models. All values have been nosmalised to the corresponding values spanning the period 1986 to 2006 for HIRHAM5-EC-EARTH.

	HIRHAM5-EC-EARTH			
	Historical	RCP2.6	RCP4.5	RCP8.5
$\langle W \rangle_{20yr}$	1.00 ± 0.03	0.98 ± 0.02	0.99 ± 0.04	0.96 ± 0.03
$\langle S \rangle_{20yr}$	1.00 ± 0.01	0.99 ± 0.02	0.98 ± 0.02	0.97 ± 0.03
$\langle L \rangle_{20yr}$	1.000 ± 0.005	0.995 ± 0.003	0.992 ± 0.005	0.986 ± 0.003
	RCA4-EC-EARTH			
	Historical	RCP2.6	RCP4.5	RCP8.5
$\langle W \rangle_{20yr}$	1.01 ± 0.03	0.99 ± 0.03	0.98 ± 0.03	0.97 ± 0.04
$\langle S \rangle_{20yr}$	0.99 ± 0.03	0.97 ± 0.02	0.95 ± 0.02	0.93 ± 0.03
$\langle L \rangle_{20yr}$	1.005 ± 0.006	0.999 ± 0.005	0.993 ± 0.004	0.987 ± 0.003
	RCA4-HadGEM2-ES			
	Historical	RCP2.6	RCP4.5	RCP8.5
$\langle W \rangle_{20yr}$	1.01 ± 0.04	0.98 ± 0.03	0.99 ± 0.04	0.97 ± 0.03
$\langle S \rangle_{20yr}$	1.00 ± 0.02	0.96 ± 0.03	0.94 ± 0.03	0.92 ± 0.02
$\langle L \rangle_{20yr}$	1.00 ± 0.005	0.995 ± 0.004	0.993 ± 0.006	0.989 ± 0.003
	RACMO22E-EC-EARTH			
	Historical	RCP2.6	RCP4.5	RCP8.5
$\langle W \rangle_{20yr}$	0.97 ± 0.02	N.A	0.97 ± 0.03	0.98 ± 0.03
$\langle S \rangle_{20yr}$	1.00 ± 0.02	N.A	0.98 ± 0.02	0.96 ± 0.02
$\langle L \rangle_{20yr}$	1.007 ± 0.004	N.A	0.996 ± 0.005	0.990 ± 0.003
	RACMO22E-HadGEM2-ES			
	Historical	RCP2.6	RCP4.5	RCP8.5
$\langle W \rangle_{20yr}$	0.97 ± 0.03	0.98 ± 0.03	0.99 ± 0.04	0.98 ± 0.03
$\langle S \rangle_{20yr}$	1.00 ± 0.03	0.99 ± 0.03	0.98 ± 0.04	0.96 ± 0.03
$\langle L \rangle_{20yr}$	1.008 ± 0.006	1.001 ± 0.006	0.997 ± 0.006	0.992 ± 0.004
	CCLM4-MPI-ESM-LR			
	Historical	RCP2.6	RCP4.5	RCP8.5
$\langle W \rangle_{20yr}$	0.98 ± 0.02	N.A	0.97 ± 0.03	1.00 ± 0.04
$\langle S \rangle_{20yr}$	1.00 ± 0.02	N.A	0.98 ± 0.02	0.92 ± 0.03
$\langle L \rangle_{20yr}$	1.000 ± 0.004	N.A	0.996 ± 0.003	0.990 ± 0.004

Table 7.6: Welch t-statistic p-values for the average wind and solar power along with consumption for the different climate scenarios within each climate model. p-values in front of "/" are evaluated by table lookup while values after "/" are evaluated by bootstrapping. Shaded p-values indicate values below the significance level of 5%. 0.00 indicates values smaller than 10^{-4}

	HIRHAM5 EC-EARTH	**RCA4 EC-EARTH**	**RCA4 HadGEM2-ES**	**RACMO22E EC-EARTH**	**RACMO22E HadGEM2-ES**	**CCLM4 MPI-ESM-LR**
			Wind			
hist-rcp26	0.01/0.00	0.05/0.05	0.03/0.02	N.A	0.88/0.88	N.A
hist-rcp45	0.19/0.18	0.01/0.02	0.19/0.16	0.36/0.36	0.25/0.32	0.24/0.32
hist-rcp85	0.00/0.00	0.00/0.00	0.00/0.00	0.83/0.83	0.38/0.50	0.11/0.13
rcp26-rcp45	0.41/0.50	0.59/0.60	0.48/0.50	N.A	0.29/0.37	N.A
rcp26-rcp85	0.12/0.15	0.10/0.08	0.22/0.25	N.A	0.77/0.43	N.A
rcp45-rcp85	0.05/0.03	0.20/0.14	0.10/0.12	0.32/0.36	0.69/0.70	0.02/0.01
			Solar			
hist-rcp26	0.56/0.63	0.02/0.01	0.00/0.03	N.A	0.27/0.30	N.A
hist-rcp45	0.00/0.00	0.00/0.00	0.00/0.00	0.01/0.01	0.03/0.04	0.00/0.00
hist-rcp85	0.00/0.00	0.00/0.00	0.00/0.00	0.00/0.01	0.00/0.00	0.00/0.00
rcp26-rcp45	0.04/0.05	0.00/0.00	0.05/0.03	N.A	0.26/0.41	N.A
rcp26-rcp85	0.01/0.01	0.00/0.00	0.00/0.00	N.A	0.00/0.00	N.A
rcp45-rcp85	0.31/0.30	0.00/0.00	0.03/0.03	0.01/0.01	0.12/0.14	0.00/0.00
			Load			
hist-rcp26	0.00/0.00	0.00/0.00	0.00/0.00	N.A	0.00/0.00	N.A
hist-rcp45	0.00/0.00	0.00/0.00	0.00/0.00	0.00/0.00	0.00/0.00	0.00/0.00
hist-rcp85	0.00/0.00	0.00/0.00	0.00/0.00	0.00/0.00	0.00/0.00	0.00/0.00
rcp26-rcp45	0.04/0.03	0.00/0.00	0.03/0.05	N.A	0.00/0.00	N.A
rcp26-rcp85	0.00/0.00	0.00/0.00	0.00/0.00	N.A	0.00/0.00	N.A
rcp45-rcp85	0.00/0.00	0.00/0.00	0.00/0.00	0.00/0.00	0.00/0.00	0.00/0.00

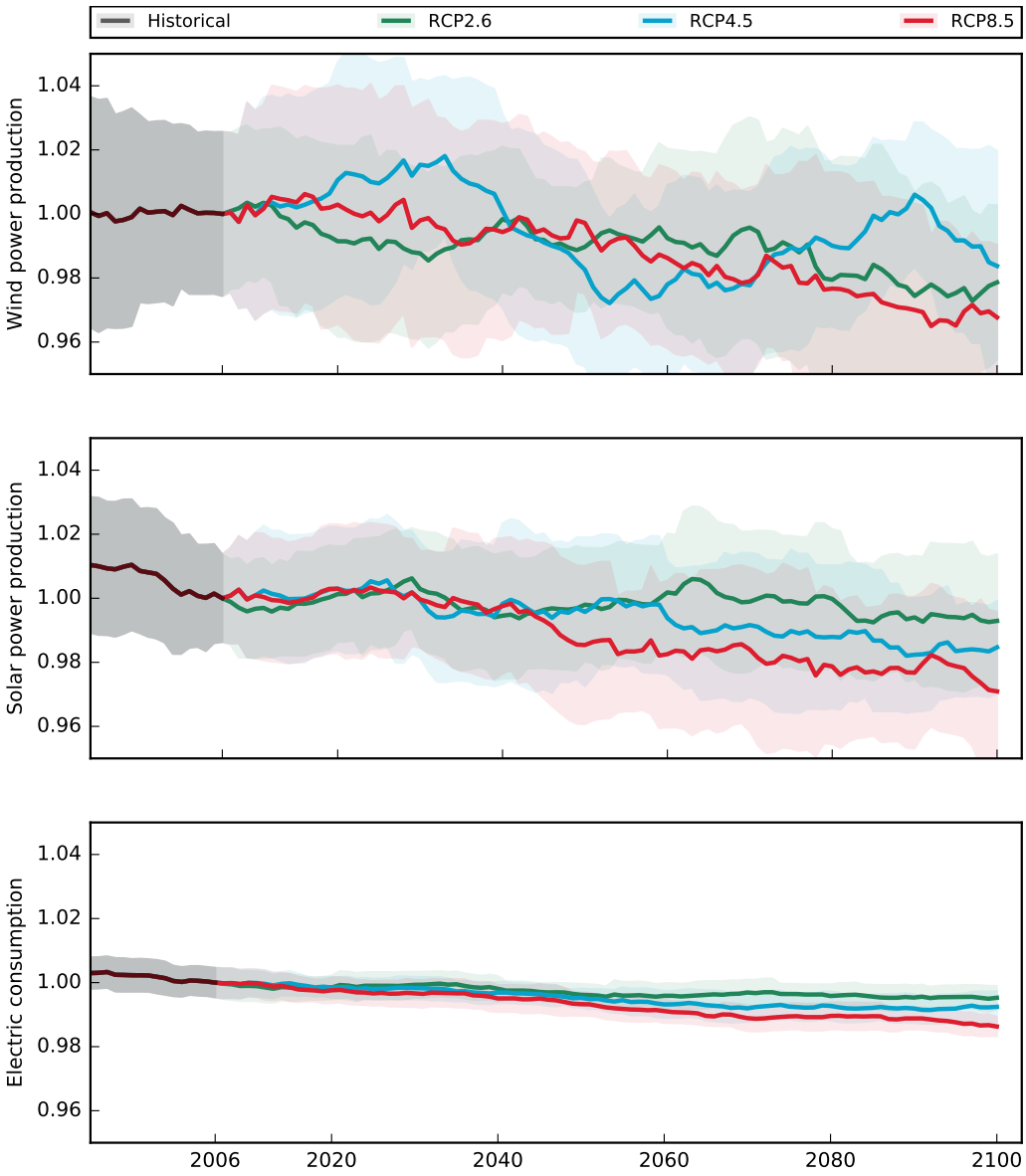

Figure 7.32: Evolution of the nosmalised wind power production, solar power production and electric consumption as a function of model year for HIRHAM5-EC-EARTH. The historical period covers 1996–2006 (black), and the future scenarios RCP2.6 (green), RCP4.5 (blue) and RCP8.5 (red) cover the years 2006–2100. The averages of the annual values are indicated with fully drawn lines, and the corresponding ranges of the one sigma standard deviation are shown with shaded areas. All key metrics are unit less as described in the methods section.

Table 7.7: Welch t-statistic p-values of the key-metrics for the different climate scenarios within each climate model. p-values in front of "/" are evaluated by table lookup while values after "/" are evaluated by bootstrapping. Shaded p-values indicate values below the significance level of 5%. 0.00 indicates values smaller than 10^{-4}.

	HIRHAM5 EC-EARTH	**RCA4 EC-EARTH**	**RCA4 HadGEM2-ES**	**RACMO22E EC-EARTH**	**RACMO22E HadGEM2-ES**	**CCLM4 MPI-ESM-LR**
			Dispatchable electricity			
hist-rcp26	0.07/0.06	0.16/0.10	0.02/0.00	N.A	0.78/0.75	N.A
hist-rcp45	0.38/0.38	0.06/0.04	0.25/0.27	0.16/0.21	0.29/0.35	0.23/0.19
hist-rcp85	0.01/0.01	0.00/0.01	0.00/0.00	0.80/0.83	0.93/0.89	0.61/0.60
rcp26-rcp45	0.44/0.48	0.74/0.67	0.32/0.33	N.A	0.19/0.23	N.A
rcp26-rcp85	0.51/0.60	0.10/0.11	0.20/0.20	N.A	0.72/0.75	N.A
rcp45-rcp85	0.18/0.11	0.13/0.08	0.05/0.04	0.24/0.21	0.33/0.36	0.12/0.14
			Benefit of transmission			
hist-rcp26	0.04/0.05	0.70/0.60	0.86/0.86	N.A	0.73/0.76	N.A
hist-rcp45	0.43/0.40	0.27/0.25	0.81/0.75	0.31/0.34	0.35/0.37	0.56/0.57
hist-rcp85	0.02/0.04	0.01/0.00	0.12/0.08	0.69/0.61	0.33/0.27	0.01/0.02
rcp26-rcp45	0.29/0.28	0.19/0.19	0.93/0.93	N.A	0.53/0.50	N.A
rcp26-rcp85	0.83/0.78	0.01/0.01	0.15/0.10	N.A	0.53/0.49	N.A
rcp45-rcp85	0.20/0.20	0.08/0.03	0.24/0.24	0.50/0.39	0.92/0.93	0.00/0.00
			Benefit of Storage			
hist-rcp26	0.00/0.00	0.58/0.64	0.00/0.01	N.A	0.51/0.51	N.A
hist-rcp45	0.80/0.84	0.01/0.02	0.00/0.00	0.00/0.00	0.05/0.08	0.00/0.00
hist-rcp85	0.30/0.32	0.00/0.00	0.00/0.00	0.00/0.00	0.00/0.01	0.00/0.00
rcp26-rcp45	0.00/0.00	0.02/0.00	0.06/0.05	N.A	0.23/0.29	N.A
rcp26-rcp85	0.03/0.04	0.00/0.00	0.00/0.00	N.A	0.02/0.04	N.A
rcp45-rcp85	0.26/0.26	0.01/0.01	0.03/0.03	0.05/0.05	0.37/0.30	0.00/0.00
			Dispatchable Capacity			
hist-rcp26	0.21/0.21	0.41/0.33	0.08/0.12	N.A	0.62/0.67	N.A
hist-rcp45	0.73/0.72	0.86/0.88	0.89/0.87	0.27/0.27	0.21/0.22	0.89/0.90
hist-rcp85	0.61/0.58	0.27/0.22	0.08/0.07	0.73/0.68	0.35/0.30	0.38/0.38
rcp26-rcp45	0.10/0.05	0.39/0.48	0.07/0.09	N.A	0.32/0.21	N.A
rcp26-rcp85	0.38/0.34	0.72/0.77	0.96/0.96	N.A	0.56/0.61	N.A
rcp45-rcp85	0.36/0.33	0.25/0.30	0.07/0.09	0.10/0.10	0.66/0.71	0.40/0.39
			Short-term variability			
hist-rcp26	0.00/0.00	0.30/0.26	0.15/0.14	N.A	0.78/0.82	N.A
hist-rcp45	0.67/0.67	0.54/0.59	0.98/0.97	0.81/0.83	0.10/0.12	0.35/0.27
hist-rcp85	0.02/0.02	0.44/0.37	0.15/0.17	0.08/0.06	0.21/0.22	0.03/0.03
rcp26-rcp45	0.01/0.00	0.59/0.67	0.16/0.13	N.A	0.20/0.24	N.A
rcp26-rcp85	0.21/0.19	0.84/0.81	0.95/0.96	N.A	0.39/0.35	N.A
rcp45-rcp85	0.11/0.16	0.78/0.85	0.17/0.17	0.17/0.17	0.52/0.60	0.01/0.01

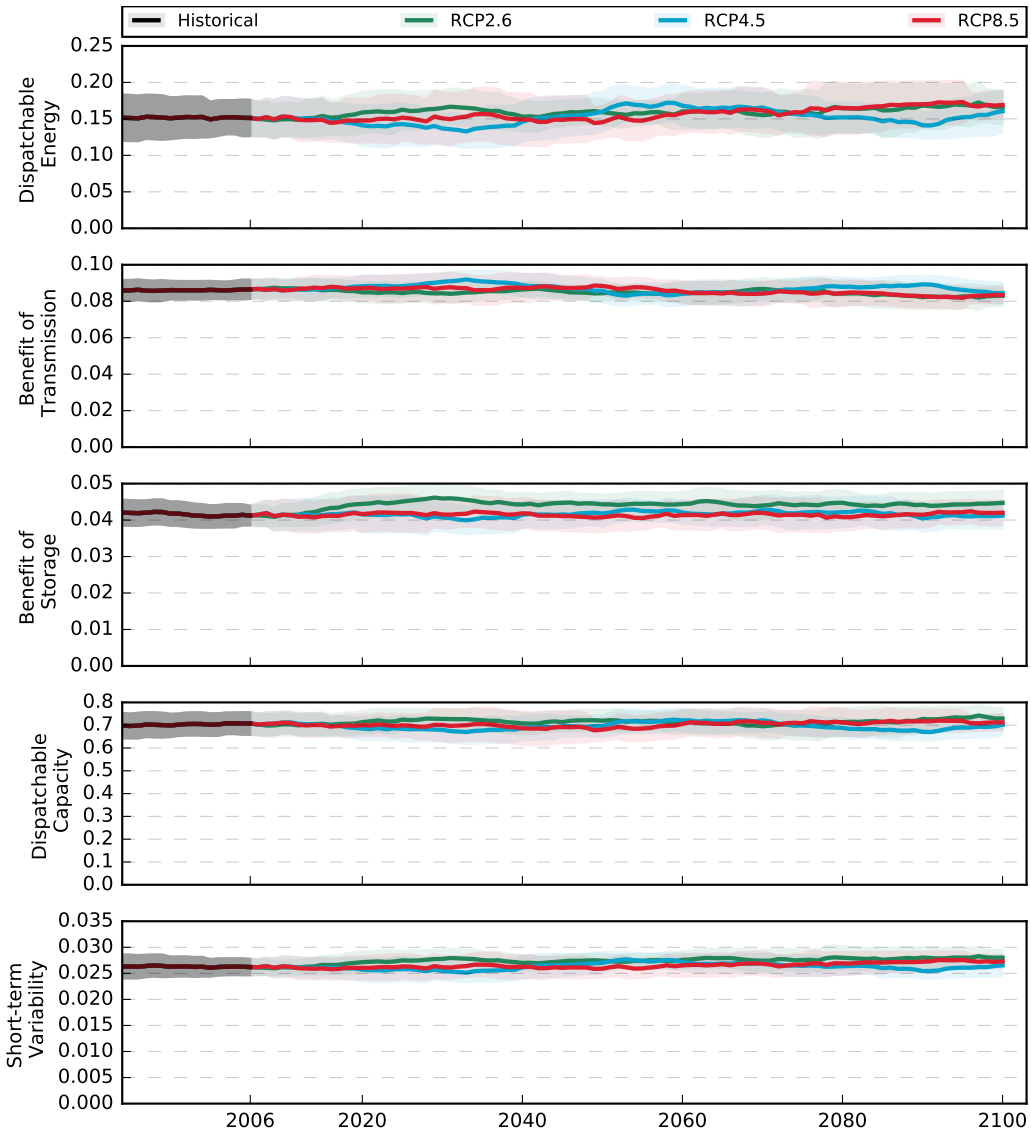

Figure 7.33: Evolution of the key metrics as a function of model year for the climate model HIRHAM5-EC-EARTH. The historical period covers 1996–2006 (black) and the future scenarios RCP2.6 (green), RCP4.5 (blue) and RCP8.5 (red) covers the years 2006–2100. The 20 year averages of the annual values are indicated with fully drawn lines, and the corresponding ranges of the one sigma standard deviation are shown with shaded areas. All key metrics are unitless as described in the methods section.

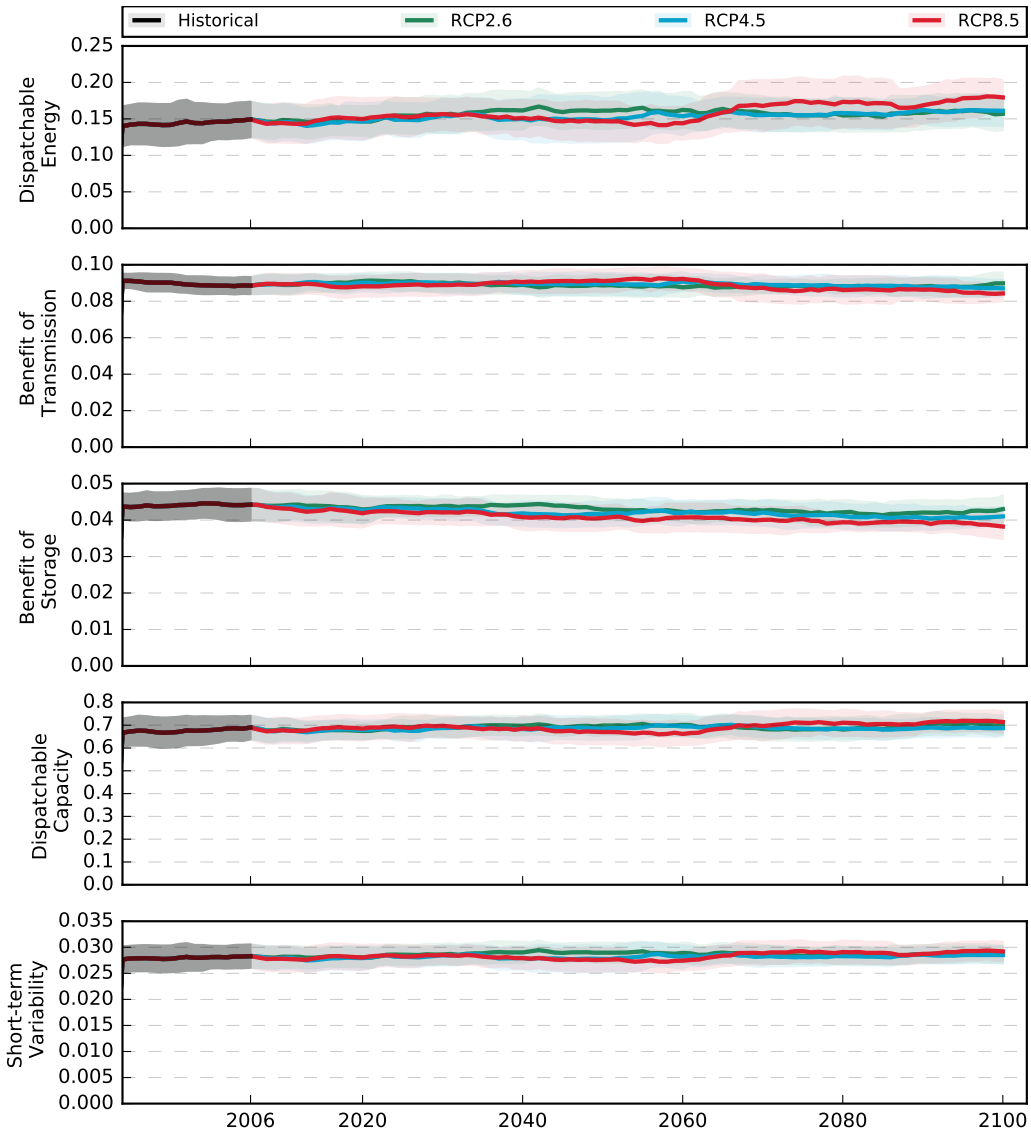

Figure 7.34: Evolution of the key metrics as a function of model year for the climate model RCA4-EC-EARTH. The historical period covers 1996–2006 (black) and the future scenarios RCP2.6 (green), RCP4.5 (blue) and RCP8.5 (red) covers the years 2006–2100. The 20 year averages of the annual values are indicated with fully drawn lines, and the corresponding ranges of the one sigma standard deviation are shown with shaded areas. All key metrics are unitless as described in the methods section.

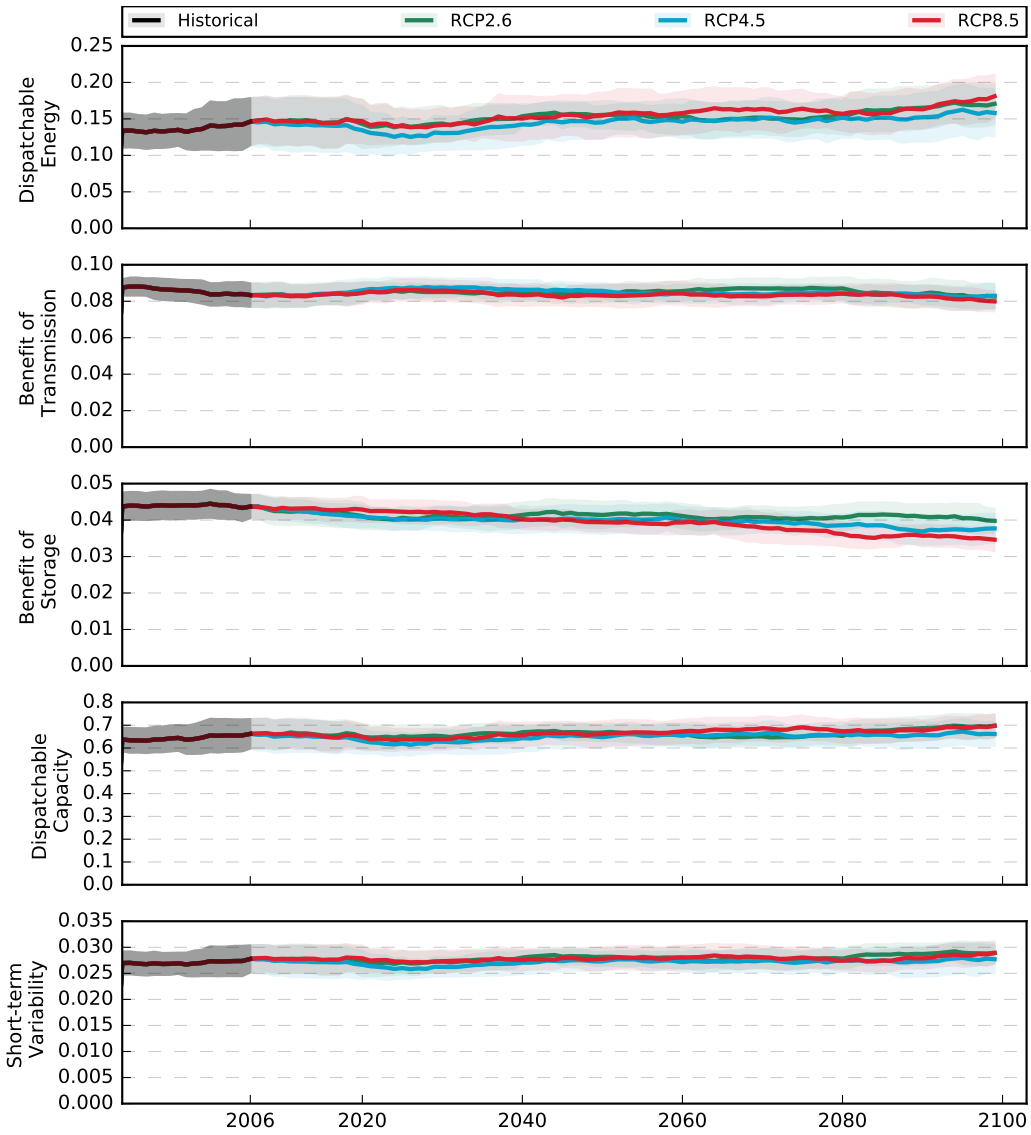

Figure 7.35: Evolution of the key metrics as a function of model year for the climate model RCA4-HadGEM2-ES. The historical period covers 1996–2006 (black) and the future scenarios RCP2.6 (green), RCP4.5 (blue) and RCP8.5 (red) covers the years 2006–2100. The 20 year averages of the annual values are indicated with fully drawn lines, and the corresponding ranges of the one sigma standard deviation are shown with shaded areas. All key metrics are unitless as described in the methods section.

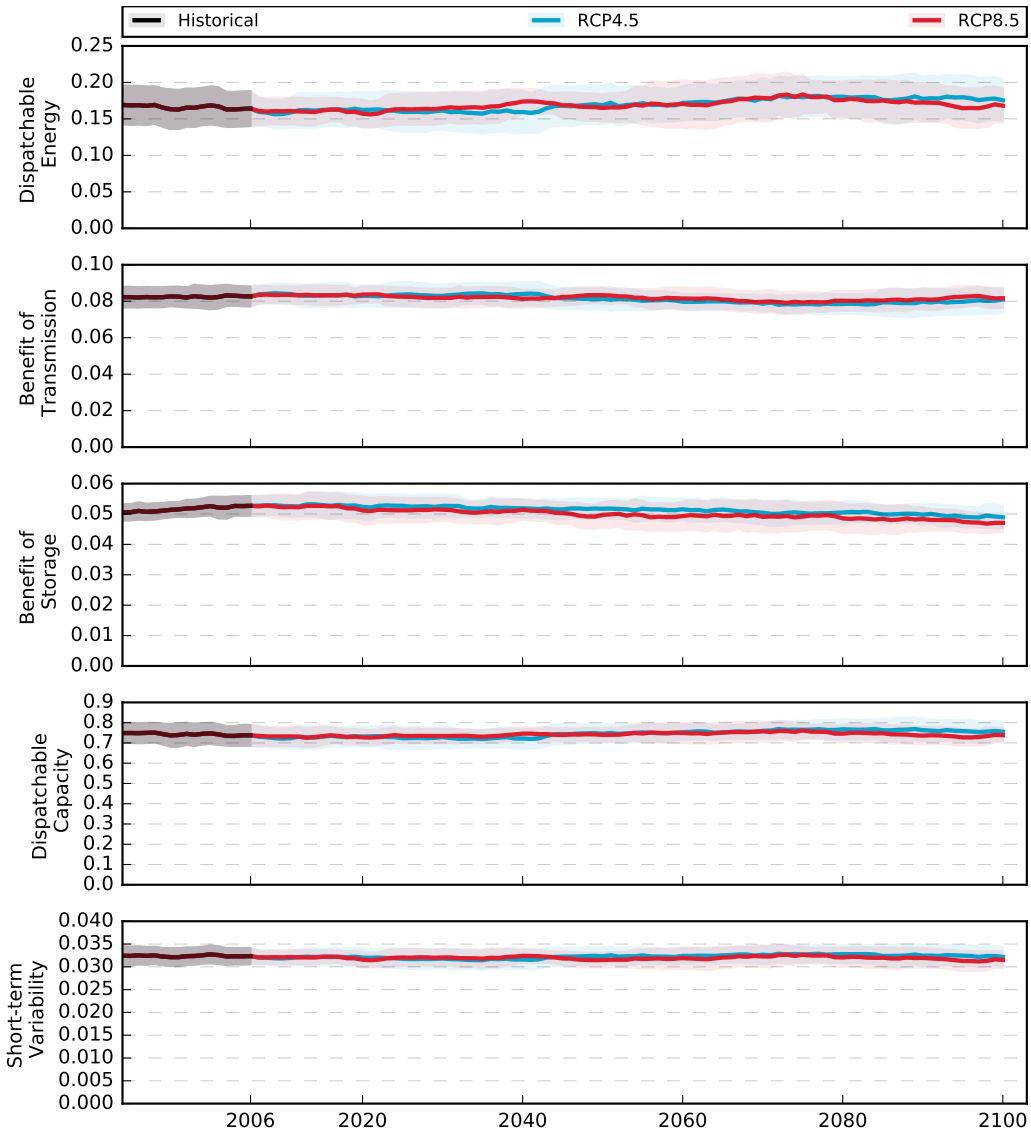

Figure 7.36: Evolution of the key metrics as a function of model year for the climate model RACMO22E-EC-EARTH. The historical period covers 1996–2006 (black) and the future scenarios RCP2.6 (green), RCP4.5 (blue) and RCP8.5 (red) covers the years 2006–2100. The 20 year averages of the annual values are indicated with fully drawn lines, and the corresponding ranges of the one sigma standard deviation are shown with shaded areas. All key metrics are unitless as described in the methods section.

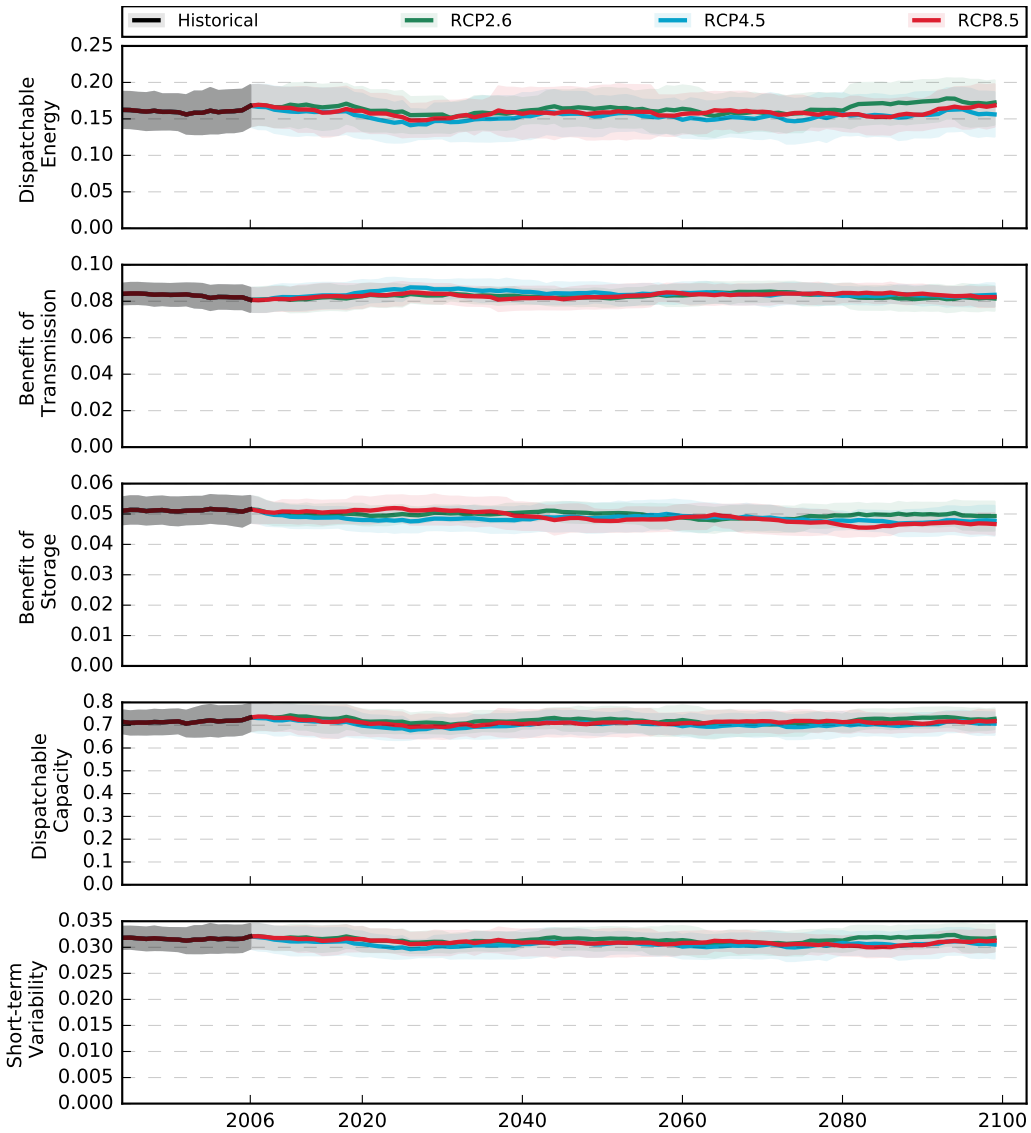

Figure 7.37: Evolution of the key metrics as a function of model year for the climate model RACMO22E-HadGEM2-ES. The historical period covers 1996–2006 (black) and the future scenarios RCP2.6 (green), RCP4.5 (blue) and RCP8.5 (red) covers the years 2006–2100. The 20 year averages of the annual values are indicated with fully drawn lines, and the corresponding ranges of the one sigma standard deviation are shown with shaded areas. All key metrics are unitless as described in the methods section.

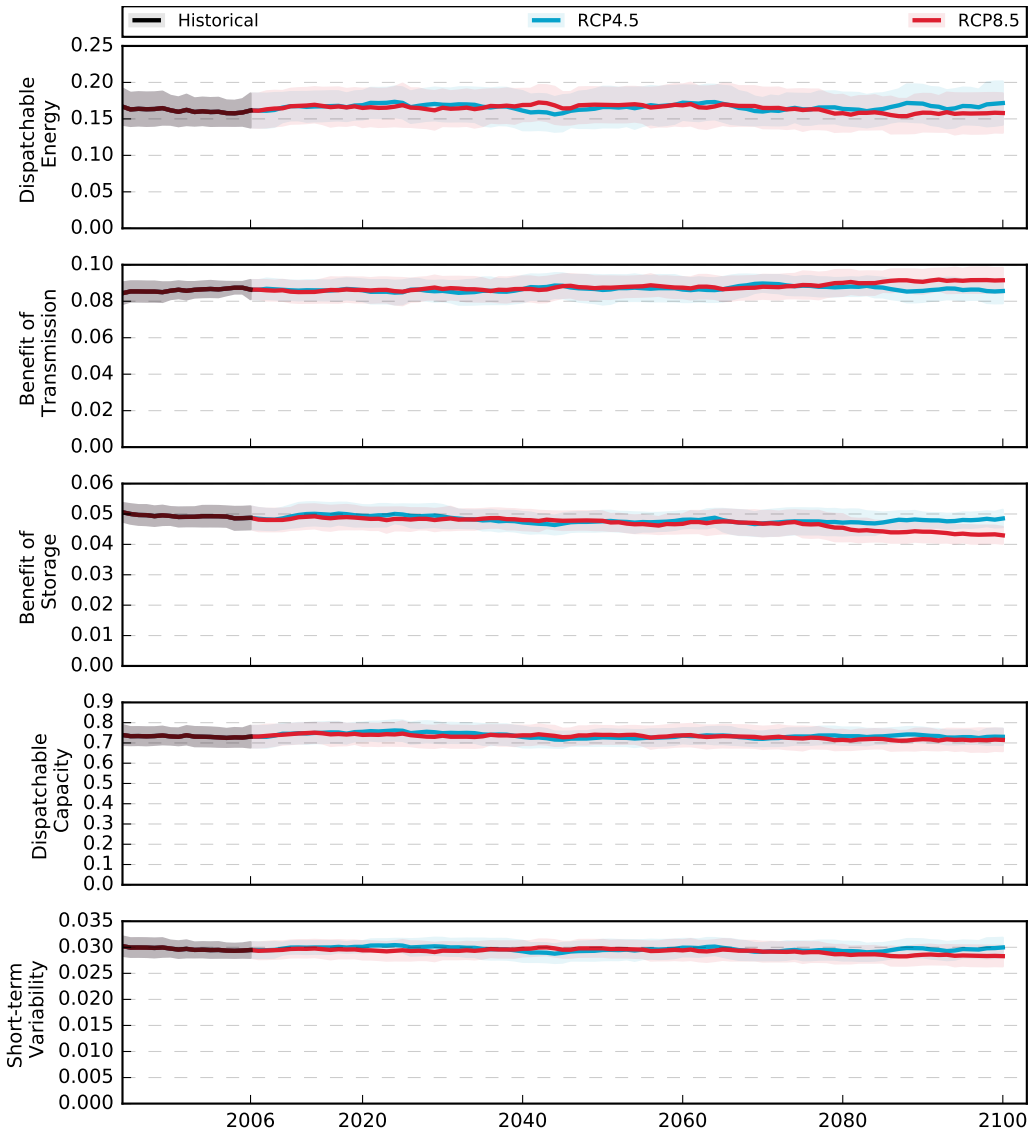

Figure 7.38: Evolution of the key metrics as a function of model year for the climate model CCL4-MPI-ESM-LR. The historical period covers 1996–2006 (black) and the future scenarios RCP2.6 (green), RCP4.5 (blue) and RCP8.5 (red) covers the years 2006–2100. The 20 year averages of the annual values are indicated with fully drawn lines, and the corresponding ranges of the one sigma standard deviation are shown with shaded areas. All key metrics are unitless as described in the methods section.

CHAPTER 8

Estimating country-specific space heating threshold temperatures from national consumption data

The material in this chapter is the Supplemental Information (SI) for the paper *Estimating country-specific space heating threshold temperatures from national consumption data*. The material is not intended for the regular reader, but only for other researchers, with special interests. Section 1 provides a general overview of the gas and electricity consumption data that is used in this project. Section 2 presents additional results.

8.1 National electricity and gas consumption data

In Figures 8.1 and 8.2 the national electricity consumption data for the countries that are used as case studies in this work are presented. The data spans from earliest 2006 to 2018. A few countries as, Austria, Switzerland, Denmark, United Kingdom show anomalies in the data. For Denmark and United Kingdom these were avoided by having data provided by national sources. For Austria data between 2006-2011 are not taken into consideration. For Switzerland data from 2015-2018 are not taken into consideration.

In Figures 8.3 and 8.4 the national gas consumption data for the countries that are used as case studies in this work are presented. The data spans from 2008 to 2018. The black plots show the gas consumption data provided by Eurostat. For a few countries, gas consumption data is available from the ENTSO-G transparency platform (red plots). For the available years these show a satisfying comparison. Gas consumption data from national sources is available for Denmark and United Kingdom (dashed green plots).

8.2 Additional results

Figures 8.5-8.7 illustrate the synergy between the monthly averaged air temperature measurements (blue curves), the heating threshold temperatures (red dashed lines) and the classified summer seasons (hatched areas) for countries that possess air temperature measurements.

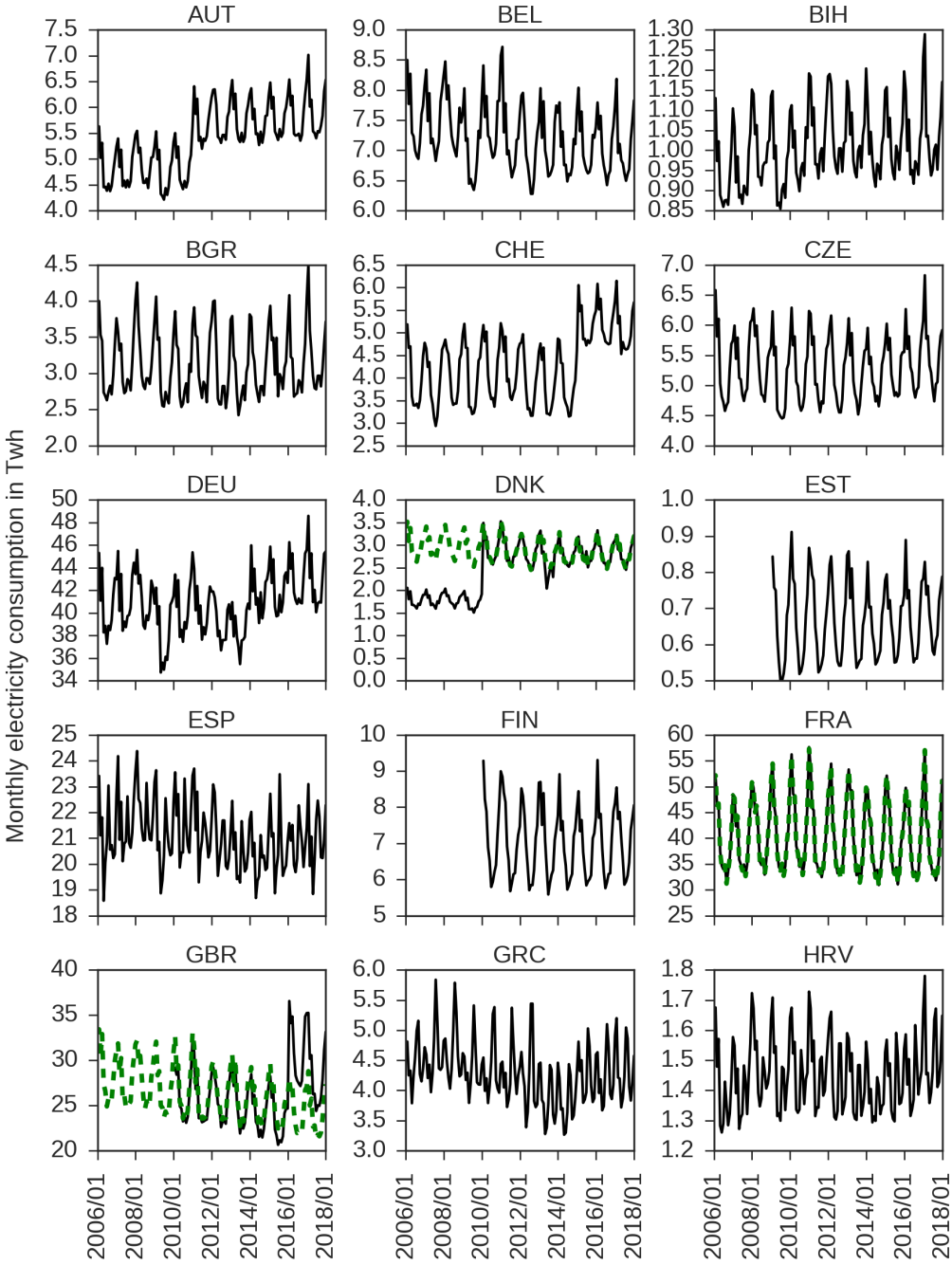

Figure 8.1: Monthly electricity consumption in TWh from earliest 2006 to 2018. Black plots illustrate electricity consumption data from ENTSO-E. Dashed green plots illustrate electricity consumption data provided by national sources.

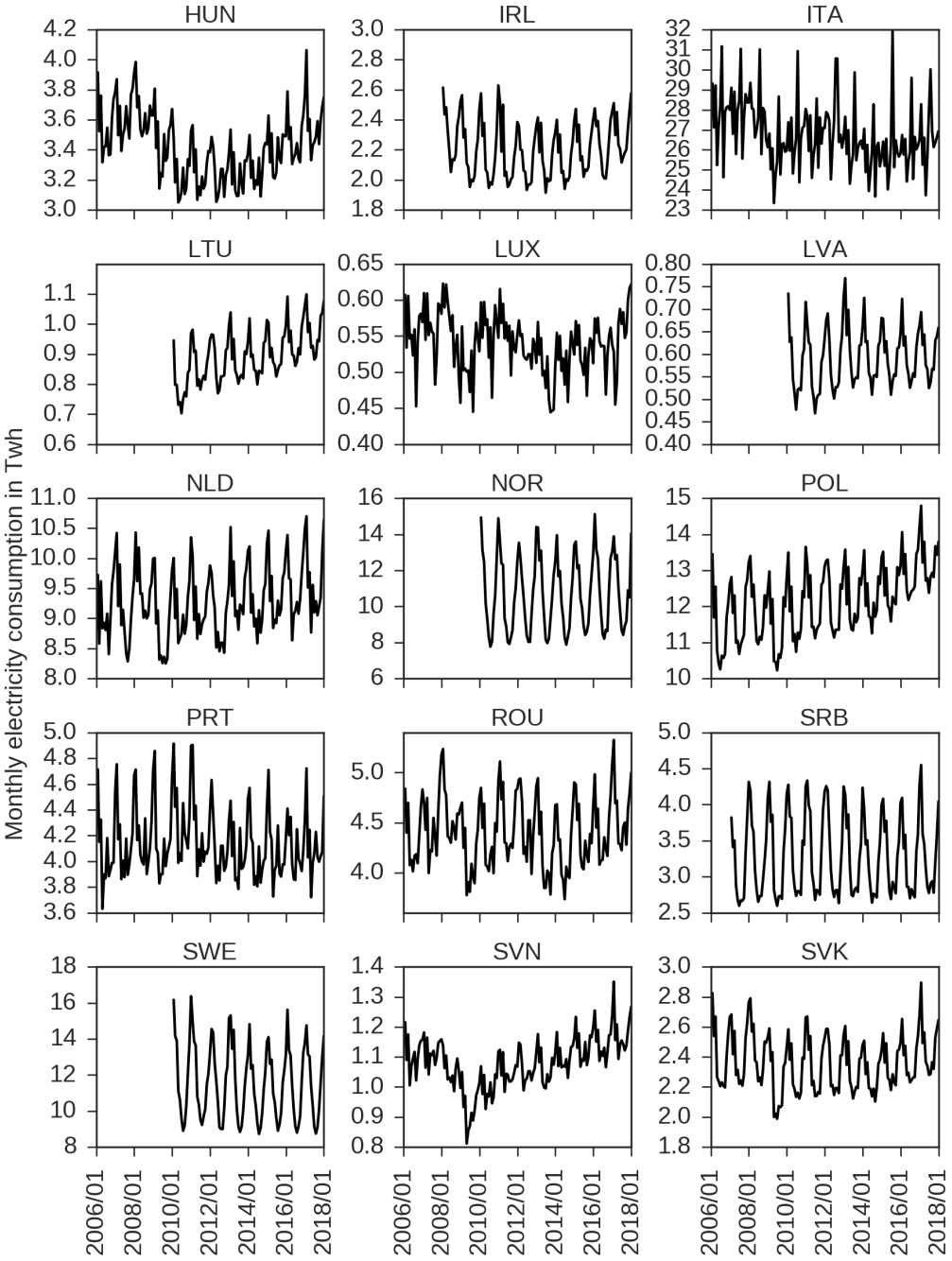

Figure 8.2: Monthly electricity consumption in TWh from earliest 2006 to 2018. Black plots illustrate electricity consumption data from ENTSO-E.

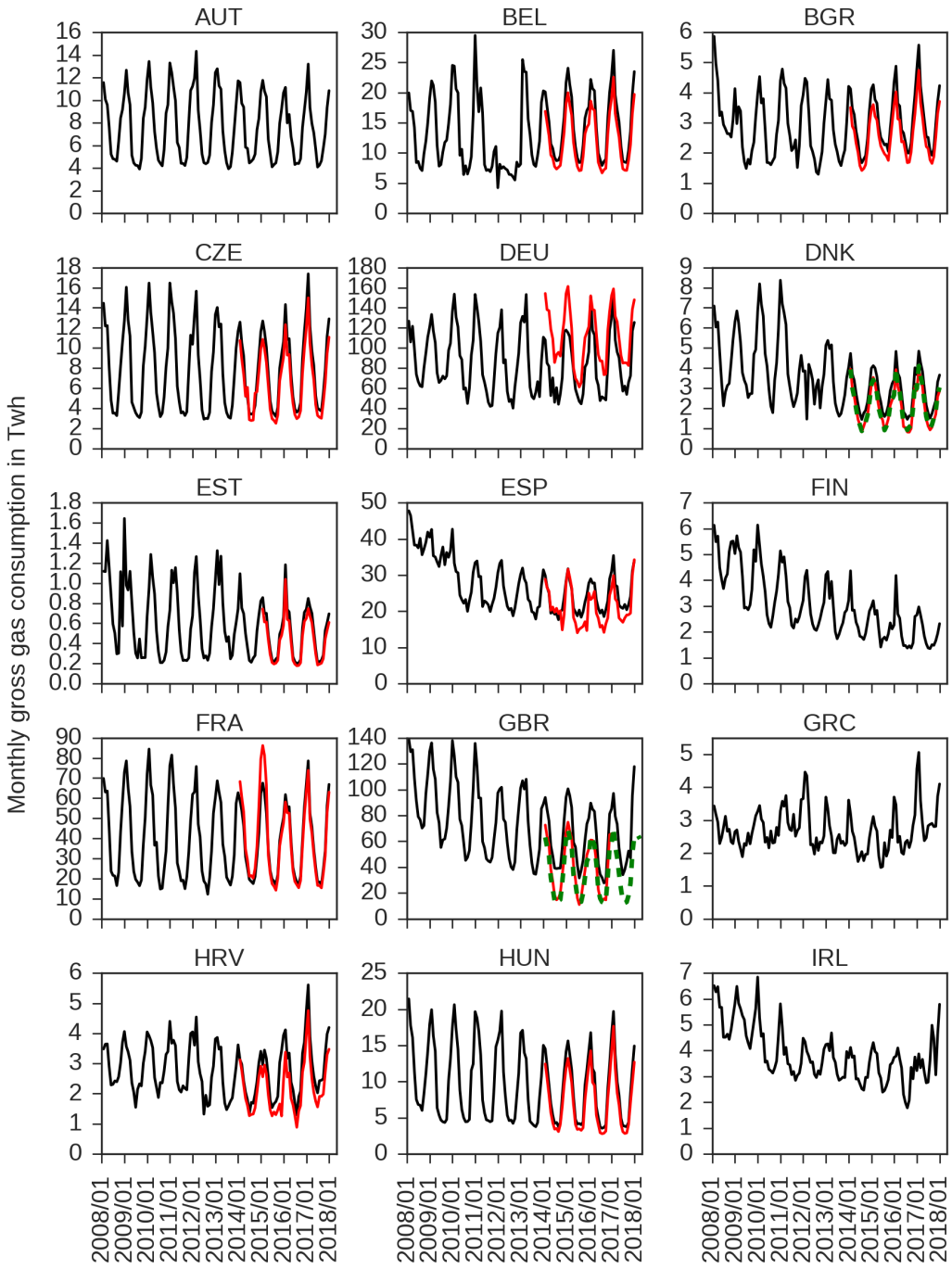

Figure 8.3: Monthly gas consumption in TWh from 2008 to 2018. Black plots illustrate gas consumption data from Eurostat. Red plots illustrate gas consumption data that is available through ENTSO-G's transparency platform. Dashed green plots illustrate data provided by national sources.

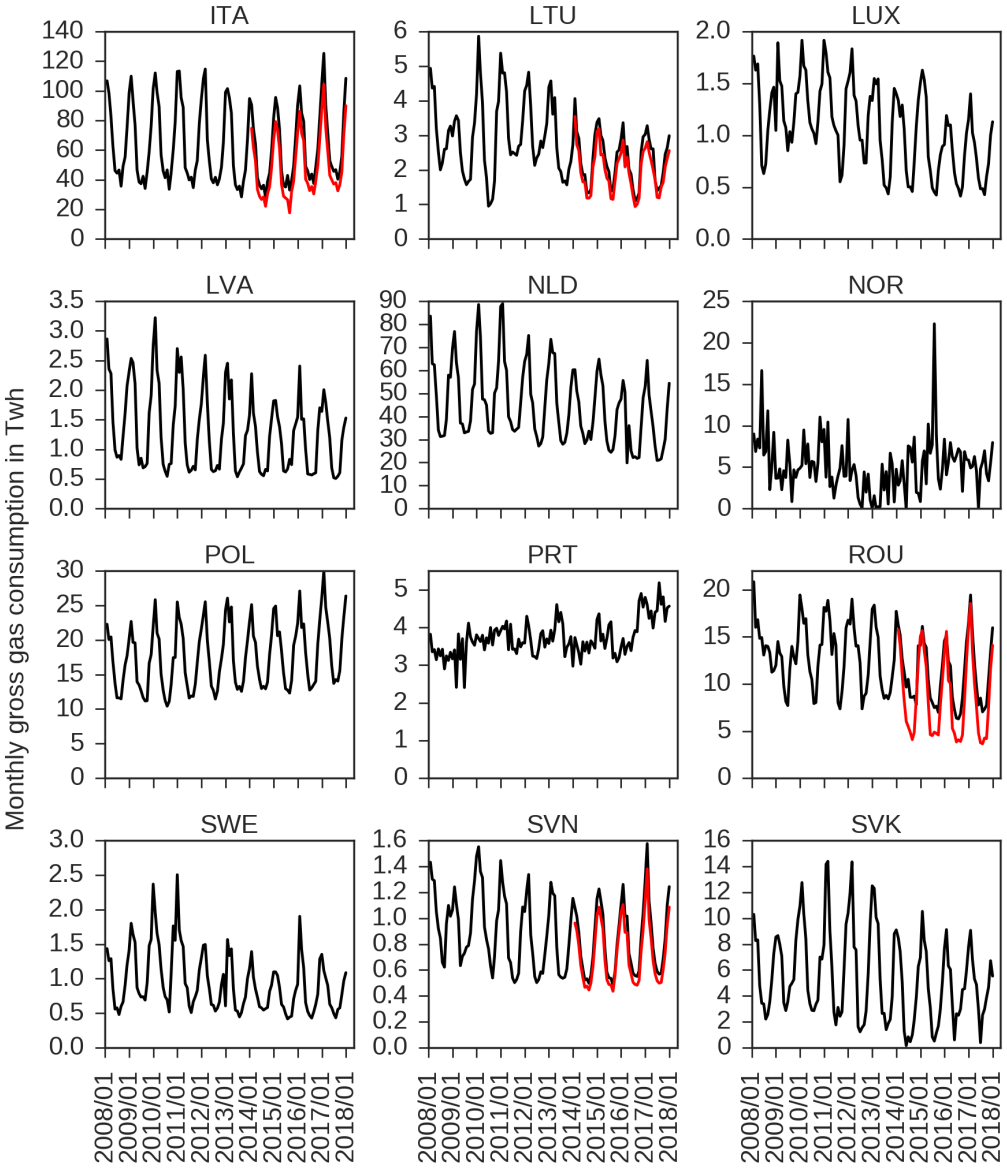

Figure 8.4: Monthly gas consumption in TWh from 2008 to 2018. Black plots illustrate gas consumption data from Eurostat. Red plots illustrate gas consumption data that is available through ENTSO-G's transparency platform.

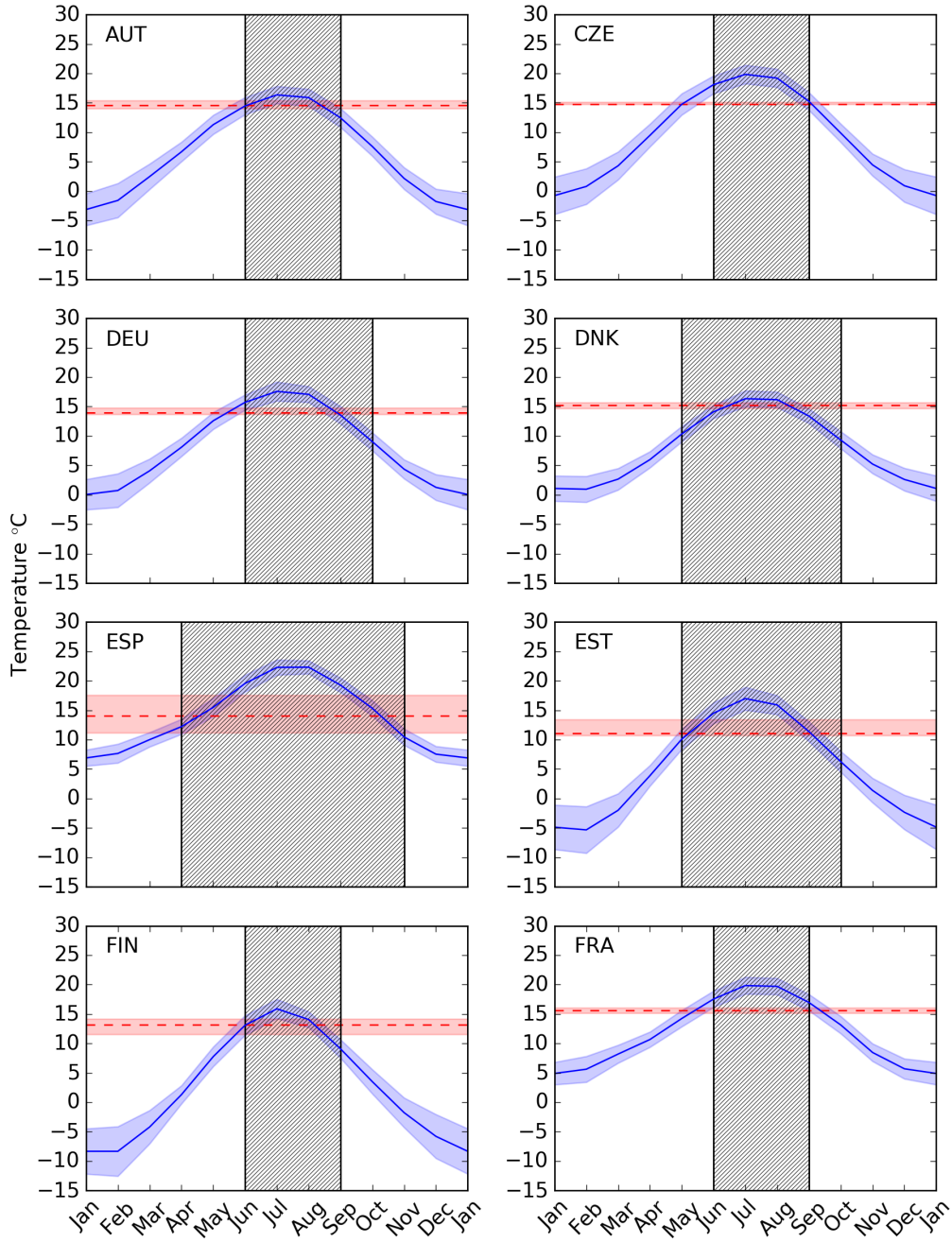

Figure 8.5: Monthly averaged temperatures from 2008 to 2017 (blue full drawn curves) with 1 sigma uncertainty ranges (shaded blue regions), heating threshold temperatures (red dashed lines) with $[q_{25\%}, q_{75\%}]$ uncertainty ranges (shaded red regions) and classified summer season (black hatched areas).

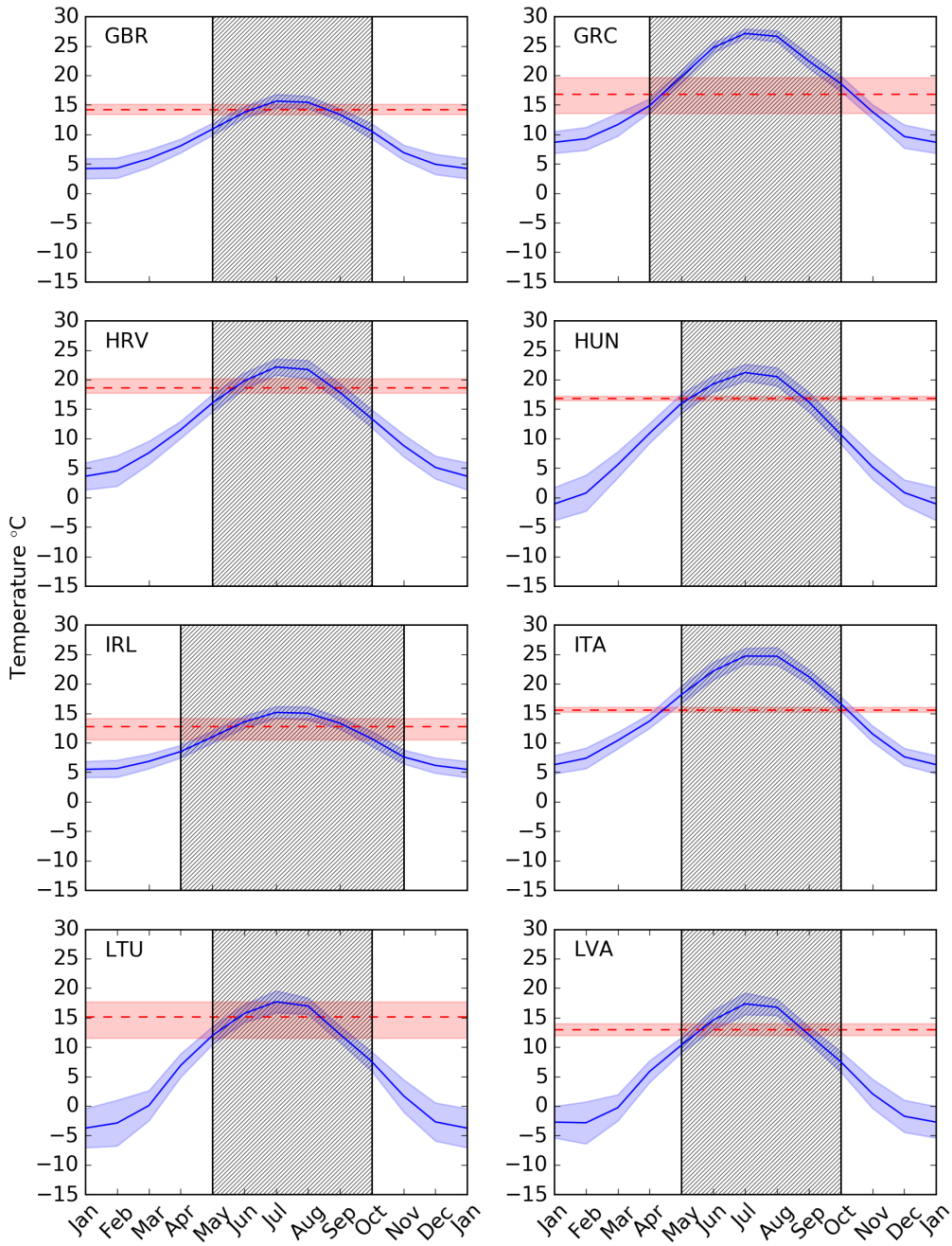

Figure 8.6: Monthly averaged temperatures from 2008 to 2017 (blue full drawn curves) with 1 sigma uncertainty ranges (shaded blue regions), heating threshold temperatures (red dashed lines) with $[q_{25\%}, q_{75\%}]$ uncertainty ranges (shaded red regions) and classified summer season (black hatched areas).

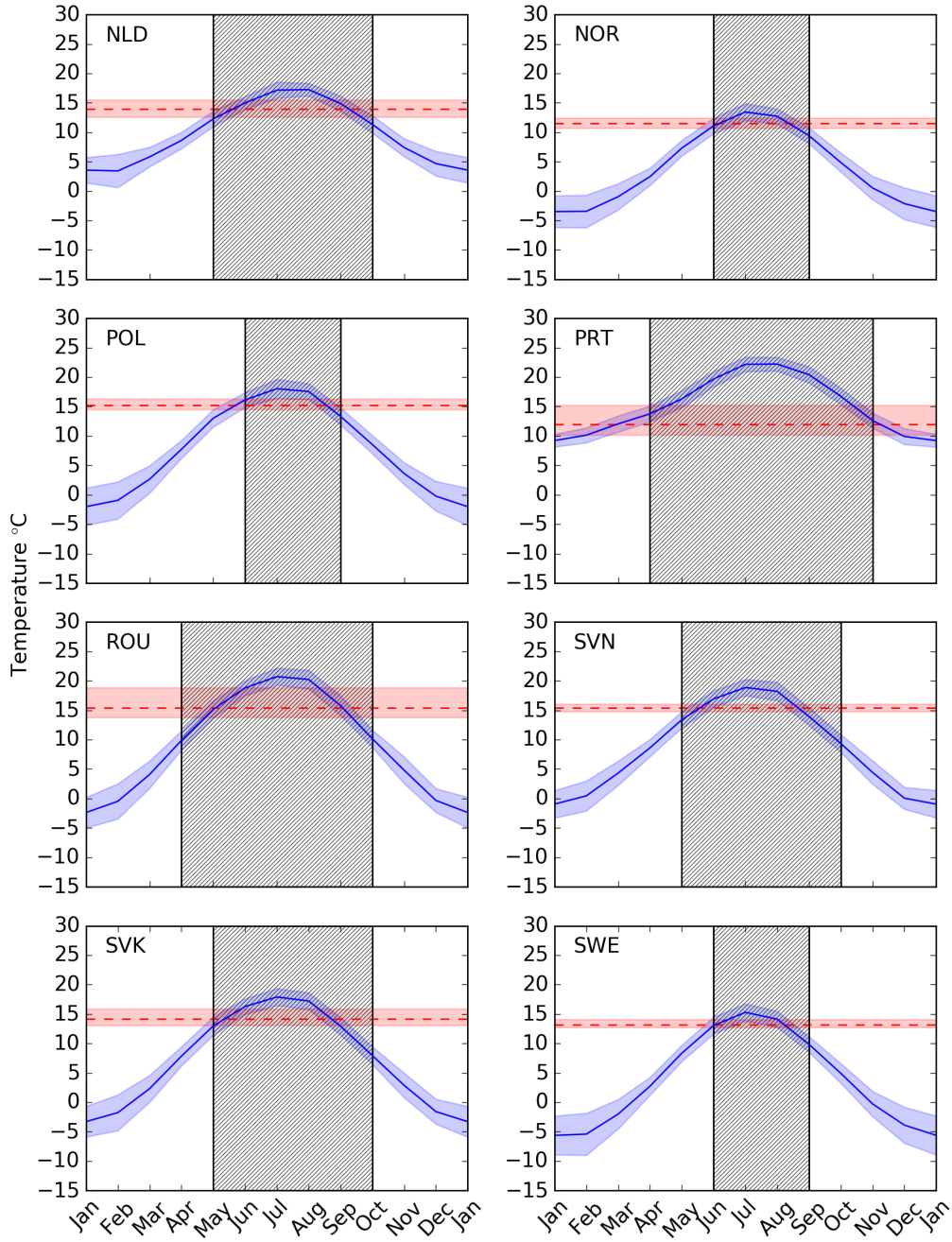

Figure 8.7: Monthly averaged temperatures from 2008 to 2017 (blue full drawn curves) with 1 sigma uncertainty ranges (shaded blue regions), heating threshold temperatures (red dashed lines) with $[q_{25\%}, q_{75\%}]$ uncertainty ranges (shaded red regions) and classified summer season (black hatched areas).

CHAPTER 9

Impact of climate change on the cost-optimal mix of decentralised heat pump and gas boiler technologies in Europe

The material in this chapter is the Supplemental Information (SI) for the paper *Impact of climate change on the cost-optimal mix of decentralised heat pump and gas boiler technologies in Europe*. The material is not intended for the regular reader, but only for other researchers, with special interests. The material of the SI is intended to give a broader perspective on the methods that are applied to conduct the technical analysis of this paper. Section 1 provides a general overview of the heating degree-days and how it used as a proxy to model the day-to-day fluctuations in the heat demand. Section 2 presents our approach to model the supply side of the residential heating sector. In section 3, the approach to model the Coefficient Of Performance (COP) of heat pumps is described. Section 4 presents the climate data that is implemented into this study. In Section 5 the discussion on the *unperturbed* pricing scheme is extended. Finally, in Section 6 the results on the impact of climate change on the heat pump coefficient of performance are discussed.

9.1 Extended experimental procedures

Heat load factors

The heat load factor, denoted as μ, is defined as the unitless ratio of the residential heat demand, L^{Total}, to the maximum possible output of heat, P^{Max}, over a given period of time, Δ, as:

$$\mu = \frac{L^{\text{Total}}}{P^{\text{Max}} \cdot \Delta} \tag{9.1}$$

where the total residential heat demand, L^{Total}, is the sum of the individual space heating and hot water components, $L^{\text{Space Heat}}$ and $L^{\text{Hot Water}}$, respectively:

$$L^{\text{Total}} = L^{\text{Space Heat}} + L^{\text{Hot Water}}$$

The decentralised nature of heating means that data on consumption is not readily available and therefore not applicable for further research. Known to the literature, the theory of heating degree-days is most frequently used as a best proxy for the variations in the day-to-day heat demand [91, 137]. In this study, a direct proportionality between the total residential space heat demand, L^{Total}, and the heating degree-days, $\text{HDD}^{\text{Space Heat}}$, is assumed as:

$$\begin{aligned} L^{\text{Total}} &= L^{\text{Space Heat}} + L^{\text{Hot Water}} \\ &= \alpha \cdot \text{HDD}^{\text{Space Heat}} + L^{\text{Hot Water}} \end{aligned} \tag{9.2}$$

α is a constant of proportionality in units of energy per heating degree-day. Inspired by [179], the accumulated heating degree-days, $\text{HDD}^{\text{SpaceHeat}}_{\Delta,\text{x}}$, for a single grid location, x, over a period of time, Δ, is given as:

$$\text{HDD}^{\text{Space Heat}}_{\Delta,\text{x}} = \int_{\Delta} (T_0 - T_{\text{x}}(t))_+ \, \text{d}t \tag{9.3}$$

$(T_0 - T_{\text{x}}(t))_+$ defines a positive value or otherwise zero [156]. To elaborate, if $T_0 > T_{\text{x}}(t)$, the output of $(T_0 - T_{\text{x}}(t))_+$ will add to the heating degree-days. On the other hand, if $T_0 \leq T_{\text{x}}(t)$, $(T_0 - T_{\text{x}}(t))_+$ will be put to zero. $(T_0 - T_{\text{x}}(t))_+$ is defined as:

$$(T_0 - T_{\text{x}}(t))_+ = \begin{cases} T_0 - T_{\text{x}}(t) & \text{if} \quad T_0 > T_{\text{x}}(t) \\ 0 & \text{if} \quad T_0 \leq T_{\text{x}}(t) \end{cases}$$

The base temperature, T_0, is defined as the outside temperature below which a building is assumed to need heating. For simplicity, the base temperature is assumed to be 17 °C although strong evidence suggests that this value vary according to region and study [179]. $T_{\mathrm{x}}(t)$ defines the gridded time series of the ambient air temperature.

The maximum output of heat, P^{Max}, is in a similar way to the total heat consumption defined by a maximum output of space heat, $P^{\mathrm{Space\ Heat}}$, and hot water, $P^{\mathrm{Hot\ Water}}$, as:

$$\begin{aligned} P^{\mathrm{Max}} &= P^{\mathrm{Space\ Heat}} + P^{\mathrm{Hot\ Water}} \\ &= \frac{\alpha\left(T_0 - T_{\mathrm{x,\,design}}\right)\cdot 1\mathrm{day}}{\Delta} + \frac{L^{\mathrm{Hot\ Water}}}{\Delta} \end{aligned} \tag{9.4}$$

The maximum output of hot water, $P^{\mathrm{Hot\ Water}}$, equals the consumption of hot water, $L^{\mathrm{Hot\ Water}}$, normalised to Δ. $P^{\mathrm{Space\ Heat}}$ is defined in a similar way to $L^{\mathrm{Space\ Heat}}$. $T_{\mathrm{x,\,design}}$ is the system design temperature and calculated as a 0.05% quantile of the gridded daily ambient temperature, $T_{\mathrm{x}}(t)$, as:

$$\int_0^{T_{\mathrm{x,\,design}}} p_{\mathrm{x}}(T_{\mathrm{x}})\,\mathrm{d}T_{\mathrm{x}} = 0.0005$$

A small quantile is used to ensure an operation time in conditions above the design temperature in 95.95% of the time. A 0.05% quantile corresponds to approximately 5 hours during a year. A 100% quantile would otherwise overestimate the technology capacity and increase the capital investments.

Finally, replacing L^{Total} and P^{Max} in Equation 9.1 by the expressions given in Equation 9.2 and 9.4 leads to:

$$\mu_{\mathrm{x}} = \frac{\alpha\cdot \mathrm{HDD}_{\Delta,\mathrm{x}}^{\mathrm{Space\ Heat}} + L^{\mathrm{Hot\ Water}}}{\left(\frac{\alpha\left(T_0 - T_{\mathrm{x,\,design}}\right)\cdot 1\mathrm{day}}{\Delta} + \frac{L^{\mathrm{Hot\ Water}}}{\Delta}\right)\Delta}$$

This can be simplified by removing the Δ in the denominator and dividing both the numerator and denominator by α as:

$$\mu_{\mathrm{x}} = \frac{\mathrm{HDD}_{\Delta,\mathrm{x}}^{\mathrm{Space\ Heat}} + \frac{L^{\mathrm{Hot\ Water}}}{\alpha}}{\left(T_0 - T_{\mathrm{x,\,design}}\right)\cdot 1\mathrm{day} + \frac{L^{\mathrm{Hot\ Water}}}{\alpha}} \tag{9.5}$$

Much like the energy demand for space heating, measurements of hot water consumption, $L^{\text{Hot Water}}$, are not available on scales that match the needs of this study. Therefore in Equation 9.5, $\frac{L^{\text{Hot Water}}}{\alpha}$, which is given in units of heating degree-days, is used as a best proxy for hot water consumption. To provide a best approximation of $\frac{L^{\text{Hot Water}}}{\alpha}$, measured hot water and space heat consumption data from Stockholm [325] are used. The general logic is to estimate the ratio of hot water to space heat for Stockholm and use this value to estimate $\frac{L^{\text{Hot Water}}}{\alpha}$. Based on the measured consumption data, the ratio of hot water to space heat is 26%, i.e.:

$$
\begin{aligned}
L^{\text{Hot Water}}_{\text{Stockholm}} &= 0.26 \cdot L^{\text{Space Heat}}_{\text{Stockholm}} \\
L^{\text{Hot Water}}_{\text{Stockholm}} &= 0.26 \cdot \alpha \cdot \text{HDD}^{\text{Space Heat}}_{\Delta,\text{Stockholm}} \\
\frac{L^{\text{Hot Water}}_{\text{Stockholm}}}{\alpha} &= 0.26 \cdot \text{HDD}^{\text{Space Heat}}_{\Delta,\text{Stockholm}}
\end{aligned}
$$

Depending on the time extent, $\frac{L^{\text{Hot Water}}_{\text{Stockholm}}}{\alpha}$ can be estimated simply by evaluating Equation 9.3. If data from other locations are known, these can in an identical way be used to estimate the heating degree-day proxy of the hot water consumption. Finally, a constant hot water consumption across space and time is assumed, which means that $\frac{L^{\text{Hot Water}}}{\alpha}$ is fixed to the value for Stockholm for each grid location, x.

Techno-economic standpoint of heat generation

The hourly accumulated cost, $X^{\text{TOT}}_{x,\theta}$, for a technology, θ, and grid location, x, depends linearly on the heat load factor, μ_x, as:

$$
X^{\text{TOT}}_{x,\theta} = X^{\text{CAP}}_{\theta} + \mu_x \cdot X^{\text{OP}}_{x,\theta}
$$

The capital expense, X^{CAP}_{θ}, is assumed to be proportional to the installed capacity, κ_θ, as shown in Equation 9.6. The per MW equipment, installation and maintenance expenses are denoted as x^{κ}_{θ}, x^{I}_{θ} and x^{FM}_{θ}, respectively. The capital cost is annuitised by the technology life time and a discount rate of 4%.

$$
X^{\text{CAP}}_{\theta} = \left(x^{\text{FM}}_{\theta} + x^{I}_{\theta} + x^{\kappa}_{\theta}\right) \cdot \kappa_\theta \tag{9.6}
$$

The marginal expense, $X^{\text{OP}}_{x,\theta}$, is proportional to the installed capacity, κ_θ as well as the ratio between the fuel price, x^{Fuel}_{θ}, and efficiency, $\text{eff}_{x,\theta}$:

$$X^{\text{OP}}_{\text{x},\theta} = \frac{x^{\text{Fuel}}_{\theta}}{\text{eff}_{\text{x},\theta}} \cdot \kappa_{\theta}$$

The efficiency takes a constant value, η_θ, for technologies different from heat pumps, as:

$$\text{eff}_{\text{x},\theta} = \begin{cases} \text{COP}_{\text{x},\theta}(t) & \text{if} \quad \theta \text{ defines a heat pump} \\ \eta_\theta & \text{otherwise} \end{cases}$$

where t defines the time. All prices and technology properties are given in Table 4.1 in Chapter 4.

Coefficient of performance (COP)

Heat pumps are implemented with a Coefficient Of Performance (COP), which defines the ratio of heat output to the amount of electricity input. COP is strongly temperature dependent, thus, long-term average values are not meaningful. An empirical relationship between the COP and the temperature difference between the heat source and heat sink, $\Delta T = T_{\text{sink}} - T_{\text{source, x}}(t)$, is presented in Equation 9.7 for air and ground based heat pumps, respectively. These are based upon the derivations in [29], updated to include new data from [326]. Furthermore, the COP for air source heat pumps was separated based on whether or not defrosting is required. Defrosting is required when outdoor temperatures fall below 5°C, lowering the COP by around 4%. For air and ground source heat pumps, $T_{\text{source, x}}$ represents the gridded air and soil temperatures, respectively. The ground temperature is estimated as an average of air temperatures over a 20 year time period. As discussed in the main paper, this corresponds to temperatures at a depth of approximately 50 meters below ground, depending on soil type and geographical location [183]. T_{sink} is assumed to be 30°C for air to air heat pumps and 55°C for large area hot water heating [29].

$$\begin{aligned} \text{COP}_{\text{Air driven, x}}(t) &= \begin{cases} 0.0012\Delta T^2 - 0.1702\Delta T + 7.855 & \text{if } T_{\text{air}} \leq 5°\text{C} \\ 0.0019\Delta T^2 - 0.2258\Delta T + 9.073 & \text{if } T_{\text{air}} > 5°\text{C} \end{cases} \\ \text{COP}_{\text{Ground driven, x}}(t) &= 0.0019\Delta T^2 - 0.2544\Delta T + 11.008 \end{aligned} \tag{9.7}$$

During winter periods, when the need for heat is high, COP takes lower values. Oppositely, during summer periods the need for heat is small but the COP increases considerably. Consequently, the yearly averaged COP for air-to-air and

air-to-water heat pumps, $\mathrm{COP}_{\mathrm{ASHP,\,x}}$, is weighted by the heating degree-days for space heating, $\mathrm{HDD}_{\mathrm{x}}^{\mathrm{Space\ Heat}}(t)$, as shown in Equation 9.8. The hot water component makes no difference to the weighting due to the assumption of constant consumption throughout the year. A similar weighting is not necessary for the ground-to-water heat pumps as temperatures at a depth of 50 meters below ground are seasonally independent [183].

$$\mathrm{COP}_{\mathrm{Air\ driven,\,x}} = \frac{1}{\mathrm{HDD}_{\mathrm{x,\Delta}}^{\mathrm{Space\ Heat}}} \sum_{t \in \Delta} \mathrm{HDD}_{\mathrm{x}}^{\mathrm{Space\ Heat}}(t) \cdot \mathrm{COP}_{\mathrm{Air\ driven,\,x}}(t) \tag{9.8}$$

9.2 Additional results

Extended discussions on the original pricing scheme

In this section, the unperturbed pricing scheme and the single technology dominance across Europe are further discussed.

Figure 9.1 shows the screening curves for all technologies that are included in this study. Since the heat pump coefficients of performance fluctuate according to the ambient temperatures, as demonstrated by Equation 9.7 and Figures 9.3-9.5, heat pumps are subject to a range of screening curves. Figures 9.3-9.5 are discussed in detail in Section 9.1. Taking the air-to-water heat pump as an example, it is seen from Figure 9.3 that the coefficients of performance fluctuate between 2.0 and 3.0. As a consequence, air-to-water heat pumps are subject to an upper and lower screening curve that define the cost region, as illustrated in Figure 9.1. Similar arguments can be made for the soil-to-water and air-to-air heat pumps. On the other hand, uniform efficiencies of biomass, oil and gas boilers result in a single screening curve for these technologies. The black shaded region defines the range of heat load factors across Europe. A spatial distribution of the heat load factors is shown in Figure 9.2 and discussed in detail in the next paragraph. From Figure 9.1 it is clear that within the range of the heat load factors, only gas boilers qualify as cost-optimal. This singularity lead to the *balanced* pricing scheme, which is used to enforce a more diverse technology distribution. This is needed in order to illustrate the potential impact of climate change on the heat generating technologies.

Figure 9.2 shows the heat load factors across Europe for the historical period and for the end-of-century periods for each climate projection. Focusing initially on the historical frame, it is clear that the cold oceanic climate increases the heat load factors significantly across the British Isles. The similar is evident for Scandinavia. The Iberian Peninsula is as well dominated by high heat load factors. This is a result of a warm Mediterranean climate, which may seem contradicting. However, the increased temperatures across these regions reduce naturally the need for space heating. As a consequence, the constant hot water consumption takes up a significant share of the total heat demand and in turn increasing the heat load factors.

A detailed investigation of Figure 9.2 reveals that it is difficult to assign any trend to the heat load factors as a function of the degree of climate change. The change in heat load factors results from a combined effect of changes in

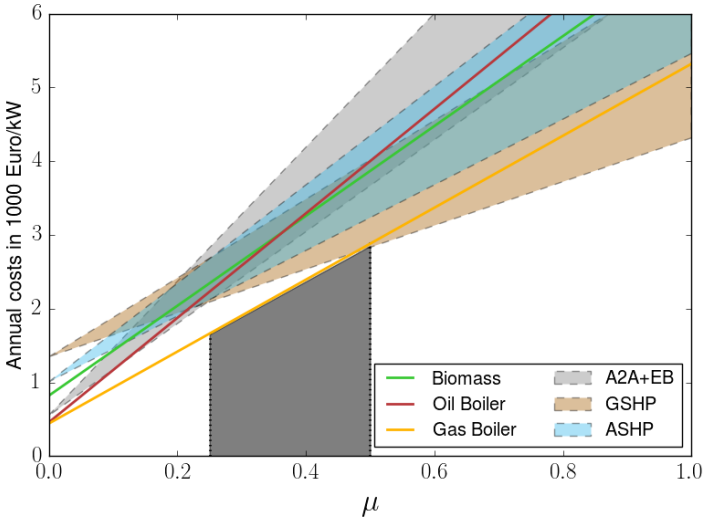

Figure 9.1: Screening curves showing the annual accumulated costs of heating in 1000 Euro/kW as a function of the heat load factor, μ. Technology prices and technology properties are taken from Table 4.1 in Chapter 4. The upper and lower screening curves for air-to-water heat pumps (ASHP) are defined by coefficients of performance equal to 2.0 and 3.0, respectively. The similar for the ground-to-water heat pumps (GSHP) are 2.5 and 4.5. For the hybrid system of air-to-air heat pumps and electricity driven boilers the combined efficiency are 3.0 and 5.0. The region shaded by a black color is constrained between 0.25 and 0.50 and defines the range of the heat load factors across Europe.

the heating degree-days and changes in the design temperatures, as seen from Equation 9.5. The Balkan countries possess almost the same heat load factors, while other parts of Europe are significantly affected by changes in the ambient temperatures. Modest temperature increases at the end-century of the RCP2.6 climate projection lead naturally to modest changes in the heat load factors. The intermediate temperature increase at the end-century of the RCP4.5 climate projection decreases the heat load factors to some extent. This change is mainly observed across the British Isles and Scandinavia. The extreme temperature increase at the end-century of the RCP8.5 climate projection leads to a significant decrease in the heat load factors in some parts of Europe as, e.g., across the British Isles, while other parts as, e.g., the Iberian Peninsula and East Europe stay almost unaffected.

Extended discussions on the heat pump COP

Figures 9.3 - 9.5 show the spatial distributions of the coefficients of performance for the three types of heat pumps in this study. Focusing initially on the air-to-water coefficients of performance in the historical time frame, it is clear that Scandinavia holds the lowest values. Higher ambient temperatures across the Mediterranean result in the highest values. In general, the values range between 2.0 and 2.7. The modest temperature increase at the end-century of the RCP2.6 climate projection does not lead to significant changes in the coefficient of performance. On the other hand, the end-century of the RCP4.5 and RCP8.5 lead to a significant increase in the coefficients of performance. In RCP8.5, the coefficients of performance increase by up to 2.5 in Scandinavia and up to 3.0 in the southern Iberian Peninsula. These changes contribute significantly to the increased distribution of heat pumps across Europe at the end-century of each climate projection. Similar arguments can be made for the ground-to-water and air-to-air heat pumps, as seen in Figures 9.4 and 9.5, respectively.

Comparing the coefficients of performance from the different heat pumps, it is evident that the values for ground-to-water heat pumps are significantly higher compared to air-to-water heat pumps. This is mainly reasoned by the stable ground temperatures, which provide a high coefficient of performance independent of the yearly seasons. The low sink temperature of the air-to-air heat pumps results in the highest coefficient of performance.

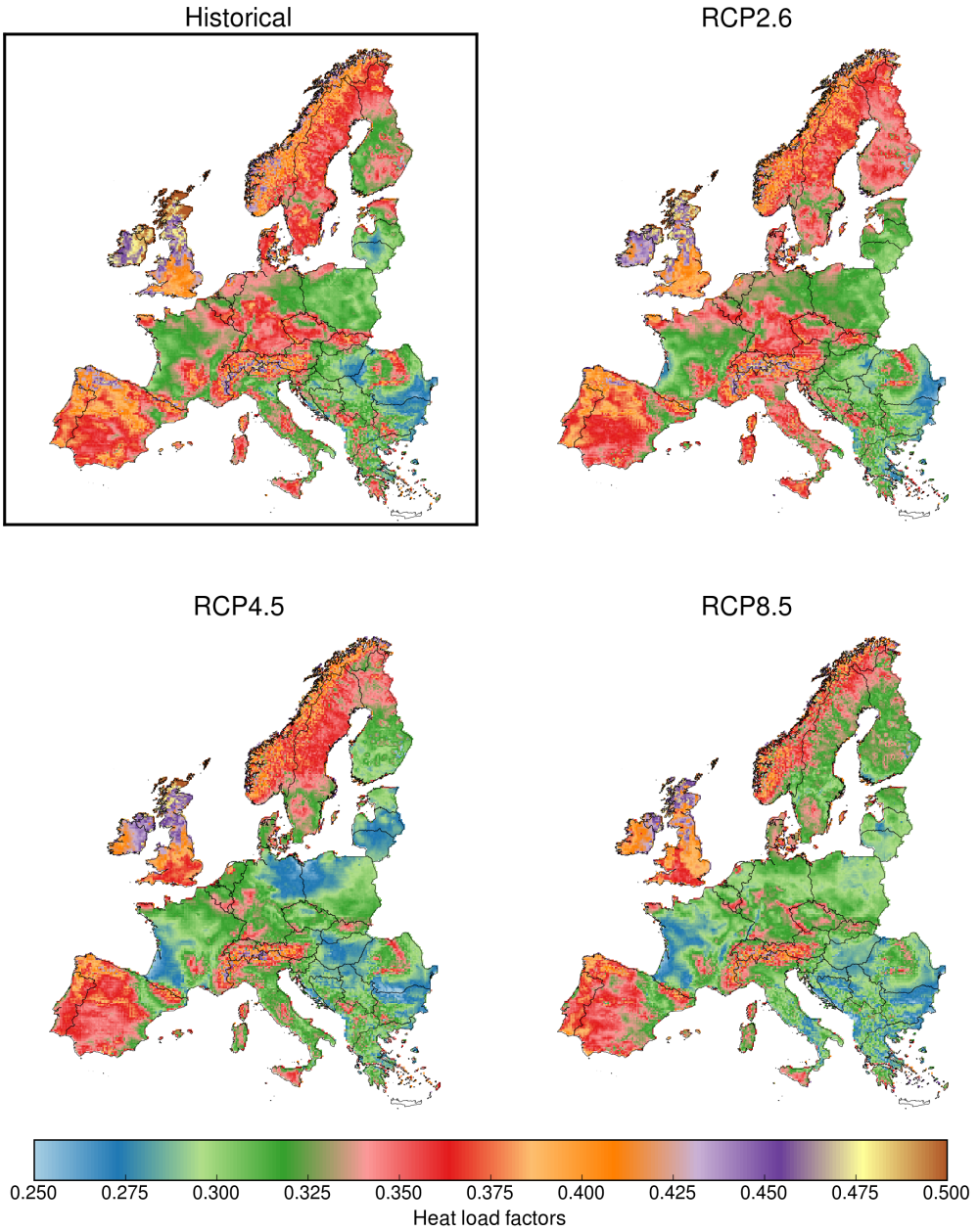

Figure 9.2: Spatial distributions of the heat load factors. The historical period is defined to span the years 1970-1990. RCP2.6, RCP4.5 and RCP8.5 spans a climatic period from 2080-2100. The figures are based on the ICHEC-EC-EARTH HIRHAM5 climate model.

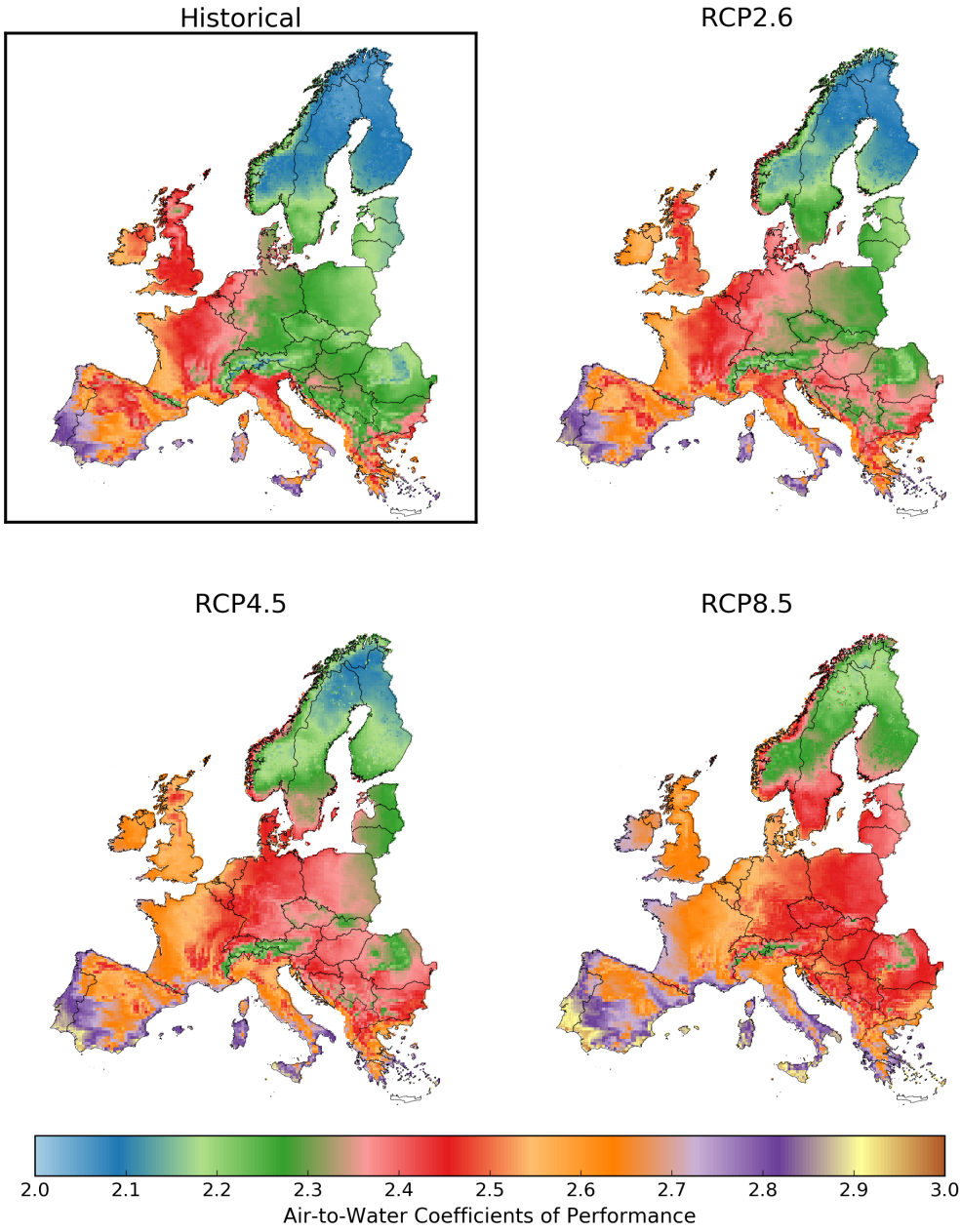

Figure 9.3: Spatial distributions of the coefficients of performance for air-to-water heat pumps with a sink temperature of 55 °C. These are weighted according the annual space heat demand as demonstrated in Equation 9.8. The historical period is defined to span the years 1970-1990. RCP2.6, RCP4.5 and RCP8.5 spans a climatic period from 2080-2100. The figures are based on the ICHEC-EC-EARTH HIRHAM5 climate model.

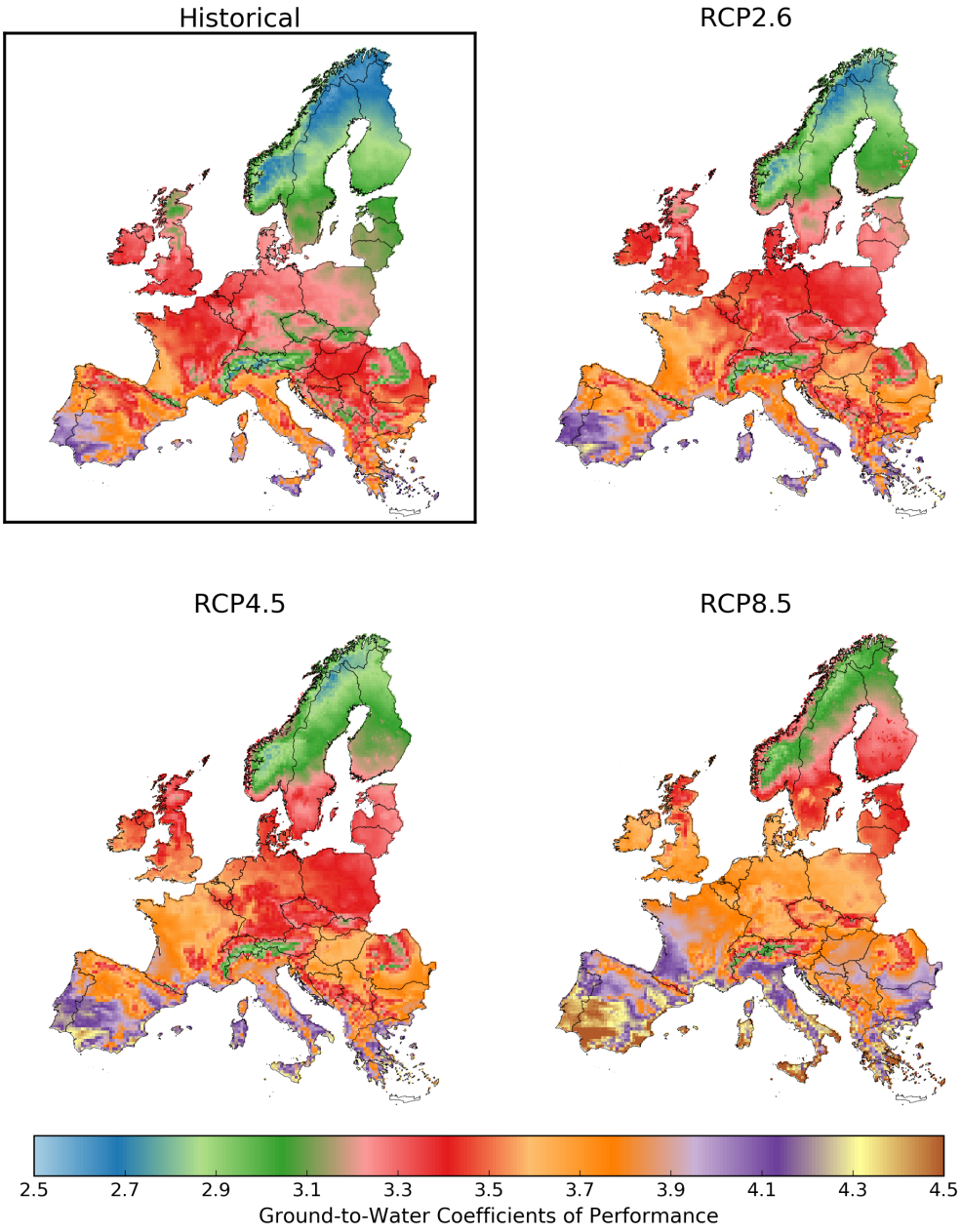

Figure 9.4: Spatial distributions of the coefficients of performance for ground-to-water heat pumps with a sink temperature of 55 °C. The historical period is defined to span the years 1970-1990. RCP2.6, RCP4.5 and RCP8.5 spans a climatic period from 2080-2100. The figures are based on the ICHEC-EC-EARTH HIRHAM5 climate model.

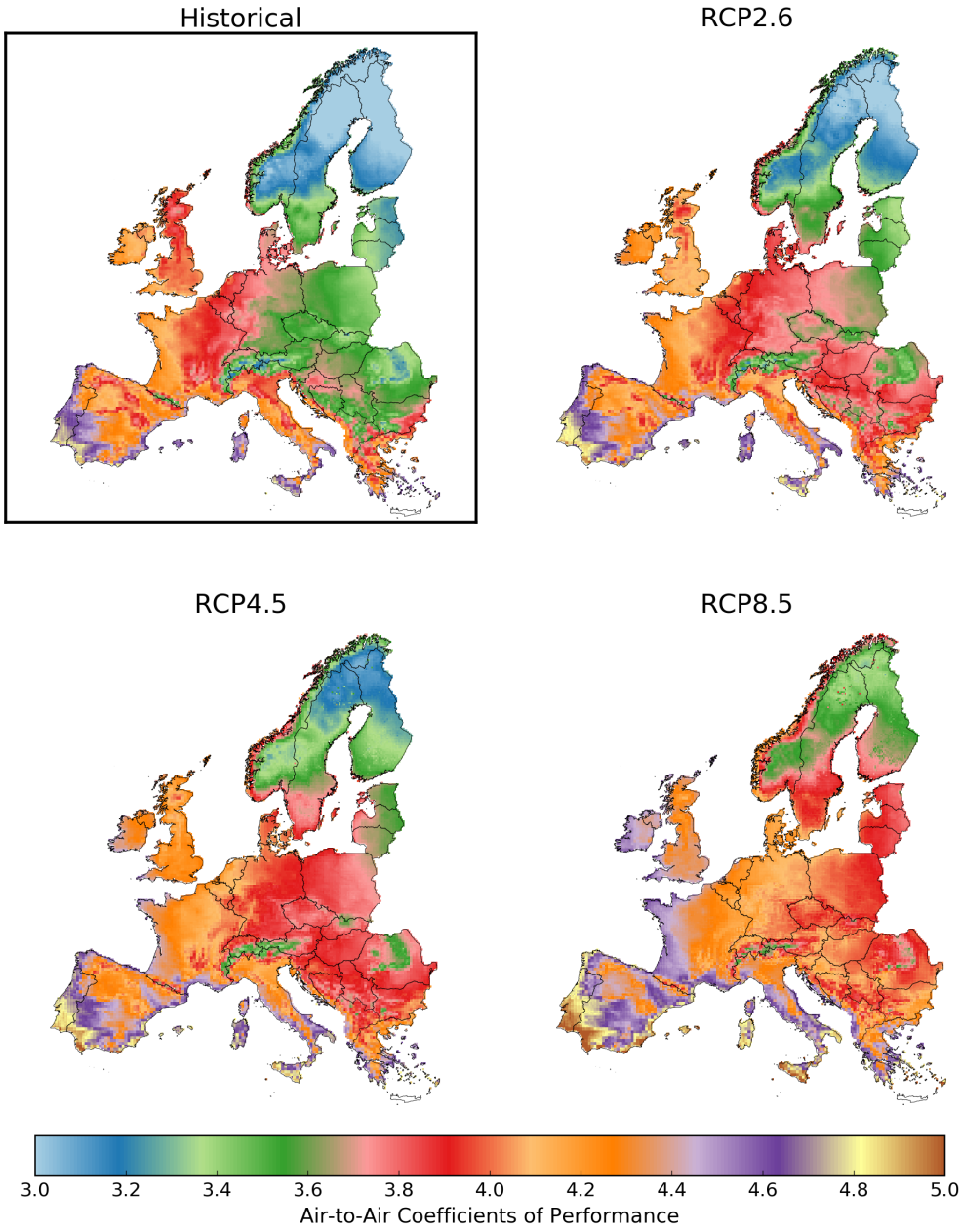

Figure 9.5: Spatial distributions of the coefficients of performance for air-to-air heat pumps with a sink temperature of 30 °C. These are weighted according the annual space heat demand as demonstrated in Equation 9.8. The historical period is defined to span the years 1970-1990. RCP2.6, RCP4.5 and RCP8.5 spans a climatic period from 2080-2100. The figures are based on the ICHEC-EC-EARTH HIRHAM5 climate model.

Subscripts	**Explanatory text**
x	Grid cell
Δ	Time period
θ	Technology
Variables	**Explanatory text**
t	time
L^{Total}	Total residential heat demand
$L^{\text{Space Heat}}$	Space heat demand
$L^{\text{Hot Water}}$	Hot water demand
P^{Total}	Total output of heat
$P^{\text{Space Heat}}$	Output of space heat
$P^{\text{Hot Water}}$	Output of hot water
T_0	Heating threshold temperature
$T_x(t)$	Gridded ambient air temperature
$T_{x,\text{ design}}$	Gridded design temperature
μ_x	Gridded heat load factor
$\text{HDD}_x^{\text{Space}}(t)$	Gridded heating degree-days as a proxy for space heating
DHW	Heating degree-days as a proxy for hot water demand
$\text{HDD}_{x,\Delta}$	Gridded heating degree-days as a proxy for the combined space heating and hot water over a time period
$\text{X}_\theta^{\text{CAP}}$	Fixed capacity expense
$\text{X}_\theta^{\text{FM}}$	Fixed yearly maintenance expense and auxiliary electricity use
$\text{X}_{x,\theta}^{\text{OP}}$	Gridded operational expense
$\text{X}_{x,\theta}^{\text{TOT}}$	Gridded yearly accumulated expense
$\text{X}_\theta^{\text{I}}$	Fixed installation expense
$\text{X}_\theta^{\text{Fuel}}$	Fixed fuel price
$\eta_{x,\theta}$	Technology efficiency
κ_θ	Installed technology capacity
$\text{COP}_{x,\theta}$	Gridded coefficient of performance
T_{source}	Temperature of hot reservoir
T_{sink}	Temperature to be met by technology

CHAPTER 10

Project contributions

Dissemination of results had a high priority in this project and was conducted in the form of journal and conference articles, data publishing, talks, conference organisation and writing grant proposal. All activities are listed in the sections to come. The project also delivered about 100 TB of high-resolution state-of-the-art climate change affected weather data to be used in later research. The data have been acquired from various Earth System Grid Federation data nodes and from personal contact to various meteorological institutes around Europe. The data have been cleaned, structured and made easy accessible on a local server for others to use. This project also leaves behind prepared state-of-the-art energy system related data.

The core contribution of this project consist of six first-authored articles. Only four are presented in this dissertation. The papers: "*Grid integration of solar PV for multi-apartment buildings*" and "*Impact of climate change on the backup infrastructure of highly renewable electricity systems*" are excluded due to missing relevance. The remaining articles are presented according to a project storyline. In the following pages, I list the main outcomes of my academic activities in this project.

Journal Articles

- Kozarcanin, Smail; Liu, Hailiang; Andresen, Gorm Bruun (2019). *21st Century Climate Change Impacts on Key Properties of a Large-Scale Renewable-Based Electricity System*. Joule, 3(4), 992-1005.
- Kozarcanin, Smail; Andresen, Gorm Bruun; Staffell, Iain (2019). *Estimating country-specific space heating threshold temperatures from national gas and electricity consumption data*. Energy and Buildings, 199, 368-380.
- Kozarcanin, Smail; Hanna, Richard; Gross, Robert; Staffell, Iain; Andresen, Gorm Bruun. *Impact of climate change on the cost optimal mix of decentralized heating in Europe*. arXiv:1907.04067. Submitted to Energy Policy.
- Kozarcanin, Smail; Andresen, Gorm Bruun. *Techno-Economic Benefits of a Fully Coupled European Electricity and Heating System in a 21st Century Climate Change*. In preparation
- Kozarcanin, Smail; Andresen, Gorm Bruun; Greiner, Martin (2018). *Impact of climate change on the backup infrastructure of highly renewable electricity systems*, J. sustain. dev. energy water environ. syst., 6(4), 710-724
- Kozarcanin, Smail; Andresen, Gorm Bruun (2018). *Grid integration of solar PV for multi-apartment buildings*. International Journal of Sustainable Energy Planning and Management, 17, 3-14.

Data Publishing

- Kozarcanin, Smail; Liu, Hailiang; Andresen, Gorm Bruun (2019). *Supplementary Data: 21st Century climate change impacts on key properties of a large-scale renewable-based electricity system*. Mendeley Data, v1

Conference Articles

- Kozarcanin, Smail; Andresen, Gorm Bruun; Greiner, Martin (2017). *Impact of climate change on the backup infrastructure of highly renewable electricity systems*. 12th Conference on Sustainable Development of Energy, Water and Environment Systems: 12th SDEWES. International Centre for Sustainable Development of Energy, Water and Environment Systems, 2017. SDEWES2017-0364.

Conference and Workshop Talks

- The 9th workshop of the Open Energy Modelling Initiative (OpenMod), Aarhus Denmark (2019) **(co-organiser)**
- 3rd World Summit on Climate Change and Global Warming, Prague Czech Republic (2019)
- Imperial College Centre for Energy Policy and Technology book club, London UK (2019)
- 5th World Conference on Climate Change, London UK (2018)
- Integrated Assessment Workshop IAM, Clermont Ferrand France (2018)
- The 8th workshop of the Open Energy Modelling Initiative (OpenMod), Zürich Switzerland (2018)
- Energy Futures Lab, London UK (2018)
- The 13th Conference on Sustainable Development of Energy, Water and Environment Systems, Dubrovnik Croatia (2017)
- Wind Energy conference, Herning Denmark (2017)
- Open Power System Data workshop (OPSD), Berlin Germany (2017)
- Institute for Geoscience - Aarhus University, Aarhus Denmark (2017)
- The 5th workshop of the Open Energy Modelling Initiative (OpenMod), Milano Italy (2016)

- Wind and solar will still work in a climate-change ravaged Europe.
  NewScientist (2019)
- Even in a warmer Europe, wind and solar could still keep the lights on.
  The Verge (2019)
- Good news! Europe's electric grid will still work even as the world crumbles.
  EurekAlert! The Global Source for Science news (2019)
- Europe's Renewable Electricity Would Survive Catastrophic Climate Change.
  INVERSE (2019)
- Vil klimaændringer også ændre forudsætningerne for vind- og solenergi?
  Ingeniøren (2019)
- Europe's power grid will survive climate change. The US, not so much.
  Cosmos - The Science of Everything (2019)
- Europe's Weather-dependent Electricity Systems Will Withstand Climate Change.
  Interesting Engineering (2019)
- Renewable energy systems will still work in a changing climate.
  Earth.com news (2019)
- Europes electricity grid will work as intended as the world heats up.
  Power Technology (2019)
- Europa mantendrá su red eléctrica a salvo del calentamiento global.
  Cienciaplus - Europa Press (2019)
- Gode nyheder: Elnettet vil fungere, selv om verden går under.
  AU VIA RITZAU (2019)
- Impacts of climate change on the electricity system design decisions for the 21st Century.
  Energy Futures Lab - Imperial College London (2018)
- Climate change and the future European electricity supply.
  Profile 2018, Department of Engineering - Aarhus University (2018)

Bibliography

[1] Benjamin D Santer, Céline JW Bonfils, Qiang Fu, John C Fyfe, Gabriele C Hegerl, Carl Mears, Jeffrey F Painter, Stephen Po-Chedley, Frank J Wentz, Mark D Zelinka, et al. Celebrating the anniversary of three key events in climate change science. *Nature Climate Change*, 9(3):180, 2019.

[2] Joeri Rogelj, Gunnar Luderer, Robert C Pietzcker, Elmar Kriegler, Michiel Schaeffer, Volker Krey, and Keywan Riahi. Energy system transformations for limiting end-of-century warming to below 1.5 °C. *Nature Climate Change*, 5(6):519, 2015.

[3] David Kennedy, Mark Bainbridge, Alice Barrs, Jenny Byars, and Liz Cassidy. Building a low-carbon economy - the UK's contribution to tackling climate change. *The Stationery Office, London*, 2008.

[4] James H Williams, Andrew DeBenedictis, Rebecca Ghanadan, Amber Mahone, Jack Moore, William R Morrow, Snuller Price, and Margaret S Torn. The technology path to deep greenhouse gas emissions cuts by 2050: The pivotal role of electricity. *science*, 335(6064):53–59, 2012.

[5] Luc Van Nuffel, J Gorenstein Dedecca, T Smit, and K Rademaekers. Sector coupling: How can it be enhanced in the EU to foster grid stability and decarbonise. *Trinomics BV Retrieved from http://www. europarl. europa. eu*, 2018.

[6] International Energy Agency, IEA. CO_2-emissions from fuel combustion, 2018.

[7] Our World in Data. Natural Disasters, 2017.
Available at: `https://ourworldindata.org/natural-disasters`
Last accessed: 27/09/19.

[8] United Nations Framework Convention on Climate Change, UNFCCC. Adoption of the Paris Agreement. Report No. FCCC/CP/2015/L.9/Rev.1,

2015.
Available at: http://unfccc.int/resource/docs/2015/cop21/eng/l09r01.pdf
Last accessed: 01/08/19.

[9] European Commision, EC. A Roadmap for moving to a competitive low carbon economy in 2050, 2011.

[10] European Commision, EC. A Clean Planet for all - A European strategic long-term vision for a prosperous, modern, competitive and climate neutral economy. *Brussels*, 28:2018, 2018.

[11] Climate Action Tracker, CAT. Pledged action leads to 2.9 °C - time to boost national climate action, 2019.

[12] Adrian E Raftery, Alec Zimmer, Dargan MW Frierson, Richard Startz, and Peiran Liu. Less than 2 °C warming by 2100 unlikely. *Nature Climate Change*, 7(9):637, 2017.

[13] Robert C Schmidt. A balanced-efforts approach for climate cooperation. *Nature Climate Change*, 5(1):10, 2014.

[14] James P Ordner. Community action and climate change. *Nature Climate Change*, 7(3):161, 2017.

[15] Richard H Moss, Jae A Edmonds, Kathy A Hibbard, Martin R Manning, Steven K Rose, Detlef P Vuuren, Timothy R Carter, Seita Emori, Mikiko Kainuma, Tom Kram, et al. The next generation of scenarios for climate change research and assessment. *Nature*, 463(7282):747, 2010.

[16] Intergovernmental Panel on Climate Change, IPCC. About the IPCC, 1988.
Available at: https://www.ipcc.ch/about/
Last accessed: 02/09/19.

[17] Rajendra K Pachauri, Myles R Allen, Vicente R Barros, John Broome, Wolfgang Cramer, Renate Christ, John A Church, Leon Clarke, Qin Dahe, Purnamita Dasgupta, et al. *Climate change 2014: synthesis report. Contribution of Working Groups I, II and III to the fifth assessment report of the Intergovernmental Panel on Climate Change*. Ipcc, 2014.

[18] Dave Jones, A Sakhel, M Buck, and P Graichen. The European Power Sector in 2018. *Sandbag/Agora*, 2018.

[19] Energy Information Administration, US EIA. Electricity data browser, 1977.
Available at: https://www.eia.gov/electricity/data/browser/
Last accessed: 24/09/19.

[20] Chinese Energy Portal. Tracking China's transition to sustainable energy, 2017.
Available at: https://chinaenergyportal.org/en/2017-electricity-other-energy-statistics-update-of-june-2018/
Last accessed: 25/09/19.

[21] Falko Ueckerdt, Robert Pietzcker, Yvonne Scholz, Daniel Stetter, Anastasis Giannousakis, and Gunnar Luderer. Decarbonizing global power supply under region-specific consideration of challenges and options of integrating variable renewables in the remind model. *Energy Economics*, 64: 665–684, 2017.

[22] Felix Creutzig, Peter Agoston, Jan Christoph Goldschmidt, Gunnar Luderer, Gregory Nemet, and Robert C Pietzcker. The underestimated potential of solar energy to mitigate climate change. *Nature Energy*, 2(9):17140, 2017.

[23] Seán Collins, Deger Saygin, JP Deane, Asami Miketa, Laura Gutierrez, Brian Ó Gallachóir, and Dolf Gielen. Planning the european power sector transformation: The remap modelling framework and its insights. *Energy strategy reviews*, 22:147–165, 2018.

[24] Clemens Gerbaulet, Christian von Hirschhausen, Claudia Kemfert, Casimir Lorenz, and P-Y Oei. European electricity sector decarbonization under different levels of foresight. *Renewable energy*, 141:973–987, 2019.

[25] Marta Victoria, Kun Zhu, Tom Brown, Gorm B Andresen, and Martin Greiner. The role of storage technologies throughout the decarbonisation of the sector-coupled european energy system. *arXiv preprint arXiv:1906.06936*, 2019.

[26] Oliver Schmidt, Adam Hawkes, Ajay Gambhir, and Iain Staffell. The future cost of electrical energy storage based on experience rates. *Nature Energy*, 2(8):17110, 2017.

[27] Francisco Díaz-González, Eduard Bullich-Massagué, Cristina Vitale, Marina Gil-Sánchez, Mònica Aragüés-Peñalba, and Francesc Girbau-Llistuella. Services of energy storage technologies in renewable-based

power systems. In *Ibero-American Congress on Information Management and Big Data*, pages 53–64. Springer, 2018.

[28] Iain Staffell and Stefan Pfenninger. The increasing impact of weather on electricity supply and demand. *Energy*, 145:65–78, 2018.

[29] Iain Staffell, Dan Brett, Nigel Brandon, and Adam Hawkes. A review of domestic heat pumps. *Energy & Environmental Science*, 5(11):9291–9306, 2012.

[30] Committee on Climate Change. Reducing UK emissions - 2018 Progress Report to Parliament, 2018.

[31] Tobias Fleiter, J Steinbach, M Ragwitz, J Dengler, B Köhler, F Reitze, F Tuille, M Hartner, L Kranzl, S Forthuber, et al. Mapping and analyses of the current and future (2020-2030) heating/cooling fuel deployment (fossil/renewables) - WP2, 2016.

[32] Richard Hanna, Robert Gross, and Bryony Parrish. Best practice in heat decarbonisation policy: A review of the international experience of policies to promote the uptake of low-carbon heat supply. UKERC Technology and Policy Assessment working paper. UK Energy Research Centre: London, UK, 2016.

[33] Jacek Zimny, Piotr Michalak, and Krzysztof Szczotka. Polish heat pump market between 2000 and 2013: European background, current state and development prospects. *Renewable and Sustainable Energy Reviews*, 48: 791–812, 2015.

[34] EHPA. European Heat Pump Market and Statistics Report. European Heat Pump Association, 2015.

[35] The Wind Power. Wind Energy Market Intelligence, 2005.
Available at: `http://www.thewindpower.net`
Last accessed: 05/09/19.

[36] Gorm B Andresen, Anders A Søndergaard, and Martin Greiner. Validation of Danish wind time series from a new global renewable energy atlas for energy system analysis. *Energy*, 93:1074–1088, 2015.

[37] Iain Staffell and Stefan Pfenninger. Using bias-corrected reanalysis to simulate current and future wind power output. *Energy*, 114:1224–1239, 2016.

[38] Marta Victoria Perez and Gorm Bruun Andresen. Using validated reanalysis data to investigate the impact of the pv system configurations at high penetration levels in european countries. *Progress in Photovoltaics: Research and Applications*, pages 1–17, 2019.

[39] Stefan Pfenninger and Iain Staffell. Long-term patterns of European PV output using 30 years of validated hourly reanalysis and satellite data. *Energy*, 114:1251–1265, 2016.

[40] European Network of Transmission System Operators for electricity, ENTSO-e. ENTSO-e at a glance, 2008.
Available at: `https://www.entsoe.eu/publications/general-publications/at-a-glance/`
Last accessed: 05/09/19].

[41] Tobias Fleiter, Rainer Elsland, Matthias Rehfeldt, Jan Steibach, Ulrich Reiter, Giacomo Catenazzi, Martin Jakob, Cathelijne Rutten, Robert Harmsen, Florian Dittman, Philippe Riviére, and Pascal Stabat. Heat Roadmap Europe - Profile of heating and cooling demand in 2015, 2017.

[42] Peter Kolp and Keywan Riahi. RCP Web-database, 2009.
Available at: `http://www.iiasa.ac.at/web-apps/tnt/RcpDb`
Last accessed: 19/10/19.

[43] Ole Bøssing Christensen, Martin Drews, Jens Hesselbjerg Christensen, Klaus Dethloff, Klaus Ketelsen, Ines Hebestadt, and Anette Rinke. The HIRHAM Regional Climate Model. Version 5 (beta). *DTU Library, Technical Information Center of Denmark*, 2007.

[44] W Hazeleger, X Wang, C Severijns, S Ştefănescu, R Bintanja, A Sterl, Klaus Wyser, T Semmler, S Yang, B Van den Hurk, et al. EC-Earth V2.2: description and validation of a new seamless earth system prediction model. *Climate dynamics*, 39(11):2611–2629, 2012.

[45] Consortium for International Earth Science Information Network, CIESIN. hematic Guide to Integrated Assessment Modeling of Climate Change, 1995.
Available at: `http://sedac.ciesin.org/mva/iamcc.tg/TGHP.html`
Last accessed: 02/09/19.

[46] Detlef P Vuuren, Elke Stehfest, Michel GJ Elzen, Tom Kram, Jasper Vliet, Sebastiaan Deetman, Morna Isaac, Kees Klein Goldewijk, Andries Hof,

Angelica Mendoza Beltran, et al. RCP2. 6: exploring the possibility to keep global mean temperature increase below 2 C. *Climatic Change*, 109 (1-2):95–116, 2011.

[47] Detlef P Vuuren, MGJ Den Elzen, PL Lucas, B Eickhout, BJ Strengers, BJ van Ruijven, MM Berk, B de Vries, MM Hoogwijk, M Meinshausen, et al. Stabilising greenhouse gas concentrations at low levels: an assessment of options and costs, 2006.

[48] Detlef P Vuuren, B Eickhout, PL Lucas, and MGJ Den Elzen. Long-term multi-gas scenarios to stabilise radiative forcingexploring costs and benefits within an integrated assessment framework. *The energy journal*, pages 201–233, 2006.

[49] Allison M Thomson, Katherine V Calvin, Steven J Smith, G Page Kyle, April Volke, Pralit Patel, Sabrina Delgado-Arias, Ben Bond-Lamberty, Marshall A Wise, Leon E Clarke, et al. RCP4.5: A pathway for stabilization of radiative forcing by 2100. *Climatic change*, 109(1-2):77, 2011.

[50] Steven J Smith and TML Wigley. Multi-gas forcing stabilization with Minicam. *The Energy Journal*, pages 373–391, 2006.

[51] Leon Clarke, James Edmonds, Henry Jacoby, Hugh Pitcher, John Reilly, and Richard Richels. Scenarios of greenhouse gas emissions and atmospheric concentrations, 2007.

[52] Marshall Wise, Katherine Calvin, Allison Thomson, Leon Clarke, Benjamin Bond-Lamberty, Ronald Sands, Steven J Smith, Anthony Janetos, and James Edmonds. Implications of limiting CO_2-concentrations for land use and energy. *Science*, 324(5931):1183–1186, 2009.

[53] Toshihiko Masui, Kenichi Matsumoto, Yasuaki Hijioka, Tsuguki Kinoshita, Toru Nozawa, Sawako Ishiwatari, Etsushi Kato, PR Shukla, Yoshiki Yamagata, and Mikiko Kainuma. An emission pathway for stabilization at 6 Wm^{-2} radiative forcing. *Climatic change*, 109(1-2):59, 2011.

[54] Yasuaki Hijioka, Yuzuru Matsuoka, Hiromi Nishimoto, Toshihiko Masui, and Mikiko KAINUMA. Global GHG emission scenarios under GHG concentration stabilization targets. *Journal of global environment engineering*, 13: 97–108, 2008.

[55] Junichi Fujino, Rajesh Nair, Mikiko Kainuma, Toshihiko Masui, and Yuzuru Matsuoka. Multi-gas mitigation analysis on stabilization scenarios using AIM global model. *The Energy Journal*, pages 343–353, 2006.

[56] Keywan Riahi, Shilpa Rao, Volker Krey, Cheolhung Cho, Vadim Chirkov, Guenther Fischer, Georg Kindermann, Nebojsa Nakicenovic, and Peter Rafaj. RCP 8.5 - A scenario of comparatively high greenhouse gas emissions. *Climatic Change*, 109(1-2):33, 2011.

[57] Shilpa Rao and Keywan Riahi. The role of Non-CO_3 greenhouse gases in climate change mitigation: Long-term scenarios for the 21st Century. *The Energy Journal*, pages 177–200, 2006.

[58] World Climate Research Programme, WCRP. About the WCRP, 1980.
Available at: `https://www.wcrp-climate.org/`
Last accessed: 02/09/19.

[59] International Geosphere-Biosphere Programme, IGBP. About IGBP, 2016.
Available at: `http://www.igbp.net/`
Last accessed: 19/10/19.

[60] Analysis, Integration and Modeling of the Earth System, AIMES. About AIMES, 2016.
Available at: `https://aimesproject.org/`
Last accessed: 19/10/19.

[61] Karl E Taylor, Ronald J Stouffer, and Gerald A Meehl. An overview of CMIP5 and the experiment design. *Bulletin of the American Meteorological Society*, 93(4):485–498, 2012.

[62] Irish Centre for High-End Computing, ICHEC. About ICHEC, 2005.
Available at: `https://www.ichec.ie/`
Last accessed: 03/09/19.

[63] WJ Collins, Nicolas Bellouin, M Doutriaux-Boucher, N Gedney, P Halloran, T Hinton, J Hughes, CD Jones, M Joshi, S Liddicoat, et al. Development and evaluation of an Earth-System model-HadGEM2. *Geoscientific Model Development*, 4(4):1051, 2011.

[64] Met Office. National Meteorological Service for the UK, 1854.
Available at: `https://www.metoffice.gov.uk/`
Last accessed: 03/09/19.

[65] Marco A Giorgetta, Johann Jungclaus, Christian H Reick, Stephanie Legutke, Jürgen Bader, Michael Böttinger, Victor Brovkin, Traute Crueger, Monika Esch, Kerstin Fieg, et al. Climate and carbon cycle changes from

1850 to 2100 in MPI-ESM simulations for the Coupled Model Intercomparison Project phase 5. *Journal of Advances in Modeling Earth Systems*, 5(3): 572–597, 2013.

[66] Institut Pierre Simon Laplace, IPSL. Earth System documentation - IPSL-CM5A-MR, 1991.
Available at: `https://view.es-doc.org/?renderMethod=id&project=CMIP5&id=4b29d25e-2968-11e0-8517-00163e9152a5`
Last accessed: 03/09/19.

[67] Institut Pierre Simon Laplace, IPSL. About IPSL, 1991.
Available at: `https://www.ipsl.fr/en/`
Last accessed: 03/09/19.

[68] CERFACS-CNRM-CM5. Model description, 2014.
Available at: `https://portal.enes.org/models/earthsystem-models/cnrm-cerfacs/cnrm-cm5`
Last accessed: 03/09/19.

[69] Filippo Giorgi, Colin Jones, Ghassem R Asrar, et al. Addressing climate information needs at the regional level: The CORDEX framework. *World Meteorological Organization (WMO) Bulletin*, 58(3):175, 2009.

[70] Sven Kotlarski, Klaus Keuler, Ole Bossing Christensen, Augustin Colette, Michel Déqué, Andreas Gobiet, Klaus Goergen, Daniela Jacob, Daniel Lüthi, Erik van Meijgaard, et al. Regional climate modeling on European scales: a joint standard evaluation of the EURO-CORDEX RCM ensemble. *Geoscientific Model Development*, 7(4):1297–1333, 2014.

[71] Sylwia Trzaska and Emilie Schnarr. A review of downscaling methods for climate change projections. *United States Agency for International Development by Tetra Tech ARD*, pages 1–42, 2014.

[72] Daniela Jacob, Juliane Petersen, Bastian Eggert, Antoinette Alias, Ole Bøssing Christensen, Laurens M Bouwer, Alain Braun, Augustin Colette, Michel Déqué, Goran Georgievski, et al. EURO-CORDEX: New high-resolution climate change projections for European impact research. *Regional environmental change*, 14(2):563–578, 2014.

[73] Patrick Samuelsson, Colin G Jones, Ulrika Willén, Anders Ullerstig, Stefan Gollvik, ULF Hansson, Christer Jansson, Erik Kjellström, Grigory Nikulin, and Klaus Wyser. The Rossby Centre Regional Climate model RCA3: Model description and performance. *Tellus A*, 63(1):4–23, 2011.

[74] Patrick Samuelsson, Stefan Gollvik, Marco Kupiainen, Ekaterina Kourzeneva, and Willem Jan van de Berg. *The surface processes of the Rossby Centre regional atmospheric climate model (RCA4)*. SMHI, 2015.

[75] Geert Lenderink and Geert Lenderink. *Simulation of present-day climate in RACMO2: First results and model developments*. Koninklijk Nederlands Meteorologisch Instituut, 2003.

[76] Julien Cattiaux, Hervé Douville, and Yannick Peings. European temperatures in cmip5: origins of present-day biases and future uncertainties. *Climate dynamics*, 41(11-12):2889–2907, 2013.

[77] Else JM Van Den Besselaar, Albert MG Klein Tank, Gerard Van Der Schrier, Mariama S Abass, Omar Baddour, Aryan FV Van Engelen, Andrea Freire, Peer Hechler, Bayu Imbang Laksono, Rudmer Jilderda, et al. International climate assessment & dataset: Climate services across borders. *Bulletin of the American Meteorological Society*, 96(1):16–21, 2015.

[78] Chiyuan Miao, Qingyun Duan, Qiaohong Sun, Yong Huang, Dongxian Kong, Tiantian Yang, Aizhong Ye, Zhenhua Di, and Wei Gong. Assessment of CMIP5 climate models and projected temperature changes over Northern Eurasia. *Environmental Research Letters*, 9(5):055007, 2014.

[79] Gerard A Meehl, Thomas F Stocker, William D Collins, Pierre Friedlingstein, T Gaye, Jonathan M Gregory, Akio Kitoh, Reto Knutti, James M Murphy, Akira Noda, et al. Global climate projections. *Cambridge, UK, Cambridge University Press*, 2007.

[80] Gunnar Myhre, Drew Shindell, François-Marie Bréon, William Collins, Jan Fuglestvedt, Jianping Huang, Dorothy Koch, Jean-Francois Lamarque, David Lee, Blanca Mendoza, et al. Anthropogenic and natural radiative forcing. *Climate change*, 423:658–740, 2013.

[81] James Hansen, Makiko Sato, Reto Ruedy, Ken Lo, David W Lea, and Martin Medina-Elizade. Global temperature change. *Proceedings of the National Academy of Sciences*, 103(39):14288–14293, 2006.

[82] Juan-Carlos Ciscar and Paul Dowling. Integrated assessment of climate impacts and adaptation in the Energy sector. *Energy Economics*, 46:531–538, 2014.

[83] Paul Dowling. The impact of climate change on the European energy system. *Energy Policy*, 60:406–417, 2013.

[84] Karoliina Pilli-Sihvola, Piia Aatola, Markku Ollikainen, and Heikki Tuomenvirta. Climate change and electricity consumption – Witnessing increasing or decreasing use and costs? *Energy Policy*, 38(5):2409–2419, 2010.

[85] G Totschnig, R Hirner, A Müller, L Kranzl, M Hummel, H-P Nachtnebel, P Stanzel, I Schicker, and H Formayer. Climate change impact and resilience in the electricity sector: The example of Austria and Germany. *Energy Policy*, 103:238–248, 2017.

[86] Leonie Wenz, Anders Levermann, and Maximilian Auffhammer. North-south polarization of European electricity consumption under future warming. *Proceedings of the National Academy of Sciences*, page 201704339, 2017.

[87] Pernille Seljom, Eva Rosenberg, Audun Fidje, Jan Erik Haugen, Michaela Meir, John Rekstad, and Thore Jarlset. Modelling the effects of climate change on the energy system – a case study of Norway. *Energy Policy*, 39 (11):7310–7321, 2011.

[88] Kirsti Jylhä, Juha Jokisalo, Kimmo Ruosteenoja, Karoliina Pilli-Sihvola, Targo Kalamees, Teija Seitola, Hanna M Mäkelä, Reijo Hyvönen, Mikko Laapas, and Achim Drebs. Energy demand for the heating and cooling of residential houses in Finland in a changing climate. *Energy and Buildings*, 99:104–116, 2015.

[89] Mojca Dolinar, Boris Vidrih, Lučka Kajfež-Bogataj, and Sašo Medved. Predicted changes in energy demands for heating and cooling due to climate change. *Physics and Chemistry of the Earth, Parts A/B/C*, 35(1):100–106, 2010.

[90] Tania Berger, Christoph Amann, Herbert Formayer, Azra Korjenic, Bernhard Pospischal, Christoph Neururer, and Roman Smutny. Impacts of climate change upon cooling and heating energy demand of office buildings in Vienna, Austria. *Energy and buildings*, 80:517–530, 2014.

[91] M Christenson, H Manz, and D Gyalistras. Climate warming impact on degree-days and building energy demand in Switzerland. *Energy Conversion and Management*, 47(6):671–686, 2006.

[92] Jonathan Spinoni, Jürgen V Vogt, Paulo Barbosa, Alessandro Dosio, Niall McCormick, Andrea Bigano, and Hans-Martin Füssel. Changes of heating and cooling degree-days in europe from 1981 to 2100. *International Journal of Climatology*, 38:e191–e208, 2018.

[93] Isabelle Tobin, Robert Vautard, Irena Balog, François-Marie Bréon, Sonia Jerez, Paolo Michele Ruti, Françoise Thais, Mathieu Vrac, and Pascal Yiou. Assessing climate change impacts on European wind energy from ENSEMBLES high-resolution climate projections. *Climatic Change*, 128(1-2): 99–112, 2015.

[94] Idar Barstad, Asgeir Sorteberg, and Michel dos-Santos Mesquita. Present and future offshore wind power potential in northern Europe based on downscaled global climate runs with adjusted SST and sea ice cover. *Renewable Energy*, 44:398–405, 2012.

[95] Isabelle Tobin, Sonia Jerez, Robert Vautard, Françoise Thais, Erik Van Meijgaard, Andreas Prein, Michel Déqué, Sven Kotlarski, Cathrine Fox Maule, Grigory Nikulin, et al. Climate change impacts on the power generation potential of a European mid-century wind farms scenario. *Environmental Research Letters*, 11(3):034013, 2016.

[96] Lynsey McColl, Erika J Palin, Hazel E Thornton, David MH Sexton, Richard Betts, and Ken Mylne. Assessing the potential impact of climate change on the UKs electricity network. *Climatic Change*, 115(3-4):821–835, 2012.

[97] Hagen Koch, Stefan Vögele, Fred F Hattermann, and Shaochun Huang. The impact of climate change and variability on the generation of electrical power. *Meteorologische Zeitschrift*, 24:173–188, 2015.

[98] Markus Schlott, Alexander Kies, Tom Brown, Stefan Schramm, and Martin Greiner. The Impact of Climate Change on a Cost-Optimal Highly Renewable European Electricity Network. *Applied Energy*, 230:1645–1659, 2018.

[99] A Bloom, V Kotroni, and K Lagouvardos. Climate change impact of wind energy availability in the Eastern Mediterranean using the regional climate model PRECIS. *Natural Hazards and Earth System Sciences*, 8(6): 1249–1257, 2008.

[100] Juliane Weber, Jan Wohland, Mark Reyers, Julia Moemken, Charlotte Hoppe, Joaquim G Pinto, and Dirk Witthaut. Impact of climate change on backup energy and storage needs in wind-dominated power systems in europe. *PloS one*, 13(8):e0201457, 2018.

[101] Jan Wohland, Mark Reyers, Juliane Weber, and Dirk Witthaut. More homogeneous wind conditions under strong climate change decrease the potential for inter-state balancing of electricity in Europe. *Earth System Dynamics*, 8(4):1047, 2017.

[102] Sonia Jerez, Isabelle Tobin, Robert Vautard, Juan Pedro Montávez, Jose María López-Romero, Françoise Thais, Blanka Bartok, Ole Bøssing Christensen, Augustin Colette, Michel Déqué, et al. The impact of climate change on photovoltaic power generation in Europe. *Nature communications*, 6:10014, 2015.

[103] Peter Berrill, Anders Arvesen, Yvonne Scholz, Hans Christian Gils, and Edgar G Hertwich. Environmental impacts of high penetration renewable energy scenarios for Europe. *Environmental Research Letters*, 11(1):014012, 2016.

[104] CF McSweeney, RG Jones, Robert W Lee, and DP Rowell. Selecting cmip5 gcms for downscaling over multiple regions. *Climate Dynamics*, 44(11-12): 3237–3260, 2015.

[105] UNEP. The Emissions Gap Report, 2017.

[106] AF Prein, Andreas Gobiet, Heimo Truhetz, Klaus Keuler, Klaus Goergen, Claas Teichmann, C Fox Maule, E Van Meijgaard, M Déqué, Grigory Nikulin, et al. Precipitation in the EURO-CORDEX 0.11° and 0.44° simulations: high resolution, high benefits? *Climate dynamics*, 46(1-2):383, 2016.

[107] Lauren Paige Seaby, Jens Christian Refsgaard, TO Sonnenborg, Simon Stisen, Jens Hesselbjerg Christensen, and Karsten Høgh Jensen. Assessment of robustness and significance of climate change signals for an ensemble of distribution-based scaled climate projections. *Journal of hydrology*, 486:479–493, 2013.

[108] Dirk Cannon, David Brayshaw, John Methven, and Daniel Drew. Determining the bounds of skilful forecast range for probabilistic prediction of system-wide wind power generation. *Meteorologische Zeitschrift*, 26(3): 239–252, 2017.

[109] Dominik Heide, Lueder Von Bremen, Martin Greiner, Clemens Hoffmann, Markus Speckmann, and Stefan Bofinger. Seasonal optimal mix of wind and solar power in a future, highly renewable Europe. *Renewable Energy*, 35(11):2483–2489, 2010.

[110] Sarah Becker, Bethany A Frew, Gorm B Andresen, Timo Zeyer, Stefan Schramm, Martin Greiner, and Mark Z Jacobson. Features of a fully renewable US electricity system: Optimized mixes of wind and solar PV and transmission grid extensions. *Energy*, 72:443–458, 2014.

[111] Hailiang Liu, Gorm Bruun Andresen, and Martin Greiner. Cost-optimal design of a simplified highly renewable Chinese electricity network. *Energy*, 147:534–546, 2018.

[112] Rolando A Rodriguez, Sarah Becker, Gorm B Andresen, Dominik Heide, and Martin Greiner. Transmission needs across a fully renewable European power system. *Renewable Energy*, 63:467–476, 2014.

[113] Rolando A Rodriguez, Magnus Dahl, Sarah Becker, and Martin Greiner. Localized vs. synchronized exports across a highly renewable pan-European transmission network. *Energy, Sustainability and Society*, 5(1): 21, 2015.

[114] Dominik Heide, Martin Greiner, Lueder Von Bremen, and Clemens Hoffmann. Reduced storage and balancing needs in a fully renewable European power system with excess wind and solar power generation. *Renewable Energy*, 36(9):2515–2523, 2011.

[115] Bethany A Corcoran, Nick Jenkins, and Mark Z Jacobson. Effects of aggregating electric load in the United States. *Energy policy*, 46:399–416, 2012.

[116] Sarah Becker, Rolando A Rodriguez, Gorm B Andresen, Stefan Schramm, and Martin Greiner. Transmission grid extensions during the build-up of a fully renewable pan-European electricity supply. *Energy*, 64:404–418, 2014.

[117] Katrin Schaber, Florian Steinke, and Thomas Hamacher. Transmission grid extensions for the integration of variable renewable energies in Europe: Who benefits where? *Energy Policy*, 43:123–135, 2012.

[118] Hannele Holttinen, Juha Kiviluoma, Ana Estanqueiro, Tobias Aigner, Yih-Huei Wan, and Michael Milligan. Variability of load and net load in case of large scale distributed wind power. Technical report, National Renewable Energy Lab. (NREL), Golden, CO (United States), 2011.

[119] Jon Olauson, Hans Bergström, and Mikael Bergkvist. Restoring the missing high-frequency fluctuations in a wind power model based on reanalysis data. *Renewable Energy*, 96:784–791, 2016.

[120] Seán Collins, Paul Deane, Brian Ó Gallachóir, Stefan Pfenninger, and Iain Staffell. Impacts of inter-annual wind and solar variations on the European power system. *Joule*, 2(10):2076–2090, 2018.

[121] José Luis Moraga, Chloé Le Coq, Machiel Mulder, and Sebastian Schwenen. Gas and the electrification of heating and transport: Scenarios for 2050, 2018.
Available at: `https://www.cerre.eu/publications/gas-and-electrification-heating-transport-scenarios-2050`
Last accessed: 02/09/19.

[122] Friends of the Earth. Delivering on the Paris Climate Agreement – The future of home heating, 2018.
Available at: `https://cdn.friendsoftheearth.uk/sites/default/files/downloads/Future%20of%20Heating_August_2018.pdf`
Last accessed: 02/09/19.

[123] Ofgem's Future Insights Series. Local Energy in a Transforming Energy System, 2017.
Available at: `https://www.ofgem.gov.uk/system/files/docs/2017/01/ofgem_future_insights_series_3_local_energy_final_300117.pdf`
Last accessed: 02/09/19.

[124] Andrea Damm, Judith Köberl, Franz Prettenthaler, Nikola Rogler, and Christoph Töglhofer. Impacts of +2 °C global warming on electricity demand in Europe. *Climate Services*, 7:12–30, 2017.

[125] Joakim Widén, Nicole Carpman, Valeria Castellucci, David Lingfors, Jon Olauson, Flore Remouit, Mikael Bergkvist, Mårten Grabbe, and Rafael Waters. Variability assessment and forecasting of renewables: A review for solar, wind, wave and tidal resources. *Renewable and Sustainable Energy Reviews*, 44:356–375, 2015.

[126] Gorm B Andresen, Rolando A Rodriguez, Sarah Becker, and Martin Greiner. The potential for arbitrage of wind and solar surplus power in Denmark. *Energy*, 76:49–58, 2014.

[127] Peter Stott. How climate change affects extreme weather events. *Science*, 352(6293):1517–1518, 2016.

[128] OECD/IEA. Energy Technology Perspectives 2017, 2017.

[129] Xiaodong Cao, Xilei Dai, and Junjie Liu. Building energy-consumption status worldwide and the state-of-the-art technologies for zero-energy buildings during the past decade. *Energy and buildings*, 128:198–213, 2016.

[130] IEA. Transition to Sustainable Buildings: Strategies and Opportunities to 2050, 2013. URL `http://www.iea.org/etp/buildings/`.

[131] IEA. CO_2 emissions from fuel combustion - highlights, 2017.

[132] Smail Kozarcanin, Hailiang Liu, and Gorm Bruun Andresen. 21st Century Climate Change Impacts on Key Properties of a Large-Scale Renewable-Based Electricity System. *Joule*, 3(4):992–1005, 2019.

[133] Roberto Schaeffer, Alexandre Salem Szklo, André Frossard Pereira de Lucena, Bruno Soares Moreira Cesar Borba, Larissa Pinheiro Pupo Nogueira, Fernanda Pereira Fleming, Alberto Troccoli, Mike Harrison, and Mohammed Sadeck Boulahya. Energy sector vulnerability to climate change: A review. *Energy*, 38(1):1–12, 2012.

[134] Iain Staffell, Daniel Scamman, Anthony Velazquez Abad, Paul Balcombe, Paul E Dodds, Paul Ekins, Nilay Shah, and Kate R Ward. The role and status of hydrogen and fuel cells across the global energy system. *engrXiv*, 2018.

[135] Tobias Fleiter, J Steinbach, M Ragwitz, J Dengler, B Köhler, et al. Mapping and analyses of the current and future (2020-2030) heating/cooling fuel deployment (fossil/renewables) - WP1, 2016.

[136] Daniel Huppmann, Joeri Rogelj, Elmar Kriegler, Volker Krey, and Keywan Riahi. A new scenario resource for integrated 1.5 °C research. *Nature climate change*, page 1, 2018.

[137] Matthias Berger and Jörg Worlitschek. A novel approach for estimating residential space heating demand. *Energy*, 159:294–301, 2018.

[138] Hailiang Liu, Tom Brown, Gorm Bruun Andresen, David P Schlachtberger, and Martin Greiner. The role of hydro power, storage and transmission in the decarbonization of the Chinese power system. *Applied Energy*, 239:1308–1321, 2019.

[139] Eurostat. The Statistical Office of the European Union. Energy statistics - cooling and heating degree days (nrg chdd), 2016.
Available at: `https://ec.europa.eu/eurostat/cache/metadata/`

en/nrg_chdd_esms.htm
Last accessed: 19/10/19.

[140] International Energy Agency, IEA. Energy efficiency indicators - highlights, 2017.

[141] Urban Persson and Sven Werner. Stratego - Quantifying the Heating and Cooling Demand in Europe, Background Report 4, 2015.

[142] Vivid Economics and Imperial College. International Comparisons of Heating, Cooling and Heat Decarbonisation Policies. Report prepared for the Department of Business, Energy and Industrial Strategy, 2017.

[143] David Connolly, David Drysdale, Kenneth Hansen, and Tomislav Novosel. Stratego - Creating Hourly Profiles to Model both Demand and Supply, background report 2, 2015.

[144] Didier Bosseboeuf. Energy efficiency trends and policies in the household & tertiary sectors in the EU27. *Results from the ODYSSEE/MURE project, Paris*, 2009.

[145] Yabin Guo, Jiangyu Wang, Huanxin Chen, Guannan Li, Jiangyan Liu, Chengliang Xu, Ronggeng Huang, and Yao Huang. Machine learning-based thermal response time ahead energy demand prediction for building heating systems. *Applied Energy*, 221:16–27, 2018.

[146] Farrokh Jazizadeh and Wooyoung Jung. Personalized thermal comfort inference using RGB video images for distributed HVAC control. *Applied Energy*, 220:829–841, 2018.

[147] Ali Ghahramani, Guillermo Castro, Simin Ahmadi Karvigh, and Burcin Becerik-Gerber. Towards unsupervised learning of thermal comfort using infrared thermography. *Applied Energy*, 211:41–49, 2018.

[148] Rochus Niemierko, Jannick Töppel, and Timm Tränkler. A D-vine copula quantile regression approach for the prediction of residential heating energy consumption based on historical data. *Applied Energy*, 233:691–708, 2019.

[149] Felix Bünning, Roozbeh Sangi, and Dirk Müller. A Modelica library for the agent-based control of building energy systems. *Applied energy*, 193: 52–59, 2017.

[150] N Gaitani, C Lehmann, M Santamouris, G Mihalakakou, and P Patargias. Using principal component and cluster analysis in the heating evaluation of the school building sector. *Applied Energy*, 87(6):2079–2086, 2010.

[151] Nil Aras. Forecasting residential consumption of natural gas using genetic algorithms. *Energy Exploration & Exploitation*, 26(4):241–266, 2008.

[152] Reed P Timmer and Peter J Lamb. Relations between temperature and residential natural gas consumption in the Central and Eastern United States. *Journal of Applied Meteorology and Climatology*, 46(11):1993–2013, 2007.

[153] Ahmet Goncu, Mehmet Oguz Karahan, Tolga Umut Kuzubas, et al. Forecasting Daily Residential Natural Gas Consumption: A Dynamic Temperature Modelling Approach. *Bogazici University, Department of Economics*, 2013.

[154] H Sarak and A Satman. The degree-day method to estimate the residential heating natural gas consumption in Turkey: a case study. *Energy*, 28(9): 929–939, 2003.

[155] Robert G Quayle and Henry F Diaz. Heating degree day data applied to residential heating energy consumption. *Journal of Applied Meteorology*, 19 (3):241–246, 1980.

[156] HCS Thom. The rational relationship between heating degree days and temperature. *Monthly Weather Review*, 82(1):1–6, 1954.

[157] Iain Staffell, Daniel JL Brett, Nigel P Brandon, and Adam D Hawkes. *Domestic microgeneration: Renewable and distributed energy technologies, policies and economics*. Routledge, 2015.

[158] Magnus Dahl, Adam Brun, and Gorm B Andresen. Decision rules for economic summer-shutdown of production units in large district heating systems. *Applied Energy*, 208:1128–1138, 2017.

[159] Hirotugu Akaike. Factor analysis and AIC. In *Selected Papers of Hirotugu Akaike*, pages 371–386. Springer, 1987.

[160] Clifford M Hurvich and Chih-Ling Tsai. Model selection for extended quasi-likelihood models in small samples. *Biometrics*, pages 1077–1084, 1995.

[161] Kenneth P Burnham and David R Anderson. *Model selection and multimodel inference: a practical information-theoretic approach*. Springer Science & Business Media, 2003.

[162] DR Anderson, KP Burnham, and GC White. Comparison of Akaike Information Criterion and Consistent Akaike Information Criterion for model selection and statistical inference from capture-recapture studies. *Journal of Applied Statistics*, 25(2):263–282, 1998.

[163] Suranjana Saha, Shrinivas Moorthi, Hua-Lu Pan, Xingren Wu, Jiande Wang, Sudhir Nadiga, Patrick Tripp, Robert Kistler, John Woollen, David Behringer, et al. The NCEP climate forecast system reanalysis. *Bulletin of the American Meteorological Society*, 91(8):1015–1058, 2010.

[164] MR Haylock, N Hofstra, AMG Klein Tank, EJ Klok, PD Jones, and M New. A European daily high-resolution gridded data set of surface temperature and precipitation for 1950–2006. *Journal of Geophysical Research: Atmospheres*, 113(D20), 2008.

[165] T Boßmann and Iain Staffell. The shape of future electricity demand: exploring load curves in 2050s Germany and Britain. *Energy*, 90:1317–1333, 2015.

[166] Energinet, 2018.
Available at: `https://energinet.dk/`
Last accessed: 19/10/19.

[167] Eurostat. Statistical Office of the European Communities: Luxembourg, 1990.

[168] ENTSO-g European Network of Transmission System Operators for gas. ENTSO-g at a glance, 2018.

[169] Aggregated Gas Stock Inventory, 2016.
Available at: `https://agsi.gie.eu/#/`
Last accessed: 19/10/19.

[170] Yu Ting Kwok, Kevin Ka-Lun Lau, Alan Kwok Lung Lai, Pak Wai Chan, Yahya Lavafpour, Justin Ching Kwan Ho, and Edward Yan Yung Ng. A comparative study on the indoor thermal comfort and energy consumption of typical public rental housing types under near-extreme summer conditions in Hong Kong. *Energy Procedia*, 122:973–978, 2017.

[171] Xiaoliang Wang, Bo Lei, Haiquan Bi, and Tao Yu. Study on the Thermal Performance of a Hybrid Heat Collecting Facade Used for Passive Solar Buildings in Cold Region. *Energies*, 12(6):1038, 2019.

[172] European Commission, EC. EU Buildings Database, 2019.
Available at: `https://ec.europa.eu/energy/en/eu-buildings-database`
Last accessed: 19/10/19.

[173] Jenni Patronen, Eeva Kaura, and Cathrine Torvestad. Nordic heating and cooling - Nordic approach to EU's Heating and Cooling Strategy, 2017.

[174] HSE, Health and Safety Executive. *Thermal comfort in the workplace guidance for employers*. Health and Safety Executive Books, 1999.

[175] DMB. Deutcher Mieterbund, 2018.
Available at: `http://www.mieterbund.de`
Last accessed: 19/10/19.

[176] Kirsti Jylhä, Kimmo Ruosteenoja, Juha Jokisalo, Karoliina Pilli-Sihvola, Targo Kalamees, Hanna Mäkelä, Reijo Hyvönen, and Achim Drebs. Hourly test reference weather data in the changing climate of Finland for building energy simulations. *Data in brief*, 4:162–169, 2015.

[177] Leticia Blázquez, Nina Boogen, and Massimo Filippini. Residential electricity demand in Spain: New empirical evidence using aggregate data. *Energy economics*, 36:648–657, 2013.

[178] Xavier Labandeira, José M Labeaga, and Xiral López-Otero. Estimation of elasticity price of electricity with incomplete information. *Energy Economics*, 34(3):627–633, 2012.

[179] S Kozarcanin, GB Andresen, and I Staffell. Estimating country-specific space heating threshold temperatures from national gas and electricity consumption data. *Energy and Buildings*, 199:368–380, 2019.

[180] Gregory Flato, Jochem Marotzke, Babatunde Abiodun, Pascale Braconnot, S Chan Chou, William Collins, Peter Cox, F Driouech, S Emori, V Eyring, et al. Evaluation of climate models, 2013.

[181] Svend Frederiksen and Sven Werner. *District heating and cooling*. Studentlitteratur, 2013.

[182] Rossano Scoccia, Tommaso Toppi, Marcello Aprile, and Mario Motta. Absorption and compression heat pump systems for space heating and DHW in European buildings: Energy, environmental and economic analysis. *Journal of Building Engineering*, 16:94–105, 2018.

[183] GIAU/GEUS. Energianlæg baseret på jordvarmeboringer - Udvikling af markedsfremmende værktøjer og best practice, 2014.
Available at: `http://geoenergi.org/xpdf/d9-temperatur_og_temperaturgradienter.pdf`
Last accessed: 19/10/19.

[184] Energinet. Technology Data for Individual Heating Plants and Energy Transport, 2016.
Available at: `https://ens.dk/sites/ens.dk/files/Analyser/technology_data_catalogue_for_heating_installations_-_marts_2018.pdf`
Last accessed: 19/10/19.

[185] Eurostat. Electricity price statistics, 2018.
Available at: `https://ec.europa.eu/eurostat/statistics-explained/index.php/Electricity_price_statistics#Electricity_prices_for_household_consumers`
Last accessed: 19/10/19.

[186] Eurostat. Natural gas price statistics, 2018.
Available at: `https://ec.europa.eu/eurostat/statistics-explained/index.php/Natural_gas_price_statistics#Natural_gas_prices_for_household_consumers`
Last accessed: 19/10/19.

[187] IEA. Monthly oil price statistics, 2019.
Available at: `https://www.iea.org/classicstats/monthlystatistics/monthlyoilprices/`
Last accessed: 19/10/19.

[188] Cross Border Bioenergy/European Biomass Association. EU Handbook - Small Scale Heating Markets, 2012.

[189] Magnus Dahl, Adam Brun, and Gorm B Andresen. Cost sensitivity of optimal sector-coupled district heating production systems. *Energy*, 166: 624–636, 2019.

[190] Iain Staffell and Richard Green. Is there still merit in the merit order stack? The impact of dynamic constraints on optimal plant mix. *IEEE Transactions on Power Systems*, 31(1):43–53, 2015.

[191] CIESIN. Documentation for the Gridded Population of the World, Version 4 (GPWv4). Palisades NY: NASA Socioeconomic Data and Applications Center (SEDAC). Center for International Earth Science Information Network - CIESIN - Columbia University, 2016.
Available at: `http://dx.doi.org/10.7927/H4D50JX4`
Last accessed: 19/10/19.

[192] International Energy Agency, IEA. CO_2 emissions from fuel combustion - highlights, 2018.

[193] Rudolf Geiger. Klassifikation der klimate nach W. Köppen. *Landolt - Börnstein - Zahlenwerte und Funktionen aus Physik, Chemie, Astronomie, Geophysik und Technik*, 3:603–607, 1954.

[194] Bas J van Ruijven, Enrica De Cian, and Ian Sue Wing. Amplification of future energy demand growth due to climate change. *Nature Communications*, 10(1):2762, 2019.

[195] Alban Kitous, Jacques Després, et al. Assessment of the impact of climate change on residential energy demand for heating and cooling. Technical report, Joint Research Centre (Seville site), 2017.

[196] Robert Gross and Richard Hanna. Path dependency in provision of domestic heating. *Nature Energy*, page 1, 2019.

[197] Bernadett Kiss, Lena Neij, and Martin Jakob. Heat pumps: A comparative assessment of innovation and diffusion policies in Sweden and Switzerland. *Energy technology innovation: Learning from historical successes and failures*, 2014.

[198] European Parliament and Council. Directive 2009/28/EC of the European Parliament and of the Council of 23 April 2009 on the promotion of the use of energy from renewable sources and amending and subsequently repealing Directives 2001/77/EC and 2003/30/EC, 2009.

[199] Colin Patrick Gleeson and Robert Lowe. Meta-analysis of European heat pump field trial efficiencies. *Energy and Buildings*, 66:637–647, 2013.

[200] Francesco Rizzi, Marco Frey, and Fabio Iraldo. Towards an integrated design of voluntary approaches and standardization processes: An analysis of issues and trends in the Italian regulation on ground coupled heat pumps. *Energy conversion and management*, 52(10):3120–3131, 2011.

[201] EC. Communication from the Commission to the European Parliament, the Council, the European Economic and Social Committee and the Committee of the Regions: An EU Strategy on Heating and Cooling. European Commission, 2016.
Available at: `https://ec.europa.eu/energy/sites/ener/files/documents/1_EN_ACT_part1_v14.pdf`
Last accessed: 19/10/19.

[202] EHPA. European Heat Pump Market and Statistics Report. European Heat Pump Association, 2017.

[203] Anouk Honoré. Decarbonisation of heat in Europe: Implications for natural gas demand. *Oxford Institute for Energy Studies*, 2018.

[204] Aditi Sahni, Alex Kazaglis, Richard Hanna, Rob Gross, Luke Kemp, Nick Kingsmill, and Ethan McCormac. International Comparisons of Heating, Cooling and Heat Decarbonisation Policies. Report prepared by Vivid Economics & Imperial College London for the Department of Business, Energy and Industrial Strategy: London, UK, 2017.

[205] EEA. Progress on energy efficiency in Europe, 2019.

[206] Lea Gynther, Bruno Lapillonne, and Karine Pollier. Energy Efficiency Trends and Policies in the Household and Tertiary Sectors: An Analysis Based on the ODYSSEE and MURE Databases. *ODYSSEE-MURE project*, 2015.

[207] EHPA. European Heat Pump Market and Statistics Report. European Heat Pump Association, 2014.

[208] Frontier Economics. Pathways to high penetration of heat pumps: Report prepared for the committee on climate change. *Frontier Economics Ltd, London*, 2013.

[209] K Papakostas, Georgios Martinopoulos, and Agis Papadopoulos. *A Comparison of Various Heating Systems in Greece Based on Efficiency and Fuel Cost. 17th Symposium on Thermal Science and Engineering of Serbia. Sokobanja, Serbia*. 17th Symposium on Thermal Science and Engineering of Serbia. Sokobanja, Serbia, 2015.

[210] SC Karytsas and IP Chaldezos. Review of the Greek Legislative Framework for Ground Source Heat Pumps (GSHPs) and Suggestions for its improvement. *Procedia environmental sciences*, 38:704–712, 2017.

[211] Diana Poputoaia and Stefan Bouzarovski. Regulating district heating in Romania: Legislative challenges and energy efficiency barriers. *Energy Policy*, 38(7):3820–3829, 2010.

[212] Stefan Bouzarovski, Luděk Sỳkora, and Roman Matoušek. Locked-in post-socialism: Rolling path dependencies in Liberec's district heating system. *Eurasian Geography and Economics*, 57(4-5):624–642, 2016.

[213] K Wojdyga and M Chorzelski. Chances for Polish district heating systems. *Energy Procedia*, 116:106–118, 2017.

[214] Lukas Kranzl, Gerald Kalt, Andreas Müller, Marcus Hummel, Christiane Egger, Christine Öhlinger, and Gerhard Dell. Renewable energy in the heating sector in Austria with particular reference to the region of Upper Austria. *Energy policy*, 59:17–31, 2013.

[215] Sophie Nyborg and Inge Røpke. Heat pumps in Denmark-From ugly duckling to white swan. *Energy Research & Social Science*, 9:166–177, 2015.

[216] Karin Ericsson. Introduction and development of the Swedish district heating systems-Critical factors and lessons learned. Lund university, 2009.
Available at: `http://www.res-h-policy.eu/downloads/Swedish_district_heating_case-study_(D5)_final.pdf`
Last accessed: 24/10/16.

[217] Jenny Sumner, Lori Bird, and Hillary Dobos. Carbon taxes: A review of experience and policy design considerations. National Renewable Energy Laboratory, 2016.
Available at: `http://www.nrel.gov/docs/fy10osti/47312.pdf`
Last accessed: 16/12/16.

[218] World Bank. State and trends of carbon pricing 2014. Washington: World Bank, 2014.
Available at: `http://documents.worldbank.org/curated/en/505431468148506727/State-and-trends-of-carbon-pricing-2014`
Last accessed: 16/12/16.

[219] AGEB. Energieverbrauch in Deutschland. Daten für das 1.-3. Quartal 2018, 2018.
Available at: https://ag-energiebilanzen.de/20-0-Berichte.html
Last accessed: 15/01/19.

[220] Even Bjørnstad. Diffusion of renewable heating technologies in households. Experiences from the Norwegian Household Subsidy Programme. *Energy Policy*, 48:148–158, 2012.

[221] Jenni Patronen, Eeva Kaura, and Cathrine Torvestad. Nordic heating and cooling: Nordic approach to EU's Heating and Cooling Strategy. Nordic Council of Ministers, 2017.
Available at: https://www.diva-portal.org/smash/get/diva2:1098961/FULLTEXT01.pdf
Last accessed: 06/06/19.

[222] Martin Forsén, Peter Roots, and Anne-Lee Bertenstam. Market status for ground source heat pumps in Europe, 2008.
Available at: https://ec.europa.eu/energy/intelligent/projects/sites/iee-projects/files/projects/documents/ground-reach_market_status_for_gchp_in_europe.pdf
Last accessed: 06/06/19.

[223] Richard Hanna, Matthew Leach, and Jacopo Torriti. Microgeneration: The installer perspective. *Renewable Energy*, 116:458–469, 2018.

[224] CCC. The Fifth Carbon Budget - The next step towards a low-carbon economy. Committee on Climate Change, 2015.

[225] CCC. Reducing UK emissions: 2018 Progress Report to Parliament. Committee on Climate Change, 2018.

[226] Anouk Honoré. The Dutch gas market: trials, tribulations, and trends, 2017.
Available at: https://www.oxfordenergy.org/publications/dutch-gas-market-trials-tribulations-trends/
Last accessed: 15/01/19.

[227] ECN - Petten, the Netherlands. National Energy Outlook 2016., 2016.

[228] Ministry of Economic Affairs. Energy agenda: Towards a low-carbon energy supply. The Hague, the Netherlands, 2017.

Available at: https://www.government.nl/documents/reports/2017/03/01/energy-agenda-towards-a-low-carbon-energy-supply
Last accessed: 06/06/19.

[229] Iain Staffell, Daniel Scamman, Anthony Velazquez Abad, Paul Balcombe, Paul E Dodds, Paul Ekins, Nilay Shah, and Kate R Ward. The role of hydrogen and fuel cells in the global energy system. *Energy & Environmental Science*, 12(2):463–491, 2019.

[230] Goran Strbac, Danny Pudjianto, R Sansom, Predrag Djapic, Hossein Ameli, Nilay Shah, Nigel Brandon, Adam Hawkes, and M Qadrdan. Analysis of Alternative UK Heat Decerbonisation Pathways. *Imperial College London: London, UK*, 2018.

[231] SD Watson, Kevin J Lomas, and Richard A Buswell. Decarbonising domestic heating: What is the peak GB demand? *Energy policy*, 126:533–544, 2019.

[232] Paul Balcombe, Dan Rigby, and Adisa Azapagic. Investigating the importance of motivations and barriers related to microgeneration uptake in the UK. *Applied Energy*, 130:403–418, 2014.

[233] UNFCCC. United nations framework convention on climate change, 1992.

[234] Mark Z Jacobson and Mark A Delucchi. A path to sustainable energy by 2030. *Scientific American*, 301(5):58–65, 2009.

[235] David Connolly, Henrik Lund, Brian Vad Mathiesen, and Martin Leahy. The first step towards a 100% renewable energy-system for Ireland. *Applied Energy*, 88(2):502–507, 2011.

[236] Henrik Lund, Poul Alberg Østergaard, David Connolly, and Brian Vad Mathiesen. Smart energy and smart energy systems. *Energy*, 137:556–565, 2017.

[237] Tom Brown, David Schlachtberger, Alexander Kies, Stefan Schramm, and Martin Greiner. Synergies of sector coupling and transmission reinforcement in a cost-optimised, highly renewable European energy system. *Energy*, 160:720–739, 2018.

[238] Maria Abou Chakra, Silke Bumann, Hanna Schenk, Andreas Oschlies, and Arne Traulsen. Immediate action is the best strategy when facing uncertain climate change. *Nature communications*, 9(1):2566, 2018.

[239] Susan Solomon. IPCC (2007): Climate change the physical science basis. In *AGU Fall Meeting Abstracts*, 2007.

[240] S Kozarcanin, R Hanna, I Staffell, R Gross, and GB Andresen. Impact of climate change on the cost-optimal mix of decentralised heat pump and gas boiler technologies in Europe. *arXiv preprint arXiv:1907.04067*, 2019.

[241] Tom Brown, Jonas Hörsch, and David Schlachtberger. PyPSA: Python for power system analysis. *arXiv preprint arXiv:1707.09913*, 2017. Available at: `https://pypsa.org/`.

[242] Kun Zhu, Marta Victoria, Tom Brown, Gorm B Andresen, and Martin Greiner. Impact of CO2 prices on the design of a highly decarbonised coupled electricity and heating system in Europe. *Applied energy*, 236:622–634, 2019.

[243] David P Schlachtberger, Tom Brown, Stefan Schramm, and Martin Greiner. The benefits of cooperation in a highly renewable european electricity network. *Energy*, 134:469–481, 2017.

[244] Karen OBrien and Linda Sygna. Responding to climate change: the three spheres of transformation. *Proceedings of Transformation in a Changing Climate*, pages 19–21, 2013.

[245] Jonas Meckling, Nina Kelsey, Eric Biber, and John Zysman. Winning coalitions for climate policy. *Science*, 349(6253):1170–1171, 2015.

[246] Elmar Kriegler, John P Weyant, Geoffrey J Blanford, Volker Krey, Leon Clarke, Jae Edmonds, Allen Fawcett, Gunnar Luderer, Keywan Riahi, Richard Richels, et al. The role of technology for achieving climate policy objectives: overview of the EMF 27 study on global technology and climate policy strategies. *Climatic change*, 123(3-4):353–367, 2014.

[247] David McCollum, Volker Krey, Peter Kolp, Yu Nagai, and Keywan Riahi. Transport electrification: A key element for energy system transformation and climate stabilization. *Climatic Change*, 123(3-4):651–664, 2014.

[248] Göran Berndes, Monique Hoogwijk, and Richard Van den Broek. The contribution of biomass in the future global energy supply: A review of 17 studies. *Biomass and bioenergy*, 25(1):1–28, 2003.

[249] Katherine Calvin, James Edmonds, Ben Bond-Lamberty, Leon Clarke, Son H Kim, Page Kyle, Steven J Smith, Allison Thomson, and Marshall

Wise. 2.6: Limiting climate change to 450 ppm CO2 equivalent in the 21st century. *Energy Economics*, 31:S107–S120, 2009.

[250] Michelle TH Van Vliet, David Wiberg, Sylvain Leduc, and Keywan Riahi. Power-generation system vulnerability and adaptation to changes in climate and water resources. *Nature Climate Change*, 6(4):375, 2016.

[251] Haewon McJeon, Jae Edmonds, Nico Bauer, Leon Clarke, Brian Fisher, Brian P Flannery, Jerome Hilaire, Volker Krey, Giacomo Marangoni, Raymond Mi, et al. Limited impact on decadal-scale climate change from increased use of natural gas. *Nature*, 514(7523):482, 2014.

[252] Susanne C Moser and Julia A Ekstrom. A framework to diagnose barriers to climate change adaptation. *Proceedings of the national academy of sciences*, page 201007887, 2010.

[253] Kristo Helin, Behnam Zakeri, and Sanna Syri. Is District Heating Combined Heat and Power at Risk in the Nordic Area? – An Electricity Market Perspective. *Energies*, 11(5):1256, 2018.

[254] EEA. Share of combined heat and power in gross electricity production in 2004, 2019.
Available at: `https://www.eea.europa.eu/data-and-maps/figures/share-of-combined-heat-and-1`
Last accessed: 01/08/19.

[255] Stefan Pfenninger, Adam Hawkes, and James Keirstead. Energy systems modeling for twenty-first century energy challenges. *Renewable and Sustainable Energy Reviews*, 33:74–86, 2014.

[256] Detlef P Van Vuuren, Jae Edmonds, Mikiko Kainuma, Keywan Riahi, Allison Thomson, Kathy Hibbard, George C Hurtt, Tom Kram, Volker Krey, Jean-Francois Lamarque, et al. The representative concentration pathways: An overview. *Climatic change*, 109(1-2):5, 2011.

[257] IPCC. Rcp database v2.0.5, 2019.
Available at: `https://tntcat.iiasa.ac.at/RcpDb/dsd?Action=htmlpage&page=compare`
Last accessed: 01/08/19.

[258] Wind Power Database. The Wind Power – Wind Energy Market Intelligence, 2005. URL `http://www.thewindpower.net`.

[259] Andreas Schröder, Friedrich Kunz, Jan Meiss, Roman Mendelevitch, and Christian von Hirschhausen. Current and Prospective Costs of Electricity Generation until 2050. DIW Data Documentation 68, 2013.
Available at: http://hdl.handle.net/10419/80348
Last accessed: 17/06/19.

[260] Natural Resources Canada, 2019.
Available at: https://www.nrcan.gc.ca/home,
Last accessed: 17/06/19.

[261] Eero Vartiainen, Gaëtan Masson, and Christian Breyer. The true competitiveness of solar PV: a European case study, tech. Rep., European technology and innovation platform for photovoltaics, 2017.
Available at: http://www.etip-pv.eu/fileadmin/Documents/ETIP_PV_Publications_2017-2018/LCOE_Report_March_2017.pdf
Last accessed: 17/06/19.

[262] Danish Energy Agency and Energinet.dk. Technology data for generation of electricity and district heating, energy storage and energy Carrier generation and conversion, 2016.
Available at: https://ens.dk/en/our-services/projections-and-models/technology-data
Last accessed: 17/06/19.

[263] Andreas Palzer. *Sektorübergreifende Modellierung und Optimierung eines zukünftigen deutschen Energiesystems unter Berücksichtigung von Energieeffizienzmaßnahmen im Gebäudesektor*. Fraunhofer Verlag, 2016.

[264] Andreas Palzer and Hans-Martin Henning. A comprehensive model for the German electricity and heat sector in a future energy system with a dominant contribution from renewable energy technologies–Part II: Results. *Renewable and Sustainable Energy Reviews*, 30:1019–1034, 2014.

[265] Mahdi Fasihi, Dmitrii Bogdanov, and Christian Breyer. Long-Term hydrocarbon trade options for the maghreb region and europe - renewable energy based synthetic fuels for a net zero emissions World. *Sustainability*, 9(2):306, 2017.

[266] Cory Budischak, DeAnna Sewell, Heather Thomson, Leon Mach, Dana E Veron, and Willett Kempton. Cost-minimized combinations of wind power, solar power and electrochemical storage, powering the grid up to 99.9% of the time. *journal of power sources*, 225:60–74, 2013.

[267] Hans-Martin Henning and Andreas Palzer. A comprehensive model for the German electricity and heat sector in a future energy system with a dominant contribution from renewable energy technologies - Part I: Methodology. *Renewable and Sustainable Energy Reviews*, 30:1003–1018, 2014.

[268] Norman Gerhardt, Fabian Sandau, Angela Scholz, Henning Hahn, Patrick Schumacher, Christina Sager, F Bergk, C Kämper, W Knörr, J Kräck, et al. Interaktion EE-Strom, Wärme und Verkehr. *Endbericht. Fraunhofer IWES*, 2015.

[269] Sonja Van Renssen. EU adaptation policy sputters and starts. *Nature Climate Change*, 3:614–615, 2013.

[270] Debra J Davidson. We still have a long way to go, and a short time to get there: A response to Fikret Berkes and Helen Ross. *Society & Natural Resources*, 26(1):21–24, 2013.

[271] Claas Teichmann, Bastian Eggert, Alberto Elizalde, Andreas Haensler, Daniela Jacob, Pankaj Kumar, Christopher Moseley, Susanne Pfeifer, Diana Rechid, Armelle Reca Remedio, et al. How does a regional climate model modify the projected climate change signal of the driving GCM: a study over different CORDEX regions using REMO. *Atmosphere*, 4(2): 214–236, 2013.

[272] Zhongfeng Xu and Zong-Liang Yang. A new dynamical downscaling approach with GCM bias corrections and spectral nudging. *Journal of Geophysical Research: Atmospheres*, 120(8):3063–3084, 2015.

[273] Chris D Hewitt. Ensembles-based predictions of climate changes and their impacts. *Eos, Transactions American Geophysical Union*, 85(52):566–566, 2004.

[274] Congbin Fu, Shuyu Wang, Zhe Xiong, William J Gutowski, Dong-Kyou Lee, John L McGregor, Yasuo Sato, Hisashi Kato, Jeong-Woo Kim, and Myoung-Seok Suh. Regional climate model intercomparison project for Asia. *Bulletin of the American Meteorological Society*, 86(2):257–266, 2005.

[275] Linda O Mearns, Ray Arritt, Sébastien Biner, Melissa S Bukovsky, Seth McGinnis, Stephan Sain, Daniel Caya, James Correia Jr, Dave Flory, William Gutowski, et al. The North American regional climate change assessment program: overview of phase I results. *Bulletin of the American Meteorological Society*, 93(9):1337–1362, 2012.

[276] Jens Hesselbjerg Christensen, Timothy R Carter, and Filippo Giorgi. PRUDENCE employs new methods to assess European climate change. *EOS, Transactions American Geophysical Union*, 83(13):147–147, 2002.

[277] Jean-Philippe Boulanger, G Brasseur, Andrea Fabiana Carril, Manuel De Castro, Nicolas Degallier, Carlos Ereño, Hervé Le Treut, Jose Antonio Marengo, Claudio Guillermo Menendez, Mario Nestor Nuñez, et al. A Europe–South America network for climate change assessment and impact studies. *Climatic Change*, 98(3):307–329, 2010.

[278] Waheed Iqbal, Wai-Nang Leung, and Abdel Hannachi. Analysis of the variability of the North Atlantic eddy-driven jet stream in CMIP5. *Climate Dynamics*, pages 1–13, 2017.

[279] Abdel Hannachi, Elizabeth A Barnes, and Tim Woollings. Behaviour of the winter North Atlantic eddy-driven jet stream in the CMIP3 integrations. *Climate dynamics*, 41(3-4):995–1007, 2013.

[280] Elizabeth A Barnes and Lorenzo Polvani. Response of the midlatitude jets, and of their variability, to increased greenhouse gases in the CMIP5 models. *Journal of Climate*, 26(18):7117–7135, 2013.

[281] Axel Lauer and Kevin Hamilton. Simulating clouds with global climate models: A comparison of CMIP5 results with CMIP3 and satellite data. *Journal of Climate*, 26(11):3823–3845, 2013.

[282] Matthew Collins, Reto Knutti, Julie Arblaster, J-L Dufresne, Thierry Fichefet, Pierre Friedlingstein, Xuejie Gao, WJ Gutowski, Tim Johns, Gerhard Krinner, et al. Long-term climate change: Projections, commitments and irreversibility. *Cambridge University*, 2013.

[283] J-LF Li, DE Waliser, G Stephens, Seungwon Lee, T L'Ecuyer, Seiji Kato, Norman Loeb, and Hsi-Yen Ma. Characterizing and understanding radiation budget biases in CMIP3/CMIP5 GCMs, contemporary GCM, and reanalysis. *Journal of Geophysical Research: Atmospheres*, 118(15):8166–8184, 2013.

[284] BJJM Van den Hurk, P Viterbo, ACM Beljaars, and AK Betts. Offline validation of the ERA40 surface scheme, 295. Technical report, ECMWF Tech. Memo, Reading, UK, 2000.

[285] Gurvan Madec et al. NEMO ocean engine. 2015.

[286] Thierry Fichefet and MA Maqueda. Sensitivity of a global sea ice model to the treatment of ice thermodynamics and dynamics. *Journal of Geophysical Research: Oceans*, 102(C6):12609–12646, 1997.

[287] ECMWF. Part I: Observation Processing, 2004.
Available at: `https://www.ecmwf.int/sites/default/files/elibrary/2004/12075-part-i-observation-processing.pdf`
Last accessed: 15/01/17.

[288] ECMWF. Part II: Data Assimilation, 2007.
Available at: `https://www.ecmwf.int/sites/default/files/elibrary/2007/9219-part-ii-data-assimilation.pdf`
Last accessed: 15/01/17.

[289] ECMWF. Part III: Dynamics and Numerical Procedures, 2007.
Available at: `https://www.ecmwf.int/sites/default/files/elibrary/2007/9220-part-iii-dynamics-and-numerical-procedures.pdf`
Last accessed: 15/01/17.

[290] ECMWF. Part IV: Physical Processes, 2007.
Available at: `https://www.ecmwf.int/sites/default/files/elibrary/2007/9221-part-iv-physical-processes.pdf`
Last accessed: 15/01/17.

[291] ECMWF. Part V: The Ensemble Prediction System, 2007.
Available at: `https://www.ecmwf.int/sites/default/files/elibrary/2007/9222-part-v-ensemble-prediction-system.pdf`
Last accessed: 15/01/17.

[292] ECMWF. Part VI: Technical and Computational Procedures, 2007.
Available at: `https://www.ecmwf.int/sites/default/files/elibrary/2007/9223-part-vi-technical-and-computational-procedures.pdf`
Last accessed: 15/01/17.

[293] ECMWF. Part VI: Technical and Computational Procedures, 2007.
Available at: `https://www.ecmwf.int/sites/default/files/elibrary/2007/9224-part-vii-ecmwf-wave-model.pdf`
Last accessed: 15/01/17.

[294] S Valcke. OASIS3 user guide (prism_2-5). *PRISM support initiative report*, 3:64, 2006.

[295] Tim C Johns, Chris F Durman, Helene T Banks, Malcom J Roberts, Alison J McLaren, Jeff K Ridley, Catherine A Senior, KD Williams, A Jones, GJ Rickard, et al. The new Hadley Centre climate model (HadGEM1): Evaluation of coupled simulations. *Journal of Climate*, 19(7):1327–1353, 2006.

[296] N Bellouin, WJ Collins, ID Culverwell, PR Halloran, SC Hardiman, TJ Hinton, CD Jones, RE McDonald, AJ McLaren, FM O'Connor, et al. The HadGEM2 family of met office unified model climate configurations. *Geoscientific Model Development*, 4(3):723–757, 2011.

[297] RLH Essery, MJ Best, RA Betts, Peter M Cox, and Christopher M Taylor. Explicit representation of subgrid heterogeneity in a GCM land surface scheme. *Journal of Hydrometeorology*, 4(3):530–543, 2003.

[298] Douglas B Clark and Nicola Gedney. Representing the effects of subgrid variability of soil moisture on runoff generation in a land surface model. *Journal of Geophysical Research: Atmospheres*, 113(D10), 2008.

[299] KJ Beven and Michael J Kirkby. A physically based, variable contributing area model of basin hydrology/Un modèle à base physique de zone d'appel variable de l'hydrologie du bassin versant. *Hydrological Sciences Journal*, 24(1):43–69, 1979.

[300] Taikan Oki and YC Sud. Design of Total Runoff Integrating Pathways (TRIP)A global river channel network. *Earth interactions*, 2(1):1–37, 1998.

[301] N Bellouin, J Rae, C Johnson, J Haywood, A Jones, and O Boucher. Aerosol forcing in the Hadley Centre CMIP5 simulations by HadGEM2-ES and the role of ammonium nitrate. *J. Geophys. Res*, 116:D20206.

[302] FM O'Connor, CE Johnson, O Morgenstern, NL Abraham, P Braesicke, M Dalvi, GA Folberth, MG Sanderson, PJ Telford, A Voulgarakis, et al. Evaluation of the new UKCA climate-composition model–Part 2: The Troposphere. *Geoscientific Model Development*, 7(1):41–91, 2014.

[303] Peter M Cox. Description of the TRIFFID dynamic global vegetation model. *Hadley Centre technical note*, 24:1–16, 2001.

[304] K Coleman and DS Jenkinson. RothC-26.3-A Model for the turnover of carbon in soil. In *Evaluation of soil organic matter models*, pages 237–246. Springer, 1996.

[305] Marco A Giorgetta, Erich Roeckner, Thorsten Mauritsen, Jürgen Bader, Traute Crueger, Monika Esch, Sebastian Rast, Luis Kornblueh, Hauke Schmidt, Stefan Kinne, et al. The atmospheric general circulation model ECHAM6-model description. 2013.

[306] Erich Roeckner, G Bäuml, L Bonaventura, Renate Brokopf, Monika Esch, Marco Giorgetta, Stefan Hagemann, Ingo Kirchner, Luis Kornblueh, Elisa Manzini, et al. The atmospheric general circulation model ECHAM 5. PART I: Model description. 2003.

[307] Erich Roeckner, Renate Brokopf, Monika Esch, Marko Giorgetta, Stefan Hagemann, Luis Kornblueh, Elisa Manzini, Ulrich Schlese, and Uwe Schulzweida. The atmospheric general circulation model ECHAM5 Part II: Sensitivity of simulated climate to horizontal and vertical resolution. 2004.

[308] TJ Raddatz, CH Reick, W Knorr, Jens Kattge, E Roeckner, Reiner Schnur, K-G Schnitzler, P Wetzel, and J Jungclaus. Will the tropical land biosphere dominate the climate–carbon cycle feedback during the twenty-first century? *Climate Dynamics*, 29(6):565–574, 2007.

[309] JH Jungclaus, Nils Fischer, Helmuth Haak, K Lohmann, J Marotzke, D Matei, U Mikolajewicz, D Notz, and JS Storch. Characteristics of the ocean simulations in the Max Planck Institute Ocean Model (MPIOM) the ocean component of the MPI-Earth system model. *Journal of Advances in Modeling Earth Systems*, 5(2):422–446, 2013.

[310] Kalle Eerola. About the performance of HIRLAM version 7.0. *Hirlam Newsletter*, 51:93–102, 2006.

[311] Per Undén, Laura Rontu, Peter Lynch, Francisco Javier Calvo Sánchez, Gerard Cats, Joan Cuxart, Kalle Eerola, Carl Fortelius, José Antonio García-Moya, Colin Jones, et al. HIRLAM-5 scientific documentation. 2002.

[312] PW White. IFS documentation CY23r4: Part IV physical processes, 2004.

[313] Gustav Strandberg, Lars Bärring, Ulf Hansson, Christer Jansson, Colin Jones, Erik Kjellström, Marco Kupiainen, Grigory Nikulin, Patrick

Samuelsson, and Anders Ullerstig. *CORDEX scenarios for Europe from the Rossby Centre regional climate model RCA4*. SMHI, 2015.

[314] Cathrine Fox Maule. *Presentation of the DMI-HIRHAM5 CORDEX AFRICA-44 simulation - v2*. 2014.

[315] E Van Meijgaard, LH Van Ulft, G Lenderink, SR De Roode, Eva Louise Wipfler, R Boers, and RMA van Timmermans. *Refinement and application of a regional atmospheric model for climate scenario calculations of Western Europe*. Number KVR 054/12. KVR, 2012.

[316] H Tennekes. The logarithmic wind profile. *Journal of the Atmospheric Sciences*, 30(2):234–238, 1973.

[317] Douglas T Reindl, William A Beckman, and John A Duffie. Diffuse fraction correlations.

[318] DT Reindl, WA Beckman, and JA Duffie. Evaluation of hourly tilted surface radiation models. *Solar energy*, 45(1):9–17, 1990.

[319] Hans Georg Beyer, Gerd Heilscher, and Stefan Bofinger. A robust model for the MPP performance of different types of PV-modules applied for the performance check of grid connected systems. *Eurosun. Freiburg*, 2004.

[320] Center for International Earth Science Information Network - CIESIN. Gridded Population of the World, Version 4 (GPWv4), 2016.

[321] Suranjana Saha, Shrinivas Moorthi, Xingren Wu, Jiande Wang, Sudhir Nadiga, Patrick Tripp, David Behringer, Yu-Tai Hou, Hui ya Chuang, Mark Iredell, Michael Ek, Jesse Meng, Rongqian Yang, Malaquias Pena Mendez, Huug van den Dool, Qin Zhang, Wanqiu Wang, Mingyue Chen, and Emily Becker. NCEP Climate Forecast System Version 2 (CFSv2) Selected Hourly Time-Series Products, 2011. URL `https://doi.org/10.5065/D6N877VB`.

[322] Bernard L Welch. The generalization ofstudent's' problem when several different population variances are involved. *Biometrika*, 34(1/2):28–35, 1947.

[323] Joan Fisher Box. Guinness, gosset, fisher, and small samples. *Statistical science*, pages 45–52, 1987.

[324] Bradley Efron and Robert J Tibshirani. *An introduction to the bootstrap*. CRC press, 1994.

[325] Fabian Levihn. Personal correspondence with Stockholm Exergi, 2018.

[326] NTB Buchs. Wärmepumpen-Testzentrum Buchs (WPZ), 2019. URL https://www.ntb.ch/fue/institute/ies/wpz/.

About the author

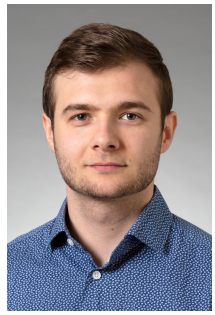

Smail Kozarcanin, the author of this book, was born in Bosnia & Herzegovina on September 1st 1990. In 2013, he obtained his BSc degree in Physics & Astronomy at the Department of Physics and Astronomy at Aarhus University. In 2015, he obtained his MSc degree in Physics & Astronomy with a minor in Mathematics at the Department of Mathematics at Aarhus University. His first encounter with energy systems took place during his Master's thesis titled: *Impact of nodal mismatch correlations on the power flows in renewable energy networks*. In this project, he concentrated on the electricity sector and had a rather restricted focus on energy systems as a whole. After obtaining his degrees, Smail worked as an assistant researcher at the Department of Engineering, Aarhus University where after he moved into teaching. In November 2016, he began his PhD project in the Renewable Energy and Thermodynamics group at the Department of Engineering, Aarhus University. Because of his personal interest in climate change and energy systems, he took up the challenge of this 3-year's Ph.D. project. His PhD focused on the impact of climate change on the European electricity and heating systems. Due to his background in physics and mathematics he had a restricted knowledge within the proposed topic at the onset of the project. The 3-year's PhD project was subject to a steep learning curve. At the time of writing, Smail has continued his career as a quantitative analyst in at Danske Commodities.